

**Characterization of *Synechocystis* sp. PCC 6803
under mixotrophic conditions**



Dissertation

**in fulfilment of the requirements for the degree “Dr. rer. nat.”
of the Faculty of Mathematics and Natural Sciences
at Kiel University**

submitted by

Xi Chen

Kiel, January 2014

First referee: _____ Prof. Dr. Rüdiger Schulz _____

Second referee: _____ Prof. Dr. Wolfgang Bilger _____

Date of the oral examination: _____ 11.02.2014 _____

Approved for publication: _____ 11.02.2014 _____

Signed: _____ , Dean

Contents

Contents	I
List of Abbreviations	I
1 Introduction	1
1.1 Cyanobacteria	1
1.2 <i>Synechocystis</i> sp. PCC 6803	4
1.3 Photosynthesis and respiration metabolism	4
1.3.1 Photosynthesis.....	4
1.3.2 Respiration.....	6
1.3.3 Cytochrome bd-type oxidase	7
1.3.4 The TCA cycle in <i>Synechocystis</i> sp. PCC 6803.....	8
1.4 Fermentation	9
1.5 Glucose degradation pathways	10
1.6 PFOR / PDH Complex.....	14
1.6.1 Pyruvate: ferredoxin / flavodoxin oxidoreductase (PFOR)	14
1.6.2 Pyruvate dehydrogenase (PDH) complex	16
1.7 Hydrogenase	17
2 Aims of the present study	20
3 Materials and Methods	21
3.1 Chemicals, buffers and media	21
3.2 Oligonucleotides	22
3.3 Plasmids and Bacteria.....	25
3.4 Restriction Enzymes.....	25
3.5 Cultivation of bacteria	26
3.5.1 Cultivation of <i>Synechocystis</i> sp. PCC 6803	26
3.5.2 Preparation of freezing cultures	26
3.5.3 Cultivation of <i>Escherichia coli</i>	26
3.6 Physiological Methods.....	29
3.6.1 Optical density	29
3.6.2 Absorption spectrum of chlorophyll a and phycocyanin	29

3.6.3	Chlorophyll content	30
3.6.4	Respiration and photosynthesis rate measurement	30
3.6.5	PAM (Pulse Amplitude Modulated) fluorescence measurement	33
3.6.6	Nuclear Magnetic Resonance (NMR)	35
3.6.7	NAD ⁺ /NADH determination	35
3.7	Molecular biological Methods	36
3.7.1	Isolation of genomic DNA from <i>Synechocystis</i> sp. PCC 6803	36
3.7.2	Polymerase Chain Reaction (PCR).....	38
3.7.3	DNA gel electrophoresis	39
3.7.4	Cloning.....	40
3.7.5	Restriction enzyme digestion	41
3.7.6	Mutants construction	42
3.7.7	RNA isolation from <i>Synechocystis</i> sp. PCC 6803.....	48
3.7.8	Denatured RNA agarose gel electrophoresis.....	48
3.7.9	DNase I digestion of RNA	49
3.7.10	Reverse transcript PCR	49
3.7.11	Quantitative real time PCR.....	50
3.8	Protein Analysis.....	51
3.9	Database and Bioinformatic programs	52
4	Results	53
4.1	Characterization of the <i>nifJ</i> - and the <i>hoxH</i> -mutant under different growth conditions	53
4.1.1	Characterization of the <i>nifJ</i> -mutant	53
4.1.2	Characterization of the <i>hoxH</i> -mutant	57
4.1.3	Activity of the cytochrome bd oxidase under mixotrophic conditions in WT and $\Delta nifJ$ cultures	58
4.1.4	Photosynthesis and respiration under mixotrophic conditions in WT and $\Delta nifJ$ cultures	59
4.1.5	Identification of excreted metabolites in WT and $\Delta nifJ$ cultures via Nuclear Magnetic Resonance (NMR).....	61
4.1.6	Transcription of selected genes in WT and $\Delta nifJ$ cultures under autotrophic, mixotrophic and fermentative conditions	67
4.1.7	Pyruvate dehydrogenase complex deletion mutant construction	69
4.1.8	Quantitative real time PCR for <i>nifJ</i> and <i>pdhA</i> genes.....	71

4.1.9	Colorimetric NADH/ NAD ⁺ Determination.....	77
4.1.10	Investigation of acetate feedback effect.....	79
4.2	Characterization of glycolytic pathways in <i>Synechocystis</i> sp. PCC 6803 ...	81
4.2.1	Construction of mutants with interrupted glucose degradation pathways in <i>Synechocystis</i> sp. PCC 6803	83
4.2.2	Construction of mutants to interrupt the potential ED pathway in <i>Synechocystis</i> sp. PCC 6803	100
4.2.3	Quantitative real time PCR for key genes of glucose degradation pathways.....	102
5	Discussion	108
5.1	Characterization of PFOR under different conditions	108
5.1.1	PFOR is an important electron sink under mixotrophic conditions	108
5.1.2	Analysis of excreted metabolites of WT and mutants under different conditions.....	112
5.1.3	Transcript expression of <i>nifJ</i> and <i>pdhA</i> under different conditions.....	115
5.2	Characterization of glucose degradation pathways	117
5.2.1	A novel glucose degradation enzyme in <i>Synechocystis</i> : glucose dehydrogenase (GDH)	117
5.2.2	Characterization of the ED pathway in <i>Synechocystis</i>	119
5.2.3	Transcription levels of the key genes of the EMP, OPP and ED pathways in <i>Synechocystis</i>	120
6	Summary	122
7	Zusammenfassung	124
8	Future perspectives	126
9	References	127
	Acknowledgement	141
	Affidavit.....	143
	Curriculum Vitae	144

List of Abbreviations

AA	Amino acid
ADP	Adenosine diphosphate
Amp	Ampicillin resistance
AOX	Alternative oxidase
ATP	Adenosine Triphosphate
BG-11	Medium for cyanobacteria
BLAST	Basic local alignment search tool
bp	Base pair
cDNA	Complementary DNA
CO ₂	Carbon dioxide
CDP	Disodium 4-chloro-3-phenyl phosphate
Chl	Chlorophyll
CoA	Coenzyme A
COX	Cytochrome c oxidase
Ct	Cycle threshold
Cyt	Cytochrome
DBMIB	2,5-dibromo-3-methyl-6-isopropyl-p-benzoquinone
DCMU	3-(3,4-dichlorophenyl)-1,1-dimethylurea
ddH ₂ O	Deionised and autoclaved water
Dig	Digoxigenin
DMSO	Dimethylsulfoxid
DNA	Deoxyribonucleic acid
DNase	Deoxy ribonuclease
dNTPs	Deoxyribonucleotide
DT	Dithionite
DTT	Dithiothreitol
<i>E. coli</i>	<i>Escherichia coli</i>
ED	Entner-Doudoroff
EDTA	Ethylene dinitro tetraacetic acid
EMP	Embden-Meyerhof-Parnas
FMN	Flavin mononucleotide
FNR	Ferredoxin: NADP oxidoreductase
g	Gram / Gravitational acceleration
GA	Glyceraldehydes
GAP	Glyceraldehyde 3-phosphate
GAPDH	Glyceraldehydes-3-phosphate dehydrogenase
GDH	Glucose dehydrogenase
H ⁺	Proton
H ₂	Hydrogen
kb	Kilobase
kD	Kilodalton
KDG	2-keto-3-deoxy-Gluconate
KDPG	2-keto-3-deoxy-6-phosphogluconate
Km	Kanamycin resistance
L	Liter
LAHG	Light Activated Heterotrophic Growth

LB	Luria Bertani nutrient medium
M	Molar
m ²	Square metre
Mb	Megabyte
min	Minute
ml	Milliliter
mM	Milimolar
MOPS	4-Morpholinopropane sulfonic acid
mRNA	Messenger ribonucleic acid
ms	Milisecond
MV	Methy viologen
N ₂	Nitrogen
NAD(H)	Nicotinamide adenine dincleotide (red/ox)
NADP(H)	Nicotinamide adenine dinucleotide Phosphate (red/ox)
NCBI	National center of biotechnology information
NMR	Nuclear magnetic resonance
O ₂	Oxygen
OD	Optical density
OPP	Oxidative Pentose Phosphate
PAM	Pulse Amplitude Modulated chlorophyll fluorescence
PC	Plastocyanin
PCC	Pasteur Culture Collection
PCP	Pentachlorophenol
PCR	Polymerase Chain Reaction
PDH	Pyruvate dehydrogenase
PEP	Phosphoenolpyruvate
PFOR	Pyruvate: ferredoxin / flavodoxin oxidoreductase
<i>pfu</i>	<i>Pyrococcus furiosus</i>
PGP	2,3-bisphosphoglycerate
PH	Potentia hydrogenii
PQ	Plastoquinone
PRK	Phosphoribulokinase
PS I	Photosystem I
PS II	Photosystem II
Q _A	Electron acceptor in Photosystem II
qRT- PCR	Quantitative real time PCR
RNA	Ribonucleic acid
RNase	Ribonuclease
rpm	Round per minute
RT	Room temperature
RT-Mix	Reverse transcription mixture
RT-PCR	Reverse transcription-polymerase chain reaction
SDH	Succinate dehydrogenase
SDS	Sodium Dodecyl Sulfonate
SOB	Super optimal broth medium
SOC	Super optimal broth + glucose
sp.	Species
SSC	Standard saline citrate
<i>Taq</i>	<i>Thermus aquaticus</i>
TBE	Tris/boric acid/EDTA buffer

TCA cycle	Tricarboxylic acid cycle
TE	Tris/EDTA buffer
TEMED	N,N,N',N'-Tetramethylethylenediamine
TES	N-tris(hydroxymethyl)methyl-2-aminoethanesulfonic acid
TPP	Thiamine pyrophosphate
Tris	2-Amino-2-(hydroxymethyl)-1,3-propanediol
Tween	Polyoxyethylene-(20)-sorbitan monolaurate
U	Unit
UV	Ultraviolet
vol	Volume
v/v	Volume/volume
WT	Wild-type
w/v	Weight/volume
X-gal	5-Bromo-4-chloro-3-indolyl- β -D-galactoside
μ E	Microeinstein
μ M	Micromole
$^{\circ}$ C	Celsius
2PG	2-phosphoglycerate
3PG	3-phosphoglycerate

1 Introduction

1.1 Cyanobacteria

Cyanobacteria (also known as blue-green bacteria, blue-green algae, cyanophyceae, or cyanophytes) constitute one of the largest groups of photosynthetic prokaryotes. They are gram-negative organisms. These bacteria consist of 150 genera and 2000 species (Schopf, 2002) with great structural diversity (Stanier, *et al.*, 1977). To date (19th Nov. 2013), the genome of 74 species are completely sequenced (http://www.ncbi.nlm.nih.gov/sutils/genom_table.cgi). The sequenced genome size is notably different, extending from 1.6 Mb to 9.0 Mb. The ancestors of cyanobacteria can be traced back to about 3.5 billion years ago by fossil records (Schopf, 1993; Schopf, 2006) and played a significant role in bringing in atmospheric oxygen to the Earth (Blankenship, *et al.*, 1998; Catling, *et al.*, 2005; Buick, 2008). Based on the endosymbiosis theory, cyanobacteria contributed to the precursors of chloroplasts of eukaryotes (Sagan, 1967; Douglas, 2004; Rodríguez-Ezpeleta, *et al.*, 2005), and they nowadays own a photosynthetic apparatus, which is prominently similar to the one enclosed in the eukaryotic chloroplast in both structural and functional respects. Some strains of cyanobacteria, like *Synechocystis* sp. PCC 6803 and *Synechococcus* sp. PCC 7002, are naturally transformable by exogenous DNA (Shestakov, *et al.*, 1970; Grigorieva, *et al.*, 1982; Koksharova, *et al.*, 2002).

Cyanobacteria can be found in many different environments, including aquatic (saltwater and freshwater), terrestrial, and extreme environments (like hypersaline waters, hot springs or even in the deserts) (Stal, *et al.*, 1997). They are also involved in symbiosis with plants, fungi or animals (Whitton, *et al.*, 2000). Cyanobacteria are a morphologically diverse group with unicellular, filamentous, and colonial forms, and they are divided into five subgroups by their morphological appearance: the Chroococcales, the Pleurocapsales, the Oscillatoriales, the Nostocales and the Stigonematales (Rippka, *et al.*, 1979).

Chlorophyll a is the only type of chlorophyll pigment in the cyanobacterial cell (Whitton, *et al.*, 2000), and these prokaryotes also harbor specific pigments such as phycocyanin and allophycocyanin which are organized with proteins to phycobilisomes on the thylakoid membrane functioning as a part of light-harvesting

complex (De Ruyter, *et al.*, 2008). These phycobiliproteins may account for about 50% of total proteins in some cyanobacteria (De Marsac, 1977). The pigment composition is affected by light intensity and light quality, like chlorophyll and phycocyanin are reduced by higher intensities of white light (Stanier, *et al.*, 1977). Likewise, nitrogen or carbon source starvation also causes a reversible destruction of phycobiliproteins in the light (Allen, *et al.*, 1969; Stanier, *et al.*, 1977; Gründel, *et al.*, 2012). Amino acids obtained by phycobiliprotein degradation can be used to supply cells with ATP by oxidative substrate-level phosphorylation (Hauf, *et al.*, 2013). Although the light energy absorbed by phycobiliproteins is majorly transferred to photosystem II (PS II), it can also be passed to photosystem I (PS I) (Jones, *et al.*, 1964; De Ruyter, *et al.*, 2008).

Cyanobacteria hold flexible energy metabolisms to adapt to various natural environments, which enable them to grow under autotrophic, fermentative and mixotrophic conditions (Yang, *et al.*, 2002; Eiler, 2006). The varying availability of light energy and exogenous substrates affect protein expression and cellular metabolism (Gill, *et al.*, 2002, Kurian, *et al.*, 2006).

Generally, heterotrophic growth of cyanobacteria takes place under two conditions: dim light or pulses of light (Anderson, *et al.*, 1991). Growth in the dark at the expense of sugars is usually much slower than phototrophic growth. When the growth conditions are changed from phototrophic to fermentative, CO₂ assimilation by the Calvin-Benson cycle is inactivated promptly by the inactivation of the key enzymes of the cycle, such as phosphoribulokinase (Pelroy, *et al.*, 1972).

For typical mixotrophic growth, glucose is utilized as exogenous carbon sources, like in *Synechocystis* sp. PCC 6803 (Yang, *et al.*, 2002). Some strains use alternative substrates, for example, the nitrogen-fixing strain *Cyanothece* 51142 prefers glycerol to glucose (Feng, *et al.*, 2010). The growth rate under mixotrophic conditions is higher than that under autotrophic conditions (Yoshikawa, *et al.*, 2013). When glucose was fed into autotrophically grown cultures of *Synechocystis*, respiration was activated and an increased amount of metabolic intermediates such as glucose-6-phosphate, 6-phospho-gluconate, ribulose-5-phosphate, ribose-5-phosphate, fructose-1,6-bisphosphate, glyceraldehyde-3-phosphate and dihydroxyacetone phosphate indicated an increased carbon flow through the OPP pathway and

glycolysis (EMP). However the amount of ribulose bisphosphate, 3-phosphoglycerate, phosphoenolpyruvate and pyruvate significantly decreased, indicating a reduced carbon flow through the Calvin-Benson cycle (Takahashi, *et al.*, 2008). The glucose also provoked a faster growth rate and a decreased photosynthetic activity (Verhees, *et al.*, 2003; Takahashi, *et al.*, 2008; Reher, *et al.*, 2010). Takahashi, *et al.* (2008) argued that the down regulation of the Calvin-Benson cycle might be caused by the repression of the enzyme activities of PRK (phosphoribulokinase) and GAPDH (glyceraldehydes-3-phosphate dehydrogenase). It was reported for the cyanobacterium *Synechococcus* 7942 that the down-regulation of the Calvin-Benson cycle was shown to be caused by the formation of GAPDH, PRK, and a small protein named CP12 associated with the decrease in the NADP(H)/NAD(H) ratio (Tamoi, *et al.*, 2005). Takahashi *et al.* (2008) detected that the NADP(H)/NAD(H) ratio in *Synechocystis* decreased from 2.3 to 1.4 upon the addition of glucose. However, some of the proteins are regulated post transcriptionally so that changes at the expression level of the transcripts are hardly detectable during the growth conditions shift (Kahlon, *et al.*, 2006; Herranen, *et al.*, 2004; Lee, *et al.*, 2007). Takahashi *et al.* (2008) demonstrated that the enhancement of glucose metabolism might be caused by the abundant supply of substrates under mixotrophic conditions and increased metabolic flux through the OPP pathway and TCA cycle.

An overflow of glucose in the growth environment of cyanobacteria can result in a Crabtree effect (De Deken, 1966; Fiechter, *et al.*, 1981; Marc, *et al.*, 2013). A limitation of respiratory capacity in Crabtree-positive cells shifts the glycolytic flux toward fermentative metabolism with ethanol, glycerol, acetate or lactate production bypassing the TCA cycle (Beck, *et al.*, 1968; Käppeli, *et al.*, 1986; Vemuri, *et al.*, 2006), this phenomenon was named “Crabtree effect”. The hypothesis to explain this effect is that NADH generated by glucose degradation pathways is far too much beyond the cellular capacity for its oxidation, and finally reduced products are produced fermentatively to maintain the redox balance. This process generates no NAD(P)H and less ATP than respiration and TCA cycle (Rieger, *et al.*, 1983; Postma, *et al.*, 1989; Gancedo, 1998; Vemuri, *et al.*, 2007). Vice versa, some intermediates are utilized as alternative carbon substrates when the cells are in the carbon-limiting state (Paczia, *et al.*, 2012). However it is important to note that, mixotrophic growth does not happen in all cyanobacteria (Rippka, 1972).

The nutritional properties of cyanobacteria have been investigated for many decades, and the distinctive and uniform pathways of carbon metabolism in light and dark have been demonstrated. Therefore analysis of the metabolism under different trophic conditions in cyanobacteria is important.

1.2 *Synechocystis* sp. PCC 6803

Synechocystis sp. PCC 6803 (hereafter *Synechocystis*) which belongs to the order of Chroococcales is a unicellular, non-nitrogen fixing organism. It was firstly recognized and listed in the Pasteur Culture Collection (PCC) in 1968 (Reed, *et al.*, 1985).

Synechocystis was the first genome-sequenced cyanobacterium (Kaneko, *et al.*, 1996) and the size is 3.9 Mb with a total of 3,725 genes (Cyanobase, <http://genome.microbedb.jp/cyanobase>). *Synechocystis* is able to survive in up to 1.2 M NaCl saline media (Reed, *et al.*, 1985). It can live photoautotrophically with oxygenic photosynthesis, it can also grow mixotrophically without any need of photosystem II in the presence of a carbon source (e.g. glucose) (Rippka, *et al.*, 1979; Williams, 1988), or even grows heterotrophically when given short light pulses in regular time intervals (every 24 h) (Anderson, *et al.*, 1991). Additionally, *Synechocystis* also operates the C₄ pathway to assimilate carbon through the PEP carboxylase and malic enzyme under mixotrophic conditions (Yang, *et al.*, 2002). *Synechocystis* is one of the most studied cyanobacteria in the laboratory, since its fast growth property, simple genome character and its ability to take up exogenous DNA as described (Grigorieva, *et al.*, 1982).

1.3 Photosynthesis and respiration metabolism

1.3.1 Photosynthesis

In *Synechocystis*, the electron transport of photosynthesis (green part in Fig. 1.1) and respiration (orange part Fig. 1.1) take place in the same membrane (thylakoid membrane) (Gantt, 1994; Vermaas, 2001) (Fig. 1.1). The plastoquinone, the cytochrome b₆f complex, cytochrome C₅₅₃ and plastocyanin (grey part in Fig. 1.1) fulfill a dual function as electron carriers (Schmetterer, 1994).

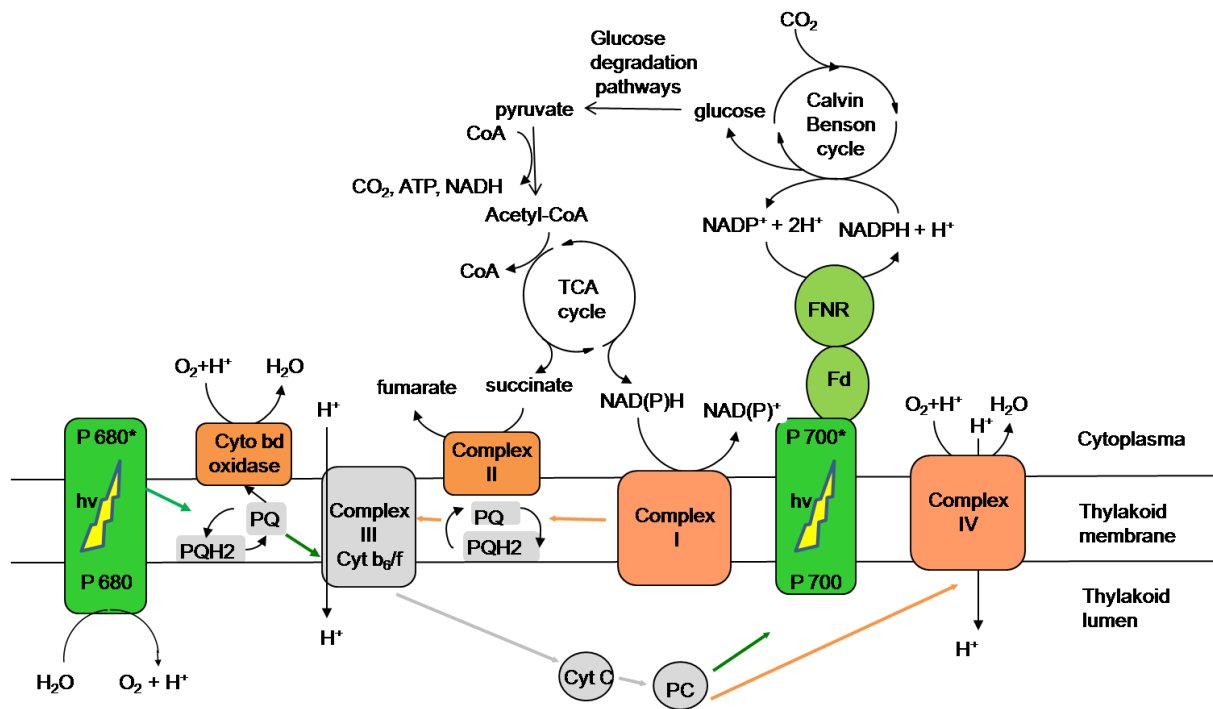


Fig.1.1. Electron transport chain of photosynthesis (green part) and respiration (orange part) in *Synechocystis* sp. PCC 6803. Calvin-Benson cycle, glucose degradation pathways and TCA (tricarboxylic acid) cycle are included. The grey parts are the shared electron carriers: plastoquinone (PQ), Complex III (cytochrome b₆f complex) and plastocyanin / cytochrome C553. Cytochrome bd oxidase is situated between PSII and cytochrome b₆f complex. Complex I: type-1 NADH dehydrogenase; Complex II: succinate dehydrogenase; Complex III: cytochrome b₆f complex; Complex IV: cytochrome c oxidase; FNR: Ferredoxin: NADP oxidoreductase; Fd: ferredoxin; PQ: plastoquinone; PC: plastocyanin; Cyt C: cytochrome c553.

The main elements of photosynthesis electron transport chain in cyanobacteria are identical to those in higher plants (Vermaas, 2001; Cournac, *et al.*, 2004). PSII (P680) and PSI (P700) both are excited by photon absorption and connected by the Complex III (cytochrome b₆f complex). The plastoquinone (PQ) which feeds the cytochrome b₆f complex is one of the main regulators for electron transfer between photosynthesis and respiration in *Synechocystis* (Fujita, *et al.*, 1987; Berry, *et al.*, 2002; Pfannschmidt, 2003; Volkmer, *et al.*, 2007). Ferredoxin: NADP oxidoreductase (FNR) catalyzed the final step providing NADPH for carbon fixation. FNR is attached to the phycobilisome (Thomas, *et al.*, 2006). NADP⁺ is the final acceptor of this photosynthetic electron transport. NADPH and ATP generated by photosynthesis are used in the Calvin-Benson cycle which is a major sink for NADPH and ATP in photosynthetic organisms to assimilate carbon. The excess carbon fixed is stored in the form of glycogen. Photosynthesis is down-regulated with the degradation of

phycobilisome in non-diazotrophic cyanobacteria under nitrogen starving conditions (Sauer, *et al.*, 2001).

1.3.2 Respiration

Respiration provides energy, which was stored in carbon compounds and carbon precursors for the biosynthesis of amino acids, lipids, porphyrins and so on (Stal, *et al.*, 1997). Respiration is mediated by the ratio of NAD(P)H / NAD(P)⁺, and the cellular concentration of ADP which controls the rates of electron transfer and ATP synthesis (Lee, *et al.*, 2007). The respiratory electron transport chain of *Synechocystis* sp. PCC 6803 is not only situated in the thylakoid membrane, but also in the cytoplasmic membranes (Peschek, 1987; Schmetterer, 1994). *Synechocystis* also harbors an active succinate dehydrogenase (SDH, Complex II, Fig. 1.1) (Cooley, *et al.*, 2000).

Respiratory activities observed in *Synechocystis* cells grown under mixotrophic and fermentative conditions were higher than those grown autotrophically (Singh, *et al.*, 2005; Osanai, *et al.*, 2005; Kahlon, *et al.*, 2006). Only little differences in the transcript levels of respiratory genes were observed in the stationary phase of mixotrophically grown compared to autotrophically grown cells (Tu, *et al.*, 2004). However, when Lee *et al.* (2007) investigated the early exponential phase of the growth of *Synechocystis* they found the respective transcript levels in cells grown under mixotrophic and fermentative conditions were significantly up-regulated compared to cells grown under autotrophic conditions.

In case of a surplus of energy, which would lead to oxidative stress in the cells, different protective mechanisms exist in cyanobacteria to dissipate an overflow of the electrons. Firstly, a large portion of light energy is converted into heat directly (Maxwell, *et al.*, 2000; Gilmore, 2004). Additionally the antennae sizes of light harvesting complexes are regulated by varying light conditions (Mc Connel, *et al.*, 2002). And the electrons can also be transferred directly from reduced ferredoxin to O₂ and recycled to H₂O by pseudocyclic electron transport (Hormann, *et al.*, 1993; Mehler, 1951; Asada, 2000). In addition, nitrate or sulfate can function as electron acceptors (Antal, *et al.*, 2005; Gutthann, *et al.*, 2007; Serebryakova, 2007). The regulation also happens on the transcriptional level, which might take hours or days (Hihara, *et al.*, 2001). It was also found that the bidirectional hydrogenases, which

catalyzes the reduction of protons (H^+) to hydrogen (H_2) or the reaction vice versa can play a role as a valve for low potential electrons generated during the light reaction of photosynthesis when dark adapted cells are brought to light (Appel, *et al.*, 2000).

Surplus electrons can also be transferred from plastoquinone to a cytochrome bd-type oxidase, which releases water (Fig. 1.1) (Berry, *et al.*, 2002). With this situation, the cytochrome b_6f complex, the complex IV and the respiratory chain are bypassed and no further electrons are pumped leading to a lower ATP yield by the ATP synthase.

1.3.3 Cytochrome bd-type oxidase

As both the plastoquinone (PQ) pool and the cytochrome b_6f (cyt b_6f) complex (Complex III) are shared by the photosynthetic and respiratory pathways, the PQ pool is the central switching point of both respiratory and photosynthetic electron transport in cyanobacteria (Fig. 1.1). PQ is the acceptor of electrons from PSII, Complex I and Complex II, and on the other hand, the source of electrons for PSI, cytochrome c oxidase (COX), and possibly alternative oxidases. It was shown that the PQ pool is important for balancing respiratory and photosynthetic electron transport and for the regulation of the different enzymes (Berry, *et al.*, 2002).

COX is a terminal oxidase found in both thylakoid and cytoplasmic membranes (Nicholls, *et al.*, 1992). Additionally, there are two alternative oxidases in *Synechocystis*: Ctall, which is located only in the cytoplasmic membrane but does not serve as a quinol oxidase in thylakoids (Pils, *et al.*, 2001; Berry, *et al.*, 2002; Huang, *et al.*, 2002); and a cytochrome bd-type oxidase (Cyt bd oxidase), which is located exclusively in the thylakoid membrane and does not only prevent an overreduction of the PQ pool under stress conditions, such as higher light intensity or a presence of excess glucose in the cell, but is also involved in other physiological functions (Pils, *et al.*, 1997; Howitt, *et al.*, 1998; Büchel, *et al.*, 1998; Berry, *et al.*, 2002). A cyt bd oxidase was identified in several bacteria and was shown to play a role as an electron sink when an external energy supply (glucose or increased light intensity) accelerates cell growth (Berry, *et al.*, 2002) similar to the function of alternative oxidase (AOX) in mitochondria (Moore, *et al.*, 1994; Jarmuszkiewicz, *et al.*, 1998; Affourtit, *et al.*, 2001).

In the presented work, the role of the Cyt bd oxidase under mixotrophic conditions in different mutants was investigated via fluorescence measurements under application of different inhibitors (Fig. 1.2).

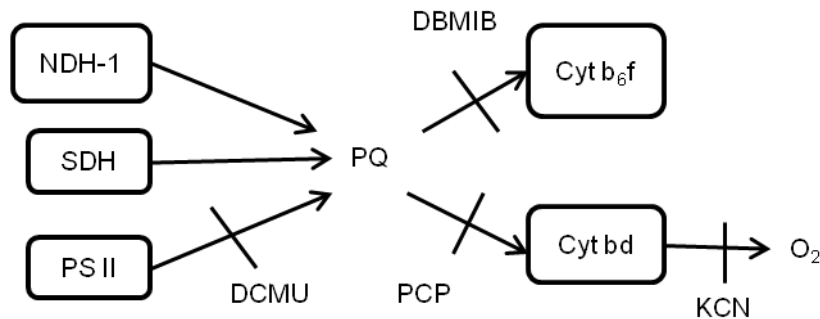


Fig. 1.2. Routes of electron transfer and sites of action for different inhibitors in the thylakoid membrane of *Synechocystis* sp. PCC 6803 according to Berry, *et al.* (2002). DBMIB: 2,5-dibromo-3-methyl-6-isopropyl-p-benzoquinone, is an inhibitor of Cyt b₆f; DCMU, 3-(3,4-dichlorophenyl)-1,1-dimethylurea, interrupts electron exchange between QA in PSII and PQ pool; PCP, pentachlorophenol, is an inhibitor of the Cytbd oxidase; KCN, is an inhibitor of all respiratory oxidases in *Synechocystis* 6803.

1.3.4 The TCA cycle in *Synechocystis* sp. PCC 6803

The glycogen and glucose degradation in *Synechocystis* can be coupled to an oxidation of pyruvate which flows in form of acetyl-CoA to the reactions of the tricarboxylic acid cycle (TCA cycle, also known as the citric acid cycle or Krebs cycle) producing carbon dioxide and reduced NADH. The electrons are finally fed into the respiratory electron chain coupled to oxidative phosphorylation (Fig. 1.1). The TCA cycle also provides essential precursor metabolites for biosynthesis of cellular components (Krebs, 1970).

However, the TCA cycle in cyanobacteria is special, since 2-oxoglutarate dehydrogenase, which converts 2-oxoglutarate to succinyl-CoA, is missing (Smith, *et al.*, 1967; Schwarz, *et al.*, 2011). Even though the organisms can assimilate acetate and activate it, acetate can serve only as a partial source of cell carbon, replacing endogenously synthesized acetyl-CoA in certain biosynthetic pathway (Smith, *et al.*, 1967). However, the full function of TCA cycle in *Synechocystis* was proven by the growth supported by citric acid (Cooley, *et al.*, 2001; Jansén, *et al.*, 2010). Alternative enzymes to 2-oxoglutarate dehydrogenase were identified in *Synechococcus* sp. PCC 7002, namely 2-oxoglutarate decarboxylase and succinic semialdehyde

dehydrogenase, which convert 2-oxoglutarate to succinate and thus functionally replace 2-oxoglutarate dehydrogenase and succinyl-CoA synthetase (Zhang, *et al.*, 2011). The genes encoding these two enzymes exist in all cyanobacterial genome except *Prochlorococcus* and marine *Synechococcus* species (Zhang, *et al.*, 2011).

1.4 Fermentation

For cyanobacteria, which are oxygenic phototrophic organism, fermentation can occur in anoxic environments such as anoxic hypolimnia, lake sediments, microbial mats or at night when cells become anoxic (Stal, *et al.*, 1997). Anoxic conditions are not the prerequisites for the induction of fermentation, but fermentation occurs at reduced oxygen concentrations (Heyer, *et al.*, 1989). The first reported cyanobacterium that was shown to be capable of fermentative energy generation was *Oscillatoria limnetica* in 1979 (Oren, *et al.*, 1979). The majority of cyanobacteria accumulate glycogen in the light and uses it as energy source in the dark. The switch from autotrophic to fermentative metabolism does not activate *de novo* enzyme synthesis, and the fermentation starts quickly (Moezelaar, *et al.*, 1994). With fermentation, cyanobacteria catabolize glycogen producing CO₂, NAD(P)H, ATP, hydrogen and carbon products such as formate, acetate, lactate and alcohols (Heyer, *et al.*, 1991; Carrieri, *et al.*, 2008; Carrieri, *et al.*, 2010; McNeely, *et al.*, 2010). However, no oxidative phosphorylation can be performed under fermentative conditions, since the oxygen, which is the terminal electron acceptor for the respiration chain is missing.

There are different types of fermentation in cyanobacteria including homolactic, heterolactic, homoacetic and mixed-acid pathways (Stal, *et al.*, 1997). In homolactic fermentation, one molecule of glucose is converted to two molecules of lactic acid. Heterolactic fermentation, in contrast, yields one molecule carbon dioxide and one molecule ethanol in addition to lactic acid. And for homoacetic fermentation, three molecules acetate are produced by one mol glucose. However, the acetate production is related to trehalose degradation instead of glycogen. Whereas in the mixed-acid fermentation pathway, the organism degrades glycogen into carbon dioxide, ethanol, acetate, lactate, formate and sometimes hydrogen. *Synechocystis* can produce acetate, lactate and hydrogen under fermentative conditions (Appel, *et*

al., 2000; Antal, *et al.*, 2005; Gutthann, *et al.*, 2007), the single steps of the pathway have not been clearly demonstrated yet.

The results of transcription profiling of *Synechococcus* sp. PCC 7002 showed that the transcript levels for genes encoding the two photosystems, electron transport proteins, phycobilisome components, and chlorophyll biosynthesis decreased under fermentative conditions compared to autotrophic conditions (Ludwig, *et al.*, 2011). ATP synthesis is produced by substrate-level phosphorylation for growth maintenance under fermentative conditions. Transcripts for the pyruvate dehydrogenase complex (*pdhA*, *pdhB*) were 10-fold lower, while *nifJ* (pyruvate: ferredoxin oxidoreductase) increased 110 to 130-fold (Xu, 2010; Ludwig, *et al.*, 2011). This suggests that glucose degradation pathway for conversion of phosphoenolpyruvate to acetyl-CoA via pyruvate dehydrogenase complex (PDH complex) is replaced by pyruvate: ferredoxin oxidoreductase (PFOR) under fermentative conditions.

Nitrate reduction can function as alternative electron sink under low oxygen concentration conditions (Gutthann, *et al.*, 2007; McNeely, *et al.*, 2010).

1.5 Glucose degradation pathways

During dark anoxic periods, cyanobacteria survive at the expense of glycogen, which was accumulated in the light and is broken down to glucose.

Glucose metabolism in prokaryotic and eukaryotic cells is followed by a variety of pathways dependent on the growth conditions. Different glucose degradation pathways exist. Glucose can be broken down to pyruvate coupled with the synthesis of ATP, NADPH or NADH alternatively via the Embden–Meyerhof–Parnas pathway (EMP), the Entner–Doudoroff pathway (ED) and the Oxidative Pentose Phosphate pathway (OPP). The amount of ATP produced by different glucose degradation pathways varies (Bar-Even, *et al.*, 2012). The net yield of NADPH, NADH and ATP for one molecule glucose for the different glucose degradation pathways and their key enzymes are listed in table 1.1.

The EMP pathway (often simply named “glycolysis”) is the ubiquitous route for glucose degradation in all domains of life (Romano, *et al.*, 1996; Kim, *et al.*, 2008;

Reher, *et al.*, 2010). Prokaryotes utilize various glycolytic alternatives beside the EMP pathway to perform glucose metabolism (Fraenkel, 1996; Kim, *et al.*, 2008).

Table 1.1. The net yields of NADPH, NADH and ATP for 1 molecule glucose degraded either via EMP, ED or OPP and the key enzymes of all three pathways.

pathway	key enzyme (No. in Fig. 1.3)	Yield for one molecule glucose		
		NADH	NADPH	ATP
EMP	phosphofructokinase (3)	2	0	2
ED	KDPG aldolase (iv)	1	1	1
OPP	G6PDH (b)	0	2	0

Variants of the ED pathways were found in archaea and also some bacteria, like *Pseudomonas putida*, *Zymomonas saccharophila* (Entner, *et al.*, 1952; Conway, 1992; Verhees, *et al.*, 2003; del Castillo, *et al.*, 2007; Flamholz, *et al.*, 2013). It was argued that the primary function of the ED pathway is the breakdown of sugar acids like gluconate rather than glucose (Sweeney, *et al.*, 1996; Peekhaus, *et al.*, 1998). Archaea hold two kinds of ED pathways modified from the classical ED pathway (Reher, *et al.*, 2010): a semiphosphorylative ED pathway which yields 1 ATP / mol glucose and a nonphosphorylative ED pathway which is not coupled to net ATP synthesis (Siebers, *et al.*, 2005) (Fig. 1.3). Fuhrer *et al.* (2005) analyzed the glucose metabolism of seven phylogenetically distinct bacteria and found that the ED pathway operated in all of them. Also they harbored genes encoding the enzymes of the EMP pathway.

Most prokaryotes and eukaryotes are capable of using the OPP pathway (Smith, 1982; Verhees, *et al.*, 2003). The OPP pathway is especially of importance for heterotrophic organisms that do not hold a Calvin-Benson-cycle as it supplies the cells with pentose phosphates that are precursors of the ribose and deoxyribose of nucleic acids, and with erythrose phosphate, which is a precursor for some aromatic amino acids. NADPH, which is produced in the OPP pathway supplies the cells with an important reductant for biosynthesis. Autotrophic organisms that hold the Calvin-Benson-cycle, however, are able to synthesize the respective intermediates via the mentioned cycle. The OPP pathway is the primary route for carbon catabolism in cyanobacteria during fermentation. Key enzymes of the OPP pathway, such as glucose-6-phosphate dehydrogenase (G6PDH, which is encoded by the *zwf* gene),

are activated in the dark (Smith, 1982; Stal, *et al.*, 1997; Yang, *et al.*, 2002; Summers, *et al.*, 1995; Kurian, *et al.*, 2006; Jansén, *et al.*, 2010; Kruger, *et al.*, 2003). Increased levels of proteins involved in EMP and OPP pathway were detected by proteomic analysis under fermentative conditions compared with autotrophic conditions in *Synechocystis* (Kurian, *et al.*, 2006). Even though both the OPP pathway and the EMP pathway are used during dark fermentative growth in *Synechocystis* (Yang, *et al.*, 2002), EMP pathway cannot compensate for the loss of the other (Jansén, *et al.*, 2010). Beside fermentative conditions, it was reported that the OPP pathway can operate in glycogen degradation under aerobic conditions (Smith, 1982). The investigation of the central metabolism of *Synechocystis* under different trophic conditions by transcriptomic and metabolomic analysis by Yoshikawa *et al.* (2013) showed that the activities of OPP pathway and EMP pathway were both elevated under mixotrophic conditions compared with autotrophic conditions. The OPP and the EMP pathway are connected to each other in the lower part of the pathways by GAP.

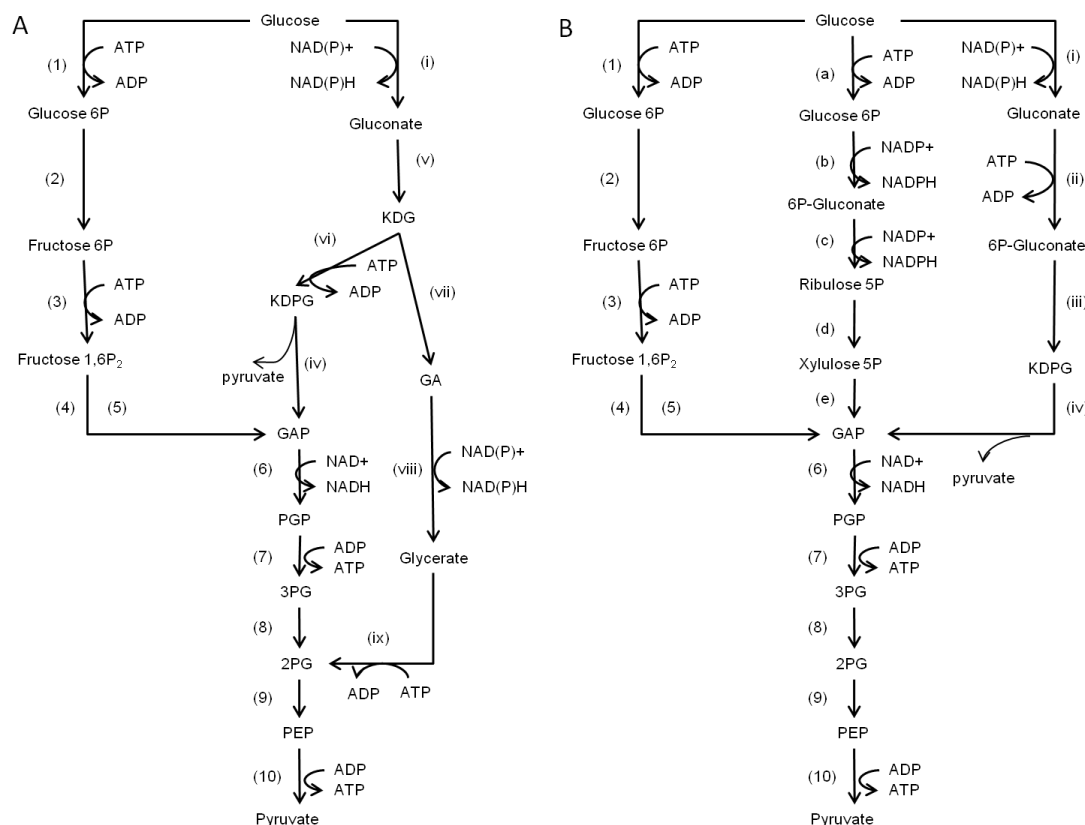


Fig. 1.3. (A) Glucose degradation in Archaea EMP (1-10) and ED pathways (semiphosphorylative part: i, v, vi, iv and 6-10; nonphosphorylative part: i, v, vii, viii, ix, 9, 10); (B) the glucose catabolism pathways in Bacteria and Eukaryote: EMP (1-10), OPP (a-e) and ED (i-iv and 6-10) according to the Verhees *et al.* (2003). Abbreviated metabolites are: P: phosphate; Fructose 1,6P₂: fructose 1,6-

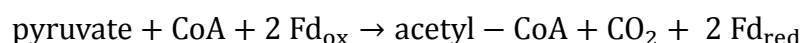
bisphosphate; KDPG: 2-keto-3-deoxy-6-phosphogluconate; GAP: glyceraldehyde 3-phosphate; PGP: 2,3-bisphosphoglycerate; 2PG: 2-phosphoglycerate; 3PG: 3-phosphoglycerate; PEP: phosphoenolpyruvate; KDG: 2-keto-3-deoxy-Gluconate; GA: glyceraldehydes. Key to enzymes: (1) (a) glucokinase; (2) phosphoglucose isomerase; (3) phosphofructokinase; (4) fructose 1,6-bisphosphate aldolase; (5) triosephosphate isomerase; (6) glyceraldehydes phosphate dehydrogenase; (7) phosphoglycerate kinase; (8) phosphoglycerate mutase; (9) enolase; (10) pyruvate kinase; (b) glucose-6-phosphate dehydrogenase; (c) 6-phosphogluconate dehydrogenase; (d) ribulose-5-phosphate 3-epimerase; (e) transketolase; (i) glucose dehydrogenase; (ii) gluconate kinase; (iii) 6-phosphogluconate dehydratase; (iv) KDPG aldolase (v) gluconate dehydratase; (vi) KDG kinase; (vii) KDG aldolase; (viii) glyceraldehydes dehydrogenase; (ix) glycerate kinase.

Flamholz *et al.* (2013) suggested that glycolytic strategy functions as a tradeoff between energy yield and protein cost, different pathways likely suit the demands of different environments or physiologies. For instance, anaerobes use the EMP pathway rather than ED pathway, while aerobes prefer ED pathway to EMP pathway, and on the other hand, facultative organisms tend to contain genes for both pathways (Fuhrer, *et al.*, 2005; Flamholz, *et al.*, 2013). The general schemes of EMP and ED pathways are quite similar: glucose is phosphorylated and then cleaved into two three-carbon units: glyceraldehydes 3-phosphate (GAP) and dihydroxyacetone phosphate for EMP pathway, while GAP and pyruvate for ED pathway. GAP is then degraded to pyruvate generating ATP by the same pathway known as “lower glycolysis” (Verhees, *et al.*, 2003). The ED pathway requires several-fold less enzymatic protein than the EMP pathway to metabolize the same amount of glucose per second (Flamholz, *et al.*, 2013). It is known from microbes that the expression of unnecessary proteins can limit their growth (Scott, *et al.*, 2010; Schuetz, *et al.*, 2012). It was found that the EMP pathway cannot compensate for the function of the ED pathway in an EMP-activated mutant of *Pseudomonas putida* which exclusively relies on the ED pathway (Chavarría, *et al.* 2013). It was suggested that this might be due to the fact that *Pseudomonas putida* has a high demand of NADPH to counteract oxidative stress. Whereas NADPH is produced by the ED pathway no NADPH is produced by the EMP pathway (Table 1.1).

1.6 PFOR / PDH Complex

1.6.1 Pyruvate: ferredoxin / flavodoxin oxidoreductase (PFOR)

The oxygen-sensitive enzyme pyruvate: ferredoxin / flavodoxin oxidoreductase (PFOR) which is encoded by *nifJ* gene (sll0741) participates in the reversible catalysis of pyruvate to acetyl – CoA with concomitant reduction of ferredoxin (abbrev: Fd) or flavodoxin (Bothe, *et al.*, 1974; Thauer, *et al.*, 1977; Neuer, *et al.*, 1982):



PFOR is found in a high number of archaea (Kletzin, *et al.*, 1996), facultatively (O₂-exclusion) (Schmitz, *et al.*, 2001) and obligate anaerobic bacteria (Thauer, *et al.*, 1977; Shah, *et al.*, 1983; Dixon, 1984). The enzyme was also shown to be central to the energy metabolism in amitochondriate eukaryotes, including those with hydrogenosomes (Müller, 1988; Horner, *et al.*, 1996). The enzyme has also been described for aerobes which might be less O₂-sensitive, like *Mycobacterium tuberculosis* and *Streptomyces coelicolor* (Plaga, *et al.*, 1992; Schmitz, *et al.*, 2001). Expression of *nifJ* under oxic conditions has been observed in *Synechocystis* (Schmitz, *et al.*, 2001). However, PFOR activity in *pdhA*-deletion cells of *Synechococcus* sp. PCC 7002 grown under oxic conditions is insufficient to compensate adequate acetyl-CoA for autotrophic growth (Xu, 2010). It was found that about 40% of all fully sequenced cyanobacterial genomes contain the gene *nifJ* (Nakao, *et al.*, 2010).

Ferredoxin and flavodoxin serve as electron acceptors for PFOR and donate electrons directly to the nitrogenase in N₂-fixing species (Knight, *et al.*, 1966; Leach, *et al.*, 1971; Bothe, *et al.*, 1974; Ragsdale, 2003). The reverse reaction of pyruvate production is also dependent on reduced ferredoxin (Neuer, *et al.*, 1982). Pyruvate synthesis by pyruvate dehydrogenase (PDH) complex with NADH as electron donor was not observed in most cyanobacteria, except *Synechococcus* 6301 (Schmitz, *et al.*, 2001).

Referred to the fermentative metabolism of *Synechococcus* 7002 (McNeely, *et al.*, 2010), pyruvate which is obtained from glucose by glucose degradation pathways in *Synechocystis* might not only be transferred into Acetyl-CoA and then be converted

into acetate by acetate kinase or ethanol by alcohol dehydrogenase, but can also be used to produce lactate, alanine and succinate by lactate dehydrogenase, alanine dehydrogenase, and the enzymes found in the TCA cycle (Stal, *et al.*, 1997; McNeely, *et al.*, 2010) (Fig. 1.4).

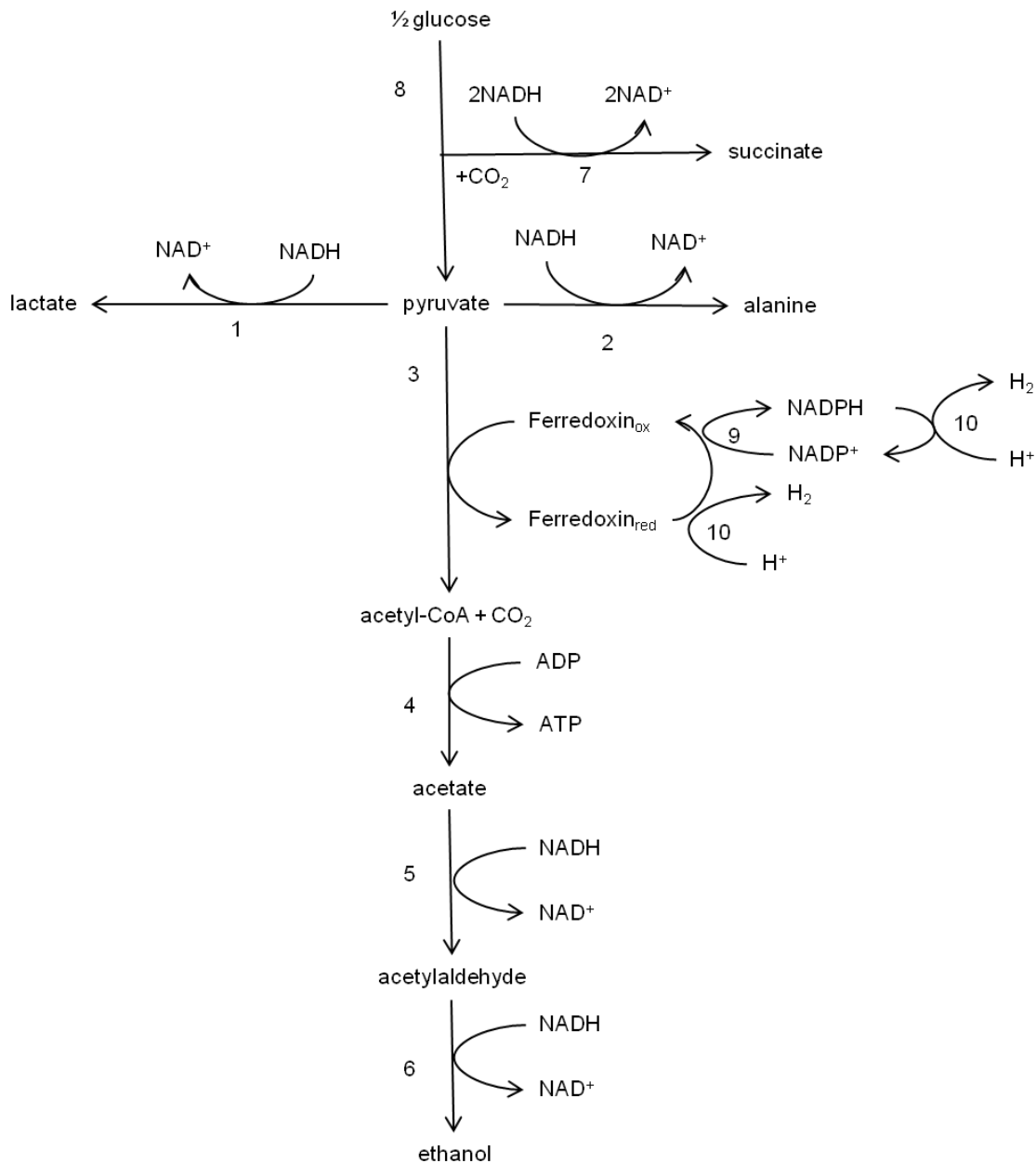


Fig. 1.4. Hypothetic fermentative metabolism of pyruvate derived from glucose degradation pathways in *Synechocystis* sp. PCC 6803 based on the sequenced genome. 1, lactate dehydrogenase; 2, alanine dehydrogenase; 3, PFOR; 4, phosphotransacetylase and acetate kinase; 5, aldehyde dehydrogenase; 6, alcohol dehydrogenase; 7, enzymes of the TCA cycle from malate dehydrogenase to succinate dehydrogenase; 8, enzymes of glycolytic pathways; 9, FNR (Ferredoxin: NADP^+ reductase); 10, hydrogenase.

1.6.2 Pyruvate dehydrogenase (PDH) complex

Pyruvate dehydrogenase (PDH) complex which consists of the pyruvate dehydrogenase enzyme (encoded by *pdhA*), dihydrolipoyl transacetylase, and dihydrolipoyl dehydrogenase (de Kok, *et al.*, 1998) catalyzes pyruvate decarboxylation and yields one molecule NADH under oxic conditions, while PFOR generates two molecules of reduced ferredoxin, which has a much lower redox potential than the NADH/NAD⁺ couple (Tittmann, 2009).

PDH complex in gram negative bacteria is inhibited by higher NADH:NAD⁺ ratio (de Kok, *et al.*, 1998). Pdh A (PDH complex) has 3 phosphorylation sites in mammals. At high NADH concentrations, Pdh A is phosphorylated in mammals and thereby inactivated (Patel, *et al.*, 2006). In *Synechocystis*, the redox poise might be elevated when growth conditions are shifted from autotrophic to mixotrophic, according to the redox state of cells supplemented with exogenous glucose during fermentation (Kujat, *et al.*, 2000).

It has been shown that the PDH complex also contributes to fermentative metabolism in *Enterococcus (Streptococcus) faecalis*, which contains both PDC and PFOR (Deibel, *et al.*, 1964). McNeely *et al.* (2011) detected that acetate is produced during fermentation, even the amount excreted was 2-fold lower in a *nifJ*-deletion mutant compared with wild type cells of the cyanobacterium *Synechococcus* sp. PCC 7002, which indicates that the PDH complex also functions under anoxic conditions, at least in the absence of PFOR.

Inhibition of acetate-CoA ligase and pyruvate dehydrogenase complex by glycerol eliminated acetate production, with a resulting loss of reductant and a 3-fold decrease in H₂ production by *nifJ* cells compared to WT cells (McNeely, *et al.*, 2011). Glycerol is a specific inhibitor of PDC, but not of PFOR.

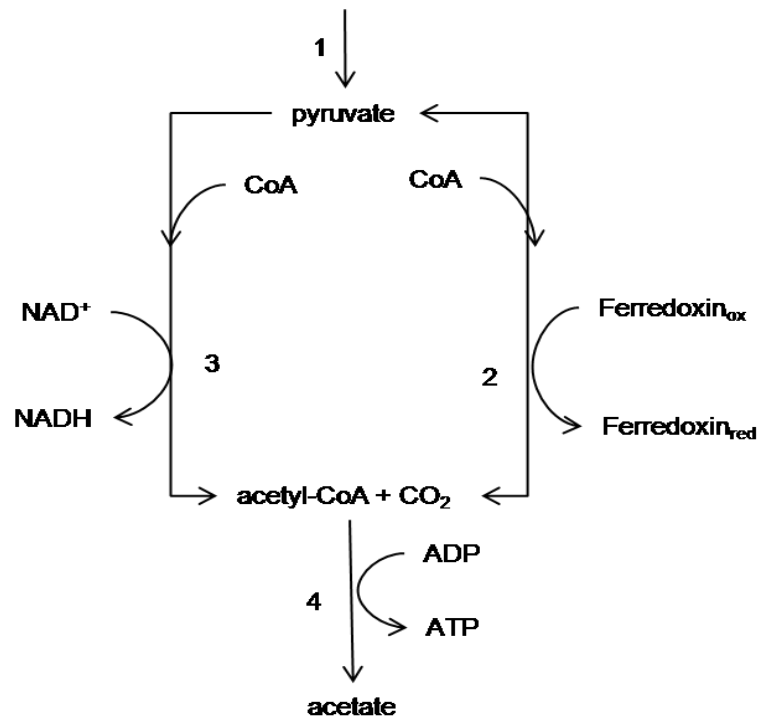


Fig. 1.5. Scheme of the reactions potentially catalyzed by PFOR and PDH complex during pyruvate metabolism in *Synechococcus* which could be supposed for *Synechocystis* sp. PCC 6803 as well. (Modified scheme from McNeely, *et al.*, 2011). 1, enzymes of glycolysis; 2, PFOR; 3, PDH complex; 4, phosphotransacetylase and acetate kinase.

The scheme of pyruvate catabolism in *Synechocystis* sp. PCC 6803 is summarized in figure 1.5. In this study, the significance of the PFOR has been characterized at the phenotypic, physiological and proteome level in *Synechocystis*. Comparisons of the WT and $\Delta nifJ$ mutant were conducted at different aspects, such as growth, photosynthetic and respiratory activities, and expression level of enzymes.

1.7 Hydrogenase

Hydrogenase catalyzes the reversible reaction of H₂ production: $2\text{H}^+ + 2\text{e}^- \rightleftharpoons \text{H}_2$.

The hydrogenases were grouped into three distinct classes according to the metal content of their catalytic subunits: the [NiFe]-hydrogenases, the [FeFe]-hydrogenases and the [Fe]-hydrogenases (Vignais, *et al.*, 2001; Shima, *et al.*, 2007). [Fe]-hydrogenases catalyze an intermediary step in CO₂ reduction with H₂ to methane. They do not catalyze the hydrogen production (Thauer, *et al.*, 1996; Thauer, 1998), and the enzyme is restricted to some methanogens (Vignais, *et al.*, 2007). Most [NiFe]-hydrogenase are found in bacteria and archaea, [FeFe]-hydrogenase are found in bacteria, anaerobic eukarya, and some algae like the green algae

Chlamydomonas reinhardtii (Vignais, *et al.*, 2001; Horner, *et al.*, 2002; Meyer, 2007; Shima, *et al.*, 2007; Vignais, *et al.*, 2007; Barz, *et al.*, 2009). [NiFe]-hydrogenase are separated into 4 different groups (Vignais, *et al.*, 2007). Most of the hydrogenases are only active under anaerobic conditions, while some [NiFe]-hydrogenase are also activated with atmospheric oxygen levels in aerobic H₂-oxidizing bacteria (Burgdorf, *et al.*, 2005). Recently, a novel group 5 NiFe-hydrogenase was determined in *Streptomyces* soil isolates (Constant, *et al.*, 2011), which is also active under ambient oxygen concentrations.

Most cyanobacteria contain two of the [NiFe]-hydrogenases: the bidirectional hydrogenase and the uptake hydrogenase. Only the bidirectional [NiFe]-hydrogenase is present in *Synechocystis* sp. PCC 6803 (Vignais, *et al.*, 2007). All completely sequenced cyanobacteria which harbor the bidirectional hydrogenase genes also harbor the gene of a pyruvate: flavodoxin / ferredoxin oxidoreductase (PFOR), *nifJ*, suggesting that the bidirectional hydrogenase is connected with PFOR during fermentation (Barz, *et al.*, 2010). The bidirectional [NiFe]-hydrogenase is sensitive to O₂. H₂ production occurs in the dark and can proceed in the light for several minutes (Cournac, *et al.*, 2004, Gutthann, *et al.*, 2007). At 1 % oxygen between 25 and 50 % of the hydrogenase remain active (McIntosh, *et al.*, 2011).

A transient outburst of H₂ was observed after re-illumination of dark-adapted cells. It was shown that this hydrogenase works as an electron valve of low-potential electrons generated at the onset of illumination (Appel, *et al.*, 2000). Hydrogen in cyanobacterial cells is produced when a surplus of reductants are present in the cells (Appel, *et al.*, 2000; Cournac, *et al.*, 2002). The hydrogenase functions as an electron valve in photosynthetic electron flow at the onset of light in dark-adapted cells (Appel, *et al.*, 2000) and additionally as a regulatory apparatus under fermentative conditions (van der Oost, *et al.*, 1989). The data also showed in *Synechococcus* sp. strain PCC 7002 that the bidirectional hydrogenase serves as a valve to reoxidize an excess of NADH formed during glycolysis (McNeely, *et al.*, 2011). Since [NiFe]-hydrogenases are more stable in the presence of oxygen they are more ideal models for hydrogenase engineering even if the H₂ production rate of [NiFe]-hydrogenase is slower than that of [FeFe]-hydrogenases (Fontecilla-Camps, *et al.*, 2007).

Beside the activity of hydrogenases, there are many other factors that influence the efficiency of hydrogen production. Until now different ways have been found to enhance the hydrogen production of cyanobacteria. Nitrogen limitation can induce hydrogen production due to the lack of alternative electron acceptors in non-nitrogen fixing strains (Beneman, *et al.*, 1974; Sveshnikov,*et al.*, 1997; Schütz,*et al.*, 2004) while by causing higher nitrogen fixation rate in nitrogen fixing strains (Serebryakova, *et al.*, 1998; Ananyev, *et al.*, 2008). Sulfur deprivation increases the hydrogen production by affecting the function of PSII to create anaerobiosis and enabling sustained hydrogen production in green algae (Melis, *et al.*, 1999). The same treatment does not result in higher H₂-production in cyanobacteria (Antal, *et al.*, 2005). Interestingly, fixed cells can produce more hydrogen than liquid cultures (Fukui, *et al.*, 1982; Tsygankov, 2004; Serebryakova, *et al.*, 2007). On the molecular level, a mutant with NDH-1 (or complex I) deletion in *Synechocystis* sp. PCC 6803 (Cournac, *et al.*, 2004, Gutthann, *et al.*, 2007), mutants lacking uptake hydrogenase in *Nostoc punctiforme* ATCC 29133 (Lindberg, *et al.*, 2002) and *Anabaena* PCC 7120 (Lindblad, *et al.*, 2002) generated higher amounts of hydrogen.

2 Aims of the present study

One of the overall aims of the working group in which this thesis was prepared is to understand the hydrogen metabolism of the fully sequenced, unicellular cyanobacterium *Synechocystis* sp. PCC 6803. The present study will investigate two different metabolic aspects that are linked to the hydrogen production of this organism with the aim to get a deeper understanding for the processes that influence the hydrogen metabolism.

- (1) Previous to this thesis it was shown in the working group that the hydrogen production in a *nifJ* deletion mutant of *Synechocystis* sp. PCC 6803 was severely reduced (Kaspar, 2010). The gene *nifJ* encodes for the pyruvate: ferredoxin / flavodoxin oxidoreductase (PFOR), which catalyzes the cleavage of pyruvate to CO₂ and acetyl-CoA while reducing ferredoxin / flavodoxin. This mutant should be further characterized in this thesis.

- (2) Investigations within this thesis revealed that both NifJ and the hydrogenase are of importance under mixotrophic conditions. The electrons that are used for the production of hydrogen under mixotrophic conditions come from the breakdown of glucose. The aim of this part of the work is to characterize the operating glucose degradation pathways in *Synechocystis* under mixotrophic conditions.

3 Materials and Methods

3.1 Chemicals, buffers and media

All chemicals used in this work were obtained from Becton, Boehringer, Biocell, Biogenes, Biomol, Bio-Rad, BioVision, Biozym, Braun, Calbiochem, Difco, Eppendorf, Fermentas, Fluka, GE, Invitrogen, Merck, Millipore, Norton, Qiagen, Promega, Roche, Roth, Sartorius, Serva, Sigma-Aldrich, Tetenal, Thermo. The water was taken from a distillation machine (Seralpur pro 90CN, O. Kohl Chemie – Pharma - Laborbedarf, Germany) and was additionally filtered and autoclaved for 20 min for molecular experiments. For primer dilution and RNA-related experiments nuclease free, sterile filtered, autoclaved water and low organic purity water (ROTH, Karlsruhe, Germany) was used.

Buffers and media used in this work are listed in table 3.1 and table 3.2.

Table 3.1: Buffer used in this work.

Name	Reagents
TBE	890 mM Tris (pH 8.3), 890 mM H ₃ BO ₃ , 25 mM Na ₂ EDTA
TE	10 mM Tris, 1 mM Na ₂ EDTA (pH 8.0)
5 x DNA loading buffer	50 % (v/v) glycerol, 50 % (v/v) 10 x buffer TBE, 0,2 mg/ml bromophenol blue
TES	0.5M TES, PH 8.0

The respective media were supplemented with 15 g/L Bacto Agar for agar plate production. All media were autoclaved for 20 min before use.

For the growth under mixotrophic conditions, 10 mM Glucose was added into the medium. For BG-11₀ medium, 5 mM arginine or 10 mM urea was used instead of NaNO₃ as a nitrogen source.

For cultures grown in low light, LAHG (Light Activated Heterotrophic Growth) agar plates served as growth medium. The agar for LAHG plate was prepared in the fume cupboard. 125 g agar was mixed with 3 L ddH₂O by magnetic stirring and was filtered

with nylon gauze twice. The filtered agar was washed twice with 2.5 L 95% (v/v) technical methanol for 15 min, and then washed twice with 2.5 L technical acetone for 15 min. Washed agar was dried overnight in the fume cupboard and was then ready to use.

Table 3.2: Media used in this work.

Name	Reagents
BG-11 medium	17.6 mM NaNO ₃ , 0.304 mM MgSO ₄ x 6 H ₂ O, 31.2 µM citric acid, 2.79 µM Na ₂ EDTA, 46.3 µM H ₃ BO ₃ , 4.15 µM MnCl ₂ x 4 H ₂ O, 1.61 µM NaMoO ₄ x 2 H ₂ O, 188.7 µM NaCO ₃ , 175.1 µM K ₂ HPO ₄ , 0.77 µM ZnSO ₄ x 7 H ₂ O, 10 mM TES (pH 8.0), 22.8 µM FeNH ₄ -citrate, 0.32 µM CuSO ₄ x 5 H ₂ O, 5 µM NiCl ₂
BG-11 ₀ medium	BG-11 medium without NaNO ₃
LB medium	1 % (w/v) NaCl, 1 % (w/v) peptone, 0,5 % (w/v) yeast extract
SOB medium	0.5 % (w/v) yeast extract, 2 % (w/v) tryptone, 10 mM NaCl, 2.5 mM KCl, 10 mM MgCl ₂ , 10 mM MgSO ₄
SOC medium	SOB medium with 20 mM glucose

3.2 Oligonucleotides

These Polymerase Chain Reaction (PCR) primers (Table 3.3) were all made by Sigma-Aldrich (Steinheim, Germany).

Table 3.3: Primers used in this work.

Name	Sequence 5'-3'
M13-F	AGGGTTTTCCAGTCACGACGTT
M13-R	GAGCGGATAACAATTTACACACAGG
Em F	GTCGACGAAAAAAGAAATTAGATAAA
Em R	GTCGACTTACTTATTAATAATTTATAGC
Cm F	TCAATAATATCGAATTCCTGCAG
Cm R	AGCGAGGTGCCGCCATCAAGCTT
Gm1	GTCGACGGATGAAGGCACGAACC
Gm2	GTCGACGAATTGTTAGGTGGCG
Km f	CCACGTTGTGTCTCAAAATCTCTGAT
Km r	ATCGCCCCATCATCCAGCCAGAAAG
Sp f	TCGCGCAGGCTGGGTGCCAA
Sp r	GCCCTCGCTAGATTTTAATGCGGAT

Ka-rt-I F	GAAACCATTGCTCACCTGCG
Ka-rt-I R	CAACGGCCTGGAGCAAATC
Ka-rt-s F	TGGCAAATGCCCAAGCTTTC
Ka-rt-s R	CTGTCCAGATAGGCCAACGG
Zwf S F	AATTTTCCACCGGCATTGGC
Zwf S R	ACCCTGGGCAAACCTCATTCC
Zwf L F	TCGTGAGCAGATGCGTAAGG
Zwf L R	ACCCTGGGCAAACCTCATTCC
pfkB1S F	ATCGTCAGTTGGGGCTTGAC
pfkB1 S R	AACTACCGTCTCCGCCAATG
pfkB1 L F	TCCCTACCGCATCCAAAGTG
pfkB1 L R	TTCCGACACCATAACCAGGC
pfkB2 S F	GATTGTCCTGGCCTCAATGC
pfkB2 S R	TGAGGCCTTAACCACTGCTC
pfkB2 L F	TGTGCCCTTTACGGATCTGG
pfkB2 L R	AGCGGCGGTAAAAGTCAGG
GDH S F	ATTACCCCGATCCCAAACCC
GDH S R	CCCGCCAAAAGCGATGTAG
GDH L F	GGGAGGCATAAGGGTTGGTC
GDH L R	CCGGTCTGGGAATTACCGTAG
16s-50r	TCATCATGCCCTTACGC
16s-50f	TCCCGACCATTGTAGTACGTG
16s-91r	AAGTCATCATGCCCTTACG
16s-91f	ATGGGATTCGCTTACTCTCG
nifJ-50r	GTCCCTATGAATATTGTGGCCA
nifJ-50f	TCAGCACAATCACCCGTTCC
nifJ-93r	GGCATACTCCACACAGATG
nifJ-93f	ATGCCAAAGACCATGATGG
pdhA-50r	CCCTCAGTGCGGGAGTTC
pdhA-50f	CCTTACCAAACAGTTCCGCCATT
pdhA-85r	CAGAGAAACCGCCTTAGTGC
pdhA-85f	GCCCCGGTAATACATCTCAG
rnpB-50r	GCTGACTAACTGGTAACTGAC
rnpB-50f	CGCACCTTTGCACCCTTAC
rnpB-80r	GGGTTTACCGAGCCAGTACC
rnpB-80f	TGACCACTGAAAAGGGTAAGG
KA-1	GGTGGAGCGGTAATCTGGAA
KA-in1	GGTTCGTGCCTTCATCCGTCGACAGGTCGATGGAATCAGTGCG
KA-in2	CGCCACCTAACAATTCGGTTCGACATGGGTAAAAGCAGGGGAGC
KA-2	TGCCCTGCCATAGATTTGGT

nifJ-1	TGGGCTATCTCTTTCCCCGG
nifJ-in1	ATCTAATTTCTTTTTTCGTGCGACAAGGGGTGATGGGATAAATGG
nifJ-2	ATTTTTGGTATTCATCTGAGTG
nifJ-in2	AATTATTTAATAAGTAAGTCGACGGTCTATTCGGAAAATCGCTTT
PGD-1	GCCAGAGCCAGAGCCATTTA
Ph-in1	AGAGATTTATCTAATTTCTTTTTTCGTGACCTTCCATTCTGACCCGGCTT
PGD-in2	GCTATAAATTATTTAATAAGTAAGTCGACAAGATCCAAAAGGCCCTCGG
PGD-2	CCTCGCAAACCTTCCCTCCA
Rbc-1	GCATCCCCTGCGTGATAAGA
Rbc-in1	ATCAGAGATTTTGAGACACAACGTGGGCCTTAAACCCTGCTTTGGC
Rbc-in2	CTTTCTGGCTGGATGATGGGGCGATCCCAACTGCTACATTCGGGT
Rbc-2	GTCCAAAGAACAGGGCCGTA
Pdha-1	TCTTATAGGGGCCACGGGAA
Pdha-in1	TTGGCACCCAGCCTGCGCGATCTATGCGAAGTCGGTCAGC
Pdha-in2	ATCCGCATTAATACTAGCGAGGGCACGTTCACCGTTTGGGAGAA
Pdha-2	GACACCCAACCGCTAATGGA
Pdhb-1	AAACATGGCACGGGCAAATC
Pdhb-in1	GGTTCGTGCCTTCATCCGTGACCCGCATCTCTCCTTGTTGGT
Pdhb-in2	CTCCACCTAACAATTCGGTCGACGACTGACCATTGTGCAACCG
Pdhb-2	CGTTTACGGCAAGGGTACT
Gdh-1	GTAACACCCACACCGTTTGC
Gdh-in1	GGTTCGTGCCTTCATCCGTGACCCCGCCAAAAGCGATGTAG
Gdh-in2	CGCCACCTAACAATTCGGTCGACTCTGAGTGGCACCACCATTC
Gdh-2	TGAGTATCTCCCGCAGACTA
pfkB1-1	CTGCCATGCCGCAAAAAGTACGAA
pfkB1-in1	ATCAGAGATTTTGAGACACAACGTGGCTCCACTGGTTAAAATACCAATGCG
PfkB1-in2	CTTTCTGGCTGGATGATGGGGCGATGGGCATTTGCCTTGGAACGATTAA
pfkB1-2	ATCTTTGTTGGAACGATCAAACATG
pfkB2-1	CTGCTTTTGAGCGGGTTCAATATGT
pfkB2-in1	TTGGCACCCAGCCTGCGCGACACCACCACTGGTCAAAAATTCCAAT
PfkB2-in2	ATCCGCATTAATACTAGCGAGGGCCCAAGTCATTGGGCATATACCTAGG
pfkB2-2	CACCATCTGGATTCAAACAGCCCCT
Zwf-1	AAGACCTGCCAATAAAGATAAATTG
Zwf-in1	TCAATAATATCGAATTCCTGCAGGGAGTCCAGTGCGGAAGGGATTTTC
Zwf-in2	AGCGAGGTGCCGCCATCAAGCTTAGGCAGAATGGTTAATTAATAAAGA
Zwf-2	GCCTCGAATACGGATGCTATTTTGT
Ldh-1	AAATGCAGGAAGAATCAGAAAATTT
Ldh-in1	ATCAGAGATTTTGAGACACAACGTGGGACGATCATAGGCTTTACTGCTAAA
Ldh-in2	CTTTCTGGCTGGATGATGGGGCGATCAAATATTGCTGAATTGAGCAGAA
Ldh2	AACAAAAGGCAGAAGTCGCCGGTTA

tag	AGACCGTGTGCGAGC
pdhA-tag1	AGACCGTGTGCGACACGGGAATCCCTTCCCCAT
pdhA-tag2	AGACCGTGTGCGACACGGGAAT
PfkB1-tag1	AGACCGTGTGCGAACACTTTGGATGCGGTAGGGA
pfkB1-tag2	AGACCGTGTGCGAACACTTTG
pfkB2-tag1	AGACCGTGTGCGATGCTCTGGATGTCCCTTACT
pfkB2-tag2	AGACCGTGTGCGATGCTCTG
nifJ-tag1	AGACCGTGTGCGAGCCAGCAAAGGGCCGATAGA
nifJ-tag2	AGACCGTGTGCGAGCCAGCAA
Rnpb-tag1	AGACCGTGTGCGACACCAATCATGGGGCAGGAA
Rnpb-tag2	AGACCGTGTGCGACACCAATCA
Zwf-tag1	AGACCGTGTGCGAAGAAGGGCACCCCCTGCCAA
Zwf-tag2	AGACCGTGTGCGAAGAAGGGCA
HoxH-tag1	AGACCGTGTGCGATGGCCAAATTGCCGTAACCGA
HoxH-tag2	AGACCGTGTGCGATGGCCA
HoxE-tag1	AGACCGTGTGCGAAGTCGCCACTCCAAACACCCG
HoxE-tag2	AGACCGTGTGCGAAGTCGCC
pdhA f	CCCTCAGTGCGGGAGTTC
pdhA r	CCTTACCAAACAGTTCCGCCATTA
Rnpb f	GCTGACTAACTGGTAACTGAC
Rnpb r	CGCACCTTTGCACCCTTAC

3.3 Plasmids and Bacteria

Table 3.4: *E.coli* plasmids and strains.

plasmid/ <i>E.coli</i>	description	reference
Top10 (<i>E. coli</i>)	F- <i>mcrA</i> Δ (<i>mrr-hsdRMS-mcrBC</i>) ϕ 80/ <i>lacZ</i> Δ M15 Δ <i>lacX74</i> <i>recA1</i> <i>araD139</i> Δ (<i>ara-leu</i>) 7697 <i>galU</i> <i>galK</i> <i>rpsL</i> (Str ^R) <i>endA1</i> <i>nupG</i>	Invitrogen
pCR2.1 TOPO	<i>lacZ</i> α pUC _{ori} Amp ^R Km ^R M13 binding site, cloning- and sequencing vector	Invitrogen

3.4 Restriction Enzymes

Table 3.5: Restriction enzymes (MBI Fermentas, St. Leon-Rot, Germany) used in this work.

enzyme	sequence (5' to 3')	buffer
EcoR I	GAATTC	unique buffer or tango buffer
Hind III	AAGCTT	red buffer or tango buffer

3.5 Cultivation of bacteria

3.5.1 Cultivation of *Synechocystis* sp. PCC 6803

Cultures of *Synechocystis* 6803 wild type strain were grown photoautotrophically in BG-11 medium (Table 3.2). Mutant strain of *Synechocystis* 6803 was supplemented with the respective antibiotics (Table 3.6). Organisms were cultured on BG-11 agar plates (Table 3.2) at 28 °C and 50 $\mu\text{E}/\text{m}^2/\text{second}$ light intensity. For light sensitive organisms, the light intensity for cultivation was 5 $\mu\text{E}/\text{m}^2/\text{second}$ light intensity. Then cultures were transferred into 100 ml conical glass flasks with 50 ml BG-11 medium on a shaker at 100 rpm (Kreisschuetzler 3020, GFL-Gesellschaft für Labortechnik, Burgwedel, Germany) at 28 °C and 50 $\mu\text{E}/\text{m}^2/\text{second}$ light intensity. These 50 ml liquid cultures were used to inoculate Kniese tubes (EYDAM, Kiel, Germany) with fresh BG-11 medium in a volume of 250 ml. They were kept in a Kniese light bench (Kniese, Uni-Marburg, Germany) at 28 °C and 50 $\mu\text{E}/\text{m}^2/\text{second}$ light intensity and were continuously bubbled with air for physiological experiments of autotrophic growth. For mixotrophic conditions cultures were supplemented with 10 mM glucose. When cultures were grown in BG-11₀ medium (Table 3.2), other nitrogen sources as nitrate were used as 5 mM arginine or 10 mM urea.

All figures showing growth curves are based on cultures that were grown at the same time in triplicate in three Kniese tubes. The OD₇₅₀ of each Kniese tube was measured in triplicate. The mean and the standard deviation of these nine measuring values are shown in the figures. All growth curves were repeated in at least five independent experiments. A typical growth curve from those five curves is shown in this work.

3.5.2 Preparation of freezing cultures

All wild type and mutant strains of *Synechocystis* sp. PCC 6803 were stored in -80 °C for long term storage. 500 μl of culture which were pre-grown in 50 ml BG-11 medium in conical glass flasks for two weeks, were mixed with 250 μl 80% (v/v) glycerol in sterile 1.5 ml reaction cups, and frozen at -80°C.

3.5.3 Cultivation of *Escherichia coli*

Transformation of *Escherichia coli* (*E. coli*) Top10 cells was performed as described by the manufacturer (Invitrogen, Karlsruhe, Germany) except that only 1/4 of the

reaction was used. Transformed *E. coli* Top10 cells (Invitrogen, Karlsruhe, Germany) were grown for 1 hour in SOC medium on a shaker at 37 °C and 180 rpm (4400 Innova Incubator Shaker, New Brunswick Scientific, Nürtingen, Germany).

Table 3.6. Mutant strains listed with their antibiotic resistance cassette and the concentration of the respective antibiotic when cultivated. The deleted genes and proteins can be seen from figure 1.3, figure 1.4 and figure 1.5.

Mutant strain	Deleted gene	Deleted protein	Resistance cassette	concentration ($\mu\text{g ml}^{-1}$)	Reference
$\Delta nifJ$	<i>nifJ</i>	PFOR	Erythromycin	25	Gutekunst, <i>et al.</i> , 2014
$\Delta hoxH$	<i>hoxH</i>	[NiFe]-bidirectional Hydrogenase	Kanamycin	50	Appel, <i>et al.</i> , 2000
$\Delta pfkB_1B_2$	<i>pfkB1</i> <i>pfkB2</i>	phosphofructokinase	Kanamycin Spectinomycin	50 20	Together with Rebekka Kirsch, unpublished.
$\Delta nifJpfkB_1B_2$	<i>nifJ</i> <i>pfkB1</i> <i>pfkB2</i>	PFOR phosphofructokinase	Erythromycin Kanamycin Spectinomycin	25 50 20	this work
Δzwf	<i>zwf</i>	glucose-6-phosphate dehydrogenase	Chloramphenicol	20	Together with Rebekka Kirsch, unpublished.
$\Delta zwfnifJ$	<i>zwf</i> <i>nifJ</i>	glucose-6-phosphate dehydrogenase PFOR	Chloramphenicol Erythromycin	20 25	this work
$\Delta zwf pfkB_1B_2$	<i>zwf</i> <i>pfkB1</i> <i>pfkB2</i>	glucose-6-phosphate dehydrogenase phosphofructokinase	Chloramphenicol Kanamycin Spectinomycin	20 50 20	this work
$\Delta pdhA$	<i>pdhA</i>	PDH complex	Spectinomycin	20	this work
Δgdh	<i>gdh</i>	Glucose dehydrogenase (SII 1709)	Gentamycin	5	this work
$\Delta gdhzwf$	<i>gdh</i> <i>zwf</i>	Glucose dehydrogenase (SII 1709) glucose-6-phosphate dehydrogenase	Gentamycin Chloramphenicol	5 20	this work

$\Delta gdhpfkB_1B_2$	<i>gdh</i> <i>phkB1</i> <i>pfkB2</i>	Glucose	Gentamycin	5	this work
		dehydrogenase (SII 1709)	Kanamycin	50	
		phosphofructokinase	Spectinomycin	20	
$\Delta gdhzwfpfkB_1B_2$	<i>gdh</i> <i>zwf</i> <i>pfkB1</i> <i>pfkB2</i>	Glucose	Gentamycin	5	this work
		dehydrogenase (SII 1709)	Chloramphenicol	20	
		glucose-6-phosphate dehydrogenase	Kanamycin	50	
		phosphofructokinase	Spectinomycin	20	
Δka	<i>eda</i>	KDPG aldolase	Gentamycin	5	this work
$\Delta kazwf$	<i>eda</i> <i>zwf</i>	KDPG aldolase	Gentamycin	5	this work
		glucose-6-phosphate dehydrogenase	Chloramphenicol	20	
$\Delta kapfkB_1B_2$	<i>eda</i> <i>pfkB1</i> <i>pfkB2</i>	KDPG aldolase	Gentamycin	5	this work
		phosphofructokinase	Kanamycin	50	
			Spectinomycin	20	
$\Delta kazwfpf kB_1B_2$	<i>eda</i> <i>zwf</i> <i>pfkB1</i> <i>pfkB2</i>	KDPG aldolase	Gentamycin	5	this work
		glucose-6-phosphate dehydrogenase	Chloramphenicol	20	
			Kanamycin	50	
		phosphofructokinase	Spectinomycin	20	
Δph	<i>gnd</i>	6-phosphogluconate dehydrogenase	Erythromycin	25	this work
$\Delta phzwf pf kB_1B_2$	<i>gnd</i> <i>zwf</i> <i>pfkB1</i> <i>pfkB2</i>	6-phosphogluconate dehydrogenase	Erythromycin	25	this work
			Chloramphenicol	20	
		glucose-6-phosphate dehydrogenase	Kanamycin	50	
		phosphofructokinase	Spectinomycin	20	
$\Delta rubisCO$	<i>rbc</i>	RuBisCo	Kanamycin	50	this work
$\Delta pepC$	<i>ppc</i>	Phosphoenolpyruvate carboxylase	Chloramphenicol	20	this work

Transformed cells of *E. coli* were plated on LB agar plates supplemented with 50 µg/ml kanamycin. They were incubated at 37 °C over night in an incubator (T5050E, Heraeus, Hanau, Germany). For short-term storage, the plates were sealed with parafilm (ROTH, Karlsruhe, Germany) and kept in a refrigerator at 4 °C. For long-term storage, freezing cultures were prepared as described for *Synechocystis* and stored at -80 °C.

3.6 Physiological Methods

3.6.1 Optical density

The optical density (OD) of liquid cultures was measured by photometrical analysis (UV 2501 PC Photometer, Shimadzu, Kyoto). A wavelength of 750 nm was chosen to measure the cell density of *Synechocystis*. The BG-11 medium which was used to inoculate the cultures was utilized as blank reference. Samples that showed an OD₇₅₀ value above 0.5 were diluted with BG-11 medium before they were measured.

3.6.2 Absorption spectrum of chlorophyll a and phycocyanin

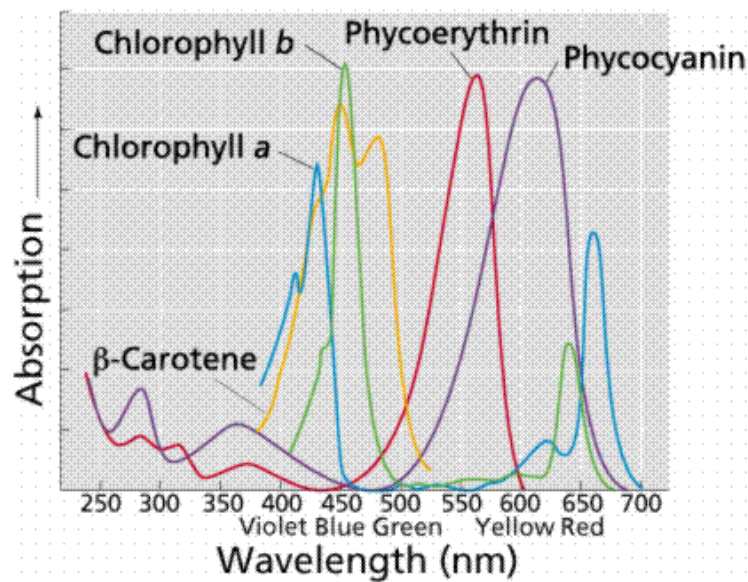


Fig. 3.1. The absorption spectrum of Chlorophyll a and b, β -carotene, phycoerythrin and phycocyanin. (<http://www.cas.miamioh.edu>)

The spectrums of chlorophyll a and phycocyanin were determined by photometrical analysis (UV 2501 PC Photometer, Shimadzu, Kyoto). The absorption spectrum (Fig. 3.1) of chlorophyll a has two peaks between 640 nm - 660 nm and between 430 nm – 450 nm. Phycocyanin absorbs light at a wavelength around 600 nm. The absorption spectrum was measured in a range from 400 nm to 800 nm. BG-11 medium was used as blank reference. In order to make sure that all samples have the same amount of cells, the lowest OD₇₅₀ value of all samples was used as standard, and all other cultures were diluted to this standard OD₇₅₀ value. Samples that had higher

OD₇₅₀ values than 0.5 were diluted. All spectrum curves were saved in jpeg and png format.

3.6.3 Chlorophyll content

For chlorophyll content measurement, 1 ml cell suspension, whose OD₇₅₀ was no more than 0.5, was centrifuged at 16,000 x g for 10 min at room temperature (Eppendorf Centrifuge 5415D, Eppendorf, Germany). 1 ml methanol was used to resuspend the pellet and the suspension was vortexed for 10 min to extract chlorophyll. Dissolved cells were centrifuged down for 10 min at 16,000 x g (Eppendorf Centrifuge 5415D, Eppendorf, Germany). Measurements of the supernatants' extinctions were carried out at 666.5 nm, 666 nm, 665.5 nm and 665 nm (UV-2501 PC, Shimadzu, Kyoto, Japan) with methanol as a blank reference. An additional measurement at 750 nm was taken to test for possible contamination by other particles.

Chlorophyll content was calculated according to the following formula after (Lichtenthaler, 1987):

$$\text{chlorophyll content } (\mu\text{g /ml}) = \frac{(\text{maximum of OD}_{666.5 \text{ to } 665}) - \text{OD}_{750}}{0.0809 \cdot \text{dilution}}$$

0.0809 = molar extinction coefficient chlorophyll

OD = optical density

3.6.4 Respiration and photosynthesis rate measurement

All oxygen production and oxygen uptake measurements were performed with a platinum electrode with a silver counter electrode (DW1 Liquid Clark Electrode, Hansatech Instruments, Norfolk, UK) with a polarizing potential of + 750 mV. The anode (silver) and cathode (platinum) of the electrode were connected by saturated KCl to conduct the electron flow. The platinum electrode was in contact with the reaction chamber with a Teflon membrane (Membrane Kit Standard, YSI Incorporated, Yellow Springs, OH), and the chamber was surrounded by water jacket with a constant temperature of 28 °C. A control box (workshop of biological department at the Philips-University, Marburg, Germany) was connected to the

electrode to amplify the signal. The signal relate to the concentration of hydrogen in the cell suspension. The signal was recorded by a chart recorder (SE-120, ABB Metrawatt, Nürnberg, Germany). The experimental set up is shown in figure 3.2 and figure 3.3.

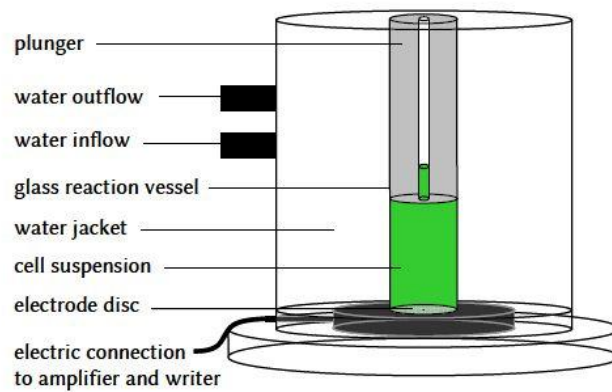


Fig. 3.2. Setup of the Clark electrode for hydrogen measurements (Kaspar, 2010).

To measure the sensitivity of the electrode, 1 ml air saturated ddH₂O (0.245 μmol oxygen per ml oxygen at 28 °C) was added to the reaction chamber and the signal was recorded. A small amount of sodium dithionite (DT), which is a reductive substrate, was used to reduce all the oxygen. The difference between the two signals corresponds to 0.245 μmol O₂.

The cultures were sampled as described in section 3.6.3. 1ml of culture with an OD₇₅₀ of 1 was added in the reaction chamber and incubated in the dark for about 3 min until the curve was stable to measure the respiration rate. Then the cultures were exposed to 277 $\mu\text{E}/\text{m}^2/\text{sec}$ light for 3 min to measure the photosynthetic rate of the cultures. After that 20 μl methyl viologen (100 mM) was added to the cultures and incubated for 3 min to measure the light-driven O₂ consumption rate by methyl viologen (Krasikov, *et al.*, 2012).

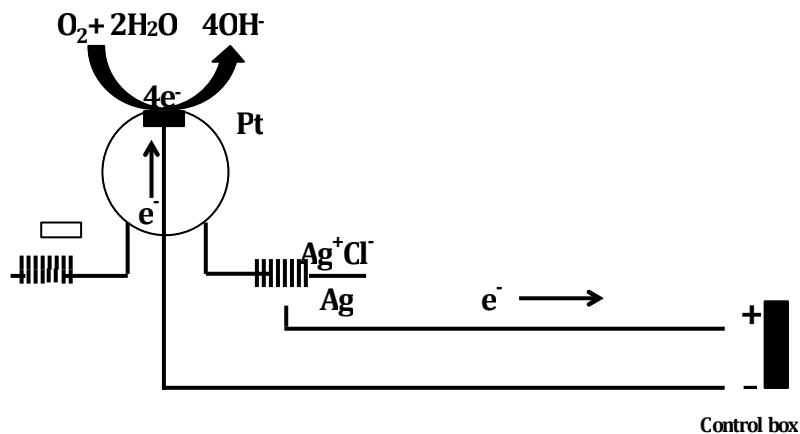


Fig. 3.3. Electron flow of oxygen electrode (Lindel, 2012).

The oxygen production or consumption rate (Fig. 3.4) was calculated by the following formula:

$$O_2 \text{ production or consumption rate } (\mu\text{mol min}^{-1}\text{OD}^{-1}) = \frac{\text{gradient} \cdot \text{recorder speed (cm min}^{-1}) \cdot 0.245 (\mu\text{mol})}{\text{calibration (cm)} \cdot \text{recorder amplification} \cdot \text{OD750}}$$

Gradient: $\Delta y/\Delta x$

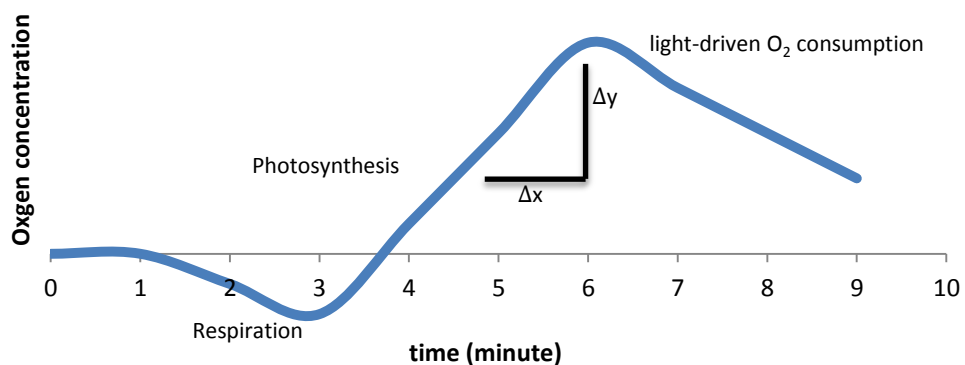


Fig. 3.4. Sample curve of O_2 production and consumption of wild type of *Synechocystis* (Lindel, 2012).

3.6.5 PAM (Pulse Amplitude Modulated) fluorescence measurement

PAM measurements were performed to determine the activity of electron transfer complexes in *Synechocystis* sp. PCC 6803. Absorbed light energy is distributed into three different ways by light-harvesting-complexes in the cells: water splitting and electron transfer to NADP⁺, fluorescence and heat. The fluorescence intensity was measured with a Multicolor PAM (Multicolor PAM, Heinz Walz GmbH, Germany) (Schreiber, *et al.*, 2012). Cultures with a concentration of 2.2 µg/ml chlorophyll were measured. The curves were drawn with the software Pam Win-3 v.3.12g.

Three supplementary chemicals were used: DBMIB (2, 5-Dibromo-6-methyl-3-isopropyl-1, 4-benzochinon) and DCMU (3-(3, 4-dichlorophenyl)-1, 1-dimethylurea). DBMIB could occupy the Q (o) site of the cytochrome (cyt) b₆f complex simultaneously and inhibit the flow of electrons between photosystems (PS) II and I (Roberts, *et al.*, 2001). Sodium acetate is used to keep DBMIB reduced, since DBMIB itself can serve as a quencher of chlorophyll fluorescence (Aoki, *et al.*, 1983; Vernotte, *et al.*, 1990). DCMU is a very specific and sensitive inhibitor of photosynthesis so that it is widespread used as herbicide. It blocks the plastoquinone binding site of photosystem II, disallowing the electron flow from photosystem II to plastoquinone, but leaves photosystem I functional (Metz, *et al.*, 1986). Under these conditions, ATP synthesis by cyclic photophosphorylation is maintained, but the generation of the photo-reductant (NADPH) necessary for CO₂ assimilation is completely arrested.

Blue light (wavelength of 440 nm) was used as measuring light for the fluorescence. The setup of slow kinetics method of Multicolor PAM used in this work is listed below (Table 3.7). The calculation method followed the one described by Schreiber, *et al.* (1986).

Table 3.7. The set up of Slow Kinetics of Multicolor PAM.

	Light intensity	Gain	Damping	Actinic light
value	1	2	2	6

2 ml cultures were incubated with 8 μ l 2.5 M sodium ascorbate (antioxidant, used to keep DBMIB reduced) for about 2 min prior to each measurement. At the very beginning of the measurement, the measuring light was turned on for 5 seconds and then actinic light with higher intensity was added. A few seconds later, 2 μ l DBMIB (final concentration 20 μ M) was added. Then every 20 seconds, a strong flash illuminated the cultures for 250 ms. Flashed for 4 times, 2 μ l DCMU (final concentration 10 μ M) was added to measure maximal fluorescence.

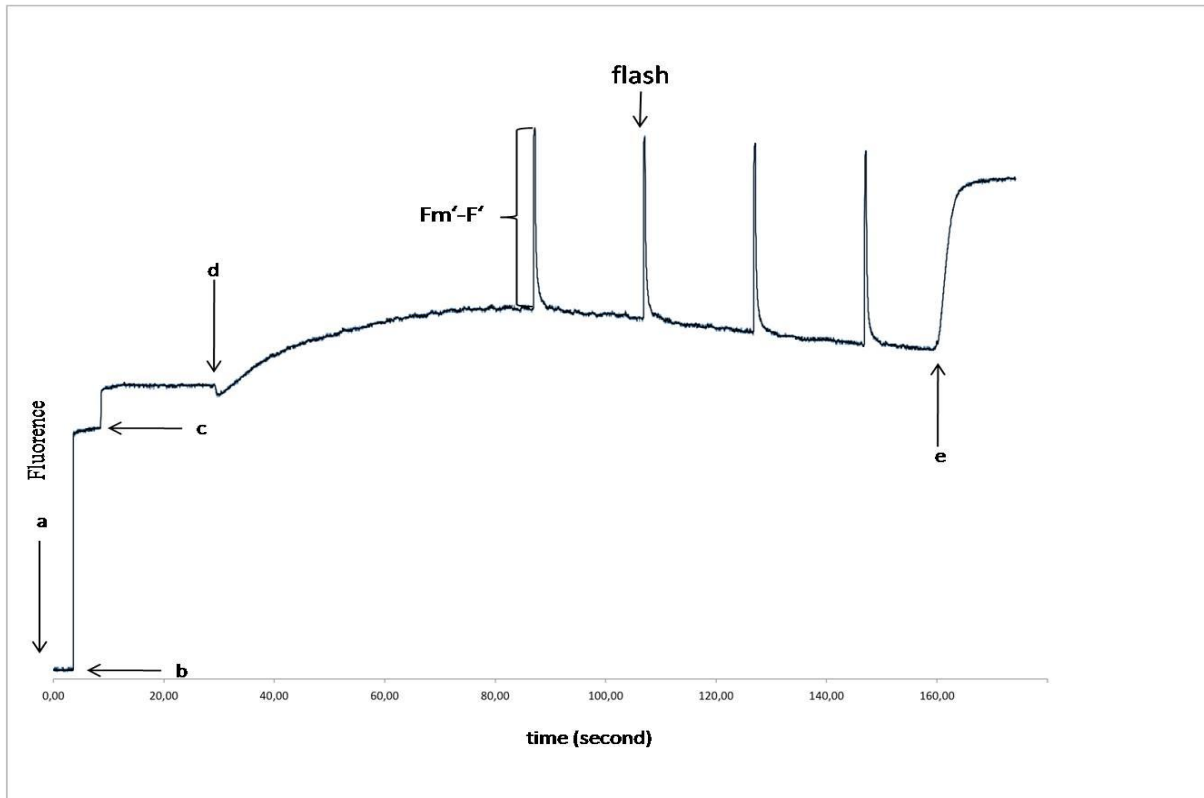


Fig. 3.5. Typical curve of a sample measured with slow kinetics at the PAM (Lindel, 2012). a: addition of 8 μ l ascorbate; b: start measuring light; c: start actinic light; d: addition of 2 μ l DBMIB; e: addition of 2 μ l DCMU.

The activity of the cytochrome bd - oxidase was calculated by the following formular:

$$\text{activity of the cytochrome bd - oxidase} = \frac{F_m' - F'}{F_m'}$$

3.6.6 Nuclear Magnetic Resonance (NMR)

NMR measurements were performed to investigate excreted metabolites in the growth medium of *Synechocystis* sp. PCC 6803. The measurements were carried out by the group of Professor Sönnichsen, Institute for Organic Chemistry, University of Kiel.

For NMR analysis cultures were grown in Kniese tubes and sampled every day. 2 ml culture were centrifuged at 16,000 x g, 4 °C for 30 min and the supernatant was transferred into new 2 ml reaction cups. The samples were stored at – 20 °C or sent to the group of Prof. Sönnichsen directly. Three repeats of each sample were made.

3.6.7 NAD⁺/NADH determination

All the cultures used for NAD⁺/NADH determination experiment were grown autotrophically and mixotrophically in 250 ml BG-11 medium. 5 ml to 10 ml cells, equivalent to approximately 10⁹ cells/ml (10 ml cultures of OD₇₅₀ of 1) were sampled for the measurements. The cells were centrifuged at 3,500 x g -9 °C for 10 min and the pellets were washed with 1 ml 20 mM cold PBS (Phosphate buffered solution, Table 3.8). The suspension was transferred to a 2 ml reaction cup and was centrifuged at 12000 x g for 1 min at -9 °C. The pellet was resuspended in 50 µl extraction buffer (Biovision, California, USA), and precooled glass beads (∅=0.18 mm) were added nearly (0.5-1 mm) to the surface of the liquid. The mixture was vortexed 4 times 1 min in the cold room (4 °C) and chilled on the ice for 1 min intermediately. 150 µl extraction buffer was added again and the mixture was centrifuged at 3,500 xg for 10 min at -9 °C. The liquid phase was transferred as much as possible into a new reaction cup and centrifuged at maximum speed for 30 min at -9 °C. The supernatant was transferred into precooled 10 kD spin columns (BioVision, California, USA). The sample was centrifuged at 10,000 x g for 10 min at -9 °C. The flow through liquid was divided into two 30 µl portions. One was incubated with 30 µl NADH extraction buffer (BioVision, California, USA) at 60 °C for 30 min and chilled on ice immediately and then was quickly spinned to remove any precipitate to determine the amount of NADH present in the cells. To the other one 30 µl NADH extraction buffer (BioVision, California, USA) was added on ice. 2 times 25 µl heated and 2 times 25 µl non-heated samples were placed in four wells of a 96 well microtiterplate, and 2.5 µl of all these samples were also placed with 22.5 µl NADH extraction buffer as concentration

control. 50 μ l NAD Cycling Mix (BioVision, California, USA) was well mixed and pipetted into each well and incubated for 5 min at room temperature. Then 10 μ l NADH developer (BioVision, California, USA) was added into each well and incubated for 1 to 4 hours before measuring absorbance at 450 nm by TECAN GENios machine (TECAN Group Ltd., Austria). The reactions can be stopped by adding stop solution (BioVision, California, USA), the color should be stable for 48 hours with the stop solution and sealed at 4 °C with foil. The values were collected by the software Magellam.

With the aid of the standard curve the different concentrations of total NAD^+ +NADH and NADH alone can be calculated. The standard curve was prepared by pipetting 0, 1, 2, 3, 4, and 5 μ l of NADH Standard (Biovision, California, USA) in wells and adjusting the volume to 25 μ l by adding NADH extraction buffer.

All the chemicals (BioVision, California, USA) mentioned in this section were from BioVison's NAD^+ /NADH Quantification Colorimetric Kit.

Table 3.8. PBS buffer (pH 7.4).

Reagent	Volume
20 mM K_2HPO_4	81% (v/v)
20 mM KH_2PO_4	19% (v/v)
NaCl	8.77 g/L

3.7 Molecular biological Methods

3.7.1 Isolation of genomic DNA from *Synechocystis* sp. PCC 6803

In order to isolate the genomic DNA of *Synechocystis* sp. PCC 6803, cells of the wild type strain or mutants were pelleted or directly scratched from one half of an agar plate and transferred into a 2 ml sterile reaction cup. The cells were resuspended in 200 μ l TE buffer (pH 7.4). Phenol chloroform isoamylalcohol (25:24:1 (v/v/v)) and an equal amount of sterile glass beads ($\phi = 0.17$ -0.18 mm), which equaled the fourfold volume of the cell pellets, and 2 μ l 10 % (w/v) SDS were added. The cell walls were disrupted by vortexing this mixture 10 x 1 min, cooled on ice in-between, and then

centrifuged at 16,000 x g for 10 min (Centrifuge 5804R, Eppendorf, Hamburg, Germany).

The aqueous supernatant containing the nucleic acids was transferred into a new 1.5 ml cup and diluted with phenol chloroform isoamylalcohol (25:24:1 (v/v/v)) whose volume was the same as the supernatant. After another centrifugation step for 2 min at 16,000 x g (Centrifuge 5804R, Eppendorf, Hamburg, Germany), three phases in the tube were formed. The upper one was transferred into a new reaction cap. This step was repeated until the interphase disappeared or was barely visible. Then the cap was filled with chloroform isoamylalcohol (24:1 (v/v)) whose volume was the same as the upper liquid phase and centrifuged for 2 min at 16,000 x g (Centrifuge 5804R, Eppendorf, Hamburg, Germany). This step extracted the phenol out of the upper phase and was repeated several times until the pink color in the upper phase mostly disappeared. The supernatant was then collected in a new reaction cap.

DNA precipitation was done by addition of the supernatant's 0.1 fold volume of 3 M sodium acetate (pH 4.8) and a 2.5 fold volume of 100 % ethanol. After at least 2 h of incubation at -20 °C, DNA was centrifuged down for 15 min at 16,000 x g and -9 °C (Centrifuge 5804R, Eppendorf, Hamburg, Germany).

The pellets were washed with 70 % (v/v) ethanol and centrifuged again for 5 min at 16,000 x g (Centrifuge 5804R, Eppendorf, Hamburg, Germany). The supernatant was discarded and the pellet was dried at 37 °C in an incubator (Memert, Schwabach, Germany). The dry pellet was dissolved in 20 - 50 µl TE buffer (pH 7.4) and stored at 4 °C.

DNA concentration was determined by two methods in parallel. A Nanodrop (NanoDrop ND-1000 Spectrophotometer, Thermo Scientific, USA) was used to measure the concentration of nucleic acids in 1 µl sample from the genomic DNA extraction. The other measuring way was to separate the DNA sample on 0.8% (w/v) agarose gels. By this way, DNA concentration was estimated by comparing the bright of the band to a λ DNA marker with defined DNA concentration.

3.7.2 Polymerase Chain Reaction (PCR)

The polymerase chain reaction (Saiki, *et al.*, 1988) is a biochemical technology to amplify nucleic acid fragments *in vitro* across several steps that are initiated by changes in temperature, generating thousands to millions of copies of these particular DNA sequences.

A detailed description of the steps used in this assay is listed in table 3.9.

Table 3.9. Steps of PCR protocol.

Steps	Cycles	Time (min)	Temperature (°C)
Initialization	1	1	95
Denaturation	30-40	0.5	95
Annealing		1	X
elongation		Y	72
elongation	1	10	72
incubation	1	∞	4

The primers were designed by Primer-BLAST (<http://www.ncbi.nlm.nih.gov/tools/primer-blast/>) and produced by Sigma-Aldrich (Steinheim, Germany). The annealing temperature was calculated depending on the specificity and affinity between DNA template and primers. The elongation time was dependent on the length of the expected PCR product. The Taq polymerase (MBI Fermentas, St. Leon-Rot, Germany) needs at least one minute to synthesize a 1 kb product.

Each PCR reaction contained in a total volume of 50 µl the following components (Table 3.10) in 200 µl caps and was programmed by the thermocycler (DNA- Engine PTC-200, Bio-Rad, USA):

Table 3.10. PCR components and their quantities.

Reagent	Volume (μ l)	Final concentration
10 x buffer (+ 500 mM KCl)	5	
MgCl ₂ (25 mM)	3	1.5 mM
Taq-Polymerase (5 U/ μ l)	0.25	0.025 U / μ l
dNTPs (2.5 mM)	4	200 μ M
Primer forward (5 μ M)	5	0.5 μ M
Primer reverse (5 μ M)	5	0.5 μ M
DNA (2-20 ng/ μ l)	5	0.2-2 ng/ μ l
H ₂ O	22.75	
total	50	

3.7.3 DNA gel electrophoresis

DNA fragments were separated on an agarose gel according to their lengths (Sambrook, *et al.*, 1989) for analytical and preparative aims. In this method, the shorter the fragments are, the faster they run. Gels were prepared by using 0.8 % (w/v) agarose and 1 μ g/ml ethidium bromide dissolved in TBE buffer (Table 3.1). The buffer was also used as an electro conductive medium in the gel chamber (Biozym, Hess. Oldendorf, Germany). RulerTM 1 kb marker (MBI Fermentas, St. Leon-Rot, Germany) was used to calibrate the size and 1 ng/ μ l Lambda DNA/HindIII marker (MBI Fermentas, St. Leon-Rot, Germany) was utilized to determine the DNA concentration of the sample. The DNA samples were supplemented with 0.2 volumes (v/v) of 5 x sample loading buffer (table 3.1). Electrophoresis was performed with power supply at 5 V/cm (High Voltage Power Pack P30, Biometra, Göttingen, Germany) for 50 min.

After the electrophoresis, gels were irradiated with a UV light (TF 20 M Vilber Lourmat, Torcy, France) to detect DNA, pictured with a PC connected live camera (Alpha Imager 2200, Cell Biosciences, Santa Clara, CA) and documented with the program Alpha View (Cell Biosciences, Santa Clara, CA).

3.7.4 Cloning

3.7.4.1 DNA recovery from the gel

After electrophoretic separation in an agarose gel, respective DNA bands were cut out from the gel and stored in sterile 2 ml reaction cups. DNA fragments recovery was carried out with the high pure PCR product purification kit (Roche, Mannheim, Germany) following the manufacturer's instructions.

3.7.4.2 Ligation

For transforming DNA fragments into chemically competent Top10 *E. coli* cells (Invitrogen, Karlsruhe, Germany), the fragments were ligated into the pCR2.1 TOPO vector (Invitrogen, Karlsruhe, Germany). The ligation was performed by using the TOPO TA cloning kit (Invitrogen, Karlsruhe, Germany) following the manufacturer's instructions, except that $\frac{1}{4}$ reactions were used. All the cups and tips here were prechilled before use.

The reagents used are listed in table 3.11.

Table 3.11. Set up of cloning reaction in 1.5 μ l.

reagent	Volume (μ l)
PCR product (DNA fragments)	x
Salt solution	0.25
pCR2.1 TOPO vector	0.25
water	add 1.5

3.7.4.3 *E. coli* transformation

25 μ l of competent Top10 *E. coli* cells were used for the transformation. The cells were thawed on ice. 1.5 μ l of the reaction (Table 3.11) were pipetted to the cells. The set up was incubated at room temperature for 10 minutes, after that the mixture was heat-shocked for exactly 30 seconds at 42°C and then cooled down immediately on ice for 5 min. Then transformed cells were supplemented with 125 μ l SOC medium

(Invitrogen, Karlsruhe, Germany) and incubated for 1 h in a shaker (4400 Innova Incubator Shaker, New Brunswick Scientific, Germany) at 180 rpm and 37°C.

1.6 mg X-galactose was supplemented on LB agar provided with antibiotic Kanamycin to select positive colonies. When X-galactose is digested by the beta-galactosidase, which is expressed by the gene *lacZ*, a blue by-product will be produced. The pCR2.1 TOPO vector carries *lacZ* in its multiple cloning sites. Therefore, if the plasmids of the cell colonies carry an inserted sequence in their multiple cloning sites, the gene *lacZ* cannot be expressed and the colonies are white. Otherwise, the cells without any insert will get a blue staining due to the cleavage of galactose. Obviously, the positive colonies with required gene appear white, while the others are blue.

After 1h incubation, cultures were spread on LB agar plates in triplicates and incubated in an incubator at 37 °C over night.

After overnight incubation, white colonies were picked with sterilized tooth-sticks and grown in 3 ml LB liquid medium with kanamycin in a shaker (4400 Innova Incubator Shaker, New Brunswick Scientific, Germany) at 180 rpm and 37°C over night.

3.7.4.4 Plasmid DNA isolation

2 ml out of overnight incubated 3 ml *E.coli* cultures were used to isolated plasmids. Nucleo Spin Plasmid Kit (MACHEREY-NAGEL, Düren, Germany) was used to do the plasmid preparation according to the manufacturer's instruction.

3.7.4.5 Sequencing

All of the plasmid and DNA sequencing was according to Sanger, *et al.* (1977) and carried out by the institute for clinical molecular biology (IKMB) in Kiel.

3.7.5 Restriction enzyme digestion

DNA digestion was performed with regard to the type of enzymes and their buffers (MBI Fermentas, St. Leon-Rot, Germany). At least 1-3 units of restriction endonuclease per 1 µg DNA were used and the mix was incubated at 37 °C 1 hour or overnight. The digested products were checked by loading them on a 0.8% (w/v) agarose gel (Section 3.7.3).

3.7.6 Mutants construction

All mutants listed in table 3.6 were constructed by inserting an antibiotic resistance cassette into the genome of *Synechocystis* via homologous recombination thereby interrupting the target gene.

3.7.6.1 Primer design

Target genes' sequences were obtained from Cyanobase (<http://genome.microbedb.jp/cyanobase/>) and NCBI (<http://www.ncbi.nlm.nih.gov/>). The primers were designed for the upstream 200 bp to 500 bp sequence of the target gene, named gene-1, gene-in1. Additional primers were designed for the downstream 200 bp to 500 bp sequence of the target gene, named gene-in2, gene-2. The primers gene-in1 and gene-in2 contained sequences of special antibiotic resistance cassettes to use them for fusion PCRs (see 3.7.6.2 and Chenchik, *et al.*, 1996). The primers are listed in table 3.3.

3.7.6.2 Fusion PCR

Before conducting fusion PCR (Fig. 3.6), three normal PCR were set up to amplify the upstream (with primer pairs: gene-1, gene-in1) and downstream (with primer pairs: gene-in2, gene-2) sequences of the target gene, and the sequences of the antibiotic resistance cassette. PCR products were run on 0.8% (m/v) agarose gels and compared to Lambda Marker to estimate the concentrations of the products. The total amount of PCR products for fusion PCR was 100 ng. The different PCR products that were set up for the fusion were applied in a ratio 1:1:1. The set up of a fusion PCR is listed in table 3.12. The temperature program steps are listed in table 3.13 (DNA-Engine PTC-200, Bio-Rad, USA).

The fusion PCR products had to be re-amplified. All the products were diluted into 1:1, 1:10, 1:100 and 1:1000 respectively. 5 µl of each dilution was used as template and gene-1, gene-2 primer pairs were used as re-amplification PCR (Table 3.10) primers.

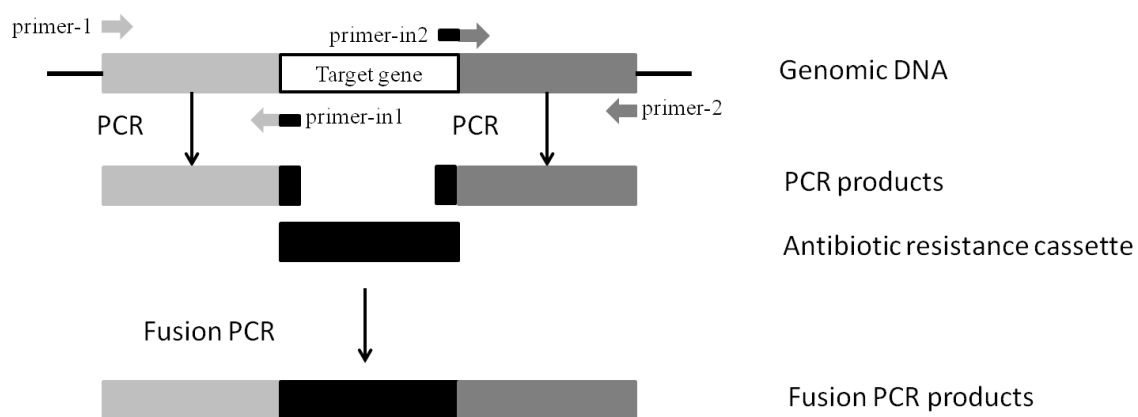


Fig. 3.6. the scheme of fusion PCR. Primers are listed in table 3.3.

Table 3.12. Set up of fusion PCR.

reagent	Volume (μ l)
Three PCR-products (100 ng)	x
dNTPs (2.5 mM)	4
10x buffer	5
Pfu-DNA-Polymerase (2 U/ μ l)	0.4
H ₂ O	40.6-x
total	50

Table 3.13. Temperature program of fusion PCR.

Steps	Cycles	Time (min)	Temperature ($^{\circ}$ C)
Initialization	1	1	95
Denaturation	30	0.5	95
Annealing		5	X
elongation		Y	72
incubation	1	∞	4

3.7.6.3 Transformation of *Synechocystis* sp. PCC 6803

The cultures of *Synechocystis* sp. PCC 6803 were inoculated at a optical density OD_{750} of 0.15 in 250 ml Kniese tubes with fresh BG-11 medium at 28 °C and 50 $\mu\text{E}/\text{m}^2/\text{second}$ light intensity and were continuously bubbled with air for 24 hours. 250 ml cultures were used for 2 transformations. On the second day, 250 ml cultures were centrifuged down at 5000 x g for 10 min at room temperature (4400 Innova Incubator Shaker, New Brunswick Scientific, Germany). The pellet was re-suspended in 1.5 ml BG-11 medium. 300 μl of the cell suspension was mixed with 6-18 μg plasmid DNA with the fusion PCR product cloned inside. The mixture was incubated in the shaker at 30 °C for 6 hours inverting the samples every 30 min of incubation. After incubation, 100 μl of cells were spread on twice-autoclaved nitrocellulose membrane filters (Poresize 0.45 μm , MACHEREY- NAGEL, Düren, Germany), which were laid on BG-11 agarose plates without any antibiotics. Triplicates were made and incubated in continuous light of 28 $\mu\text{E}/\text{m}^2/\text{s}$ at 30 °C for 2 days. Then the filters were transferred to new plates supplemented with the corresponding antibiotic as described in Table 6. Two weeks later, single colonies could be picked and streaked onto new agar plates with antibiotic. For mutants with deletions in genes that are important in the light, such as Δpep , $\Delta rubisCo$, the colonies were grown on LAHG agar plate in dim light with 5 $\mu\text{E}/\text{m}^2/\text{second}$ light intensity.

For the double mutant or triple mutant construction, the same procedure was used as described above. The only difference was that mutant cells instead of wild type *Synechocystis* sp. PCC 6803 cells were used for the transformation and that transformed cells were first incubated on agar-plates that contained the antibiotic for the mutant and subsequently incubated on plates with multiple antibiotics.

3.7.6.4 Southern blotting

3.7.6.4.1 DNA labeling

The Dig (Digoxigenin) system (Boehringer Mannheim, Mannheim, Germany) as a nonradioactive probe is safe, effective and re-usable. PCR-DIG labeling Mix (Roche, Mannheim, Germany) was incorporated into DNA by PCR. The PCR procedure was almost the same as described in 3.7.2, with the only difference that 4 μl of PCR-DIG labeling Mix instead of 5 μl of dNTP was used with a final concentration of 160 μM .

3.7.6.4.2 Genomic DNA restrict digestion

About 200 ng genomic DNA of wild type and mutants was digested with HindIII enzyme (Section 3.7.5) over night. Digested DNA was loaded on a long 0.8% (m/v) agarose gel and run for about 2 hours at 180 V/cm. Dig marked lambda-DNA/HindIII-Marker (DNA-Molecular-Weight Marker II, Boehringer Mannheim, Mannheim, Germany) was used to check the size of the bands.

3.7.6.4.3 Southern blotting

After the electrophoresis of the digested DNA, the gel was soaked in denaturation buffer (Table 3.14) twice for 15 min and then submerged in neutralization buffer (Table 3.14) twice for 15 min at room temperature. The DNA was blotted by capillary transfer to a nylon membrane (Poresize 0.20 μm , MACHEREY- NAGEL, Düren, Germany) using 20 x SSC (Table 3.14) buffer over night. Whatman paper soaked with 2 x SSC was used to help transferring the DNA (Fig. 3.7). The DNA was bound to the nylon membrane by a UV-crosslinker (UV-Stratalinker 2400, STRATAGENE, USA). The membrane with DNA could then be used immediately or it could be stored dry at room temperature for further use.

Table 3.14. Buffers for Southern blotting.

buffer	reagent
Denaturation buffer	0.5 N NaOH
	1.5 M NaCl
neutralization buffer	0.5 M Tris-HCl, pH 7.5
	3 M NaCl
20x SSC	300 mM Sodium citrate, pH 7.0
	NaCl

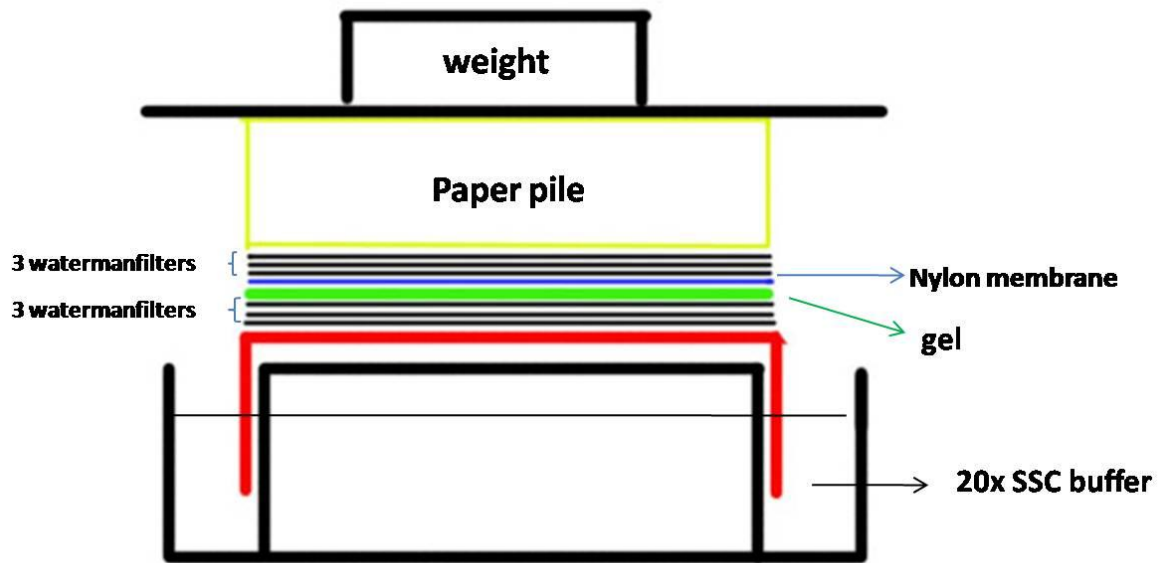


Fig. 3.7. Set up of Southern blotting.

3.7.6.4.4 Pre-hybridization and hybridization

Table 3.15. Buffers for Pre-hybridization and hybridization.

buffer	reagent
prehybridization buffer	5 x SSC buffer, 0.1% (w/v) Sodium lauroylsarcosine, 0.02% (w/v) SDS, 1% (w/v) Blocking reagent
hybridization buffer	7% (w/v) SDS, 50% (v/v) Deionized formamide, 5x SSC buffer, 2% (w/v) Blocking reagent, 50 mM Sodium phosphate, pH 7.0, 0.1% (w/v) Sodium lauroylsarcosine
2 x washing buffer	2 x SSC buffer, 0.5% (w/v) SDS
0.5 x washing buffer	0.5 x SSC buffer, 0.1% (w/v) SDS

The membrane was incubated with 30 ml prehybridization buffer (Table 3.15) for 1 hour at 68 °C in a hybridization tube in an oven (Biometra, Goettingen, Germany). Then the prehybridization buffer was discarded and the hybridization buffer (Table 3.15) with 25 ng/ml Dig-labeled probe which had been previously denaturated by

heating at 100 °C for 10 min and chilled directly on ice was added. The hybridization was incubated over night. On the next day, the membrane was washed twice 5 min with 2 x washing buffer (Table 3.15) at room temperature and then was washed twice for 15 min with 0.5 x washing buffer (Table 3.15) at 68 °C. All these four washing steps were performed in the hybridization tube.

3.7.6.4.5 Detection

After hybridization the membrane was taken out in a clean box and was equilibrated in buffer 1 (Table 3.16) for 1 min at room temperature. Then the membrane was incubated in buffer 2 (Table 3.16) without antibody for at least 1 hour at room temperature. After that the buffer was exchanged with buffer 2 supplemented with 1/10000 dilution of 750 units/ml Anti-Dig-Antibody (Anti-Digoxigenin-AP Fab fragments, Boehringer Mannheim, Mannheim, Germany) and the membrane was incubated for exactly 30 min. The membrane was washed gently in buffer 1 with 0.3% (v/v) Tween twice for 15 min at room temperature and then shortly equilibrated in detection buffer 3 (Table 3.16) for 1 min. The membrane was then incubated with 3 ml buffer 3 supplemented with 30 µl CDP-Star (Boehringer Mannheim, Mannheim, Germany) for 5 min. The extra substrate was removed from the membrane. The membrane was sealed in a clean plastic bag. The membrane was exposed to a standard X-ray film (GE healthcare, Buckinghamshire, UK) for 10 min to 1 hour.

The film was developed in a developer liquid (Roentoroll HC, Tetenal, Norderstedt, Germany) for 5 min, shortly washed in water and then fixed with in a fixation liquid (Superfix MRP, Tetenal, Norderstedt, Germany) for 10 min. After that, the film was washed in water for at least 30 min and dried.

Table 3.16. Buffers for DIG detection.

buffer	reagent
buffer 1 pH 7.5	0.1 M Maleic acid, 0.15 M NaCl
buffer 2	10% blocking reagent in buffer 1
buffer 3	100 mM Tris-HCl, pH 9.5, 100 mM NaCl

3.7.7 RNA isolation from *Synechocystis* sp. PCC 6803

All cultures were sampled at the amount equivalent to approximately 10^9 cells/ml. Cultures were centrifuged with ice-cubes (autoclaved) at 3,500 x g for 10 min at 4 °C and the pellets were resuspended with 4 x volumes break buffer (Table 3.17) and added quickly to the tube with 4 x volumes glass beads ($\varnothing=0.5$ mm, baked for 8 hours before using) and 4 x volume phenol-chloroform-isoamylalcohol (25:24:1) (v/v/v). The mixture was vortexed for 1 min 10 times and kept on ice for 1 min after each vortexing in the cold (4 °C) room. The mixture was centrifuged at 16,000 x g for 5 min to separate the aqueous phase from the organic phase. The upper phase was transferred into a new 1.5 ml reaction-cup and extracted one or two times with the same volume phenol-chloroform-isoamylalcohol (25:24:1) (v/v/v) until the interphase was barely visible. After that, the extracted mixture was extracted with the same volume chloroform-isoamylalcohol (24:1) (v/v) to get rid of phenol. The aqueous phase should be light pink and clear. 0.1 volume 3 M sodium acetate (pH 5.6-6.5) and 2.5 volume ice cold 99% (v/v) ethanol were added and kept at -20 °C overnight to precipitate nucleic acids. The mixture was centrifuged at 16,000 x g at 4 °C for 10 min and the pellet was washed with 1 ml ice cold 70% (v/v) ethanol. The dried pellet was dissolved in 200 μ l TE buffer. In order to separate RNA from DNA, 200 μ l 5 M lithium chloride was added and kept at -20 °C for at least 1.5 hours to precipitate the RNA. The cups were inverted every 20 min to prevent them from freezing. The mixture was centrifuged at 16,000 x g at -9 °C for 30 min and the pellet was resuspended in 200 μ l TE buffer again. The RNA precipitation steps were repeated once more. The pellet was dissolved in 20 μ l of RNase free water and stored at -80 °C.

3.7.8 Denatured RNA agarose gel electrophoresis

All RNA electrophoresis apparatus was submerged in 0.1 N NaOH for 15 min and washed twice with autoclaved water. The RNA agarose gel was made by using 1.2% (w/v) agarose with 6% (v/v) Formaldehyde in 0.1 volumes (v/v) 10 x MOPS buffer (Table 3.17). 1 μ l RNA was supplemented with 3 μ l RNA loading buffer (Table 3.17) and incubated at 65 °C for 10 min and chilled immediately on ice. RNA electrophoresis was run with 1 x MOPS buffer with 1V/cm for about 16 hours. RNA

concentration was determined by Nano Drop and estimated by comparing the bands in the gel with the Lambda Marker (see section 3.7.3).

Table 3.17. Buffers of RNA extraction.

buffer	reagent
break buffer	32 ml TE 50/100 (50 mM Tris-HCl, pH 8.0, 100 mM EDTA), 150 μ l Triton X-100, 600 μ l 25% (w/v) Sodium lauroylsarcosine, 20% (w/v) Sodium dodecyl sulfate
10x MOPS	200 mM MOPS (pH 6.3), 50 mM Sodium acetate, 1mM EDTA, pH 7.
RNA loading buffer	0.1 volume (v/v) of 10 x MOPS, 0.19 volume (v/v) of 37% (v/v) formaldehyde, 0.58 volume (v/v) of deionized formamide, 0.1 volume loading buffer (0.05% Bromphenolblue, 60% Glycerine in 1x MOPS buffer), add H ₂ O to 1volume

3.7.9 DNase I digestion of RNA

15 μ l of RNA (1 μ g) was incubated at 37 °C for 2 hours with 2 μ l Dnase (10 U/ μ l, MBI Fermentas, St. Leon-Rot, Germany) in 2 μ l 10 x DNase buffer (MBI Fermentas, St. Leon-Rot, Germany) and supplemented with 1 μ l Ribolock RNase Inhibitor (40 U/ μ l, MBI Fermentas, St. Leon-Rot, Germany) and quickly cooled down on ice. 2 μ l 50 mM EDTA was added in the mixture and incubated at 65 °C for 10 min and quickly cooled down on ice to get rid of the Dnase I and buffer.

To check the digestion efficiency, 1 μ l DNase I digested RNA was used as a template for PCR reaction. 1 μ l genomic DNA and 1 μ l H₂O were used as positive and negative controls respectively. PCR products should not been seen in the DNase I digested RNA sample nor in the H₂O sample.

3.7.10 Reverse transcript PCR

Reverse transcript PCR reactions were performed with RT-PCR kit (Applied biosystems, Karlsruhe, Germany) according to the manufacturer's instruction. The set up and negative control are listed below (Table 3.18). The reaction mixture was

first incubated at 37 °C for 1 hour. The mixture was further heated at 95 °C for 5 min and then chilled at 4 °C. cDNA can be stored at -20 °C for at least several months.

Control PCR (Section 3.7.2) was also made to check the cDNA. PCR product should be seen in PCR reaction with RT-Mix, while no band should be seen in the negative control.

Table 3.18. Set up of Reverse transcript PCR.

	reagent
Reverse transcript PCR	9 µl digested RNA, 10 µl 2x buffer, 1 µl RT-Mix
negative control	9 µl digested RNA, 10 µl 2x buffer, 1 µl H ₂ O

3.7.11 Quantitative real time PCR

Quantitative real time PCR (qRT-PCR) was performed with Power SYBR Green PCR Master Mix Kit (Applied biosystems, Karlsruhe, Germany) in qRT-PCR machine (Rotor-Gene Q, Bio-Rad, USA). The reaction set up is listed in table 3.19. The program was according to the manufacturer's instruction (Table 3.20). Three repeats of each reaction were made. Threshold was always set up as 0.1000.

Table 3.19. Set up of qRT-PCR.

reagent	volume (µl)
SYBR Green Reaction Mix	7.5
Forward Primer of target gene	1.5
Reverse Primer of target gene	1.5
cDNA	4.5

Table 3.20. Temperature program of qRT-PCR.

Step	Enzyme activation	PCR	
	Hold	Cycles (40 cycles)	
		Denature	Anneal/Extend
Time	10 min	15 sec	60 sec
Temperature (°C)	95	95	60

Before the expression levels of the genes of interest were tested, the efficiency of primers of target genes was investigated. One cDNA sample was diluted into 1/30, 1/300, 1/900 and 1/3000. The primers were checked by qRT-PCR with all four cDNA dilutions. A trend line was created with the Ct value plotted on the y-axis and the dilution plotted at the x-axis. The slope of the trend line was used to calculate the efficiency (E): $E = 10^{-(\text{logarithmic slope})^{-1}}$. The efficiency should be around 2 to show a high amplification rate and thereby a high primer quality, since 2 means that the amount of amplified DNA is doubled in each cycle.

At least two house-keeping genes were used as reference genes. The target gene expression level was compared to the expression level of the reference genes and was then calculated according to the formula shown below.

$$\text{target gene expression ratio} = \frac{E_{\text{primers of target gene}}^{\Delta C_{t\text{target gene}}(\text{untreated condition}-\text{treated condition})}}{E_{\text{primers of reference gene}}^{\Delta C_{t\text{reference gene}}(\text{untreated condition}-\text{treated condition})}}$$

3.8 Protein Analysis

In order to search the genome of *Synechocystis* for homologs that might fulfill specific functions well characterized proteins with the function in question were retrieved from the literature from different prokaryotes if possible. The sequences of these proteins were downloaded from the Genebank at (<http://www.ncbi.nlm.nih.gov/>) and were used as baits to search cyanobase (<http://genome.microbedb.jp/cyanobase/>) or NCBI microbes (http://www.ncbi.nlm.nih.gov/sutils/genom_table.cgi) with blastP using the default settings. In order to evaluate the function of the found proteins, the literature and the NCBI site (<http://www.ncbi.nlm.nih.gov/Structure/cdd/cddsrv.cgi>) were searched for conserved amino acids within the characterized protein. It was checked whether these conserved amino acids were also found in the candidate protein of *Synechocystis*.

To predict the localization of the protein the SignalP tool of the cbs prediction server (<http://www.cbs.dtu.dk/services/>) set for gram-negative bacteria was used.

3.9 Database and Bioinformatic programs

All database and bioinformatic programs used in this work are list below:

Database:

Cyanobase: <http://genome.microbedb.jp/cyanobase/>

NCBI: <http://www.ncbi.nlm.nih.gov/tools/primer-blast/>

NCBI microbes: http://www.ncbi.nlm.nih.gov/sutils/genom_table.cgi

NCBI proteins: <http://www.ncbi.nlm.nih.gov/Structure/cdd/cddsrv.cgi>

GOS: <http://camera.calit2.net/>

KEGG: <http://www.genome.jp/kegg/>

Programs:

BLAST: <http://www.ncbi.nlm.nih.gov/Blast.cgi>

Primer-Blast: <http://www.ncbi.nlm.nih.gov/tools/primer-blast/>

Bioedit7.0.9: <http://www.mbio.ncsu.edu/BioEdit/bioedit.html>

Nebcutter V2.0: <http://tools.neb.com/NEBcutter2/>

4 Results

4.1 Characterization of the *nifJ*- and the *hoxH*-mutant under different growth conditions

4.1.1 Characterization of the *nifJ*-mutant

The wild-type (WT) of *Synechocystis* sp. PCC 6803 and its $\Delta nifJ$ -mutant (Gutekunst, *et al.*, 2014) were grown under autotrophic (light) and mixotrophic (light and medium supplemented with 10 mM glucose) conditions (Section 3.5). The cultures were continuously bubbled with air and the OD₇₅₀ values of the cultures were recorded daily to monitor their growth (Fig. 4.1). It can be seen from the growth curves that $\Delta nifJ$ grew as well as the WT under autotrophic conditions, while its growth was impaired compared to the WT under mixotrophic conditions. $\Delta nifJ$ utilized glucose to grow nearly as fast as the WT before day 5, however the maximum OD₇₅₀ value of $\Delta nifJ$ (OD₇₅₀ around 4.5) was lower than the maximum OD₇₅₀ value of the WT (OD₇₅₀ was around 6). After day 5 the mixotrophic growth of $\Delta nifJ$ was severely affected compared to the WT, while the WT reached its stationary phase.

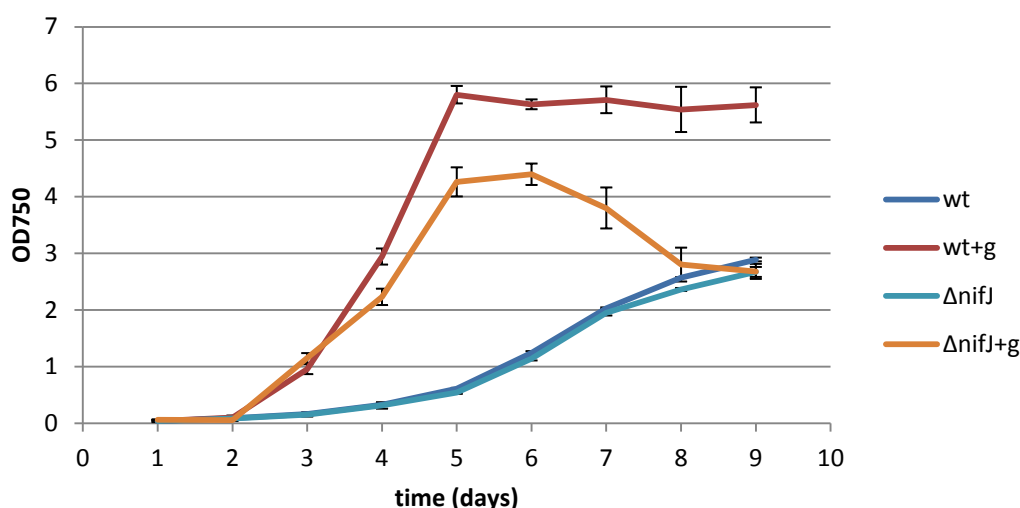


Fig. 4.1. Growth curves of WT and $\Delta nifJ$ under autotrophic and mixotrophic (+g) conditions.

Glucose is degraded to pyruvate which is converted into acetyl-CoA either by the pyruvate-dehydrogenase-complex or alternatively by NifJ (PFOR) (Neuer, *et al.*, 1982; de Kok, *et al.*, 1998). If this reaction is catalyzed by NifJ, ferredoxin or flavodoxin is reduced. Electrons from reduced ferredoxin can be passed to nitrate, to reduce it to

ammonia, which can be used for the cell metabolism. It was hypothesized that $\Delta nifJ$ could be affected under mixotrophic conditions due to their limited ability to reduce nitrate to ammonium. In order to test this hypothesis, nitrate in the growth medium of the mixotrophic cultures was replaced by 5 mM arginine. Arginine can be metabolized directly by the cells as nitrogen source. In contrast to nitrate, arginine does not need to be reduced by ferredoxin. When the growth medium was supplemented with arginine, $\Delta nifJ$ grew faster than without arginine (Fig. 4.2). However, if the growth medium was supplemented with both arginine and glucose, $\Delta nifJ$ was unable to grow (Fig. 4.2).

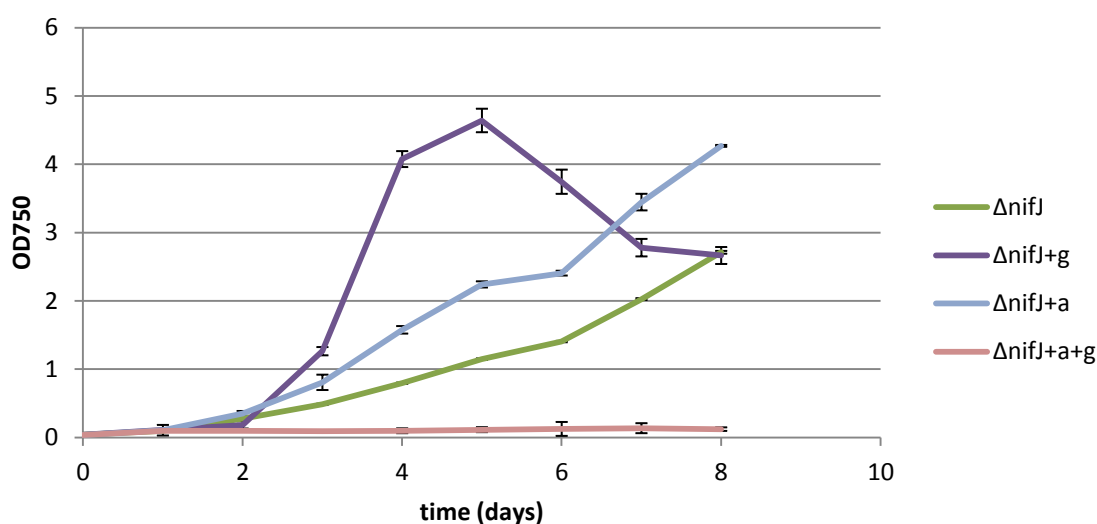
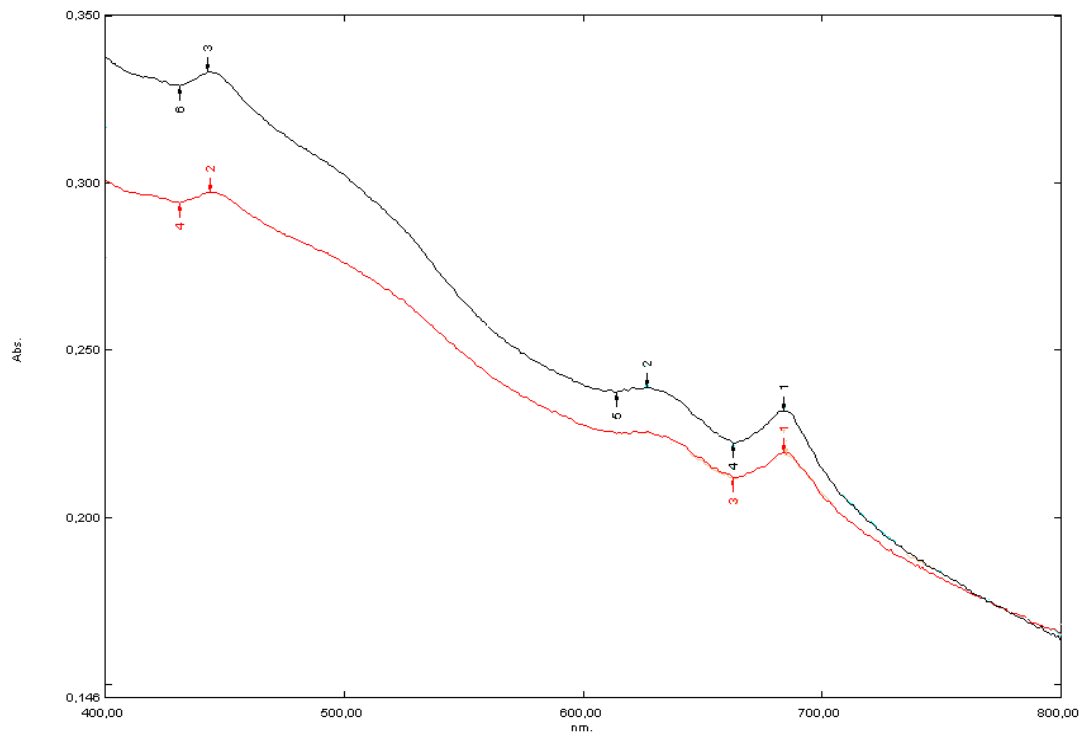


Fig. 4.2. Growth curves of $\Delta nifJ$ cultures on BG-11 medium with nitrate, or BG-11₀ medium with arginine instead of nitrate ($\Delta nifJ+a$), or BG-11₀ medium with glucose and arginine instead of nitrate ($\Delta nifJ+a+g$).

The color of mixotrophic cultures grown with arginine turned from green to yellow. In order to survey the variation of pigments in the cultures, an absorption spectrum from 400 nm to 800 nm (Section 3.6.2) was measured daily in autotrophic and mixotrophic cultures grown with arginine.

The peaks at 430 nm and 660 nm indicate the amount of chlorophyll a, the peaks at 620 nm represent the amount of phycocyanin. Figure 4.3 (a) shows the absorption spectrums of the first inoculation day of $\Delta nifJ$ cultures under autotrophic and mixotrophic conditions. The absorption spectrum at the 4th day of these two cultures can be seen in figure 4.3 (b). It is obvious that almost no phycocyanin and only a small amount of chlorophyll a existed in mixotrophic cultures grown with arginine

(a)



(b)

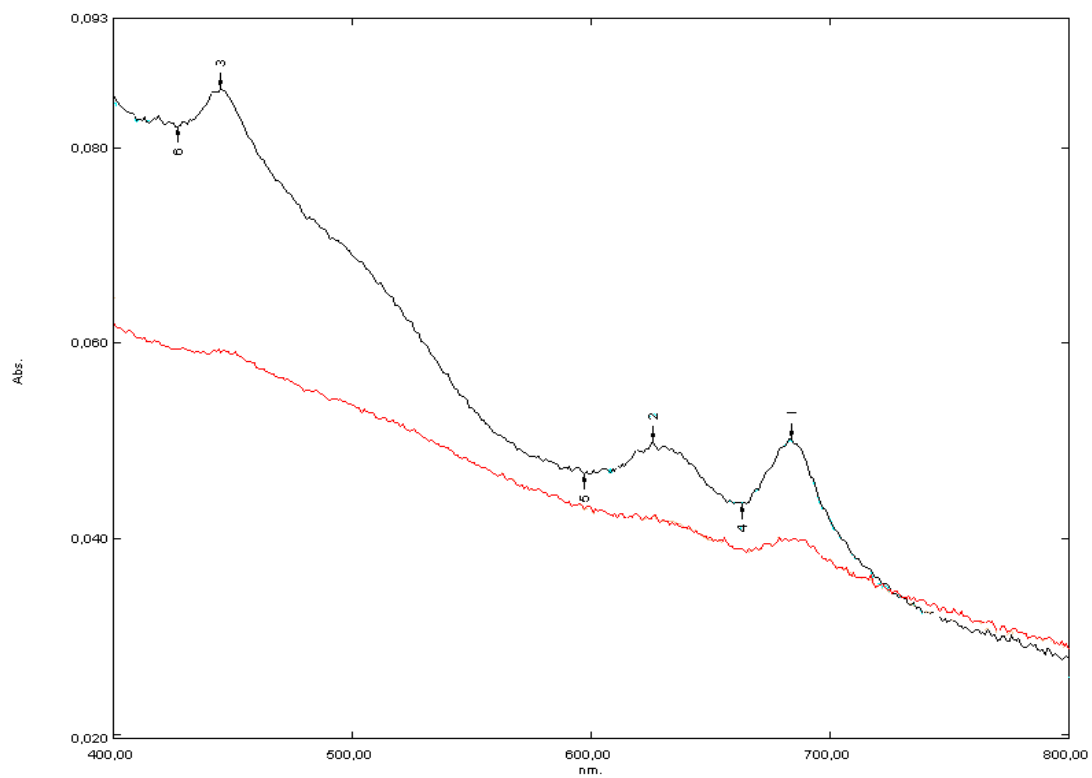


Fig. 4.3. Absorption spectrum of autotrophic $\Delta nifJ$ cultures (black lines) and mixotrophic $\Delta nifJ$ (red lines) cultures with arginine at the first (a) and the 4th (b) cultivation day.

compared to the first day. In contrast the amount of both pigments was more or less unchanged in the autotrophic cultures over this time range.

The degradation of the phycobilisome (Fig. 4.3) is consistent with the hypothesis that $\Delta nifJ$ cultures are affected under mixotrophic conditions due to their limited ability to reduce nitrate to ammonium, which could result in nitrogen shortage.

It was therefore further hypothesized that the phenotype of $\Delta nifJ$ cultures under mixotrophic conditions could be due to a surplus of electrons from the oxidation of water via photosynthesis and the oxidation of glucose. To test this hypothesis 10 μ M DCMU was added to the growth medium from mixotrophic cultures in order to interrupt the electron flow from PS II to plastoquinone (PQ). As a consequence, the cells could only accept electrons from glucose oxidation but no longer from the photosynthetic electron flow. The growth of both WT and $\Delta nifJ$ was monitored under these conditions (Fig. 4.4). The results from figure 4.4 show that the growth of $\Delta nifJ$ ($\Delta nifj+g+d$) is similar to the growth of the WT ($wt+g+d$) if DCMU was added to the medium that was supplemented with 10 mM glucose. The measurement of the mixotrophic $\Delta nifJ$ culture was stopped on day 8 as the cultures were totally bleached (Fig. 4.4). The mixotrophic cultures that were supplemented with DCMU grew slower than the mixotrophic cultures. Both WT and $\Delta nifJ$ did only reach the OD_{750} that was reached by the mixotrophic $\Delta nifJ$ culture. However whereas the mixotrophic $\Delta nifJ$ culture showed a reduced OD_{750} from day 5 on, the cultures with DCMU kept their OD_{750} values, instead of dying. This result supports the hypothesis that mixotrophic $\Delta nifJ$ cultures might suffer from a surplus of electrons. The result that WT grown on both glucose and DCMU grew slower than cultures grown on glucose alone was as expected, as the WT had to grow heterotrophically (respiration only) in the first case but could grow mixotrophically (respiration and photosynthesis) in the second case.

The presented results show that NifJ might be important to reduce nitrate under mixotrophic conditions as an electron sink.

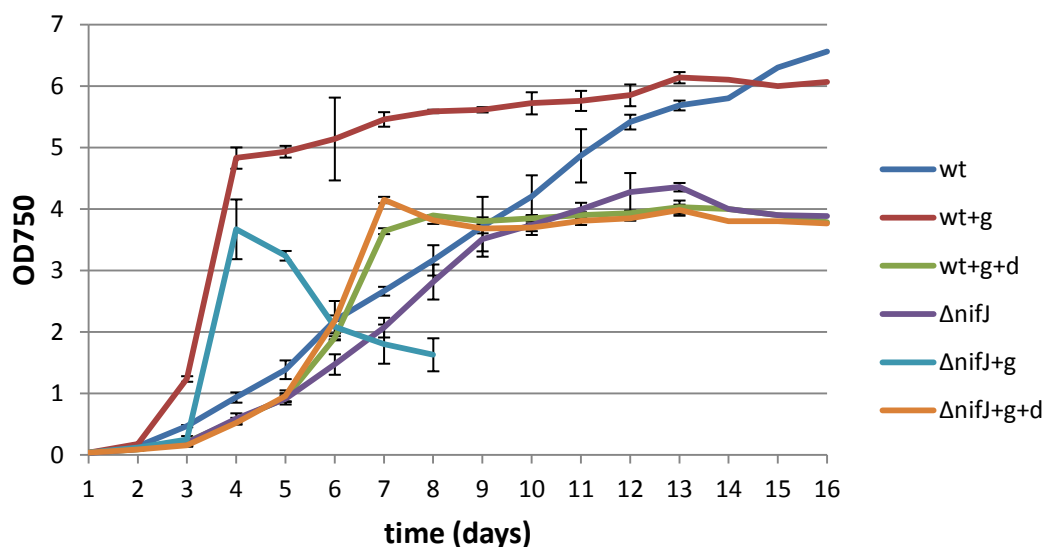


Fig. 4.4. Growth curves of WT and $\Delta nifJ$ cultures grown on BG-11 medium (wt, $\Delta nifJ$) and on BG-11 medium supplemented with glucose (+g) or glucose and DCMU (+g+d).

4.1.2 Characterization of the *hoxH*-mutant

Appel *et al.* (2000) demonstrated that the bidirectional hydrogenase of *Synechocystis* sp. PCC 6803 works as an electron valve in dark-adapted cells at the onset of photosynthesis. It was shown that the hydrogenase in *Synechocystis* is reduced by ferredoxin and that hydrogen production is connected to NifJ under fermentative conditions (Gutekunst, *et al.*, 2014). The $\Delta hoxH$ mutant (Appel, *et al.*, 2000), in which the large hydrogenase subunit was deleted, was further characterized. In order to study the effect of glucose on $\Delta hoxH$, the cells were cultivated under mixotrophic growth conditions.

When grown on BG-11 medium, $\Delta hoxH$ had no phenotype compared to the WT (Fig. 4.5). Unlike $\Delta nifJ$, the $\Delta hoxH$ cultures could use glucose as well as the WT (data not shown). However, when the cultures were cultivated under a dark:light (12h:12h) regime, with anoxic conditions during the dark period, $\Delta hoxH$ could not grow on glucose plus arginine as $\Delta nifJ$ (Fig. 4.5).

This is the first time that a strong growth phenotype of the hydrogenase-free mutant of *Synechocystis* sp. PCC 6803 could be shown. These results indicate that both NifJ and the hydrogenase might withdraw a surplus of low-potential electrons under anaerobic, mixotrophic and nitrate limiting conditions.

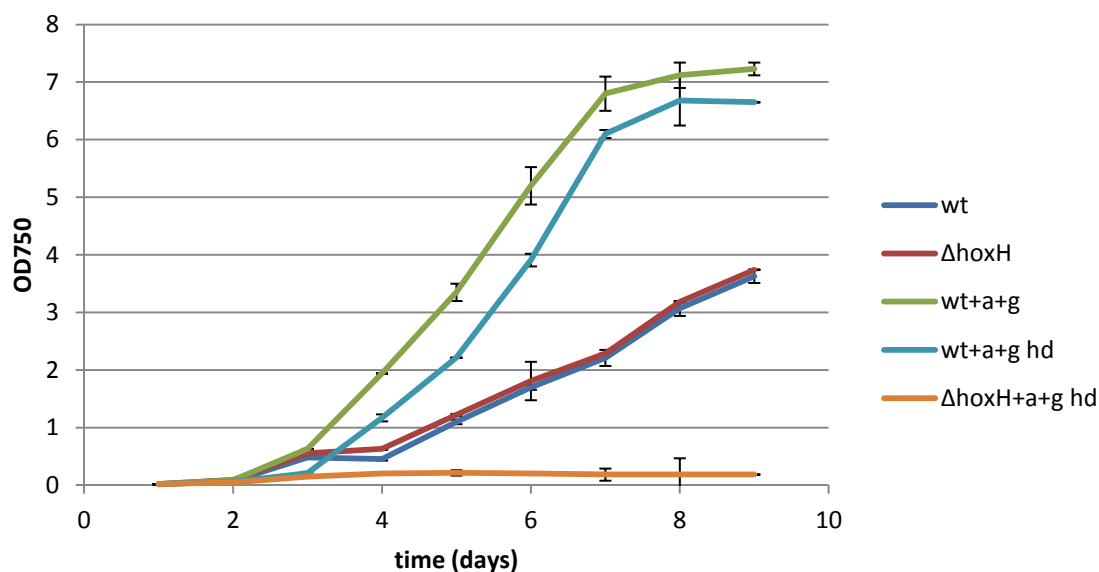


Fig. 4.5. Growth curves of WT and $\Delta hoxH$ cultures grown on BG-11 medium or BG-11₀ medium with arginine and glucose (+a+g) or BG-11 medium with glucose and arginine under a dark:night regime (+a+g hd).

4.1.3 Activity of the cytochrome bd oxidase under mixotrophic conditions in WT and $\Delta nifJ$ cultures

The cytochrome bd oxidase is located in the thylakoids of *Synechocystis* and reduces oxygen to water. The enzyme receives its electrons directly from the plastoquinone (PQ) pool and prevents over reduction under certain culture conditions when the cytochrome b₆f complex alone is not able to forward the electrons to acceptors in the photosynthetic electron chain (Berry, *et al.*, 2002). A high activity of the cytochrome bd oxidase thus indicates that the photosynthetic electron chain is overreduced. As it was hypothesized that the $\Delta nifJ$ cultures suffer from a surplus of electrons under mixotrophic conditions, the activity of the cytochrome bd oxidase was measured via PAM (Section 3.6.5).

WT and $\Delta nifJ$ cultures were grown under autotrophic and mixotrophic conditions. Their growth was monitored by OD₇₅₀ measurements. As shown in figure 4.6 $\Delta nifJ$ grew slower than the WT on days 2-4. Aliquots of the mixotrophic cultures were used for PAM measurements using a slow kinetic at 440 nm in order to determine the activity of the cytochrome bd oxidase. As shown in figure 4.7 the cytochrome bd

activity of mixotrophic $\Delta nifJ$ cultures had a trend to be higher on the days on which their growth was decreased compared to the WT.

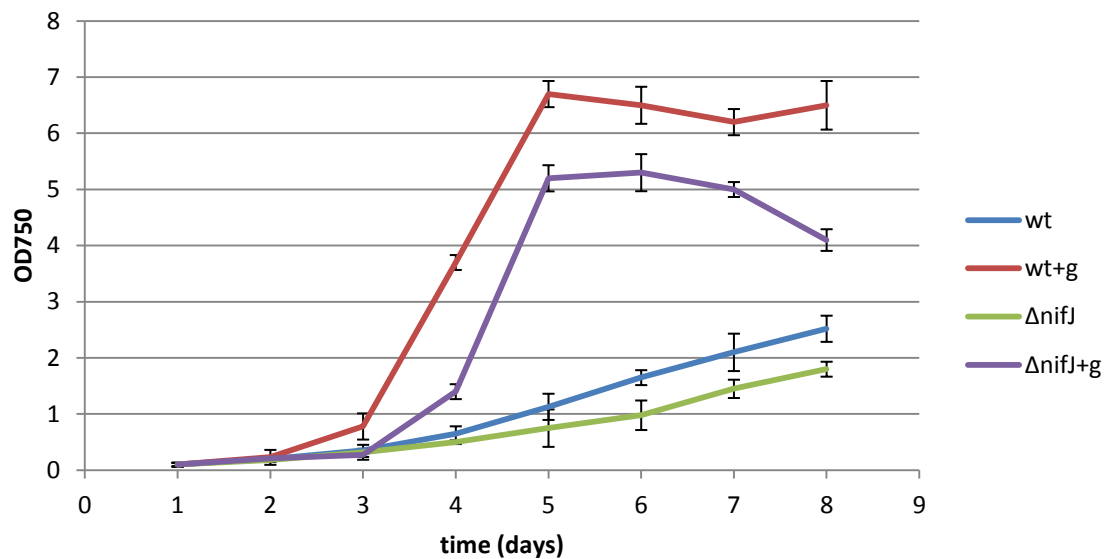


Fig. 4.6. Growth curves of wt and $\Delta nifJ$ under autotrophic and mixotrophic conditions for PAM measurement.

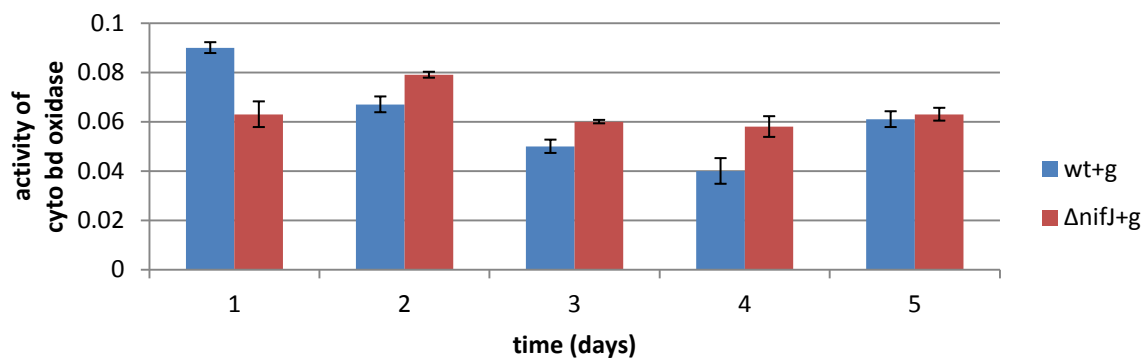


Fig.4.7. Comparison of cytochrome bd oxidase activities between wt and $\Delta nifJ$ mixotrophic cultures by PAM measurement with 440 nm slow kinetic method. The measurements were performed in triplicate.

4.1.4 Photosynthesis and respiration under mixotrophic conditions in WT and $\Delta nifJ$ cultures

In order to further characterize $\Delta nifJ$ and WT under mixotrophic conditions, their photosynthesis rate and respiration rate were determined via a clark-electrode

(Section 3.6.4). Over a period of a week both oxygen evolution in the light and oxygen consumption in the dark were monitored daily.

4.1.4.1 Photosynthesis rate

In order to measure the photosynthetic rate, cells were firstly incubated for three minutes in the dark and subsequently illuminated for three minutes. The oxygen evolution in the light was recorded and the photosynthesis rate was determined.

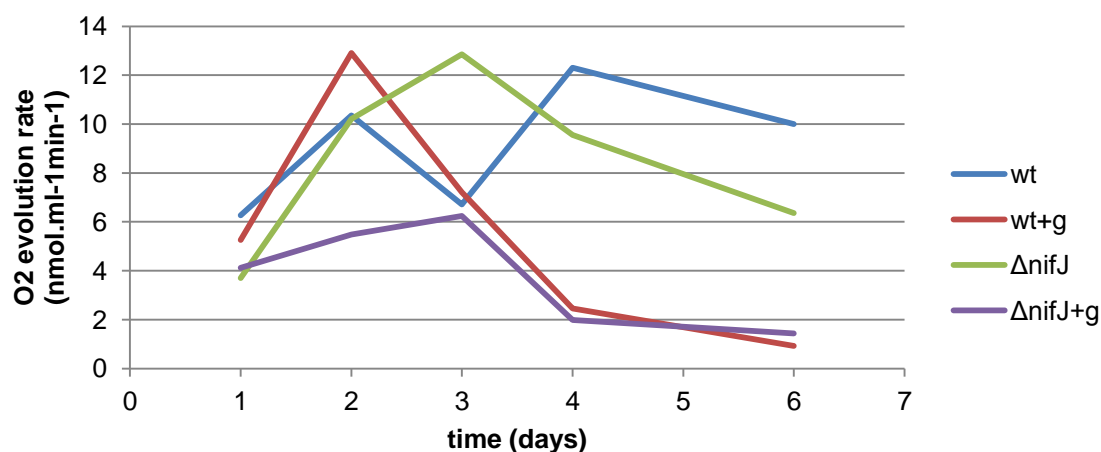


Fig. 4.8. Photosynthesis rate of WT and $\Delta nifJ$ grown with BG-11 medium and BG-11 medium with glucose (+g) measured as oxygen evolution at the Clark-electrode. The measurement was performed in 1 ml culture with an OD₇₅₀ of 1. One of two independent measurements is shown here.

As shown in figure 4.8, the rate of photosynthesis of both WT and $\Delta nifJ$ dropped under mixotrophic conditions within a week, whereas the photosynthetic rate of the autotrophic cultures fluctuated.

4.1.4.2 Respiration rate

For the respiration rate measurement, the cultures were incubated in the dark for 3 minutes.

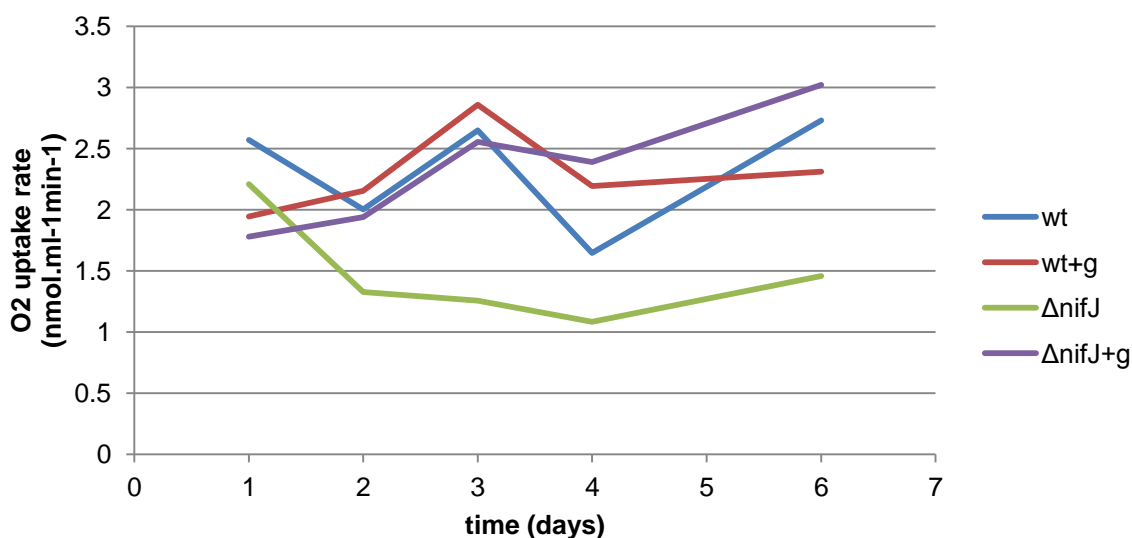


Fig. 4.9. Respiration rate of WT and $\Delta nifJ$ grown with BG-11 medium and BG-11 medium with glucose (+g) measured as oxygen uptake at the Clark-electrode. The measurement was performed in 1 ml culture with an OD_{750} of 1. The measurement was performed only once.

Respiration was higher in mixotrophic $\Delta nifJ$ cultures compared to autotrophic cultures (Fig. 4.9). The respiration rate in the mixotrophic WT culture dropped when the culture reached its stationary growth phase.

These measurements indicate that glucose is preferentially metabolized under mixotrophic conditions, as photosynthesis is down-regulated and respiration is up-regulated.

4.1.5 Identification of excreted metabolites in WT and $\Delta nifJ$ cultures via Nuclear Magnetic Resonance (NMR)

Nuclear magnetic resonance (NMR) spectroscopy is a powerful analytical technique to identify and quantify the small-molecule water-soluble metabolites. All the measurements demonstrated here were performed by ^1H NMR (Section 3.6.6).

4.1.5.1 Analysis of fermentatively excreted metabolites via NMR

In order to identify the fermentative metabolites excreted from WT and $\Delta nifJ$ cultures, cells were cultivated to an optical density (OD_{750}) of 3. 30 ml of these cultures were transferred into 50 ml tubes and sealed with a rubber septum. The cells were flushed with nitrogen for 10 min to expel the oxygen. The tubes were wrapped with aluminum

foil to prevent oxygen evolution from photosynthesis. The samples were incubated in a water bath at 28°C in the dark for 8 days. 2 ml samples were taken each day for NMR measurements.

The metabolites were analyzed in the supernatant. Typical metabolites for WT, $\Delta nifJ$ and $\Delta hoxH$ cultures were acetate, lactate, alanine, succinate, 3-hydroxybutyrate and formate. Figure 4.10 shows the metabolites in the supernatant of WT culture over a time period of 8 days. The excreted metabolites were measured five times in independently cultivated cultures. The growth medium without cells was measured as a control. No significant differences were visible between WT, $\Delta nifJ$ and $\Delta hoxH$ cultures concerning the metabolites highlighted in figure 4.10. Acetate was already present from the very first day on, so its production might already have started under autotrophic conditions. The peaks of 3-hydroxybutyrate, alanine and lactate however appeared later and were therefore interpreted as fermentatively produced metabolites.

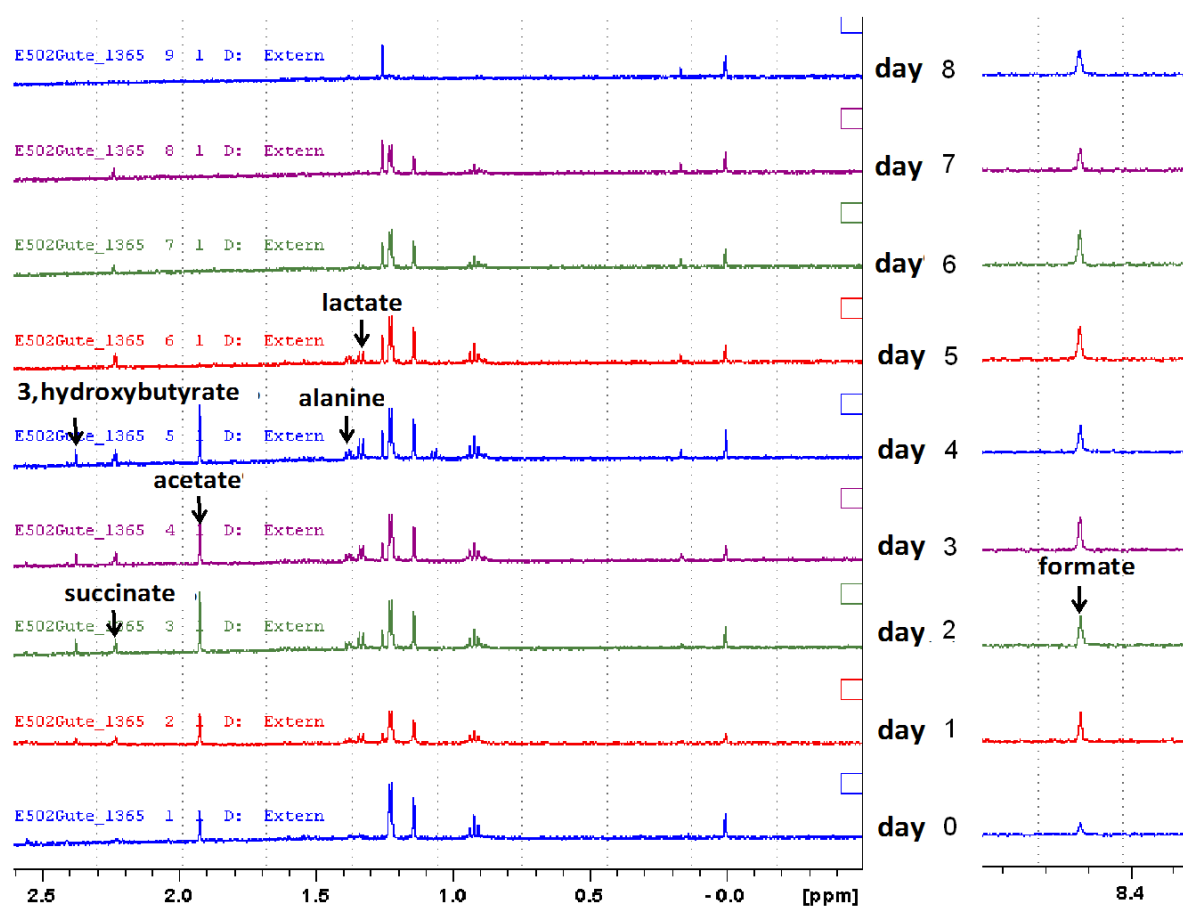


Fig. 4.10. The time course of excreted metabolites under fermentative conditions in the WT over 9 days. On the y-axis, arbitrary units are shown.

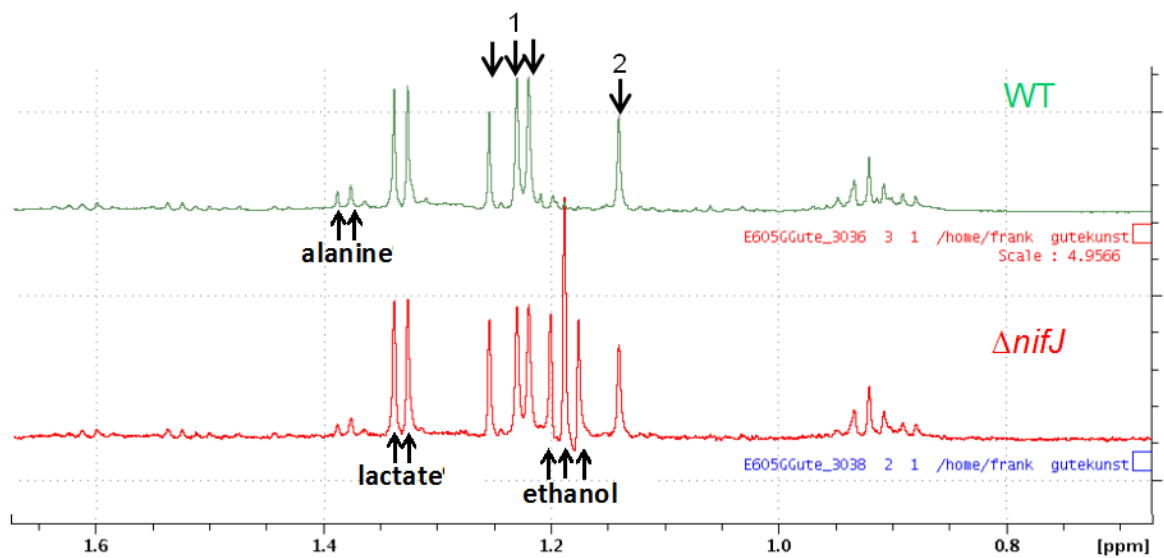


Fig. 4.11. Alanine, lactate and ethanol excretion on the seventh day under fermentative conditions in WT and $\Delta nifJ$ cultures. The peaks of Number 1 and 2 are still not identified. On the y-axis, arbitrary units are shown.

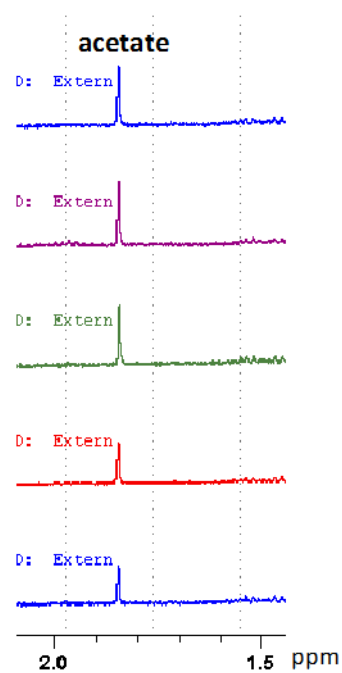


Fig. 4.12. Acetate excretion in $\Delta nifJ$ cultures over 5 days. On the y-axis, arbitrary units are shown.

In some experiments, ethanol could be detected in the $\Delta nifJ$ cultures but not in the WT cultures (Fig. 4.11). As ethanol was present from the very beginning it cannot be ruled out, that ethanol was produced under autotrophic conditions already.

Interestingly, *ΔnifJ* cultures produced acetate under fermentative conditions as the WT. As these cells lack NifJ, pyruvate was probably converted via the pyruvate dehydrogenase complex to acetyl-CoA and further to acetate (Fig. 4.12). If pyruvate is converted to acetyl-CoA via NifJ, electrons are transferred to ferredoxin (Fig. 1.4). However if this reaction is catalyzed by the pyruvate dehydrogenase complex, electrons are transferred to NAD⁺. The production of ethanol could thus be a way to regenerate NAD⁺ for a further breakdown of glucose.

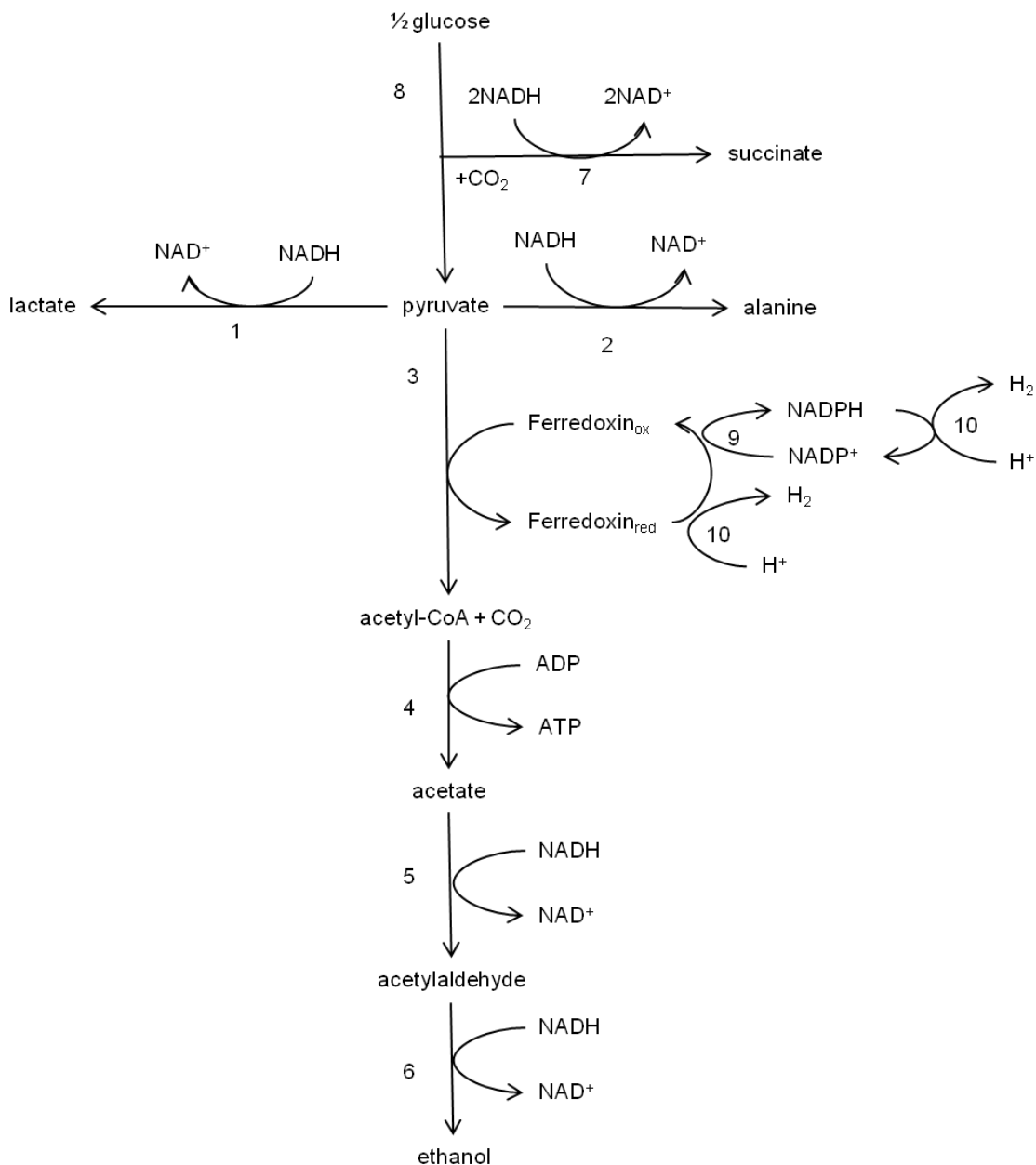


Fig. 4.13. Hypothetic fermentative metabolism of pyruvate derived from glycolytic pathways in *Synechocystis* sp. PCC 6803 based on the sequenced genome. 1, lactate dehydrogenase; 2, alanine dehydrogenase; 3, PFOR; 4, phosphotransacetylase and acetate kinase; 5, aldehyde dehydrogenase;

6, alcohol dehydrogenase; 7, enzymes of the TCA cycle from malate dehydrogenase to succinate dehydrogenase; 8, enzymes of glycolytic pathways; 9, Pyruvate formate-lyase; 10, 3-hydroxybutyrate dehydrogenase; 11, FNR (Ferredoxin: NADP+ reductase); 12, hydrogenase.

The NMR analyses show that *Synechocystis* excretes several metabolites under fermentative conditions. A hypothetical scheme of the respective pathways shown in figure 4.13 is confirmed by our results. All enzymes shown in figure 4.13 are annotated in the genome of *Synechocystis*.

4.1.5.2 Analysis of mixotrophically excreted metabolites via NMR

In order to further investigate the differences between *Synechocystis* WT and $\Delta nifJ$ under mixotrophic conditions, their excreted metabolites were analyzed under mixotrophic conditions. WT and $\Delta nifJ$ were cultivated under autotrophic and mixotrophic (light and 10 mM glucose) conditions (Fig. 4.14). The supernatants of mixotrophically grown cells were analyzed via NMR.

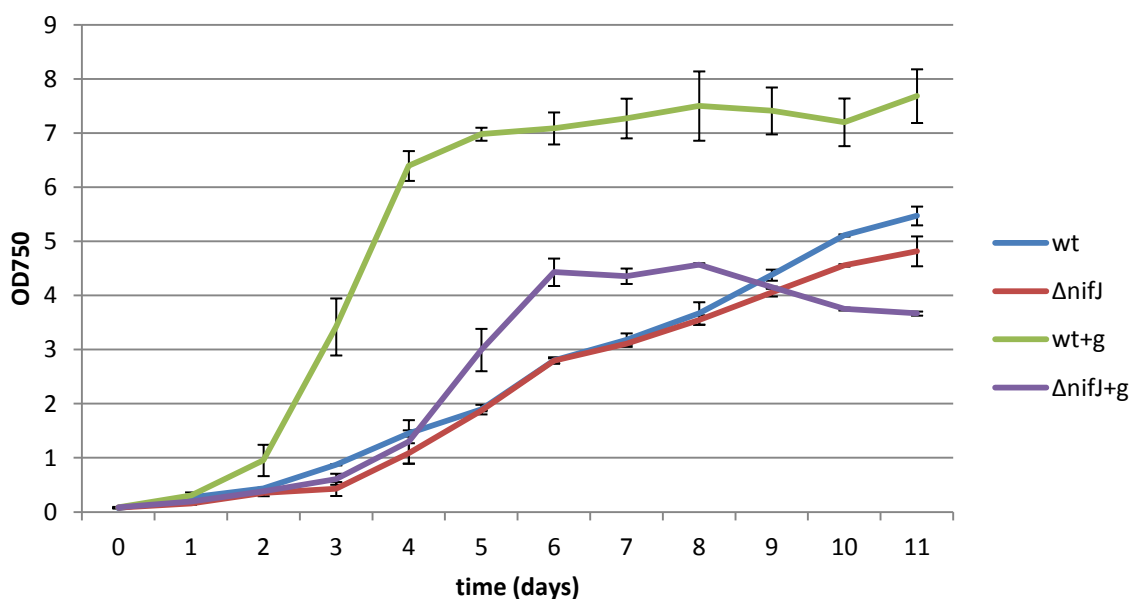


Fig. 4.14. Growth curves of autotrophic and mixotrophic WT and $\Delta nifJ$ cultures analyzed via NMR, qRT – PCR and NAD+ / NADH determination.

Figure 4.15 shows that WT cultures consumed the glucose within the first five days whereas $\Delta nifJ$ cultures consumed the glucose within the first six days. As soon as the glucose was taken up, the cultures entered their stationary growth phase (Fig. 4.14, Fig. 4.15).

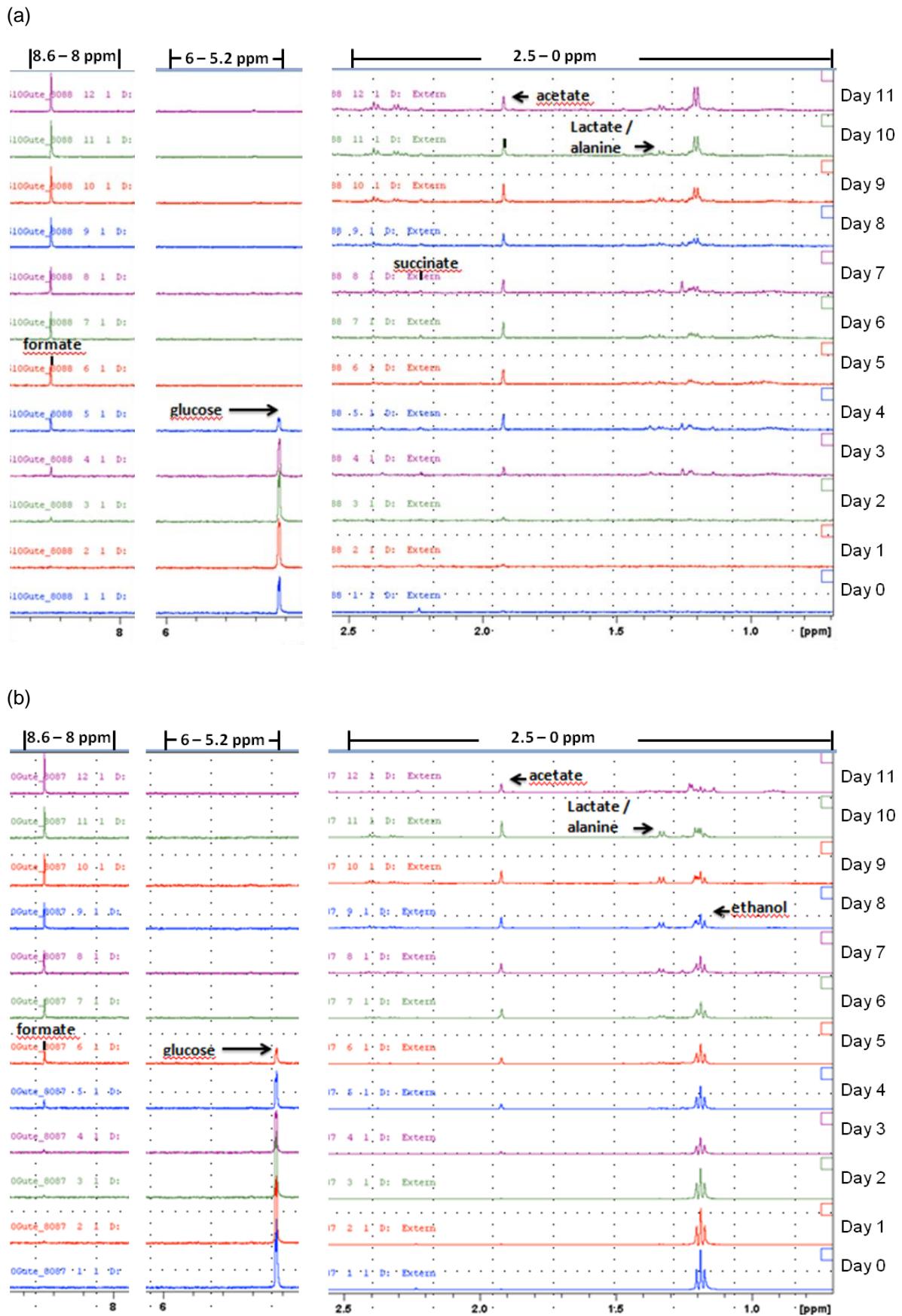


Fig. 4.15. NMR spectrum of the growth medium of (a) WT and (b) $\Delta nifJ$ cultivated under mixotrophic conditions. On the y-axis, arbitrary units are shown.

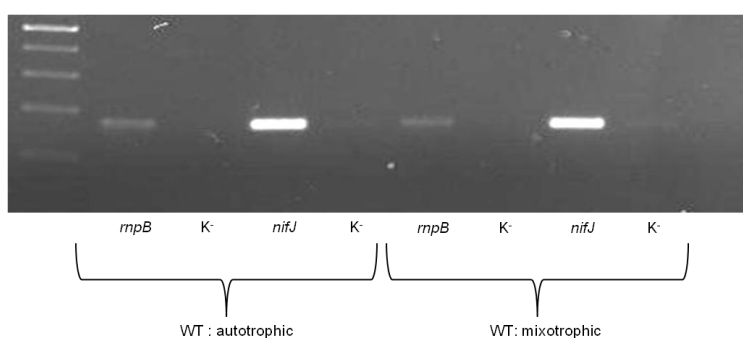
The NMR spectrum shows that acetate and formate were the dominant excretion products under mixotrophic conditions of both WT and $\Delta nifJ$ (Fig. 4.15). Acetate and formate appear both in the supernatant of the WT and $\Delta nifJ$ from day 3 on. Lactate could be detected in WT cultures from day 3 on, while it was found from day 6 on in $\Delta nifJ$ cultures. The growth medium of $\Delta nifJ$ contained ethanol from the very first day on, which was not detected in the growth medium of the WT.

The transcription of selected genes in WT and $\Delta nifJ$ cultures was investigated via qRT-PCR and the NADH/NAD⁺ ratio was determined colorimetrically.

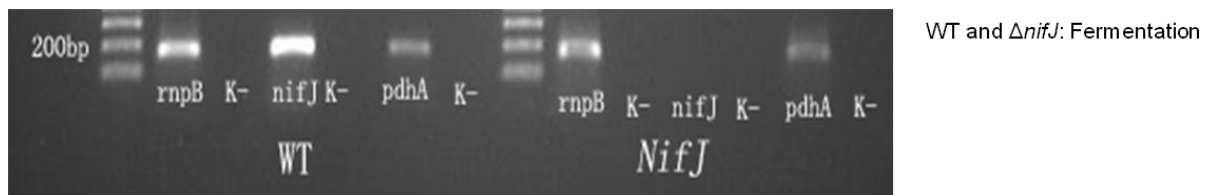
4.1.6 Transcription of selected genes in WT and $\Delta nifJ$ cultures under autotrophic, mixotrophic and fermentative conditions

NifJ codes for the pyruvate: ferredoxin oxidoreductase, which is described as an oxygen sensitive enzyme in many organisms (Bothe, *et al.*, 1974; Thauer, *et al.*, 1977; Neuer, *et al.*, 1982). It was however shown that *nifJ* is transcribed under aerobic conditions in the cyanobacteria *Synechococcus* sp. PCC 6301 and *Synechocystis* sp. PCC 6803 (Schmitz, *et al.*, 2001). Since the $\Delta nifJ$ mutant had a phenotype under mixotrophic conditions, its transcription was investigated via RT-PCR (Section 3.7.10) to gain an indication whether this phenotype was due to a direct or indirect effect of the deletion of *nifJ*. Beside *nifJ*, *pdhA* which codes for a subunit of the pyruvate-dehydrogenase complex and catalyzes a similar reaction as *nifJ* (Fig. 1.5) was tested. RNA was isolated from cells that were grown autotrophically or mixotrophically to an OD₇₅₀ of around 3. The cells for fermentative conditions were taken from cultures that were grown autotrophically to an OD₇₅₀ of around 3 and were incubated anaerobically for 7 days. As a reference gene *rnpB* was used. A sample in which RNA was replaced by water was used as a control (K).

(a)



(b)



(c)

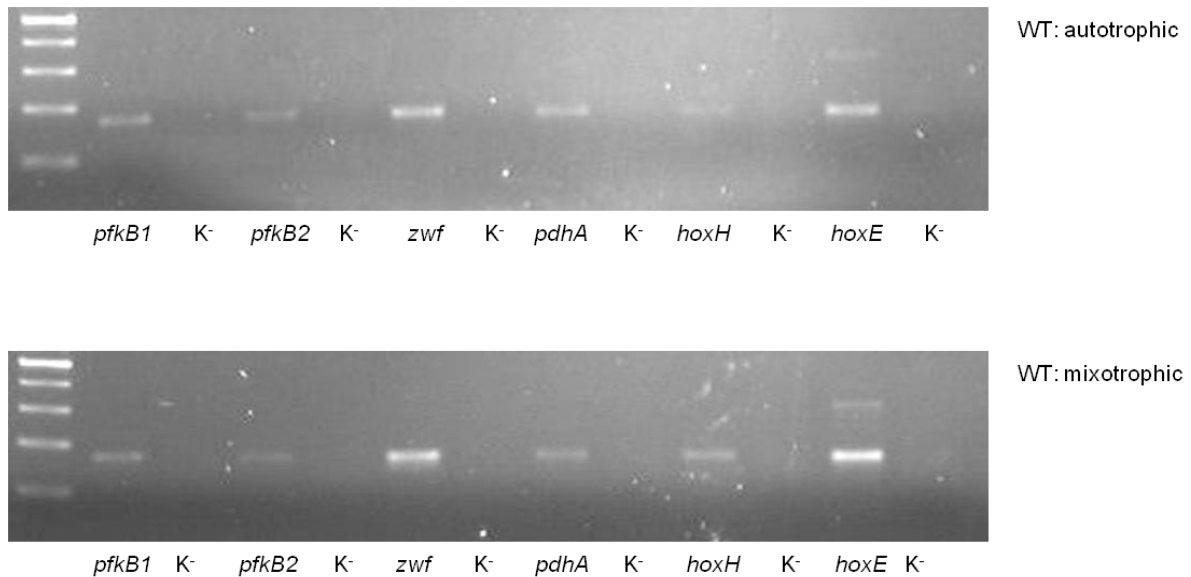


Fig. 4.16. Reverse transcription of *rnpB*, *nifJ*, *pdhA*, *hoxE*, *hoxH*, *pfkB1* and *pfkB2* under autotrophic, mixotrophic and fermentative conditions. *rnpB* used as reference gene and water as negative control (K⁻) (a) *nifJ* gene expression under autotrophic and mixotrophic conditions in WT (b) *nifJ* and *pdhA* genes expression under fermentative conditions in WT and $\Delta nifJ$ (c) *pfkB1*, *pfkB2*, *zwf*, *pdhA*, *hoxE* and *hoxH* genes expression under autotrophic and mixotrophic conditions in WT.

Figure 4.16 a and b show that *nifJ* is transcribed under autotrophic, mixotrophic and fermentative conditions in the WT, but as expected not under fermentative conditions in the $\Delta nifJ$ mutant. The expression of *nifJ* under mixotrophic conditions is consistent with the results for the growth of $\Delta nifJ$. Also *pdhA* was transcribed under autotrophic, mixotrophic and fermentative conditions (Fig. 4.16).

Previous to this study, it was shown in our group that NifJ might transfer electrons via ferredoxin / flavodoxin to the hydrogenase while catalyzing the oxidative cleavage from pyruvate and coenzyme A to acetylCoA and CO₂ (Kaspar, 2010). Hydrogen production is thus connected to the glucose degradation. In order to further characterize the glucose degradation pathways in *Synechocystis* under autotrophic

and mixotrophic conditions, the transcription of the key enzymes of the known glycolytic pathways were also investigated. The key enzyme of glycolysis, the 6-phosphofruktokinase is encoded by *pfkB1* and *pfkB2*. The key enzyme of the oxidative phosphate pentose pathway, the glucose-6-phosphate dehydrogenase is encoded by *zwf* (Fig. 1.3). Additionally *hoxH* and *hoxE* coding for subunits of the bidirectional [NiFe]-hydrogenase were also analyzed. As shown in figure 4.16 all genes were transcribed under both autotrophic and mixotrophic conditions in the WT.

Reverse Transcript-PCR (RT-PCR) only allows determining if a gene is transcribed or not. In order to analyze the expression level of genes in detail, quantitative real time PCR (qRT-PCR) has to be performed.

4.1.7 Pyruvate dehydrogenase complex deletion mutant construction

A targeted mutagenesis of *Synechocystis* is greatly facilitated by its natural transformability and spontaneous recombination.

In order to further analyze the function and interplay of NifJ and the pyruvate dehydrogenase complex it was attempted to construct a mutant without a functioning pyruvate dehydrogenase complex (Section 3.7.6).

Table 4.1. The subunits of PDH complex

Enzyme	Abbrev.	Cofactor(s)	# subunits prokaryotes
pyruvatedehydrogenase	E1	TPP (thiamine pyrophosphate)	24
dihydrolipoyl transacetylase	E2	lipoate coenzyme A	24
dihydrolipoyl dehydrogenase	E3	FAD NAD ⁺	12

The Pyruvate dehydrogenase complex is organized in cubic symmetry in prokaryotes, having 60 subunits (Table 4.1) in three functional proteins (Mattevi, *et al.*, 1992). The E1 (pyruvate dehydrogenase) - catalyzed process is the rate-limiting step of the reaction. PDH complex's key genes are *pdhA* and *pdhB*, which encode complex E1 component alpha and beta subunits respectively. For the construction of the mutant, *pdhA* should be replaced by a spectinomycin resistance cassette (Sp).

In order to obtain a *pdhA* mutant, homologous regions up- and down-stream of the open reading frame of *pdhA* were fused to the spectinomycin resistance cassette by fusion PCR. The sequence of *pdhA* and the primers used are shown below:

The sequence of *pdhA* was obtained from NCBI:

pdhA slr1394 pyruvate dehydrogenase E1 component subunit alpha [*Synechocystis* sp. PCC 6803]

>gi|16329170:2230332-2231668 *Synechocystis* sp. PCC 6803 chromosome, complete genome

```
GGCTACCGATTACCAATGAAACACTCACAATGCTCAAAGACCAAAGTGATCAGATTGTGTTCTATC
CTACCCCGACTAGATGGGGCTGACCGACTTCGCATAGAATCTAACAGGGATATAAAACCCCTTCC
CCTTTATCTACTGCAAATTGTAATGTTTCAGAACGCATTTTGCCTGAATTGAACACCGCAGAA
ATTTCCCTGGACAGAGAAACCGCCTTAGTGCTTACGAAGACATGGTCCTGGGTGCGTTCTTCGA
GGATAAATGCGCTGAGATGTATTACCGGGGCAAATGTTTGGTTTTGTCCACCTCTACAACGGCC
AGGAAGCGGTGTCCTCTGGGATAATCAAAGCCATGCGCCAGGATGAGGATTACGTTTGCAGTAC
CTATCGAGACCATGTTTCATGCCCTCAGTGCGGGAGTTCCAGCTCGGGAAGTAATGGCGGAACTG
TTTGGTAAGGAAACCGGTTGCAGTCGGGGTCGGGGTGGTTCTATGCACCTATTTTCTCGGCC
ATAATCTCCTGGGGGGCTTTGCGTTCATCGGGGAAGGATTCCCGTGGCCCTGGGAGCGGCGT
TTCAAATAAGTACCGCCGGGAAGTGTGAAAGATGACGGCTACGACCAAGTTACCGCCTGTTTC
TTCGGTGATGGCACCAGTAATAACGGCCAGTTTTTTGAATGCCTGAACATGGCCGCCCTGTGGAA
ACTGCCCATTTCTGTTTGTGGTGGAAAATAATAAATGGGCGATCGGTATGGCCCACGAGCGGGCA
ACGTCCCAACCAGAAATCTACAAAAAAGCCAGTGTGTTCAACATGGTGGGGGTAGAAGTGGATG
GTATGGATGTGGTGGCAATGCATAAAGTAGCAACGGAAGCAGTGGCTAGGGCCAGGGCAGGCG
AAGGGCCTACCTTGATTGAAGCGTTGACCTATCGTTTCCGGGGTCACTCCCTAGCGGATCCCGAT
GAACTCCGTTCTGCCGAAGAAAAACAGTTTTTGGGCTGCCCGGGACCCAATTAAGAAATTTGCCGC
TTTCATGACGGAACACGAATTAGCCAGCAATGAAGAGCTAAAGGCGATCGATAAACGCATTCAAG
AAGTAATTGACGATGCCCTGGCCTTTGCCGAGTCTAGCCCCGAACCAATCCCGAAGATCTGAG
GAAATATATTTTCGCCGATTAGTATGCTGGGGGAGCGGCGCAATACGTTACCGTTTGGGAGAAT
GGAATAGTTAACCGTGGGAGTTTGTATGATTGTGCTCCTGATCGATTAAGTGCCTATTTTCT
CCTACCCCTGTGCATGGAATCTAAGTTGCTGAGTGCAAATCAA
```

The parameters of primers used to construct the $\Delta pdhA$ mutant are listed in table 4.2.

Table 4.2. The primers used for the PDH complex mutant construction.

(a) Primers used in this work for amplifying *pdhA* upstream sequence

name	pdha-1 (Table 3.3)	pdha-in1 (Table 3.3)
Length (bp)	20	40
GC%	55	62.5
Tm (°C)	60	
Product length (bp)	155	

(b) Primers used in this work for amplifying *pdhA* downstream sequence

name	pdha-in2 (Table 3.3)	pdha-2 (Table 3.3)
Length (bp)	45	20
GC%	50	55
Tm (°C)	60	
Product length (bp)	311	

(c) Primers used in this work for amplifying spectinomycin resistance gene

name	Sp f (Table 3.3)	Sp r (Table 3.3)
Length (bp)	20	25
GC%	70	48
Tm (°C)	60	
Product length (bp)	1747	

The fusion product of *pdhA*-fragments and spectinomycin resistance cassette were cloned into the Topo-Vector and its sequence was verified by sequencing. The construct was used to transform the *Synechocystis* WT. However it was not possible to obtain $\Delta pdhA$ mutants. The pyruvate dehydrogenase complex might thus be essential for the survival of *Synechocystis*.

4.1.8 Quantitative real time PCR for *nifJ* and *pdhA* genes

Transcription levels of the *nifJ* and *pdhA* were investigated in WT cells and $\Delta nifJ$ cells under autotrophic and mixotrophic conditions by quantitative real time PCR (qRT-PCR, see section 3.7.11). *16S* and *rnpB* were used as reference genes.

The primer efficiencies (Table 4.3) were investigated and calculated accordant to the formula shown in 3.7.11. Primers creating two different amplicon lengths (approx. 50 bp and 90 bp) were used. The differences in amplicon lengths had no influence on the efficiency with which genes were amplified.

The transcription of *nifJ* and *pdhA* was compared between autotrophic and mixotrophic conditions in WT and $\Delta nifJ$ cultures (Fig. 4.14).

Table 4.3. Efficiency of different genes with different primer lengths.

gene	Primer pair (see table 3.3)	Product length (bp)	Primer efficiency
<i>16S</i>	16s-50f, 16s-50r	50	2.026
	16s-91f, 16s-91r	91	2.030
<i>rnpB</i>	rnpB-50f, rnpB-50r	50	2.031
	rnpB-80f, rnpB-80r	80	1.986
<i>nifJ</i>	nifJ-50r, nifJ-50f	50	2.140
	nifJ-93r, nifJ-93f	93	1.951
<i>pdhA</i>	pdhA-50f, pdhA-50r	54	1.972
	pdhA-85f, pdhA-85r	85	1.983

RNA was isolated on day 0, 3, 5, 7 and 11. *16S* and *rnpB* were chosen to serve as reference genes. The expression ratios (mixotrophic expression / autotrophic expression) of both genes were in the range of 0.99 – 1.02 which showed that the transcript expression of housekeeping genes were not changed during growth conditions shift and two primers have little expression difference (Fig. 4.17). *RnpB* and *16S* were used to calculate the expression ratio of target genes.

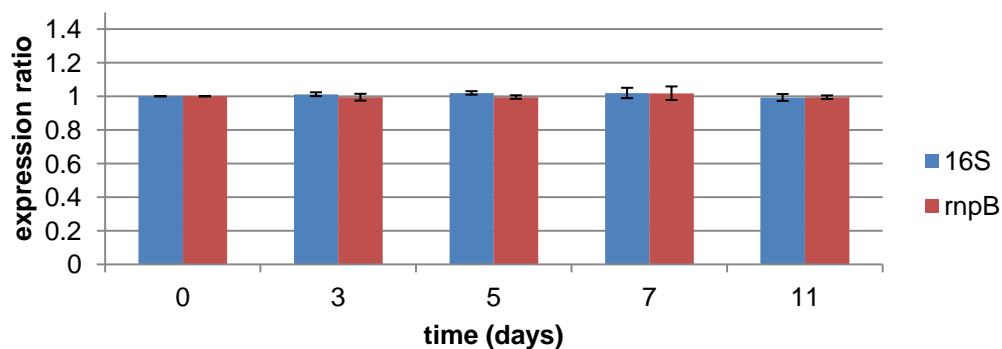


Fig. 4.17. Expression ratio of reference genes *16S* and *rnpB* under mixotrophic / autotrophic conditions on day 0, 3, 5, 7, and 11 in WT cultures.

As the expression ratios of *nifJ* transcription under mixotrophic to autotrophic conditions in the WT is shown in figure 4.18 and figure 4.19. The transcription of *nifJ* was slightly up-regulated under mixotrophic conditions at day 5, but after that no expression was observed at day 7 and day 11 (Fig. 4.18 a). The expression level of *pdhA* was already higher under mixotrophic conditions on day 3 and increased

further on day 5 (about 6 fold) (Fig. 4.18 b). When the growth reached the stationary phase, the expression of *pdhA* was repressed to the level in autotrophic cultures and even lower at Day 11. The relative expression of *pdhA* in $\Delta nifJ$ cultures was up-regulated from day 3 to day 7 under mixotrophic conditions but dropped on day 11 (Fig. 4.18 c). The expression of both *nifJ* and *pdhA* was most strongly enhanced in the mixotrophic cultures on day 5. The relative drop down in the transcription of both genes on day 7 can be attributed to the fact, that the glucose had been consumed on day 7 in both WT and $\Delta nifJ$ cultures (Fig. 4.15).

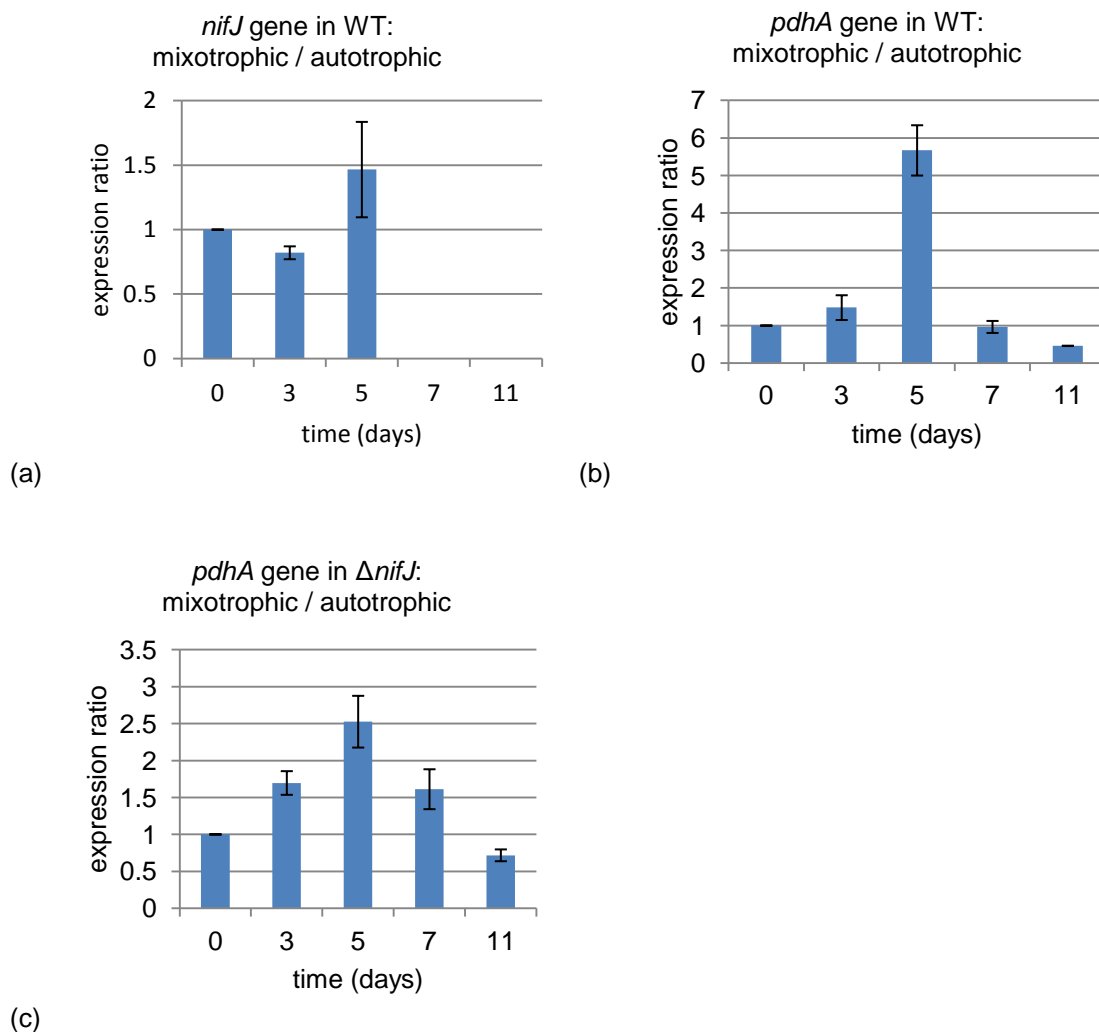


Fig. 4.18. qRT-PCR results about the expression ratio of the transcripts of *nifJ* and *pdhA* under mixotrophic conditions to autotrophic conditions at different time points. *RnpB* used as reference gene. (a) Expression ratio of *nifJ* under mixotrophic / autotrophic conditions on day 0, 3, 5, 7, and 11 in WT cultures. (b) Expression ratio of *pdhA* under mixotrophic / autotrophic conditions on day 0, 3, 5, 7, and 11 in WT cultures. (c) Expression ratio of *pdhA* under mixotrophic / autotrophic conditions on day 0, 3, 5, 7, and 11 in $\Delta nifJ$ cultures.

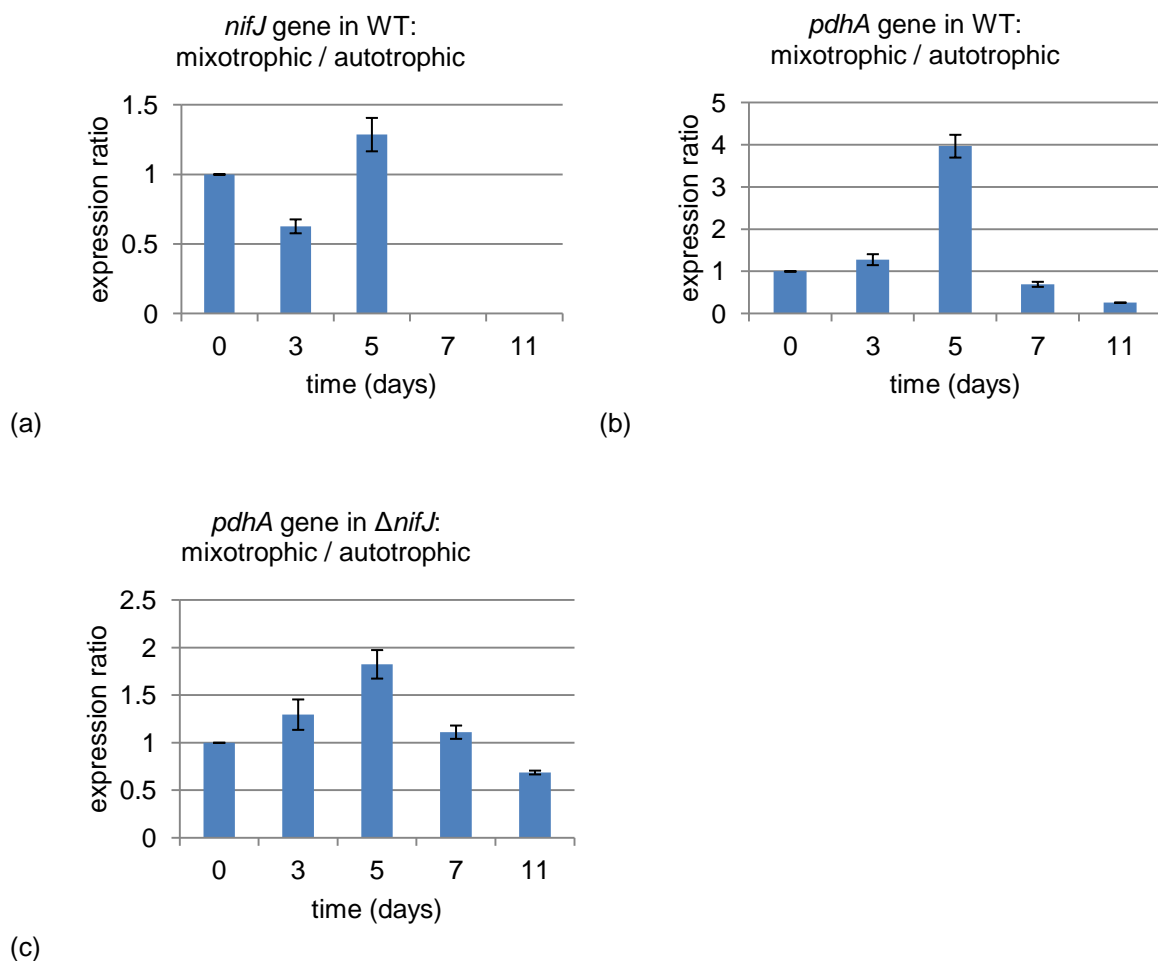


Fig. 4.19. qRT-PCR results about the expression ratio of the transcripts of *nifJ* and *pdhA* under mixotrophic conditions to autotrophic conditions at different time points. *16S* used as reference gene. (a) Expression ratio of *nifJ* under mixotrophic / autotrophic conditions on day 0, 3, 5, 7, and 11 in WT cultures. (b) Expression ratio of *pdhA* under mixotrophic / autotrophic conditions on day 0, 3, 5, 7, and 11 in WT cultures. (c) Expression ratio of *pdhA* under mixotrophic / autotrophic conditions on day 0, 3, 5, 7, and 11 in $\Delta nifJ$ cultures.

To get a more detailed picture of the expression of *nifJ* and *pdhA* under mixotrophic conditions earlier time points (0h, 0.5h, 6h, 24h, 48h, 72h after addition of glucose) were chosen for RNA extraction (Fig. 4.20). Neither *nifJ* nor *pdhA* were up-regulated upon the addition of glucose within the first 24 hours in the WT (Fig. 4.21 a and c). The expression of *pdhA* increased 48h after glucose addition and the expression of *nifJ* slightly increased after 72h in the WT. The onsets of decreasing growth detected here were different with ones shown in figure 4.14, this might be due to the utilization of different batch of cultures. The start incubation OD_{750} of these batch cultures was around 2, while the others were around 0.04. Also slight differences in the medium

that can never be totally excluded, in the light intensity, and temperature might also affect the transcript expression.

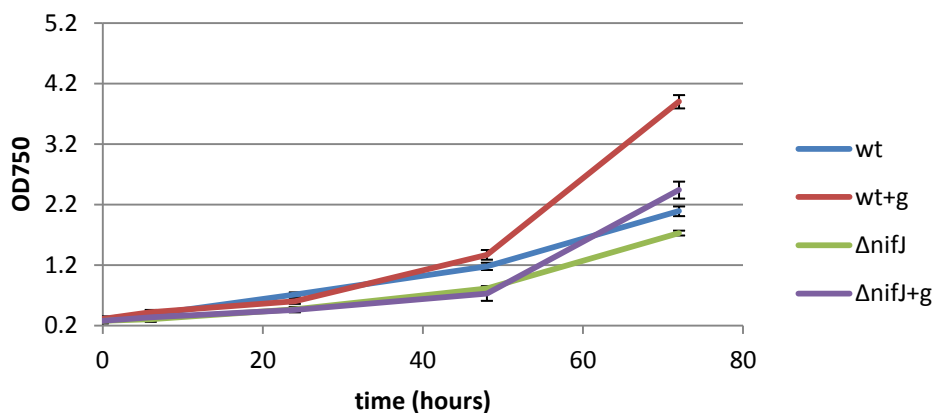


Fig. 4.20. Growth curves of WT and $\Delta nifJ$ mutants under autotrophic and mixotrophic conditions for qRT-PCR experiments.

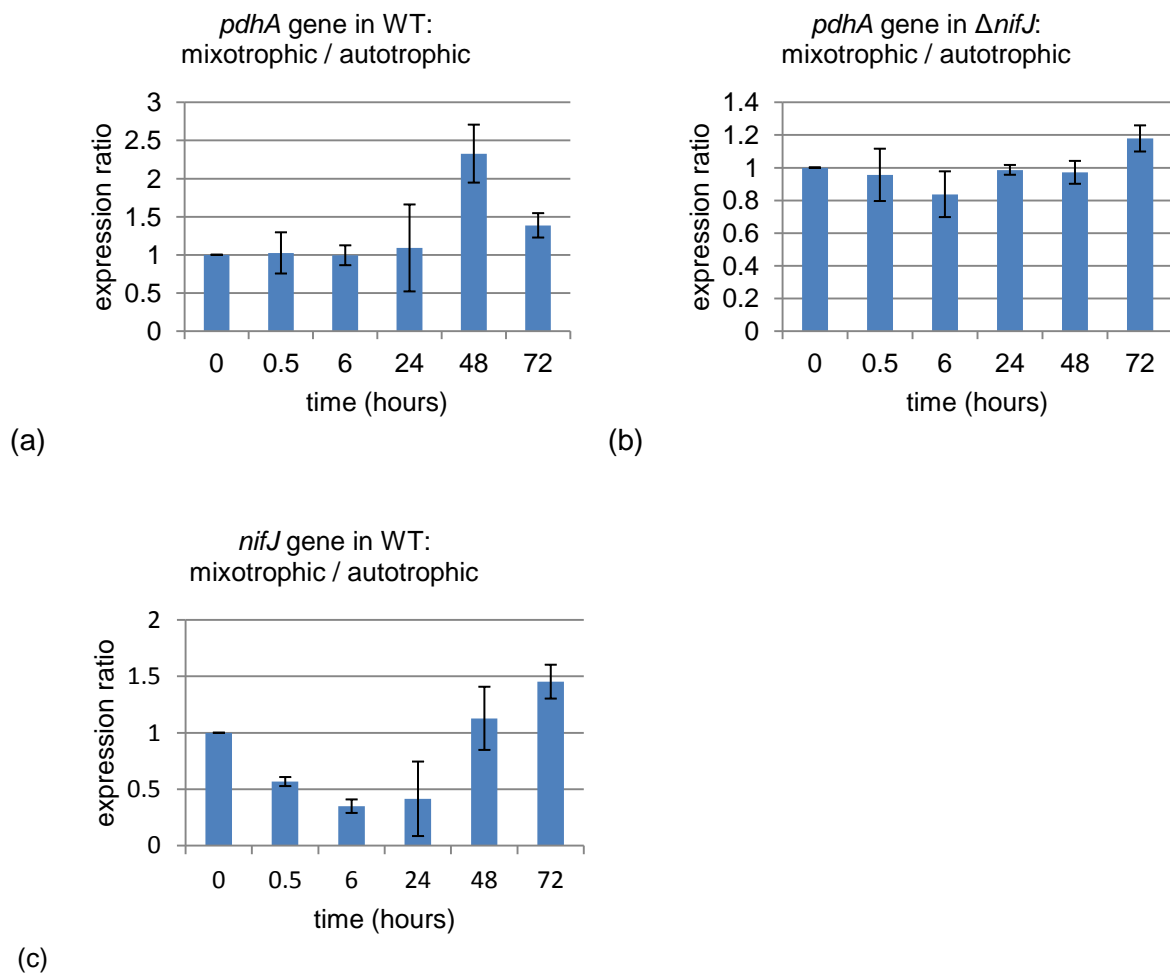


Fig. 4.21. qRT-PCR results about the expression ratio of the transcripts of *nifJ* and *pdhA* under mixotrophic conditions to autotrophic conditions at different time points. *RnpB* used as reference gene.

(a) Expression ratio of *pdhA* under mixotrophic / autotrophic conditions 0h, 0.5h, 6h, 24h, 48h and 72 after addition of glucose in WT cultures; (b) Expression ratio of *pdhA* under mixotrophic / autotrophic conditions 0h, 0.5h, 6h, 24h, 48h and 72 after addition of glucose in $\Delta nifJ$ cultures; (c) Expression ratio of *nifJ* under mixotrophic / autotrophic conditions 0h, 6h, 24h, 48h and 72 after addition of glucose in WT cultures.

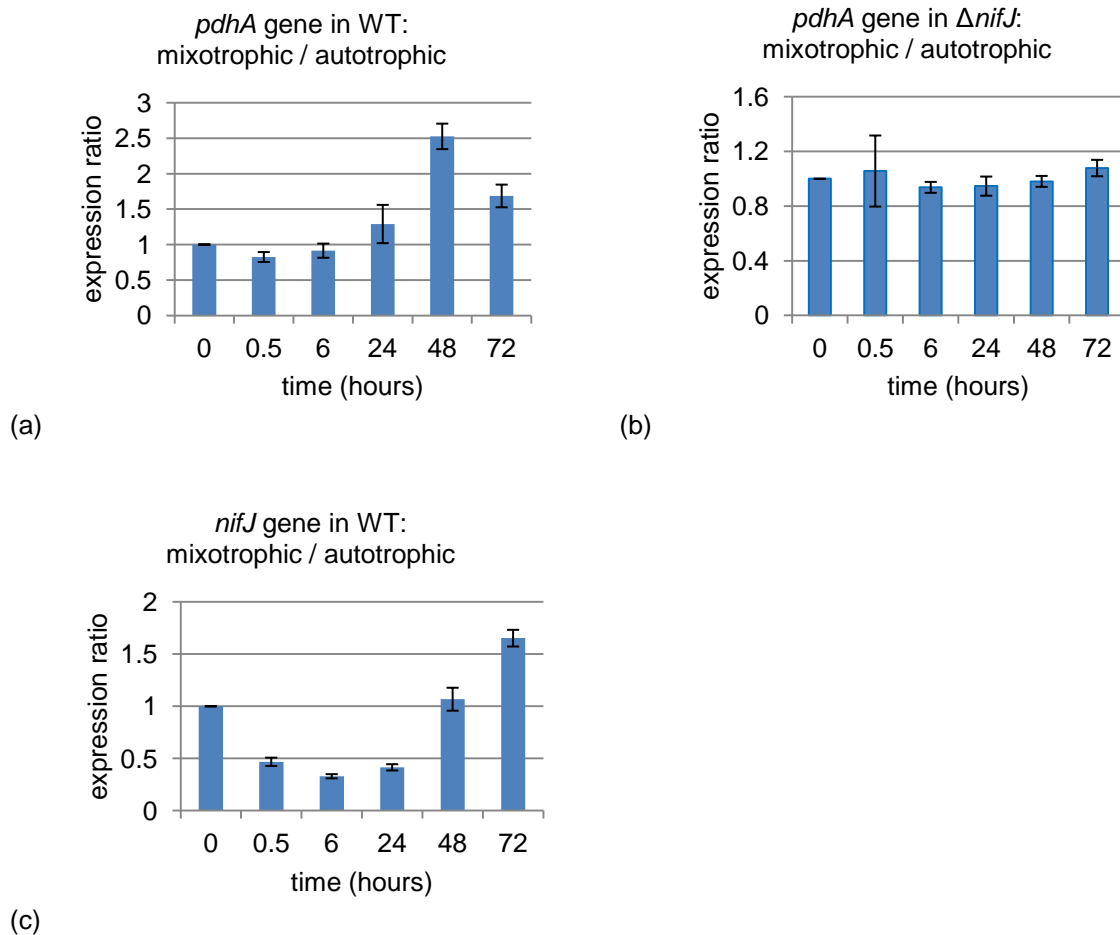
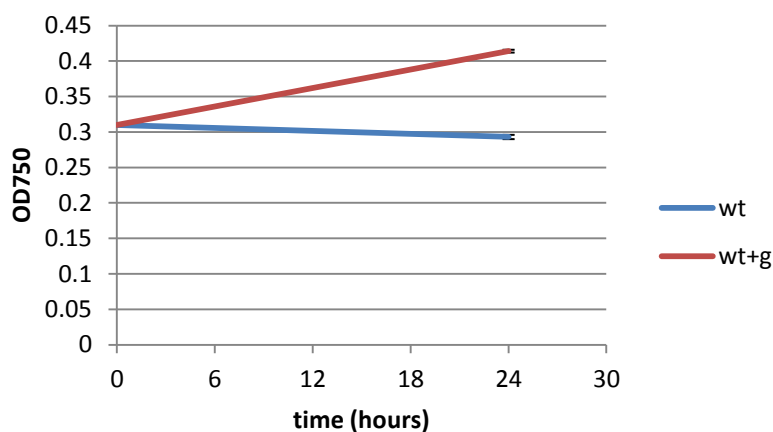


Fig. 4.22. qRT-PCR results about the expression ratio of the transcripts of *nifJ* and *pdhA* under mixotrophic conditions to autotrophic conditions at different time points. *16S* used as reference gene. (a) Expression ratio of *pdhA* under mixotrophic / autotrophic conditions 0h, 0.5h, 6h, 24h, 48h and 72 after addition of glucose in WT cultures; (b) Expression ratio of *pdhA* under mixotrophic / autotrophic conditions 0h, 0.5h, 6h, 24h, 48h and 72 after addition of glucose in $\Delta nifJ$ cultures; (c) Expression ratio of *nifJ* under mixotrophic / autotrophic conditions 0h, 6h, 24h, 48h and 72 after addition of glucose in WT cultures.

Whether *16S* or *rnpB* were used as reference genes had no influence on the trend of the expression ratios (Fig. 4.18 and Fig. 4.19, Fig. 4.21 and Fig. 4.22).

(a)



(b)

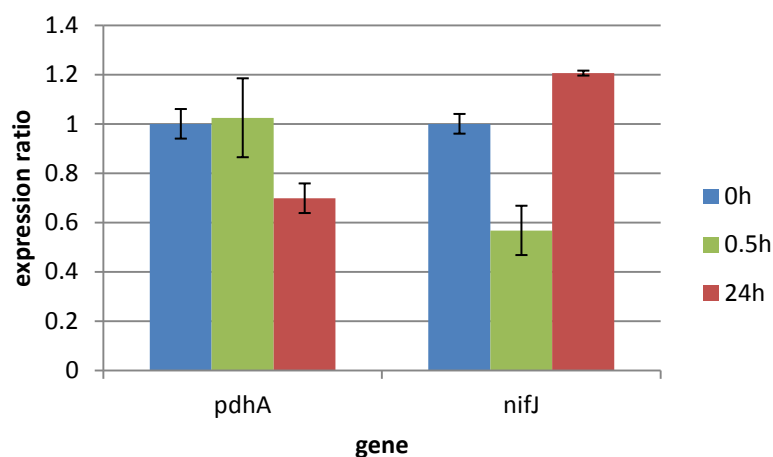


Fig. 4.23. Expression ratio of *pdhA* and *nifJ* under mixotrophic / autotrophic conditions after 0h, 0.5h and 24h of dark incubation in WT cultures. (a) the growth curves of wt autotrophic and mixotrophic cultures; (b) qRT-PCR results for expression ratio of *pdhA* and *nifJ*, *mpB* used as reference gene.

Additionally, the expression ratio of *pdhA* and *nifJ* was monitored in mixotrophic to autotrophic cultures that were bubbled with air and grown for one day in the dark (Fig. 4.23). Within 24h the expression ratio of *pdhA* decreased slightly and the expression level of *nifJ* increased under these conditions.

4.1.9 Colorimetric NADH/ NAD⁺ Determination

The transcriptional analyses show that both *pdhA* and *nifJ* are expressed under mixotrophic conditions. They furthermore tend to be up-regulated, when glucose is metabolized. As both enzymes basically catalyze the same reaction (Fig. 1.5), the

question remains to be answered why the pyruvate dehydrogenase complex is not able to functionally replace NifJ in the $\Delta nifJ$ mutants under mixotrophic conditions. One difference between the reaction catalyzed by the pyruvate dehydrogenase complex and NifJ is that NAD^+ is reduced to NADH in the first case, but ferredoxin is reduced in the latter case. It was therefore hypothesized that $\Delta nifJ$ mutants might suffer from a high NADH/ NAD^+ ratio under mixotrophic conditions that might slow down the glucose breakdown due to missing NAD^+ . A lack of NAD^+ might also block the cleavage of pyruvate via the pyruvate dehydrogenase complex, which would leave NifJ as the only enzyme to carry out the reaction. It is additionally known from some gram negative bacteria cells that high NADH concentrations in the cells result in the phosphorylation of the *pdhA* subunit of the pyruvate dehydrogenase complex which inactivates the enzyme complex (de Kok, *et al.*, 1998). For the case that this should happen in *Synechocystis*, NifJ might be an essential enzyme under mixotrophic conditions to cleave pyruvate. Therefore the NADH/ NAD^+ ratio of WT and $\Delta nifJ$ cultures was determined (Section 3.8.1) under autotrophic and mixotrophic conditions.

The intracellular concentrations of NAD^+ and NADH were determined in the cultures shown in figure 4.14 0 h, 6 h, 24 h and then further every 24 hours over 10 days (Fig. 4.24).

The ratio of NADH to NAD^+ in WT and $\Delta nifJ$ cultures was similar under autotrophic conditions over the 10 days and was stable at a rather low level (Fig. 4.24). However under mixotrophic conditions the NADH to NAD^+ was higher in $\Delta nifJ$ cultures compared to WT cultures. NADH concentrations raised in both mixotrophic cultures during the exponential growth phase (Fig. 4.14) in which glucose was metabolized (Fig. 4.15) and reached its maximum after 120 h on day 5. When the cultures reached the stationary growth phase, the NADH/ NAD^+ ratio decreased.

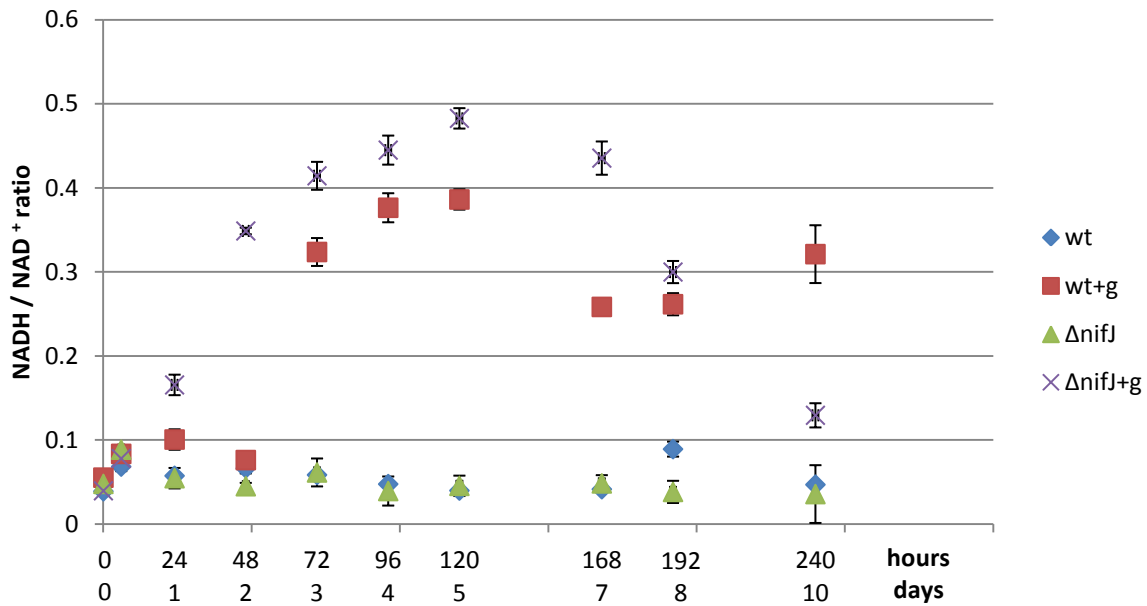
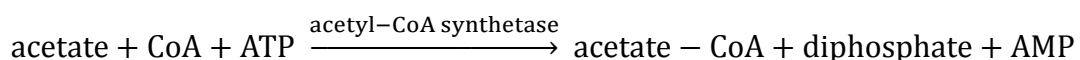


Fig. 4.24. Time course of the NADH / NAD⁺ ratio (0h, 24h, 48h, 72h, 96h, 120h, 168h, 192h, 240h) in WT and $\Delta nifJ$ cultures under autotrophic and mixotrophic (+g) conditions.

These results confirm the hypothesis that $\Delta nifJ$ cultures have a higher NADH/NAD⁺ ratio under mixotrophic conditions, which might partly explain their difficulty to metabolize glucose with the same efficiency as WT cultures.

4.1.10 Investigation of acetate feedback effect

If the pyruvate dehydrogenase complex should be inactivated due to the high NADH/NAD⁺ ratio in WT and $\Delta nifJ$ cultures at a certain time point under mixotrophic conditions, the $\Delta nifJ$ cells might have problems to supply the TCA cycle with acetyl-CoA. This would result in a lack of metabolic intermediates that are normally provided by the TCA cycle. In order to check whether this could be the reason for the decreased growth of $\Delta nifJ$ under mixotrophic conditions, the cultures were supplemented with 10 mM acetate. Acetate can be converted to acetyl-CoA to supply the TCA cycle:



It can be seen in figure 4.25 that the addition of 10 mM acetate had no big effect on the growth of the WT under mixotrophic conditions. However, when acetate was added to the mixotrophic $\Delta nifJ$ cultures, their growth had not the characteristic bend

around day 7 but the cultures continued to grow (compare *nifJ*+g and *nifJ*+g+ac in figure 4.25).

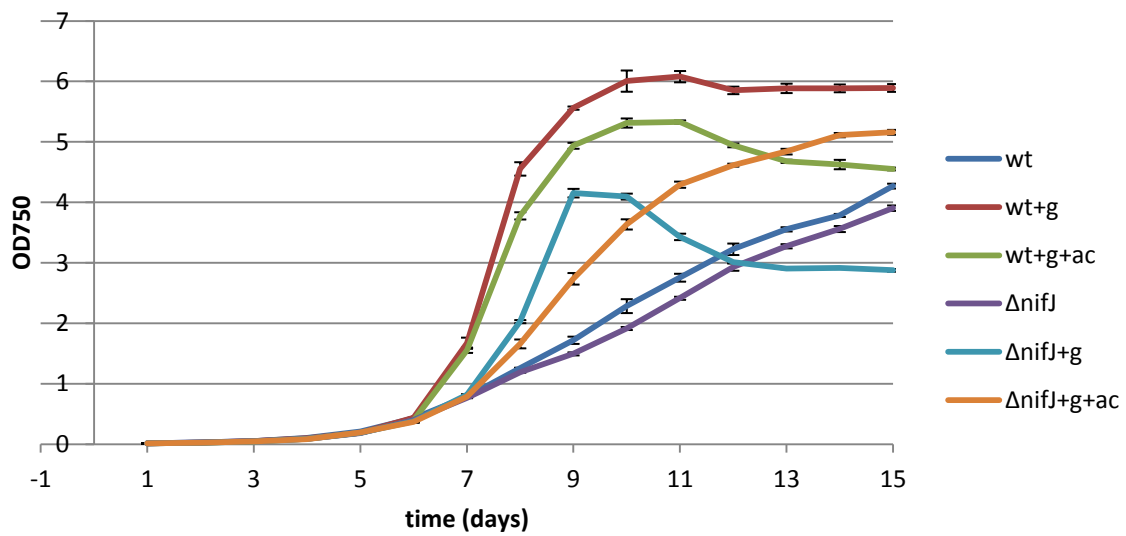


Fig. 4.25. Growth curves of WT and $\Delta nifJ$ cultures grown autotrophically, mixotrophically (+g) or mixotrophically with acetate (+g+ac).

These results thus confirm the hypothesis that the decreased growth of $\Delta nifJ$ under mixotrophic conditions might be due to a restricted operation of the TCA cycle.

4.2 Characterization of glycolytic pathways in *Synechocystis* sp. PCC 6803

As the results have already shown in 4.1, exogenous glucose has a different physiological effect on the WT of *Synechocystis* compared to the $\Delta nifJ$ mutant of *Synechocystis*. The $\Delta nifJ$ cultures were not able to reach the same optical density at 750 nm as the WT when their medium was supplemented with the same amount of glucose (Fig. 4.1), and the activity of Cyt bd oxidase was elevated at the early stage (the second day of incubation, Fig. 4.7) under mixotrophic conditions in the mutant. These results might indicate that PFOR is involved in the glucose degradation in *Synechocystis* in the light beside the PDH complex. This is in agreement with the qRT-PCR results which show that the transcripts of *nifJ* and *pdhA* were both expressed under mixotrophic conditions (Fig. 4.15). This phenomenon is consistent with the reports by Schmitz, *et al.* (2001) who found that *nifJ* is expressed under aerobic conditions even though the enzyme is regarded as being inactivated by oxygen (Neuer, *et al.*, 1982). We could show that the hydrogenase is connected to NifJ and furthermore that the hydrogenase is essential under mixotrophic nitrate-limiting conditions (Fig. 4.13, Gutekunst, *et al.*, 2014). In order to understand the physiology of NifJ and the hydrogenase in more detail, the glucose degradation pathways were investigated.

It is known that glucose catabolism in *Synechocystis* is carried out through the Embden-Meyerhof-Parnas pathway (EMP, often simply “glycolysis”) and alternatively through the oxidative pentose phosphate pathway (OPP) (Yoshikawa, *et al.*, 2013). However, it is still under debate how these two different glycolytic pathways cooperate with each other and which one is more important under mixotrophic conditions in *Synechocystis*.

In order to get a more detailed picture of the situation under mixotrophic conditions the key enzymes of both glucose degradation pathways were deleted. The phosphofructokinase (encoded by *pfkB1* and *pfkB2*, Table 1.1 and Fig. 4.26) was knocked out to interrupt the EMP pathway and the glucose-6-phosphate dehydrogenase (G6PDH encoded by *zwf*, Table 1.1 and Fig. 4.26) was knocked out to interrupt the OPP pathway. Furthermore a triple mutant was constructed in which both key enzymes of the EMP pathway (*pfkB1*, *pfkB2*) as well as the key enzyme of

the OPP pathway (*zwf*) were deleted. The gene *nifJ* was also deleted in the Δzwf and the $\Delta pfkB1B2$ mutant. The $\Delta nifjzwf$ and $\Delta nifjpfkB1B2$ mutant were however not yet characterized.

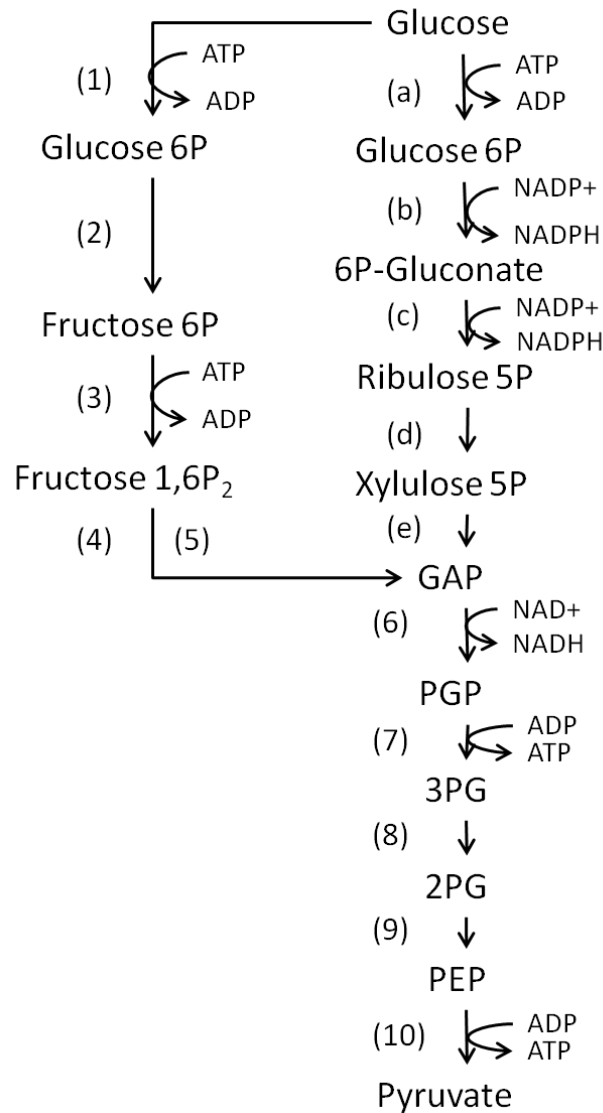


Fig. 4.26. Routes of glucose catabolism in *Synechocystis* based on glucose catabolism in bacteria and archaea as shown by Verhees, *et al.* (2003): EMP (1-10), OPP (a-e, 6-10). Abbreviated metabolites are: P, phosphate; Fructose 1,6P₂, fructose 1,6-bisphosphate; GAP, glyceraldehyde 3-phosphate; PGP, 2,3-bisphosphoglycerate; 2PG, 2-phosphoglycerate; 3PG, 3-phosphoglycerate; PEP, phosphoenolpyruvate. Key to enzymes: (1) (a) glucokinase; (2) phosphoglucose isomerase; (3) phosphofructokinase; (4) fructose 1,6-bisphosphate aldolase; (5) triosephosphate isomerase; (6) glyceraldehydes phosphate dehydrogenase; (7) phospholycerate kinase; (8) phosphoglycerate mutase; (9) enolase; (10) pyruvate kinase; (b) glucose-6-phosphate dehydrogenase; (c) 6-phosphogluconate dehydrogenase; (d) ribulose-5-phosphate 3-epimerase; (e) transketolase.

4.2.1 Construction of mutants with interrupted glucose degradation pathways in *Synechocystis* sp. PCC 6803

4.2.1.1 Mutant construction

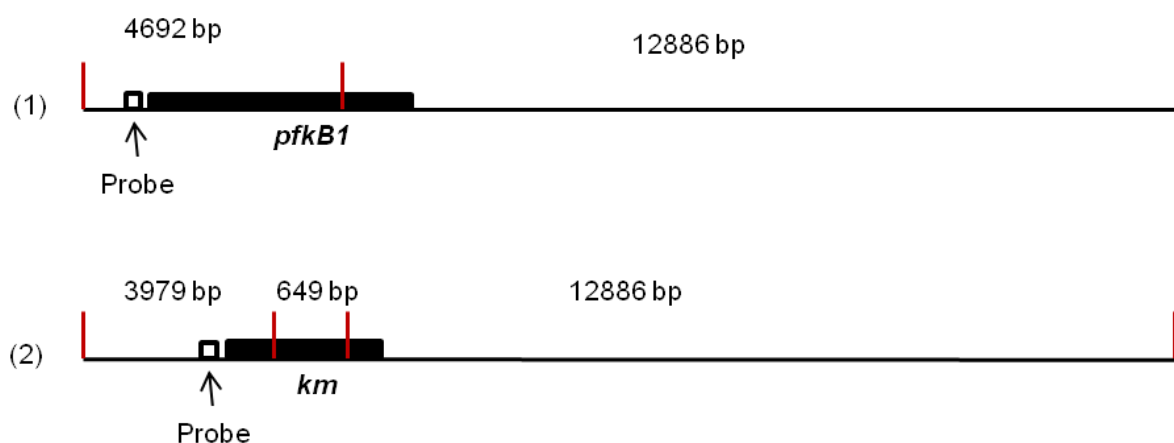
The mutation strategy was as previously described in section 3.7.6.

The gene *zwf* was replaced by a chloramphenicol-resistance cassette (primer pairs: *zwf*-1, *zwf*-in1, *zwf*-2, *zwf*-in2, Cm r, Cm f, see Table 3.3), *pfkB1* by a kanamycin-resistance cassette (primer pairs: *pfkB1*-1, *pfkB1*-in1, *pfkB1*-2, *pfkB1*-in2, Km f, Km r, see Table 3.3), *pfkB2* by a spectinomycin-resistance cassette (primer pairs: *pfkB2*-1, *pfkB2*-in1, *pfkB2*-2, *pfkB2*-in2, Sp f, Sp r, see Table 3.3) and *nifJ* by erythromycin resistance cassette (*nifJ*-1, *nifJ*-in1, *nifJ*-2, *nifJ*-in2, Em F, Em R, see Table 3.3).

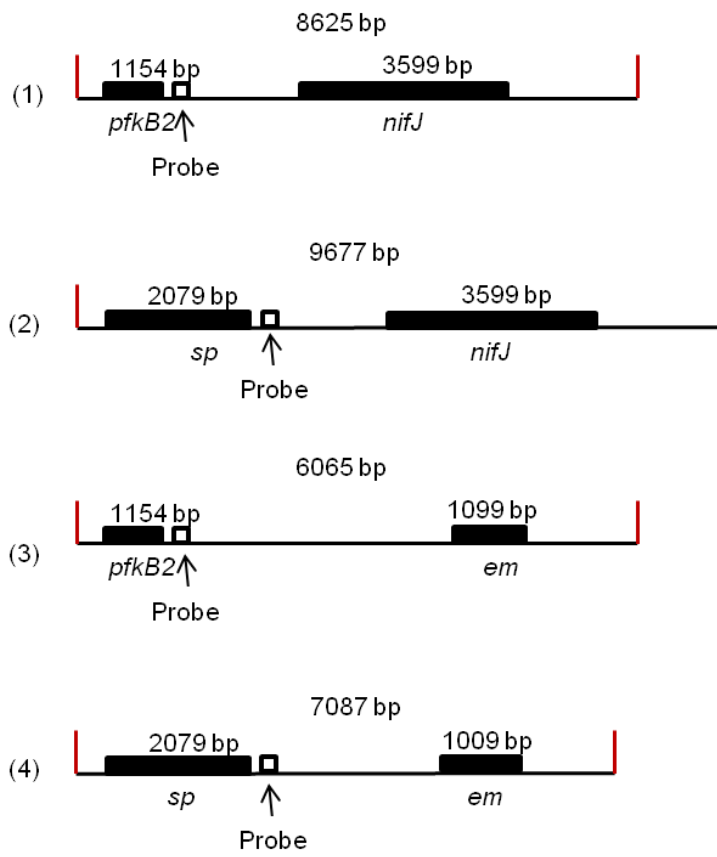
As *Synechocystis* harbors multiple copies of its genomes (Stal, *et al.*, 1997), it was checked by Southern blot whether the gene had been deleted out of each genome copy.

The genomic DNA of WT and all mutants were isolated and digested with HindIII.

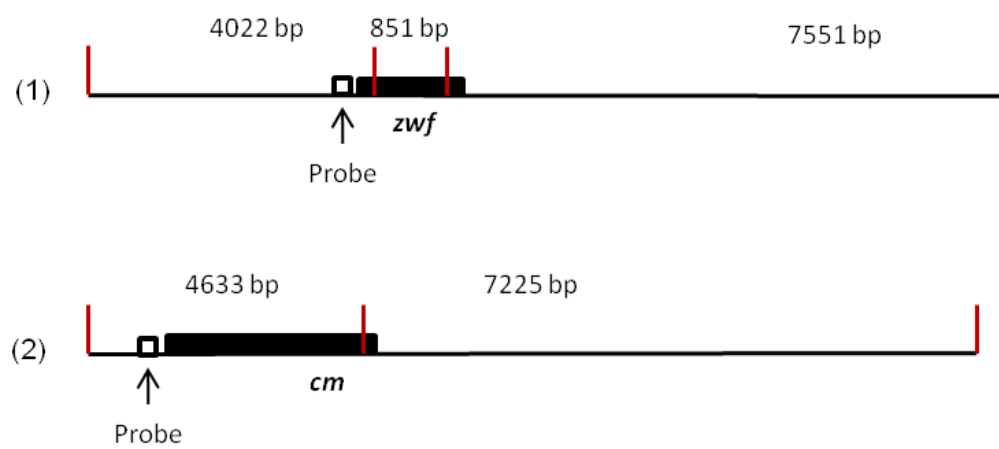
(a)



(b)



(c)



(d)

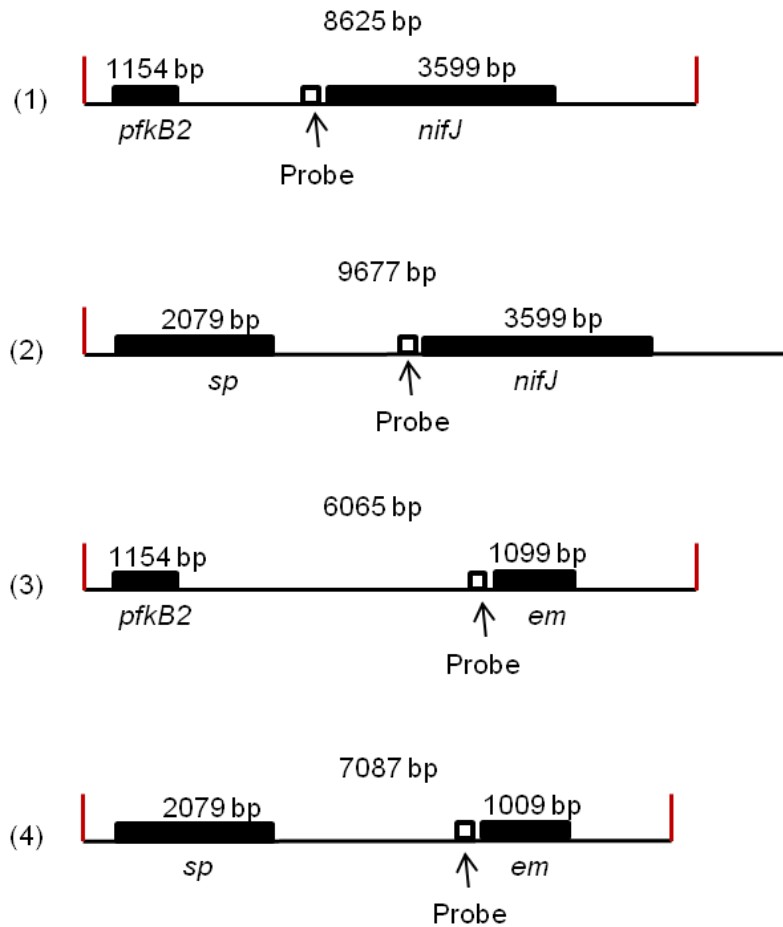


Fig. 4.27. Position of HindIII restriction sites (shown in red) and hybridization site of applied PCR-probe in different genes. (a) Gene *pfkB1*: mutation in WT (1) and *pfkB1pfkB2*, *zwf**pfkB1B2*, *nifJ**pfkB1B2* (2); (b) Gene *pfkB2*: mutation in WT (1) and *pfkB1pfkB2*, *zwf**pfkB1B2* (2), *nifJ**pfkB1B2* (4), and not mutated in *zwfnifJ* (3); (c) Gene *zwf*: mutation in WT (1) and *zwf**pfkB1B2*, *zwfnifJ* (2); (d) Gene *nifJ*: mutation in WT (1) and *zwfnifJ* (3), *nifJ**pfkB1B2* (4), and not mutated in *pfkB1pfkB2*, *zwf**pfkB1B2* (2). km = kanamycin resistance cassette; sp = spectinomycin resistance cassette; em = erythromycin resistance cassette; cm = chloramphenicol resistance cassette

As shown in figure 4.27 the restriction enzyme HindIII cuts in the open reading frame of *pfkB1* once, not in *pfkB2*, twice in *zwf* and not in *nifJ*. The enzyme cuts in the kanamycin-resistance cassette twice, not in the spectinomycin-, once in the chloramphenicol- and not in the erythromycin- resistance cassettes (Fig. 4.27). This allowed us to discriminate between WT copies and mutated copies in the cultures. The expected visible band sizes from WT and mutants in the Southern blot with the different probes are listed in table 4.4.

Table 4.4. Expected visible bands in the Southern blot dependent on the WT/mutant hybridized with different probes (for explanation see figure 4.27).

WT/mutant	probe	fragment size in Southern blot (in bp)
WT	pfkB1	4692
<i>pfkB1</i>	pfkB1	3979
<i>pfkB1B2</i>	pfkB1	3979
<i>zwf</i> <i>pfkB1B2</i>	pfkB1	3979
<i>nifJ</i> <i>pfkB1B2</i>	pfkB1	3979
<i>zwfnifJ</i>	pfkB1	4692
WT	pfkB2	8625
<i>pfkB2</i>	pfkB2	9677
<i>pfkB1B2</i>	pfkB2	9677
<i>zwf</i> <i>pfkB1B2</i>	pfkB2	9677
<i>nifJ</i> <i>pfkB1B2</i>	pfkB2	7087
<i>zwfnifJ</i>	pfkB2	6065
WT	zwf	4022
<i>zwf</i>	zwf	4633
<i>pfkB1B2</i>	zwf	4022
<i>zwf</i> <i>pfkB1B2</i>	zwf	4633
<i>nifJ</i> <i>pfkB1B2</i>	zwf	4022
<i>zwfnifJ</i>	zwf	4633
WT	nifJ	8625
<i>nifJ</i>	nifJ	6065
<i>pfkB1B2</i>	nifJ	9677
<i>zwf</i> <i>pfkB1B2</i>	nifJ	9677
<i>nifJ</i> <i>pfkB1B2</i>	nifJ	7087
<i>zwfnifJ</i>	nifJ	6065

Note that *pfkB2* and *nifJ* are located in neighborhood in the genome in *Synechocystis* which had an influence on the band sizes in cultures with multiple mutations.

Dig-labeled PCR probes were synthesized with the primer pairs: *pfkB*-1 and *pfkB*-in1, *zwf*-1 and *zwf*-in1, *nifJ*-1 and *nifJ*-in1 for the region close to the open reading frames of *pfkB1*, *zwf* and *nifJ* respectively, and primer pair *pfkB2*-2 and *pfkB2*-in2 for the region downstream sequence of gene *pfkB2* (Table 3.3).

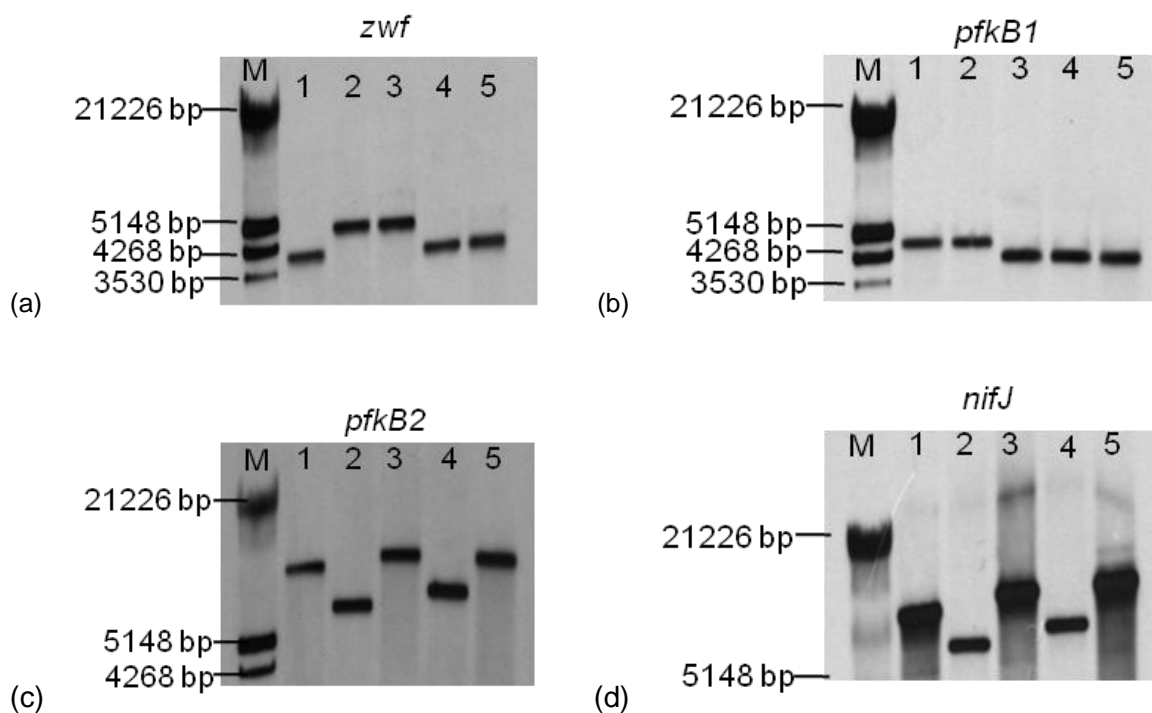


Fig. 4.28. Southern blot genomic DNA of wt (1), *zwfnifJ* (2), *zwfpfkB1B2* (3), *nifJpfkB1B2* (4) and *pfkB1B2* (5) with HindIII digestion. M is the Dig-marked λ -(HindIII)-marker. (a) The DNA samples were hybridized with *zwf* probe; (b) The DNA samples were hybridized with *pfkB1* probe; (c) The DNA samples were hybridized with *pfkB2* probe; (d) The DNA samples were hybridized with *nifJ* probe.

The Southern blots (Fig. 4.28) show that the respective genes were successfully deleted from all genomic copies in the constructed mutants and that therefore all mutants were fully segregated.

4.2.1.2 Growth characterization of mutants with interrupted EMP and OPP pathways

In order to learn more about the significance of the EMP and the OPP pathway under mixotrophic conditions, the mutant with interrupted EMP pathway (Δ *pfkB1B2*) and the mutant with interrupted OPP pathway (Δ *zwf*) were characterized under autotrophic and mixotrophic conditions (Fig. 4.29).

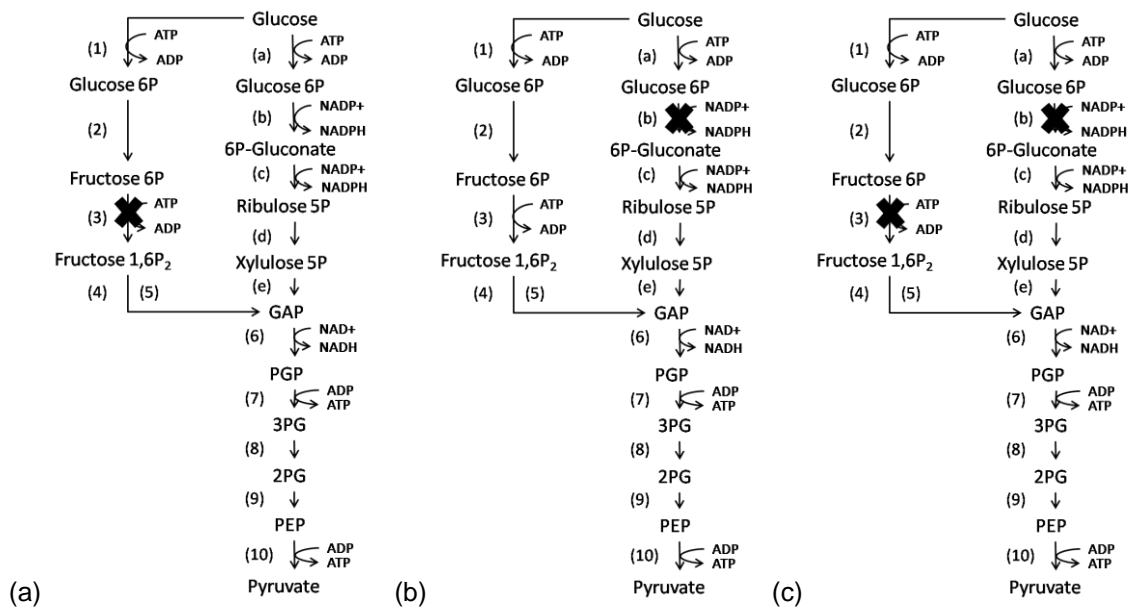


Fig. 4.29. Different mutants of glycolytic pathways in *Synechocystis*. EMP (1-10), OPP (a-e, 6-10). (a) $\Delta pfkB1B2$: the mutant with interrupted phosphofructokinase of EMP pathway; (b) Δzwf : the mutant with interrupted G6PDH of OPP pathway; (c) $\Delta zwf pfkB1B2$: the mutant which both EMP and OPP glucose degradation pathways were interrupted.

The growth rate of both mutants was similar to the growth rate of the WT under autotrophic conditions. Figure 4.30 shows that both $\Delta pfkB1B2$ and Δzwf were able to enhance their growth rate when glucose was added to their medium and that they reached an optical density at 750 nm which was similar to the one of the WT. From these results it was concluded that both pathways might compensate for each other in the mutants and that both pathways are operating under mixotrophic conditions. This is in agreement with the DNA microarray analysis and metabolic analysis from Yoshikawa *et al.* (2013) which showed the activities of OPP pathway and EMP pathway were both elevated under mixotrophic conditions compared with autotrophic conditions. However, there are studies showing that the OPP pathway is inactivated in the light (Kruger, *et al.*, 2003).

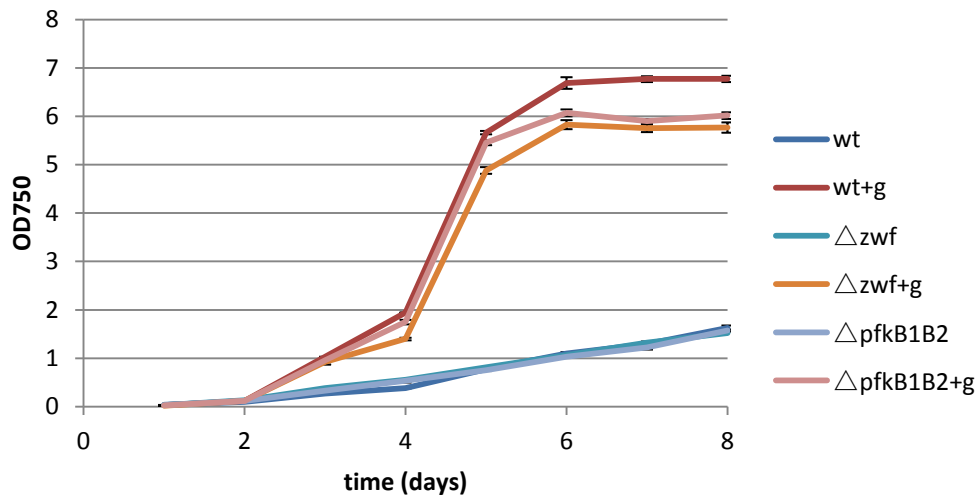


Fig. 4.30. Growth of mutants with interrupted EMP ($\Delta pfkB1B2$) and OPP (Δzwf) pathway and the WT of *Synechocystis* sp. PCC 6803 under autotrophic and mixotrophic (+g) conditions.

Following, also the growth of the triple mutant $\Delta zwf pfkB1B2$ in which both known glucose degradation pathways were interrupted, was analyzed under autotrophic and mixotrophic conditions. Surprisingly this mutant did not differ from the WT under both autotrophic and mixotrophic conditions (Fig. 4.31). The $\Delta zwf pfkB1B2$ mutant was thus still able to metabolize glucose and to enhance its growth under mixotrophic conditions. This finding contradicts the widely held belief that *Synechocystis* relies on the EMP and OPP pathway to degrade glucose under mixotrophic conditions.

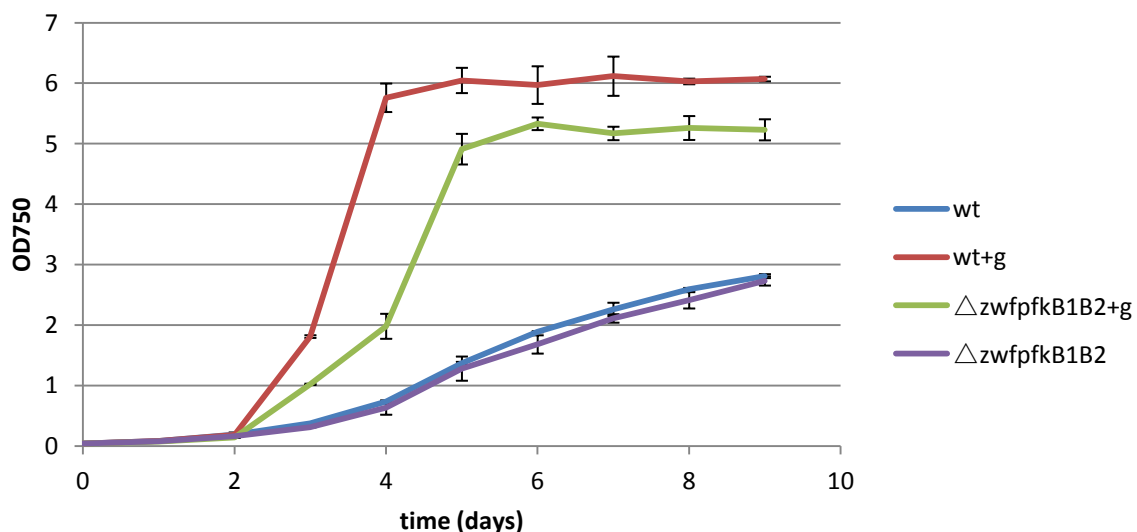


Fig. 4.31. Growth analysis of $\Delta zwf pfkB1B2$ mutants in comparison with wt cultivated in BG-11 medium and with continuous light under autotrophic and mixotrophic conditions.

It was thus hypothesized that *Synechocystis* might bypass the classical EMP and OPP pathway to metabolize glucose. It is widely accepted that exogenous glucose is phosphorylated to glucose-6-phosphate via glucokinase in a first step and then further degraded in the EMP or OPP pathway in *Synechocystis* (Yang, *et al.*, 2002; Kurian, *et al.*, 2006; Jansén, *et al.*, 2010; Yoshikawa, *et al.*, 2013) (Fig. 1.3). Some bacteria oxidize glucose to gluconate via a glucose dehydrogenase (GDH), which transfers the electrons to NAD⁺. Instead of phosphorylating the glucose itself, gluconate is then phosphorylated to 6P-gluconate in the following step (Fig. 1.3).

In order to check whether *Synechocystis* might hold a glucose dehydrogenase, its genome was searched for putative genes (Fig. 4.32, see section 3.8). Two candidate genes could be identified. *Sll1709* is annotated in the data bank cyanobase as glucose dehydrogenase and/or alternatively as 3-ketoacyl-acyl carrier protein reductase. It contains the Rossmann fold typical for dehydrogenases binding NAD(P)⁺. Highest similarities are to the short-chain dehydrogenases (3-ketoacyl-acyl carrier protein reductase) of *Pseudomonas syringae* and the glucose dehydrogenases of a number of prokaryotes. The second candidate is the gene *slr1608*, which is annotated as a putative periplasmic glucose dehydrogenase in cyanobase. The closest homologs of this gene in other cyanobacteria are annotated as glucose/sorbosone dehydrogenases. These proteins do not contain a Rossmann-fold, so they do not use NAD(P)⁺ as substrate. According to the Signa IP tool of the cbs prediction server (<http://www.cbs.dtu.dk/services/>) it is localized to the periplasm with a cleavage site between position 20 and 21 between the two Serin residues in the sequence ALS-SCG. Its localization indicates that it might reduce plastoquinone when oxidizing glucose.

Sdeg-GSDH	1	MKARPAKRDTHPVRRFIFASTLTCLSATL	SHIASANTASGTYQQFCASCHGKNLDGGLG
Ttherm-GSDH	1	-----MDRRRFLVGLLGL	---GLARG
Mmar-GSDH	1	-----MRV-----VASLVAATGLTSSGLAQ	-----
S6803-slr1608	1	-----MLIPFLFKL-----TIPLASGIALSSCGTLP	---EADLGTAAGNQTS
Tery-GSDH	1	MFQYNFFSQPEQKILDI FYGLI IKKSTL	LFRTATAALLGIVSCRTEIKLESSTATQTQN
Psyr-ShortDH2	1	-----MTLSSAPITLITGASQR	-----
Thermoplasma-GDH	1	-----MGHHHHHHMEEFTDKVAIVTGGSSG	-----
Bacillus-GDH	1	-----MYKDEGKVVVITGSSIG	-----
Tacid-GDH	1	-----MDENRGSRIA	INLTGKIALLVTGSSSG
Save-GDH	1	-----METTGSDGRQPLAPQLLKGQKALVTGANSG	-----
Psyr-ShortDH1	1	-----MHSLSKQQVAIVTGAASSG	-----
Chut-GDH	1	-----MSELKLGKQTAALITGGDSSG	-----
S6803-sll1709	1	-----MELTGKTAALVTGGGIR	-----
Mlot-ShortDH	1	-----MSKATAAALVTGGAKR	-----

Sdeg-GSDH	61	PSLIDDEWKHGADDAS	IAKSI	INKG	PTAG	MPAWERVL	DANQVRALI	IYIQEEQ	KRAKLS
-----------	----	------------------	-------	------	------	----------	-----------	---------	--------

```

Ttherm-GSDH      19  -----QGLRVEEVVVGLEVP-----
Mmar-GSDH        21  -----SDIHETEQ-----ADFRMEAVAEGLFPP-----
S6803-slr1608   41  EPTNSVEIVQANQ-----PEIKAVPVLDGLEHP-----
Tery-GSDH        61  KSRINSSVSDAENMTSISDYQKITLVKNLEHP-----
P syr-ShortDH2   17  -----VGLHLCALRLLEHGHR-----
Thermoplasma-GDH 26  -----TGLAVVDAIVRYGAK-----
Bacillus-GDH     19  -----TGKSMAREFAATEKAK-----
Tacid-GDH        27  -----TGAAIAKYMARAGAK-----
Save-GDH         31  -----TGKATAIGLGRVGAD-----
P syr-ShortDH1   19  -----TGAGAARALAEAGAA-----
Chut-GDH         20  -----TGKGIALKMAAGAN-----
S6803-sll1709   17  -----VGRALVMAALAEAGCN-----
Mlot-ShortDH     17  -----TGKATIVEDLAGHGFA-----

```

```

Sdeg-GSDH        120  KKSASNTGGVYKSELHNFTVEKFVDLPGI IWSISTNNNTFI-----ATIKDGRLFTEI
Ttherm-GSDH      34  -----WALAFIPDGGML-----TAERPGRIRLF
Mmar-GSDH        44  -----WSMAFIPDGRLL-----VSERAGRRLRLI
S6803-slr1608   69  -----WGMALPNGDIL-----TTERPGRRLRIV
Tery-GSDH        93  -----WSIALIPDGKIL-----TTERPGRRLRIF
P syr-ShortDH2   32  -----VITSRTEHASV-----TELROAGAVAI
Thermoplasma-GDH 41  -----VVSVSDEKSDVN-----VSDH-----F
Bacillus-GDH     34  -----VVVNYRSKEDANSVLEEIKKVGGELIAV
Tacid-GDH        42  -----VAVHYRSKDRADAIVDEIKNDGGFAMAF
Save-GDH         46  -----VVVNYVAGRDAEEVVREIESFGVRAVYAH
P syr-ShortDH1   34  -----VVVNYNSKPEPAEKLAEEIRAAGGKALAV
Chut-GDH         35  -----ILVNYNSDKDAEETVAQIKVLGASAIICY
S6803-sll1709   32  -----VFVHYGNSQTGALEVQQEVEALGRKAFETY
Mlot-ShortDH     32  -----VAIHANRSQGEADALAAGINQSGGRATVV

```

```

Sdeg-GSDH        174  TNG--KAQETITGV-----PKVWNHSQAGMLEVMPHPQYAKNGWIYLSYVDEISSMIS
Ttherm-GSDH      57  REGRLSTYAELSV-----YHRGESGLIGLAIHPRFPQEPYVYARTVA-EGGLR
Mmar-GSDH        67  EGDTLRRAPVAGL-----PDIMVEGQGLIGLAVHPDFADNGLIYFAY---AECISA
S6803-slr1608   92  RDGVLDPETAGVAVSTVSAQQLFASQQGLLDIAIHPRFAENRFVYFTY---SHGTQ
Tery-GSDH        116  RDGILEPTPISGV-----PQVFAFGQGLLDVSAHPRFAENRFIYLTYS---SHGDR
P syr-ShortDH2   55  YGDFSCETGIMAF-----IDLKLTQTSSTRAVVH-----NASEW
Thermoplasma-GDH 59  KIDVINEEEVKEA-----VEKTKKYGRIDILVN-----NAGLE
Bacillus-GDH     63  KGDVIVESDVINL-----VQSAIKEFGKLDVMIN-----NAGLE
Tacid-GDH        71  YGDVSKKEDVQKL-----FSEIDSKLGTVDILVN-----NAGLD
Save-GDH         75  EADVSEQEDQVADM-----VSRMVKEFGTIDVMA-----NAGLQ
P syr-ShortDH1   63  GADVSKEDVERL-----FAKTEHFCAIDILVA-----NSGLQ
Chut-GDH         64  QADVSEADVQNM-----FREAVKHFCTIDILVN-----NAGLQ
S6803-sll1709   61  SADLSDAQATQGI-----IPKAQEVFGQVDILTN-----SASVF
Mlot-ShortDH     61  GADLTDNAVAGL-----VQQAEEALGPISLILVN-----NASLF

```

```

Sdeg-GSDH        224  SKGMTAIVRGKIKN--KWVEEQQLFKTDESFYLSGCVHFGSRFAF-KDDYLLFFSIGERG
Ttherm-GSDH      105  N----QVRLRHLGE--RGVLDRVVLDGIPARP--HGLHSCGRIAFGPDGMLYVTTGEV-
Mmar-GSDH        115  NANHTALARGRINDATALTEVETLEQVNFDFKE--RGFHFGRILQFLPDSTLLTLGDGG
S6803-slr1608   148  QANRTRVARAVFDGE--KLTDWQVLEFVQTKP--GQHFCSRIITWLPDETLLVSIKDGG
Tery-GSDH        164  SNNRTRIARARLENN--TLGDLKVLFEVVSQTKP--GAQHFCSRIITWLPDGLTVASIGDGG
P syr-ShortDH2   89  L-----AETPGE--EADNFTRMESVHMLAPYLINLHCEPLI-----
Thermoplasma-GDH 93  Q-----YSPHLT--PTEIWRRTIDVNVNGSYLMAKYTIPVM-----
Bacillus-GDH     97  N-----PVSSHEM--SLSDWNKVIDTNLTGAFVLSREAIKYF-----
Tacid-GDH        105  G-----KRELVEGD--DPDDWEKVIENVLMGPYYCAREAVKRM-----
Save-GDH         109  R-----DAPVIDM--TMAQWQKVIDVNLTGQFLCAREAAKEF-----
P syr-ShortDH1   97  K-----DASIVDM--SLEDWNTVINVNLTGQFLCAREAAALRQF-----

```

Chut-GDH 98 Q-----DAAFVIM--TLKQWIKVLSVNLTGQFLCAREAVREF-----
 S6803-sll1709 95 P-----LEDKFFQV--DLDLWEWTFEAVNLRAPFQLSQAFQQV-----
 Mlot-ShortDH 95 V-----DDSIEDF--DWQAWDRHEATHVKTPALLARNFARAL-----

Sdeg-GSDH 281 -----RQDDAQDGLPNPKTIRIHS DGS PKDNP FVNKNKAYPTIWSYGHRNTQG
 Ttherm-GSDH 156 -----YERELAQD LASLGKTLRLTPEGEPA GNPFLGRRGAPPEVYSLGHRNPQG
 Mmar-GSDH 173 -----LHRNEAQDITNHLGTIIRLND DGTVPFDNPFVSARGARPEIYTYGHRNVQG
 S6803-slr1608 204 NPPVELEGDFIRQQQRASHL GKTIIRLND DGTVPADNPFERNPKAAPEVWSYGHRNIQG
 Tery-GSDH 220 NPPIEFNGEFIRQQQRNSHF GKVIIRLND DGSIPSNPFATSTDAKPAWLSYGHRNIQG
 Psyr-ShortDH2 123 -----TASEVADIVHISDDVTRKGS SKHIAYCATKAGLES-----
 Thermoplasma-GDH 128 -----LAIGHGSIINIASVQSYAATKNAAYVTSKHALGL-----
 Bacillus-GDH 132 -----VENDIKGTVINMSSVHEKIPWPLFVHYAASKGCMKLM-----
 Tacid-GDH 141 -----KPKKSGVITINITSVHEYVPSGVTAYSSAKAGLSMF-----
 Save-GDH 144 -----MRRGVVPEVSRSAKTIICMSSVHQIIPWAGHVNYAASKGVLM-----
 Psyr-ShortDH1 132 -----IKQMRPEVSRAMGKIICMSSVHQIIPWAGHVNYAASKGVLDL-----
 Chut-GDH 133 -----TKRGARPEISKALGKIICISSVHEVIIPWGGHVNYAASKGVMMI-----
 S6803-sll1709 131 -----AGDRQGIININDARIIPRPDHFVYRLTKRGLWDM-----
 Mlot-ShortDH 130 -----PEGREGIIVNIDQRVWRTPRYVFSYALSKSALWTQ-----

Sdeg-GSDH 331 LAIHPVTGDLWETEHGPRGG----DEVNIINPALNYGWPVITYGMNYN-GTPEMDATHTK
 Ttherm-GSDH 207 LAWHPKTGE LFSSEHGSGEQYGHDEVNLIIVPGNYGWPR-----VVGRGND
 Mmar-GSDH 224 IAINPQTGSVWAHEHGARGG----DELNLVPEGRNYGWPLVTVYGVNYN-GTPISDATHG
 S6803-slr1608 264 LAYDPVTQKVWATEHCSRGG----DELNLIQKGNKYGWVVSFSKEYSTDQPVPATSR
 Tery-GSDH 280 ITLDPTKNRVWATEHCSRGG----DELNLIERGENYGWVVTHTSREYS-GGLISPETS R
 Psyr-ShortDH2 159 -----TLSFAAREFAPL-----VKVNGIAPALL-----MFQPKDD
 Thermoplasma-GDH 164 -----TRSVAIYAPK-----IRCNVAVCPGT-----IMTPMVI
 Bacillus-GDH 169 -----TETLALEYAPKG-----IRVNNIGPGA-----INTPINA
 Tacid-GDH 177 -----TKALAQEELSDYN-----IRVVAIAPGA-----IKTPINK
 Save-GDH 188 -----MATLAQELAPHR-----IRVNAVAPGA-----IRTPINR
 Psyr-ShortDH1 176 -----MRSIAQEVGELK-----IRVNSVAPGA-----IRTPINA
 Chut-GDH 177 -----MKSMAQELGGLK-----IRINSIGPGA-----IKTDINN
 S6803-sll1709 167 -----TELLALELAFN-----ITVNGLALCQ-----IIEA
 Mlot-ShortDH 166 -----TQMLAQALGPR-----IRVNAIGPG-----PTLK

Sdeg-GSDH 385 EGMEOQLHYWVPSIATGGIDFYQGDAPFKWQNSL L ASGMGSOELHRVMSINDKH----DAV
 Ttherm-GSDH 255 PRYRDELYFWPQGFPPGNLAFF-----RGDIYVAGLRGQALRLVLE-GERGRWRVL
 Mmar-GSDH 278 DGLEQPIWFDWPSIAPSGIAFYDGDGFENWQGD AFVGVALVGSRIVREFEVGD----RIT
 S6803-slr1608 319 PDMVDELQIWTPIAPSGITIIYNGDRHPEWQGTIFAGGLVDRGIRHRLDENN----QIT
 Tery-GSDH 334 PGLVDEKVIWTPSIAPSGIAFYNGDRFPQWRGNIFAGGLVSQDIRRQLDPGG----NVI
 Psyr-ShortDH2 188 AAYRA-----NAAKAKS-----ALGIEPGAETVYQSLRVLDS-----TVV
 Thermoplasma-GDH 192 KAAKMEV---GEDENAVERKIEEWGRQHMPGRIGRPEEVAEVVAFLASDRS----SEI
 Bacillus-GDH 198 EKFADE---EQRADV-ESMI-----PMGYIGEPETIAAVAANLASEA----SMV
 Tacid-GDH 206 DVWGNP---ESTKDL-LNKI-----AMPRIGEVDDIGQAAVFLASDLA----SYI
 Save-GDH 217 SAWDTP---EAEADL-LRLI-----PYRRVGDPIIDANAVAVLASFDF----DYV
 Psyr-ShortDH1 205 DARGK---DAEKEM-LKLI-----PYGRIGEPEDVANAVLWLASDAS----DYV
 Chut-GDH 206 EAWETP---EAAEKL-LKLI-----PYNRIGETEDIGNVAVWLASDES----DYV
 S6803-sll1709 192 PEAPDE---EFVDRYAERRI-----PLKMTGNPKVVTDAAALYLQO-----DFL
 Mlot-ShortDH 190 NVRQD---DSDFDAQLAGL-----ILKRGPELPEFGATIRVWDA-----RSV

Sdeg-GSDH 441 TGDETL LFKGLGRVVDVLSAPDGLIYVALNPNGG----APGAIYVLKPAK---
 Ttherm-GSDH 306 RVEIALSGFG-RLREVOVQVPDGAIVVTTSNRDCRGQVRPGDDRVLRLLL----
 Mmar-GSDH 333 SREELLVGRGERIDVTTGADGSLVILTDERAG-----SVLRLVPVIP
 S6803-slr1608 375 DETTISI--GQVRVDVRQGPDPGHVYVLTQNNC-----QLLRLES---

Tery-GSDH	390	AQNSIP--GQVRDVRQGPDGLVLTDDRNG-----QLIRLEPMGK
Psyr-ShortDH2	223	IGTTLTVNGGRHVK-----
Thermoplasma-GDH	243	TGACITVDGGLLSK----LPIS--T ^N NADNSHH-----
Bacillus-GDH	240	IGITLTFADGGMTQ-----YPSFQAGRG-----
Tacid-GDH	248	IGTTLVVDGGMAL-----YPDFKHG-C-----
Save-GDH	259	VGTTLYVDGGMTL-----YPGFATG-C-----
Psyr-ShortDH1	246	HGTTLFVDGGMTL-----YPEFRGN-C-----
Chut-GDH	248	HGTTLFVDGGMTL-----YPGFASN-C-----
S6803-sll1709	234	SGTTLRLDGAEE-----YLKF-----
Mlot-ShortDH	230	TGQMLALDGGQHLA-----WQTE ^D DVTGMTE-----

Fig. 4.32. Alignment of glucose dehydrogenase, short chain dehydrogenases and glucose/sorbose dehydrogenases with the two putative candidate proteins of *Synechocystis* sp. PCC 6803. The different proteins are from *Saccharophagus degradans* (Sdeg-GSDH), *Thermus thermophilus* Hb8 (Ttherm-GSDH), *Maricaulis maris* MCS10 (Mmar-GSDH), *Trichodesmium erythraeum* IMS101 (Tery-GSDH), *Pseudomonas syringae* pv. *phaseolicola* 1448A (Psyr-ShortDH2), *Thermoplasma volcanium* (Thermoplasma), *Bacillus megaterium* (Bacillus-GDH), *Thermoplasma acidophilum* (Tacid-GDH), *Streptomyces avermitilis* MA-4680 (Save-GDH), *Pseudomonas syringae* pv. *syringae* B728a (Psyr-ShortDH1), *Mesorhizobium loti* MAFF303099 (Mlot-ShortDH). Structural information is available in the proteindatabase (www.pdb.org) for the proteins of *Bacillus megaterium*, *Thermoplasma acidophilum*, *Thermus thermophiles* Hb8 under the IDs 1GCO, 3VTZ and 2ISM, respectively.

First the gene sll1709 (*gdh* in this work) was knocked out in *Synechocystis* by inserting a gentamycin resistance cassette into the open reading frame. The gene was deleted in the WT, Δzwf , $\Delta pfkB1B2$, and $\Delta zwf pfkB1B2$, leading to the mutants Δgdh , $\Delta gdh zwf$ (*gz*), $\Delta gdh pfkB1B2$ (*gb*), and $\Delta gdh zwf pfkB1B2$ (*gzb*). In order to check whether the gene had been deleted from all genomic copies, southern blots were carried out.

The genomic DNA of WT and all mutants were isolated and digested with HindIII.

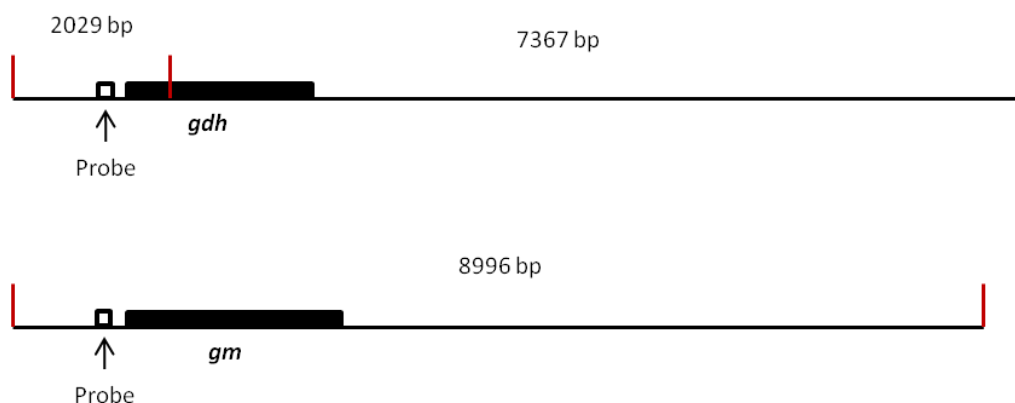


Fig. 4.33. Position of HindIII restriction sites and hybridization site of applied PCR-probe in WT (upper drawing) and *gdh* mutant (lower drawing).

There is a restriction site for HindIII in the open reading frame of *gdh* but there is no restriction site in the gentamycin resistance cassette (Fig. 4.33). Digestion of the WT DNA with HindIII results in two fragments of 2029 bp and 7267 bp in the region of *gdh* whereas only one fragment of 8996 bp exists in mutants, in which *gdh* was replaced by the gentamycin-resistance cassette (Fig. 4.33). A dig-labeled PCR probe was synthesized with the primer pair *gdh*-1 and *gdh*-in1 (see table 3.3) which is homolog to the region upstream of the ATG of *gdh*. Incubating genomic WT DNA with this probe thus results in a band of 2029 bp whereas incubation of a fully segregated genomic Δ *gdh* results in a band of 8996 bp.

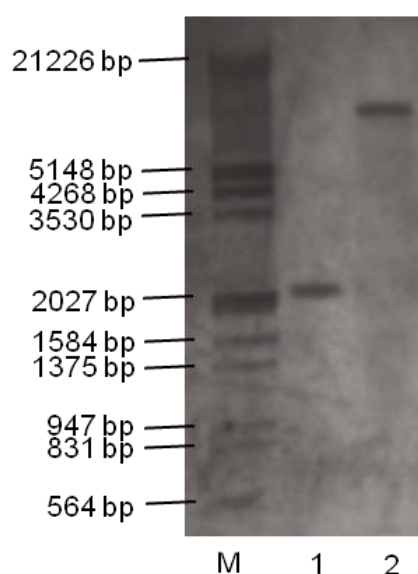


Fig. 4.34. Southern blot with genomic DNA of WT (1) and Δ *gdh* mutant (2) with a probe against the upstream region of *gdh*. Lane M is the Dig-labeled λ -(HindIII)-marker (Roche).

Additionally to the single mutant, *gdh* was also deleted from the genomes of Δ *zwf*, Δ *pfkB1B2*, and Δ *zwf**pfkB1B2*.

As shown in figure 4.34, *gdh* could be successfully deleted from the genome of Δ *zwf* and Δ *pfkB1B2*, so fully segregated Δ *gdhzwf* and Δ *gdhpfkB1B2* were obtained. However, Δ *gdhzwf**pfkB1B2* could not be completely segregated. This mutant kept *gdh* in some of its genomic copies, resulting in the merodiploid mutant *gdh*/ Δ *gdhzwf**pfkB1B2* (Fig. 4.35). That *gdh* could not be completely deleted from *Synechocystis* when the EMP and OPP pathways were interrupted might indicate that this enzyme is essential in this genetic background.

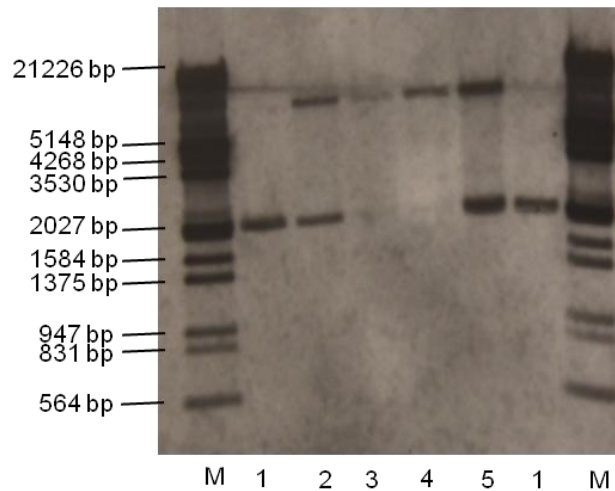
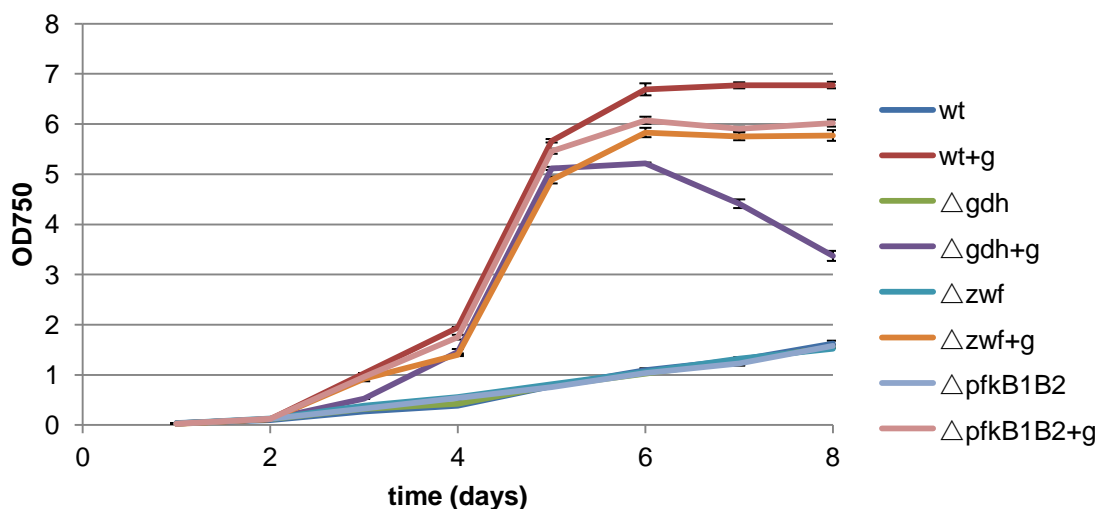


Fig. 4.35. Southern blot with genomic DNA of WT (1,6), *gdh*/ Δ *gdhzwf**pfkB1B2* (2,5; abbreviated as *gzb* / Δ *gzb*), Δ *gdhzwf* (3, abbreviated as Δ *gz*), and Δ *gdhpfkB1B2* (4, abbreviated as Δ *gb*) with a probe against the upstream region of *gdh*. The Dig-labeled λ -(HindIII)-marker (Roche) was used (lane M) to determine the sizes of the bands.

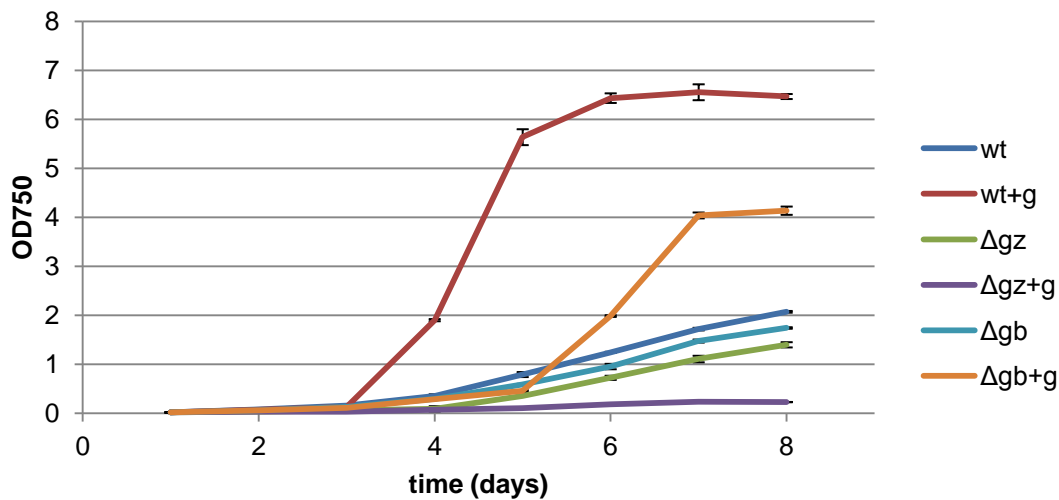
4.2.1.3 Growth characterization of different Δ *gdh* mutants

In order to analyze the importance of the putative glucose dehydrogenase (Sll1709, *gdh*) under mixotrophic conditions, the growth of Δ *gdh* was compared to WT, Δ *zwf* and Δ *pfkB1B2* under autotrophic and mixotrophic conditions. Δ *gdh* grew similar to WT, Δ *zwf* and Δ *pfkB1B2* under autotrophic conditions (Fig. 4.36 a). Under mixotrophic conditions however the optical density at 750 nm decreased in Δ *gdh* when the other cultures reached their stationary phase, indicating that the enzyme encoded by *sll1709* might be of importance in this growth phase (Fig. 4.36 a).

(a)



(b)



(c)

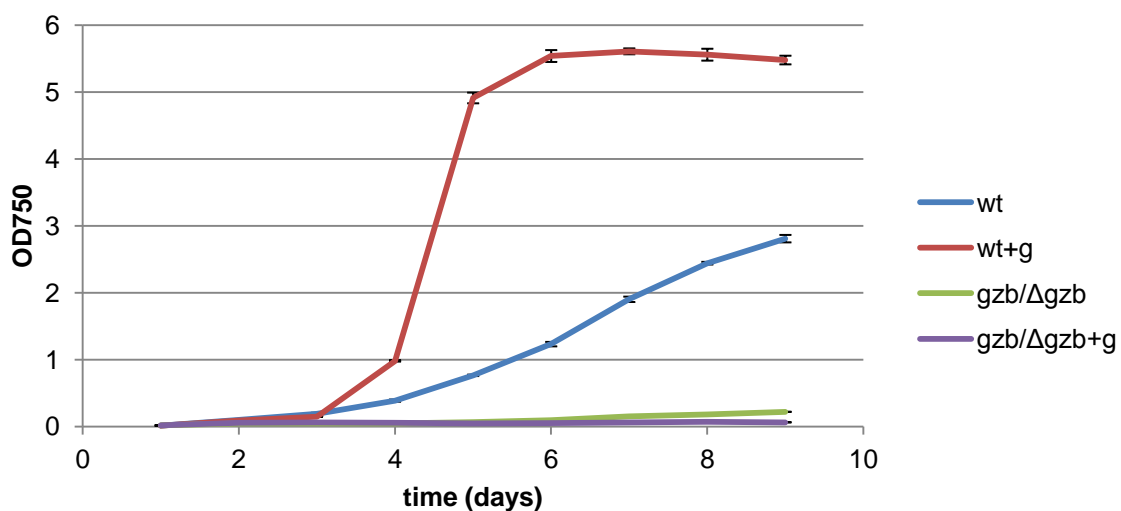


Fig. 4.36. Growth of different mutants and the WT under autotrophic and mixotrophic (+g) conditions: (a) WT, Δzwf , $\Delta pfkB1B2$, and Δgdh ; (b) WT: Δgz ($\Delta gdhzwf$), Δgb ($\Delta gdhpfkB1B2$); (c) WT and $gzb/\Delta gzb$ ($gdh/\Delta gdhzwfpkB1B2$).

In order to further investigate the significance of the putative glucose dehydrogenase (*sll1709*) the growth of $\Delta gdhzwf$ (Δgz), $\Delta gdhpfkB1B2$ (Δgb) and mrodiplid $gdh/\Delta gdhzwfpkB1B2$ ($gzb/\Delta gzb$) was compared to the WT under autotrophic and mixotrophic conditions (Fig. 4.36 b, c). All mutants grew similar to the WT under autotrophic conditions (Fig. 4.36 b). However, under mixotrophic conditions $\Delta gdhpfkB1B2$ started to metabolize glucose with a delay of two days and did not reach the same optical density at 750 nm as the WT (Fig. 4.36 b). $\Delta gdhzwf$ could not

grow with glucose at all (Fig. 4.36 b). The merodiploid mutant in which both EMP and OPP pathways were interrupted and *gdh* was partly deleted (*gzb/Δgzb*) could neither grow under autotrophic nor under mixotrophic conditions in liquid cultures (Fig. 4.36 c). On agar plates however this mutant was able to grow. These results show, that the enzyme encoded by *sll1709*, which might be a glucose dehydrogenase has an effect on growth under mixotrophic conditions. It might be a bypass for the cells in which both EMP and OPP pathway are interrupted. The fact that this gene could not be completely deleted from this mutant and that even the merodiploid mutant was no longer able to grow neither under autotrophic nor under mixotrophic conditions, indicates that it might be essential in this genetic background. However, it is not yet clarified whether *sll1709* really encodes for a glucose dehydrogenase. So these results have to be interpreted cautiously.

The construction of a mutant with a deletion of the second candidate gene, which might encode for a glucose dehydrogenase (*slr1608*) is underway. Further experiments are needed to find out if any of the enzymes encoded by these genes (*sll1709* or *slr1608*) really catalyzes the oxidation of glucose to gluconate.

For the case that a glucose dehydrogenase (i in Fig. 4.38) should be able to bypass the glucokinase (1 in Fig. 4.38) in *Synechocystis*, the question remains to be answered, whether 6-phosphogluconate is further metabolized to ribulose-5-phosphate and thereby enters the OPP pathway or whether another pathway is used to convert glucose to pyruvate (Fig. 4.38).

The Entner-Doudoroff pathway (ED) is besides EMP and OPP another glucose degradation pathway, which is found in archaea and many bacteria (Flamholz, *et al.*, 2013). As shown in figure 4.38, 6P-gluconate is converted to 2-keto-3-desoxy-6-phosphogluconate (KDPG), which is split by the KDPG aldolase into pyruvate and glyceraldehyde-3-phosphat (GAP). The KDPG aldolase is the key enzyme of the Entner-Doudoroff pathway. To date it has not been shown that the Entner-Doudoroff pathway operates in cyanobacteria. As the $\Delta zwf pfk B 1 B 2$ mutant, in which both the EMP as well as the OPP pathway were interrupted, is still able to enhance its growth on glucose, it seemed plausible to hypothesize that *Synechocystis* might hold an additional pathway to degrade glucose. The ATP yield for one molecule glucose differs between all three glucose degradation pathways. 0 ATP are gained per

molecule glucose in the OPP pathway, 1 ATP in the ED, and 2 ATP in the EMP pathway. Most anaerobic bacteria and archaea use the EMP pathway exclusively, whereas the ED pathway is found in facultative anaerobic and aerobic microorganisms more frequently, probably due to the fact that these organisms are able to gain ATP via aerobic respiration (Flamholz, *et al.*, 2013).

In order to find out whether *Synechocystis* might hold the Entner-Doudoroff pathway, its genome was searched for the gene encoding the key enzyme (KDPG aldolase) of this pathway in the cyanobacterial data bank cyanobase. It was found that the gene *sll0107* is annotated as KDPG aldolase. As its function has not been investigated experimentally, the protein sequence of the well characterized KDPG aldolase (ID-Code 1EUN) from *E.coli* (Allard, *et al.*, 2001), was used as a bait. A protein alignment between the KDPG aldolase from *E.coli* and *Synechocystis* was carried out at NCBI (Fig. 4.37).

```

KDPG E.coli          1  MKNWKTSAESILTTGPVVPVIVVKKLEHVAVPMAKALVAGCVRVLEVTLRTECAVDATRAI
Sll0107 Synechocystis 1  -----MIRQHRATAVVIRTDSIDLSIQAKVAIEAGMGLVEITWNSDQPGETIAHL

KDPG E.coli          61  AKEVPEAIVGAGTVLNPQQIAEVTEAGAQFAISPLGLTEPLIKAAITEGTIPPIPGISTVSE
Sll0107 Synechocystis 51  RQVQPHCAVGTGTVLSQEDLLQAVASGAQFCFTPHSEPELITSAVAHGLPPIPGAFSPTE

KDPG E.coli          121  LMLGMDYGLKEKRFPPAEANGGVKALQAIAGEFSQVRFRCPTGCTSPANYRDYLAALKSVLC
Sll0107 Synechocystis 111  IVQAWQRGATAVAVVPEPIKTLGGVDYIQALQGELGQPLIPTGGVTLANAQAFLLAAGATAV

KDPG E.coli          181  IGGSWLVVADALEAGDYDRITKLAAREAVEGAKL---
Sll0107 Synechocystis 171  GLSGQLFEPNLVAIKAWREIIGDLIRTLIKEIQTPRG

```

Fig. 4.37. Protein alignment between known KDPG aldolase from *E.coli* (1EUN) and putative KDPG aldolase (*sll0107*) from *Synechocystis* sp. PCC 6803 (black: conserved amino acid sequences; grey: conservative amino acid substitutions)

Crystals of the KDPG aldolase from *E. coli* soaked with pyruvate showed that four conserved amino acids (Glu45, Arg49, Thr73 and Lys133, Table 4.5) in the active site are involved in the binding of pyruvate, indicating that their existence is essential for the functioning of the KDPG aldolase (Allard, *et al.*, 2001). Lysin 133 binds pyruvate covalently whereas the other amino acids form hydrogen bonds to stabilize the enzyme substrate complex. Additional conserved amino acids in the KDPG aldolase from *E. coli* were further identified via NCBI (<http://www.ncbi.nlm.nih.gov/Structure/cdd/cddsrv.cgi>), which additionally marked amino acids 20, 94, 135 and 160 as being conserved.

Table 4.5. Occurrence of conserved amino acids in KDPG aldolase in *E. coli* and *Synechocystis*. V, valine; E, glutamic acid; R, arginine; N, asparagine; T, threonine; P, proline; K, lysine; F, phenylalanine.

organism	conserved amino acids							
	20	45	49	73	94	133	135	160
<i>E.coli</i>	V	E	R	T	P	K	F	T
<i>Synechocystis</i>	V	E	N	T	P	K	F	T

As shown in table 4.5 the conserved amino acids of the *E.coli* KDPG aldolase at positions 20, 49, 73, 93, 133, 135 and 160 all occur in the annotated KDPG aldolase of *Synechocystis* (*sl10107*). Only the arginine (R) at position 49 is replaced by an asparagine (N). However as the amino acid at position 49 is also an asparagine in the bacterium *Clostridium pasteurianum* it is likely that the protein in *Synechocystis* might be a KDPG aldolase (Fuchs, *et al.*, 2006).

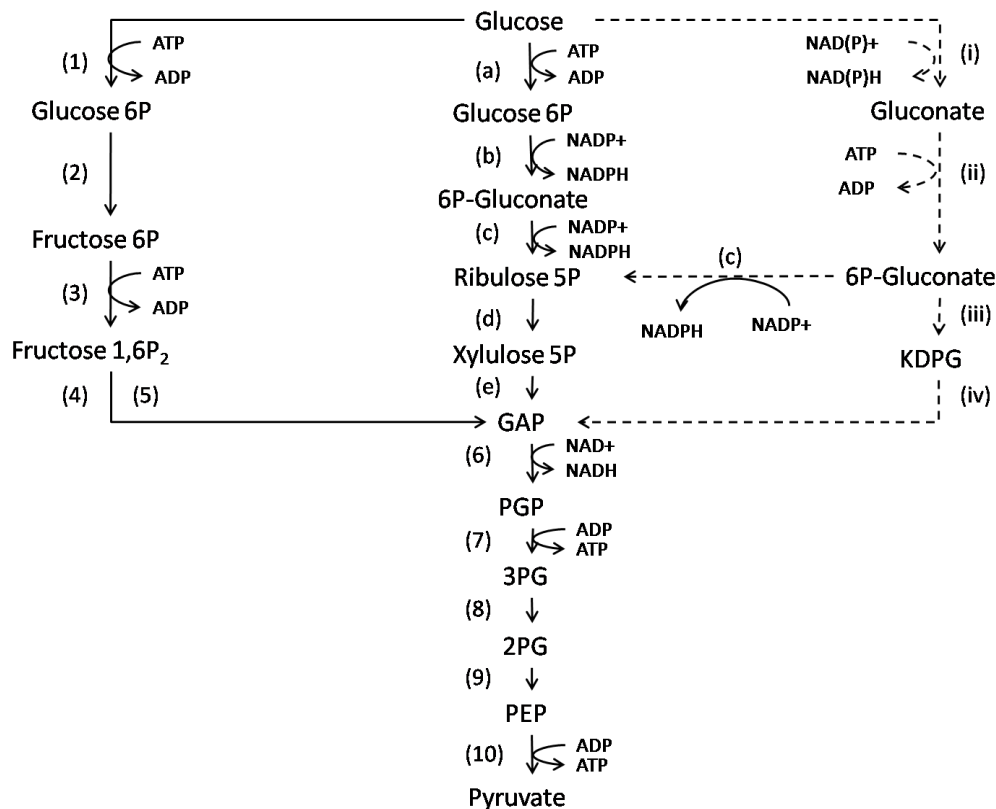


Fig. 4.38. Hypothesis of the route of glucose catabolism in *Synechocystis* based on glucose catabolism in bacteria and archaea as shown by Verhees *et al.* (2003): EMP (1-10), OPP (a-e, 6-10), ED (i-iv, 6-10). Abbreviated metabolites are: P, phosphate; Fructose 1,6P₂, fructose 1,6-bisphosphate; KDPG, 2-keto-3-deoxy-6-phosphogluconate; GAP, glyceraldehyde 3-phosphate; PGP, 2,3-bisphosphoglycerate; 2PG, 2-phosphoglycerate; 3PG, 3-phosphoglycerate; PEP,

phosphoenolpyruvate; KDG, 2-keto-3-deoxy-Gluconate; GA, glyceraldehydes. Key to enzymes: (1) (a) glucokinase; (2) phosphoglucose isomerase; (3) phosphofructokinase; (4) fructose 1,6-bisphosphate aldolase; (5) triosephosphate isomerase; (6) glyceraldehydes phosphate dehydrogenase; (7) phosphoglycerate kinase; (8) phosphoglycerate mutase; (9) enolase; (10) pyruvate kinase; (b) glucose-6-phosphate dehydrogenase; (c) 6-phosphogluconate dehydrogenase; (d) ribulose-5-phosphate 3-epimerase; (e) transketolase; (i) glucose dehydrogenase; (ii) gluconate kinase; (iii) 6-phosphogluconate dehydratase; (iv) KDPG aldolase.

In order to make the Entner-Doudoroff pathway complete the enzymes gluconate kinase (ii in Fig. 4.38) and 6-phosphogluconate dehydratase (iii in Fig. 4.38) are needed beside the glucose dehydrogenase and the KDPG aldolase (Table 4.6). A gluconate kinase is not annotated in the genome of *Synechocystis*. Similarity searches for homologous genes with the gluconat kinase from the cyanobacterium *Oscillatoria* revealed similarities to the shikimate kinase gene (*sll1669*) (e-value: 0,005) and to the hypothetical protein *slr0207* gene (e-value: 0,005) and with the glucono kinase from *Roseiflexus* with the glycerol kinase gene (*slr1672*) (e-value 2×10^{-9}) from *Synechocystis*. A BLAST-P search showed that the hypothetical protein Slr0207 has a conserved gluconate kinase domain. This gene is therefore despite its relatively low expected value an attractive candidate for a gluconate kinase.

Table 4.6. Candidate genes in *Synechocystis* that encode for enzymes that might be involved in the Entner-Doudoroff pathway

Number in figure 4.38	Name of enzyme	candidate gene in <i>Synechocystis</i> sp. PCC 6803
i	glucose dehydrogenase	sll1709, slr1608
ii	gluconate kinase	slr0207, sll1669, slr1672
iii	6-phosphogluconate dehydratase	slr0452
iv	KDPG aldolase	sll0107

4.2.2 Construction of mutants to interrupt the potential ED pathway in *Synechocystis* sp. PCC 6803

The construction of several mutants to interrupt a potential Entner-Doudoroff pathway in *Synechocystis* was started (Table 4.7).

Table 4.7. Mutant strains to interrupt the potential ED pathway in *Synechocystis* listed with concentration of their respective antibiotic resistance cassette.

mutant strains	Antibiotic resistance cassette	concentration ($\mu\text{g ml}^{-1}$)	Primer pairs for target genes
Δka	Gentamycin	5	KA-1, KA-in1, KA-2, KA-in2, Gm1, Gm2
$\Delta kazwf$	Gentamycin	5	
	Chloramphenicol	20	
$\Delta kapfkB_1B_2$	Gentamycin	5	
	Kanamycin	50	
	Spectinomycin	20	
$\Delta kazwfpfkB_1B_2$	Gentamycin	5	
	Chloramphenicol	20	
	Kanamycin	50	
	Spectinomycin	20	
Δph	Erythromycin	25	PGD-1, Ph-in1, PGD-2, PGD-in2, Em F, Em R
$\Delta phzwf pfkB_1B_2$	Erythromycin	25	
	Chloramphenicol	20	
	Kanamycin	50	
	Spectinomycin	20	

The KDPG aldolase (iv, Fig. 4.38) which is the key enzyme of the ED pathway and is encoded by sll0107 (*eda*) was deleted from the genome of *Synechocystis*. The open reading frame of *eda* was replaced by a gentamycin-resistance cassette.

In order to check whether the mutant is fully segregated, genomic DNA from Δka was digested with HindIII. There is a HindIII restriction site in the open reading frame of *eda* but none in the gentamycin cassette (Fig. 4.39). As shown in figure 4.39, a PCR probe that hybridizes upstream of *eda*, would result in a Southern blot with a band of 631 bp in Δka and a band of 2717 bp in the WT. A Dig-labeled PCR probe was synthesized with the primer pair ka-1 and ka-in1, which results in a product that hybridizes upstream of *eda* (Fig. 4.39). The Δka mutant will be analyzed as soon as it has been inoculated for at least six times on new agar plates.

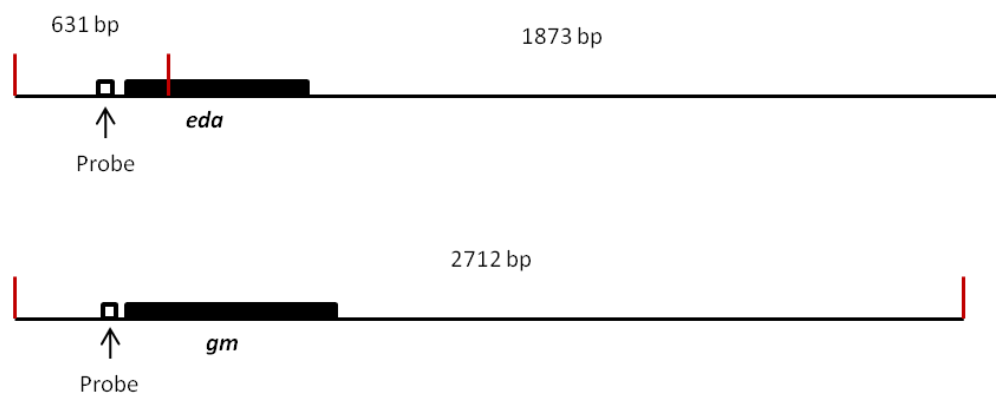


Fig. 4.39. Position of HindIII restriction sites and hybridization site of applied PCR-probe in WT (upper drawing) and *eda* mutant (lower drawing).

4.2.3 Quantitative real time PCR for key genes of glucose degradation pathways

The transcription levels of the key genes of the EMP, OPP and ED pathway (*pfkB1*, *pfkB2*, *zwf*, *gdh*, *eda*) were investigated in the WT under autotrophic and mixotrophic conditions via quantitative real time PCR (qRT-PCR). As housekeeping genes *16S* and *mnpB* were used. The primer efficiency of each gene was investigated and calculated by the formula shown in 3.7.11. Two primer pairs were constructed per gene that resulted in two different amplicon lengths (approx. 50 bp and approx.90 bp). As listed in table 4.8, the primer efficiencies of all primers resulting in the shorter amplicons (around 50 bp) ranged from 1.893 (*gdh*) to 2.058 (*pfkB2*) and those of all primers resulting in longer amplicons (around 90 bp) were in the range between 1.914 (*eda*) to 2.344 (*pfkB1*). For the analysis shown in this work, the primers producing the smaller amplicons were used.

The transcription was compared between autotrophic and mixotrophic conditions, in order to check the influence of the presence of glucose on the key genes of the three glucose degrading pathways.

WT cells were grown under autotrophic and mixotrophic (10 mM glucose) conditions. RNA was isolated before glucose was added (day 0) and 72 hours (day 3), 120 hours (day 5), 168 hours (day 7) and 268 hours (Day 11) after the addition of glucose.

Table 4.8. The primer efficiency of genes encoding key enzymes of the EMP, OPP and ED pathway with different amplicon lengths.

gene	Primer pair (see table 3.3)	Product length (bp)	Primer efficiency
<i>gdh</i>	GDH S F, GDH S R	60	1.893
	GDH L F, GDH L R	90	2.034
<i>eda</i>	Ka-rt-s F, Ka-rt-s R	59	2.005
	Ka-rt-l F, Ka-rt-l R	91	1.914
<i>pfkB1</i>	pfkB1S F, pfkB1 S R	51	2.043
	pfkB1 L F, pfkB1 L R	85	2.344
<i>pfkB2</i>	pfkB2 S F, pfkB2 S R	48	2.058
	pfkB2 L F, pfkB2 L R	88	2.324
<i>zwf</i>	Zwf S F, ZwfS R	53	2.045
	Zwf L F, Zwf L R	82	2.173

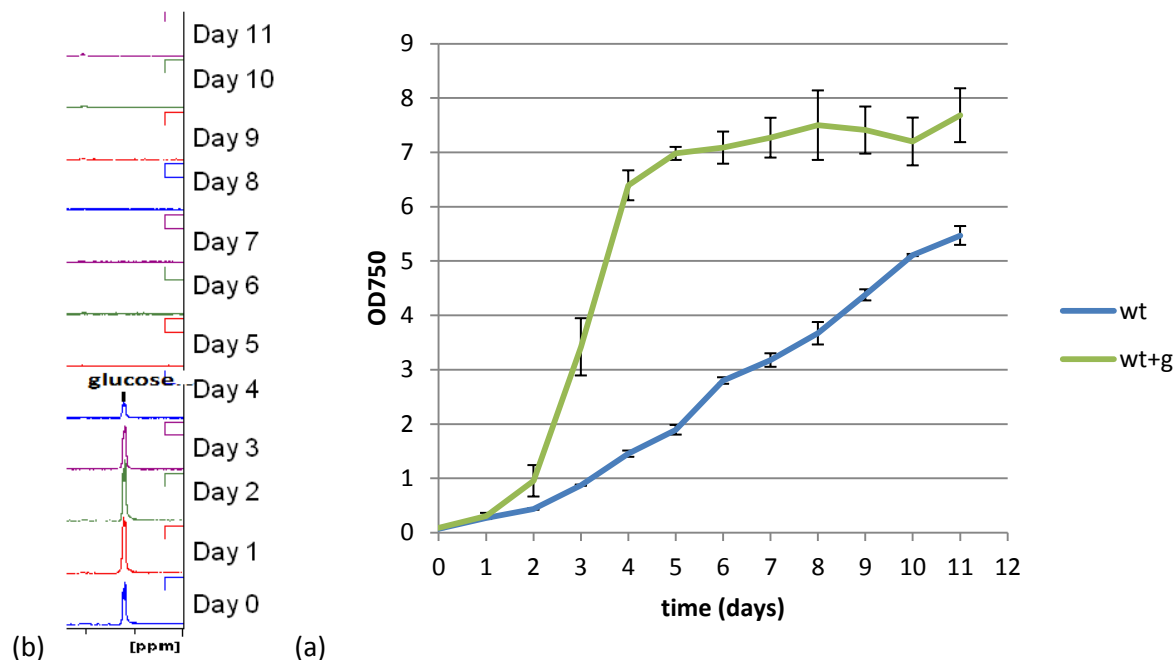


Fig. 4.40. Growth curves of autotrophic and mixotrophic WT cultures (a) and the glucose present in the growth medium as measured by NMR (b).

The growth of the WT was elevated already from day 2 on when fed with glucose as seen in figure 4.40 a. The glucose in the mixotrophic WT culture was used up on day

5 when the cultures reached its stationary growth phase as analyzed by NMR (Fig. 4.40 b). Therefore to understand the significance of the different pathways under mixotrophic conditions the transcription on days 3 and 5 is especially important. The transcription of the key enzymes of EMP pathway PfkB1 and PfkB2 were rather down than upregulated on days 3 and 5. Also the transcription of Zwf, the key enzyme of the OPP pathway was not up regulated on these days. The transcription of the genes that might participate in the ED pathways however, namely the putative *gdh* (sll1709) and and KDPG aldolase *eda*, were both slightly up regulated 1.6 times under mixotrophic conditions (Fig. 4.41). Whether *16S* or *rnpB* were used as reference genes did not influence the calculated expression ratios (Fig. 4.41).

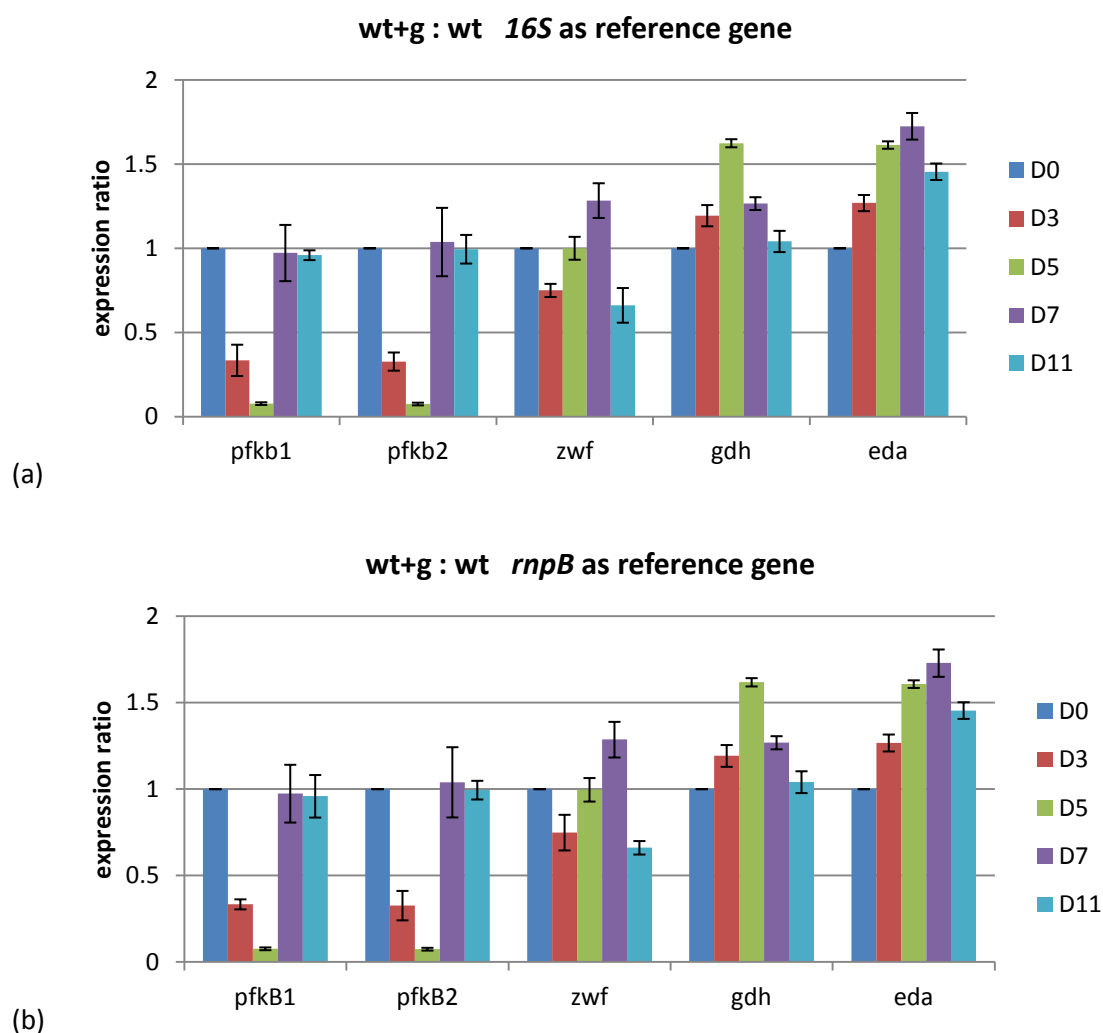


Fig. 4.41. Expression ratio of *pfkB1*, *pfkB2*, *zwf*, *gdh*, *eda* at day 3, day 5, day 7 and day 11. (a) *16S* used as reference gene; (b) *rnpB* used as reference gene.

In order to find out, how the transcription of the genes may react to glucose before day 3 (72 hours), a second growth experiment was set up, in which RNA was isolated

again before the addition of glucose (0 hours), 0.5 hours, 6 hours, 24 hours, 48 hours and 72 hours (equal to day 3 in the first experiment) after the addition of glucose. As seen in the respective growth curve, the mixotrophic cultures showed an elevated growth from about 48 hours on after the addition of glucose. Again the transcription of the key enzymes of EMP was not up regulated as in the first experiment (Fig. 4.43). The transcription of *zwf* was slightly (1.3 times) up regulated under mixotrophic conditions, whereas the putative *gdh* and *eda* were again up regulated 1.69 and 1.8 after 72 hours under mixotrophic conditions, *gdh* even 1.9 times after 48 hours (Fig. 4.43). Again whether *16S* or *rnpB* were used as reference genes had no influence on the calculated expression ratios (Fig. 4.43).

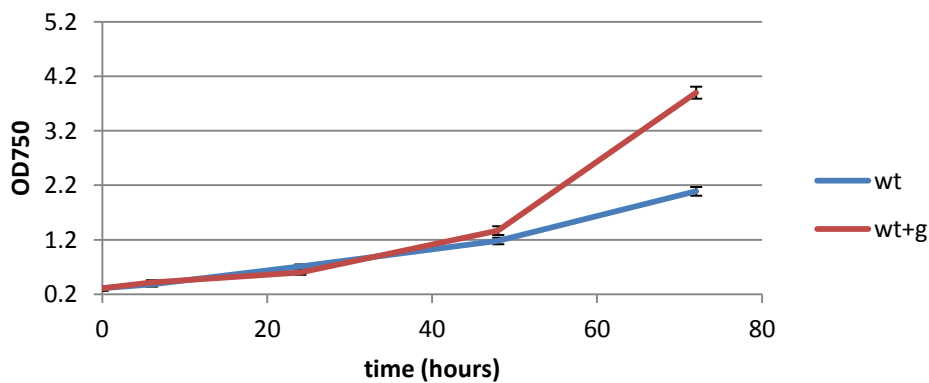
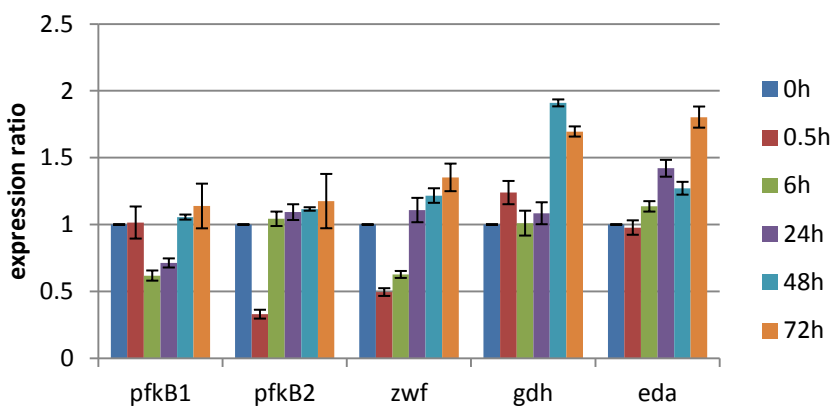


Fig. 4.42. Growth curves of autotrophic and mixotrophic WT cultures for 72 hours (3 days).

(a)



(b)

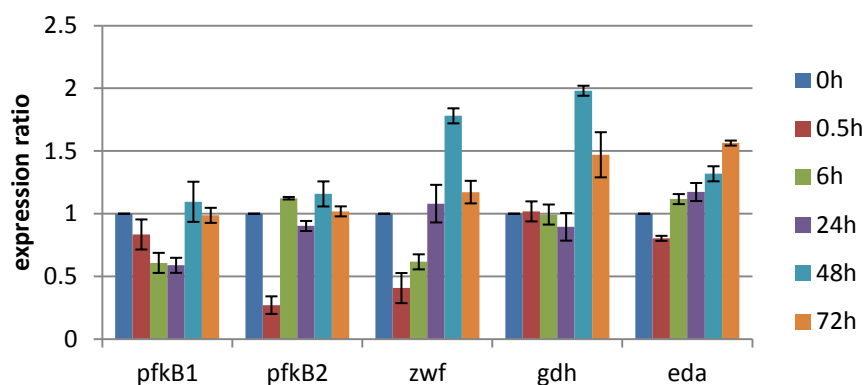


Fig. 4.43. Expression ratio of *pfkB1*, *pfkB2*, *zwf*, *gdh*, *eda* before addition of glucose (0 hour) and , 0.5 hours, 6 hours, 24 hours, 48 hours and 72 hours after addition of glucose. (a) *16S* used as reference gene; (b) *rnpB* used as reference gene.

It has been shown for higher plants that the OPP pathway is inactivated in the light (Kruger, *et al.*, 2003). Therefore the expression of all investigated key enzymes of the EMP, OPP and ED pathways were also analyzed when cultures were supplemented with 10 mM glucose in the dark (heterotrophic conditions). *16S* was used as reference gene. For this purpose, a WT culture without glucose and a Wt culture with glucose (10 mM) were incubated for 24 hours in darkness. The optical density at 750 nm slightly declined in the culture without glucose whereas the heterotrophic culture did enhance its optical density (Fig. 4.44). RNA was isolated before glucose was added in the light (0 hours), and 0.5 hours after addition of glucose in the light and 24 hours after addition of glucose in darkness. Contrary to the results obtained under mixotrophic conditions in the light, the transcription ratios of *pfkB1* and *pfkB2* were 1.4 times higher and of *zwf* 1.3 times higher under heterotrophic conditions. The transcription of the putative *gdh* gene and of *eda* were however rather down regulated (0.69 and 0.49 times respectively) under heterotrophic conditions (Fig. 4.45).

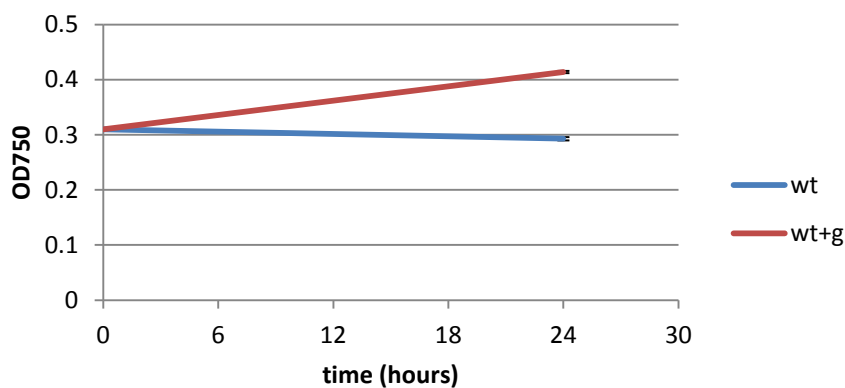


Fig. 4.44. Growth curves of WT autotrophic and heterotrophic (10 mM glucose) cultures incubated for one day in the dark.

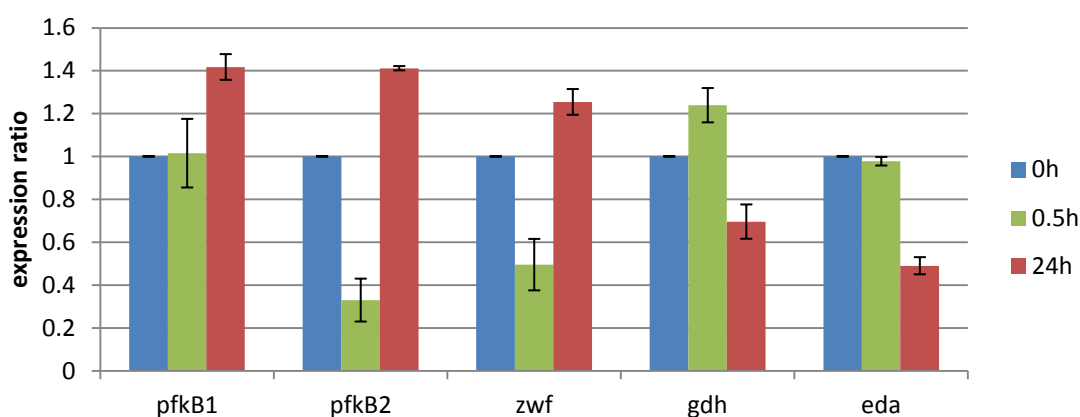


Fig. 4.45. Expression ratio of *pfkB1*, *pfkB2*, *zwf*, *gdh*, and *eda* before glucose was added in the light (0 hour), 0.5 hours after addition of glucose in the light, and 24 hours after dark incubation with glucose. *16S* was used as reference gene.

These results show on a transcriptional level, that the Enter Doudoroff pathway may be induced under mixotrophic conditions (10 mM glucose and light) whereas the Embden-Meyerhof-Parnas and oxidative pentose phosphate pathway may be induced under heterotrophic conditions (10 mM glucose and darkness). It was repeatedly suggested that the addition of glucose to *Synechocystis* cultures might rather influence metabolic processes on the enzymatic level and not on the transcriptional level (Tu, *et al.*, 2004). Which of the glucose degradation pathway is active and to what extend cannot be said from the shown results. However they give a first idea, that the ED pathway might be important under mixotrophic conditions. The fact that the mutants in which both EMP and OPP pathway were deleted, could grow under mixotrophic conditions as fast as the WT points in the same direction.

5 Discussion

The cyanobacterium *Synechocystis* sp. PCC 6803 serves as one of the most prominent model organisms. Most of the research on cyanobacteria focuses on the autotrophic or fermentative mode of their life. These, however, do not give credit to the fact that the environments which cyanobacteria face are sometimes rich in nutrients and simultaneously full of sunlight. Mixotrophic conditions are thus scientifically underestimated for this organism. Especially senescent blooms may go along with enhanced concentrations of dissolved carbon (Wetz, *et al.*, 2004). Bacteria that hold glycolytic exoenzymes are able to break down the dissolved organic carbon to short sugar chains (Teeling, *et al.*, 2012), thereby creating mixotrophic conditions where the phytoplankton is supplied with both glucose and sunlight.

5.1 Characterization of PFOR under different conditions

5.1.1 PFOR is an important electron sink under mixotrophic conditions

Various nutrient substances in the environment can provide glucose to cyanobacteria. It was reported that the cyanobacterium *Synechocystis* sp. PCC 6803 is able to consume exogenous glucose and that it grows better than under autotrophic conditions (Rippka, *et al.*, 1979; Feng, *et al.*, 2010; Yoshikawa, *et al.*, 2013). The respiration activities are enhanced under mixotrophic conditions (Kahlon, *et al.*, 2006), while strong negative effects on the CO₂ fixation by exogenous carbon sources were observed (Feng, *et al.*, 2010). In our study, *Synechocystis* had an exponential growth phase from the second day of incubation with 10 mM glucose in the light, and started to enter the stationary growth phase around day 5 (Fig. 4.1) when the glucose had been consumed in the medium (Fig. 4.14). The observed elevated exponential growth phase might be due to a maximal utilization of glucose which can not only provide NAD(P)H, ATP and intermediates for the cell metabolism, but also reduces the energy costs for carbon fixation (Bar-Even, *et al.*, 2012). During the rapid growth phase, the respiration rate was slightly up-regulated from the second day of incubation on, while the photosynthetic rate sharply decreased from this time point on (Fig. 4.8 and Fig. 4.9). These results indicate that glucose is preferentially metabolized and can provide enough energy and reductants (ATP and NAD(P)H) to support growth under mixotrophic conditions.

A $\Delta nifJ$ mutant was characterized in detail in this study. The gene *nifJ* encodes for the enzyme NifJ/PFOR (pyruvate: ferredoxin/ flavodoxin oxidoreductase), that catalyzes the cleavage of pyruvate to acetyl-CoA and CO₂ under reduction of ferredoxin/ flavodoxin. Compared to the WT, no significant growth defect was detected in the $\Delta nifJ$ cultures under autotrophic conditions. The reaction that is catalyzed by PFOR can alternatively be catalyzed by the PDH-complex (pyruvate dehydrogenase complex) (Fig. 1.5). It could be shown in this study that *pdhA*, which encodes a subunit of the PDH complex as well as *nifJ* are transcribed under autotrophic conditions (Fig. 4.18, 4.19, 4.21, 4.22), indicating that the PDH complex can probably overtake the function of PFOR under autotrophic conditions. Whereas the PDH complex transfers electrons to NAD⁺, PFOR reduces either ferredoxin or flavodoxin (Fig. 1.5). It has additionally been shown that PFOR is only active under anoxic conditions (Neuer, *et al.*, 1982). Even though PFOR is transcribed in the presence of oxygen, as was also shown by Schmitz, *et al.*, (2001), the enzyme might not have any importance under autotrophic conditions. In this study, however, it was observed that the $\Delta nifJ$ mutant could not grow as well as the WT under mixotrophic conditions in cultures that were continuously bubbled with air. In order to make sure that these cultures did not turn anoxic under mixotrophic conditions, the oxygen concentration was determined. These measurements showed oxic conditions in the cultures (Gutekunst, unpublished). It can thus be concluded that NifJ (PFOR) seems to be activated under oxic conditions in *Synechocystis*. As ferredoxin is reduced in the course of photosynthesis at PSI under autotrophic conditions, NAD⁺, which is reduced by the PDH-complex, might be a more suitable electron acceptor under autotrophic conditions. Under mixotrophic conditions, the photosynthetic rate of $\Delta nifJ$ sharply declined as in the WT (Fig. 4.8). Most important the growth of the $\Delta nifJ$ mutant was impaired under mixotrophic conditions (Fig. 4.1). It is easy to explain the decreased photosynthetic and increased respiration rate in both WT and $\Delta nifJ$ under mixotrophic conditions. As the exogenous glucose supplies the cells with ATP, reductants and intermediates, photosynthesis can be down regulated. However, exogenous glucose did not strongly suppress the photosynthetic rate in the nitrogen-fixing strain *Cyanothece* 51142 (Feng, *et al.*, 2010). Nevertheless, precise determination of the photosynthetic and respiratory activities is difficult, as the metabolic behavior fluctuates strongly due to its circadian rhythm (Toepel, *et al.*, 2008).

PFOR catalyzes the degradation of glucose under reduction of ferredoxin or flavodoxin. The reduced ferredoxin can be used to reduce nitrate to ammonia in the cells. It was therefore hypothesized that a limited ability to reduce nitrate in the $\Delta nifJ$ mutant might be the reason for its impaired growth under mixotrophic conditions from day 5 on (Fig. 4.1). This hypothesis was supported by the measured absorption spectra of mixotrophic $\Delta nifJ$ cultures, which showed that the pigments were degraded after a few days growth (Fig. 4.3). Nitrogen starvation was shown to cause the destruction of phycobiliproteins, whereas cyclic photophosphorylation around PSI is activated to provide ATP (Krasikov, *et al.*, 2012). During nitrogen starvation, terminal oxidases and hydrogenases are significantly up-regulated which provided alternative sinks for excess electrons that are no longer used in carbon fixation or nitrate reduction (Stanier, *et al.*, 1977; Krasikov, *et al.*, 2012).

However, the replacement of nitrate by arginine in the growth medium, which can be metabolized directly as nitrogen source could not rescue the growth phenotype of $\Delta nifJ$ under mixotrophic conditions. It even prevented the growth of $\Delta nifJ$ from the first day of inoculation under mixotrophic conditions, whereas the WT was able to grow (Fig. 4.5). This finding supports the hypothesis that the mutant cells suffer from a surplus of electrons under mixotrophic conditions. When a part of the photosynthetic electron flow was cut by DCMU under mixotrophic conditions in the mutant, $\Delta nifJ$ grew as well as the WT under the same conditions (Fig. 4.4).

The bidirectional NiFe-hydrogenase in *Synechocystis* works as an electron valve (Appel, *et al.*, 2000) and is connected to PFOR for fermentative hydrogen production (Gutekunst, *et al.*, 2014). The same phenotype that was observed for $\Delta nifJ$ under mixotrophic conditions with arginine as nitrogen source was also observed in the hydrogenase free mutant $\Delta hoxH$ when it was cultivated with arginine and glucose under a dark: light regime with anoxic conditions during the dark period (Fig. 4.5 and Gutekunst, *et al.*, 2014). The most important sinks for reduced ferredoxin under autotrophic conditions are the Calvin-Benson cycle and the reduction of nitrate. Both sinks are closed under mixotrophic conditions when nitrate is replaced by arginine. The addition of glucose inactivates the Calvin-Benson cycle (Oesterhelt, *et al.*, 2007) and the absence of nitrate closes this sink for reduced ferredoxin. In contrast to the WT, which was able to metabolize glucose and arginine, $\Delta nifJ$ and $\Delta hoxH$ were not (Fig. 4.5). This shows that PFOR and the hydrogenase are important electron sinks

for reduced ferredoxin under mixotrophic, nitrate-limiting conditions (Gutekunst *et al.*, 2014). A surplus of electrons under mixotrophic conditions could also explain the higher respiration rate in the $\Delta nifJ$ cultures compared to the WT. It was argued that a higher photosynthetic efficiency in the $\Delta nifJ$ cells of the cyanobacterium *Synechococcus* led to a 20% faster growth under diurnal growth conditions (McNeely, *et al.*, 2011). This could not be observed in $\Delta nifJ$ cells of *Synechocystis* in this study.

There are various metabolic strategies to dissipate the electrons from light energy or exogenous carbon sources. The energy can be converted into heat (Gilmore, 2004) or be recycled in the pseudocyclic electron transport chain (Asada, 2000). Electrons can be consumed by sinks such as nitrate (Serebryakova, 2007; Gutthann, *et al.*, 2007) or protons via the hydrogenase (Appel, *et al.*, 2000; Cournac, *et al.*, 2004; Gutthann, *et al.*, 2007). The uptake of energy coming from light can be limited by a reduced absorbance via a regulation of the light harvesting complexes (McConnel, *et al.*, 2002). Additionally different types of terminal oxidases are present in cyanobacteria cells that function as electron sinks when the external energy is beyond the capacities of the electron transport chain. In *Synechocystis* the three terminal oxidases cytochrome c oxidase (Nicholls, *et al.*, 1992), Cta II (Huang, *et al.*, 2002), and cytochrome bd oxidase (cyt bd oxidase) (Berry, *et al.*, 2002) were described. The cyt bd oxidase is able to take up electrons from the plastoquinone (PQ) pool and to transfer them to oxygen, which results in the production of water. A high activity of the cyt bd oxidase indicates an over-reduction of the plastoquinone pool in the cells. The activity of the cyt bd oxidase was measured via PAM in this study in order to get hints about the reduction state of the photosynthetic electron transport chain in both the WT and $\Delta nifJ$ under different conditions. As shown in (Fig. 4.7) the activity of the Cyt bd oxidase was elevated in $\Delta nifJ$ cultures under mixotrophic conditions compared to the WT on those days on which the growth of $\Delta nifJ$ was impaired compared to the WT. The trend of a higher cyt bd oxidase activity in $\Delta nifJ$ cells continued until day 5 when the glucose was consumed (Fig. 4.7). This indicates that $\Delta nifJ$ cells truly suffer from an elevated electron pressure under mixotrophic conditions.

5.1.2 Analysis of excreted metabolites of WT and mutants under different conditions

In order to verify the hypothesis about the fermentative metabolism of pyruvate derived from glucose degradation pathways in *Synechocystis* sp. PCC 6803 (Fig. 1.4), metabolites of WT, $\Delta nifJ$ and $\Delta hoxH$ mutants were determined by NMR measurement. It was shown in the cyanobacterium *Synechococcus* 7002 that the majority of the metabolites produced by fermentation were hydrogen, lactate, acetate, alanine, succinate and carbon dioxide (McNeely, *et al.*, 2010). WT, $\Delta nifJ$ and $\Delta hoxH$ mutants of *Synechocystis* sp. PCC 6803 excreted acetate, lactate, alanine, succinate, 3-hydroxybutyrate and formate into the medium (Fig. 4.10). Lactate, alanine, succinate and 3-hydroxybutyrate appeared after the onset of fermentation so they can be interpreted as fermentatively produced metabolites in the WT and mutant cells. However acetate and formate were already present in the medium before fermentative conditions were induced, which indicates that these two metabolites were already produced under autotrophic conditions. Acetate which is supposed to be produced via PFOR under fermentative conditions was also one of the fermentative end products in the $\Delta nifJ$ mutant (Fig. 4.12). The acetate that was present at the beginning of the fermentation might have been produced under autotrophic conditions by the PDH complex. However as shown in figure 4.12, the amount of acetate clearly increased indicating that the PDH complex took over the reaction catalyzed by PFOR under fermentative conditions. If the latter is true NADH would be produced by the PDH complex under fermentative conditions. This could explain why ethanol was detected in some $\Delta nifJ$ cultures, as the production of ethanol would serve to regenerate NAD^+ for the reaction catalyzed by the PDH complex. Fermentative ethanol production has also been reported in other cyanobacteria, such as *Arthrospira (Spirulina) maxima* (Stal., *et al.*, 1997; Carrieri, *et al.*, 2010), while in *Synechococcus* sp. PCC 7002 it was not detectable (Deng, *et al.*, 1999).

The NMR analyses of WT and $\Delta nifJ$ under mixotrophic conditions (Fig. 4.15) showed that glucose was consumed within 5 days and 6 days in the WT and $\Delta nifJ$ cultures respectively and that both cultures turned into their stationary phase of growth from this point on. The fact that the maximally reached optical density (OD_{750}) differed between WT and $\Delta nifJ$ even though the amount of consumed glucose was the same, can partly be explained by the higher activity of the cyt bd oxidase in $\Delta nifJ$ (Fig. 4.7),

as it reduces the ATP yield by consuming electrons coming from the PQ pool producing water. Alternatively $\Delta nifJ$ cells might redirect electrons to a higher extent into fermentative metabolism than the WT as described by the Crabtree effect (De Deken, 1966; Fiechter, *et al.*, 1981; Marc, *et al.*, 2013). It is known e.g. from *Saccharomyces cerevisiae* that an overflow of NADH generated by glucose degradation pathways may lead to a flux toward fermentative metabolism with the production of ethanol, glycerol, acetate or lactate in the presence of oxygen thereby bypassing TCA cycle and respiration to maintain the redox balance (Rieger, *et al.*, 1983; Postma, *et al.*, 1989; Gancedo, 1998; Vemuri, *et al.*, 2007). It was hypothesized that the Crabtree effect might get important when the NADH/NAD⁺ ratio overcharges the respiratory capacity of a cell (Marc, *et al.*, 2013). The cells therefore switch from respiration to fermentation under oxic conditions. It is obvious that the optical density that a culture can reach when exogenous glucose is fermented instead of respired is less, as less ATP and metabolic intermediates are produced. Whether the Crabtree effect plays a role under mixotrophic conditions in the $\Delta nifJ$ mutant and also to a maybe lesser extent in the WT, cannot be decided from the data gathered in this study. However the observed excretion of products such as lactate, alanine, succinate, and formate in both WT and $\Delta nifJ$ and the production of ethanol in the $\Delta nifJ$ mutant indicate, that the Crabtree effect might be of importance for both WT and $\Delta nifJ$ cultures.

WT and $\Delta nifJ$ excreted acetate and formate as the predominant mixotrophic end products. Acetate might be produced both by the PDH complex and PFOR under mixotrophic conditions. The expression of *nifJ* was observed under oxic conditions in *Synechocystis* (Schmitz, *et al.*, 2001). The fact that $\Delta nifJ$ has a phenotype under mixotrophic conditions heavily indicates that PFOR is expressed, active and of physiologic importance under these conditions. Lactate and alanine were detected from day 6 in $\Delta nifJ$ mutant cells, which was later than in the WT. Ethanol was only found in the supernatant of the mutant. It is not clear from these measurements whether ethanol had already been produced in the precultures of $\Delta nifJ$ or whether the cells started to produce ethanol under mixotrophic conditions. In the $\Delta nifJ$ mutant only the PDH complex is able to catalyze the reaction from pyruvate to acetyl-CoA both under autotrophic and mixotrophic conditions. Whereas NifJ reduces ferredoxin, the PDH complex reduces NADH ($E_{0 \text{ NAD}^+ / \text{NADH}} = -315 \text{ mV}$) in this reaction. The production of ethanol ($E_{0 \text{ acetaldehyde} / \text{ethanol}} = -197 \text{ mV}$) in the $\Delta nifJ$ mutant might

therefore serve the function to regenerate NAD^+ thereby keeping the reaction catalyzed by the PDH complex running. From day 3 on, acetate was produced. After glucose had been consumed NAD^+ was regenerated via lactate/alanine production (E_0 pyruvate / lactate = -185 mV) in both WT and $\Delta nifJ$. Since the redox potential of acetylaldehyde / ethanol is slightly less positive than that of pyruvate / lactate, there might be a mechanism for the cells to reduce acetylaldehyde preferentially over lactate / alanine production. The fact that only the $\Delta nifJ$ mutant produced ethanol might be due to the fact, that 2 NAD^+ are regenerated when acetate is reduced to ethanol but only 1 NAD^+ is regenerated when pyruvate is reduced to either lactate or alanine (Fig. 4.13).

High $\text{NADH} / \text{NAD}^+$ ratio resulting from glucose degradation pathways or the reaction catalyzed by the PDH complex might have the side effect that the PDH complex is phosphorylated and inactivated as known from e.g. *Azotobacter vinelandii* and mammals (de Kok, *et al.*, 1998; Patel, *et al.*, 2006). It was observed in *Synechocystis* that the $\text{NADH} / \text{NAD}^+$ ratio rose, when the cells were shifted from autotrophic to mixotrophic conditions (Takahashi, *et al.*, 2008). It could be shown by colorimetric $\text{NADH} / \text{NAD}^+$ measurements in this study that the intracellular $\text{NADH} / \text{NAD}^+$ ratio was higher in the $\Delta nifJ$ mutant under mixotrophic conditions compared to the WT whereas the ratio remained stable in the autotrophic cultures (Fig. 4.24). And interestingly, the $\text{NADH} / \text{NAD}^+$ ratio decreased as soon as the glucose had been consumed and the growth of the cultures reached the stationary phase. The fact that the $\text{NADH} / \text{NAD}^+$ ratio was elevated in the $\Delta nifJ$ mutant compared to the WT under mixotrophic conditions is well in line with the assumption that the mutant suffers of a surplus of electrons. A lacking amount of sufficient NAD^+ could hinder the activity of the PDH complex and could thus be responsible for the impaired growth of $\Delta nifJ$ under mixotrophic conditions. If the PDH complex should be inactivated by a high NADH concentration in the $\Delta nifJ$ mutant, this might result in a lack of acetyl-CoA for the TCA cycle. Consequently, the intermediates generated from the TCA cycle would also be missed which might lead to the impaired growth of the $\Delta nifJ$ mutant under mixotrophic conditions. This assumption could be supported by mixotrophic growth experiments in which the phenotype of the $\Delta nifJ$ mutant could be rescued by the addition of acetate, which can be converted into acetyl-CoA (Fig. 4.25).

It was impossible to delete *pdhA* in order to obtain a mutant with an inactivated PDH complex. Therefore, it can be concluded that the PDH complex is essential for *Synechocystis* and that its function cannot be compensated by PFOR. However *Synechocystis* needs PFOR to support a WT like growth under mixotrophic conditions.

5.1.3 Transcript expression of *nifJ* and *pdhA* under different conditions

As discussed above, PFOR has a function under mixotrophic conditions and the PDH complex might also be expressed under fermentative conditions in *Synechocystis* sp. PCC 6803. Expression of *nifJ* under oxic conditions has been observed in some cyanobacteria such as *Synechococcus* 6301, *Synechococcus* 6803, and *Synechococcus* 7002 (Schmitz, *et al.*, 2001). In the cyanobacterium *Synechococcus* 7002 deletion of *pdhA* resulted in a mutant with inactivated PDH complex. This mutant was auxotrophic for acetate indicating that PFOR could not produce the required acetyl-CoA to compensate for the lack of the PDH complex under oxic conditions (Xu, 2010). This result indicates that, under aerobic conditions PFOR is unable to support the autotrophic growth of this cyanobacterium (Xu, 2010). For the PDH complex, it was found that it contributes to the fermentative metabolism in the PFOR-deletion mutant of *Synechococcus* 7002 (McNeely, *et al.*, 2011). In this study, RT-PCR was performed to investigate the expression of *nifJ* and *pdhA* in WT and mutant cells under different conditions. As expected, *nifJ* is transcribed under fermentative conditions in the WT but not in $\Delta nifJ$ mutant (Fig. 4.16). The expression of *nifJ* under autotrophic and mixotrophic conditions is consistent with the results above. Also *pdhA* was expressed under fermentative conditions (Fig. 4.16), which shows that the PDH complex might have a function under these conditions. RT-PCR results can only reveal whether a gene is transcribed or not. To further study the gene expression in *Synechocystis* in more detail quantitative real-time PCR (qRT-PCR) was carried out.

The expression ratios of *nifJ* and *pdhA* under mixotrophic to autotrophic conditions were analyzed by qRT-PCR. There was no difference in the transcription level of both genes within the first 24 h, which is well in line with the growth curves in which no difference was detectable in this time period (Fig. 4.20, 4.21, 4.22). After 48 h the optical density at 750 nm drifted apart between autotrophic and mixotrophic cultures.

At this time point the transcription of both *pdhA* and *nifJ* started to be more strongly expressed under mixotrophic compared to autotrophic conditions in the WT (Fig. 4.21, 4.22). The transcription of *pdhA* was only slightly upregulated after 72 h in the $\Delta nifJ$ mutant. This indicates that cells need time to adapt to the new growth environment and to shift their metabolism. When cells of *Synechococcus* sp. strain PCC 7002 were transferred from autotrophic conditions to fermentative conditions, *nifJ* transcription levels increased within 30 min (McNeely, *et al.*, 2011). The time span, which was only 30 min, is much shorter than 24 h in our experiments (Fig. 4.21). This might be due to the fact that the cells need time to sense the glucose first and then switch their metabolism. This can also be seen from our photosynthesis and respiration results (Fig. 4.8 and Fig. 4.9). As seen in figure 4.18 the transcription of both *nifJ* and *pdh* was mostly upregulated five days after the addition of glucose. The same was true for the transcription of *pdh* in the *nifJ* mutant. When the transcription of *pdh* and *nifJ* was analyzed in a more detailed timeframe after the addition of glucose, it became evident that the transcription of *pdh* peaked after 48 h whereas the transcription of *nifJ* peaked after 72 h. This is as expected as the PDH complex might be most important under autotrophic conditions whereas PFOR becomes activated when autotrophic conditions change to mixotrophic ones.

When cultures in growth medium supplemented with glucose and without glucose were incubated for one day in the dark, the transcription of *nifJ* was up-regulated in the WT with glucose, while *pdhA* was down-regulated (Fig. 4.23). Many studies corroborate this result. Within 30 min or 1 h after fermentative incubation, a more than 100-fold increase in *nifJ* transcription and a decrease in transcription of the PDH complex was observed in *Synechococcus* 7002 (McNeely, *et al.*, 2011; Ludwig, *et al.*, 2011). The transcription of the PDH complex was not totally inactivated which supports the hypothesis of the partitioning of PDH complex and PFOR pathways under fermentative conditions.

However, since there are many possible post-transcriptional regulation mechanisms, the gene expression alone cannot tell for sure whether an enzyme is active or not (Feng, *et al.*, 2010).

5.2 Characterization of glucose degradation pathways

As discussed in 5.1, exogenous glucose has a different physiological effect on the WT of *Synechocystis* compared to the $\Delta nifJ$ mutant. The stationary growth of mixotrophic $\Delta nifJ$ cultures did not reach the same optical density at 750 nm as the WT (Fig. 4.1), and the activity of cytochrome bd oxidase under mixotrophic conditions in the mutant was up-regulated at the early stage (the second day of incubation, Fig. 4.7). These results indicate that PFOR is involved in the glucose degradation in *Synechocystis* in the light beside the PDH complex even though the enzyme is regarded as being inactivated by oxygen (Neuer, *et al.*, 1982). This hypothesis is supported by the reports that *nifJ* is expressed under aerobic conditions (Schmitz, *et al.*, 2001). This idea is in good agreement with the qRT-PCR results, which show that the transcripts of *nifJ* and *pdhA* were both expressed under mixotrophic conditions (Fig. 4.18). Recent studies in our group show that the hydrogenase is connected to NifJ and furthermore that the hydrogenase is essential under mixotrophic nitrate-limiting conditions (Gutekunst, *et al.*, 2014). In order to understand the hydrogen metabolism in *Synechocystis* under mixotrophic and fermentative conditions in more detail, the glucose degradation pathways under these conditions were studied.

5.2.1 A novel glucose degradation enzyme in *Synechocystis*: glucose dehydrogenase (GDH)

It was widely accepted that the Embden-Meyerhof-Parnas pathway (EMP, often simply “glycolysis”) and alternatively the oxidative pentose phosphate pathway (OPP) are the main glucose catabolism pathways in *Synechocystis* (Yoshikawa, *et al.*, 2013). In *Synechocystis*, exogenous glucose is phosphorylated to glucose-6-phosphate via glucokinase first and then further degraded in the EMP or OPP pathway (Yang, *et al.*, 2002; Yoshikawa, *et al.*, 2010). However, it is still not clear how these two different pathways cooperate with each other and which one is more important under mixotrophic conditions in *Synechocystis*. Glucose can also be degraded by another enzyme named glucose dehydrogenase (GDH) besides glucokinase in some bacteria (Flamholz, *et al.*, 2013). By GDH, glucose is converted into gluconate then connected into 6P-gluconate, which can flow into the OPP pathway or the ED (Entner-Doudoroff) pathway known in other organisms (Verhees, *et al.*, 2003). The ED pathway has never been described in cyanobacteria. In order to

find out which glucose degradation pathway is of importance under mixotrophic conditions in *Synechocystis*, different mutants were constructed in which known key enzymes of the different pathways were knocked out. It was shown in Southern blots that *zwf* (encoding the key enzyme G6PDH of the OPP pathway) or *pfkB1*, *pfkB2* (encoding two isoforms of the key enzyme phosphofructokinase of the EMP pathway) or all three genes could be deleted from all genomic copies of *Synechocystis* (Fig. 4.28). *Gdh*, which encodes one (*sll1709*) of two putative glucose dehydrogenases, could also be deleted in the WT, Δzwf and $\Delta pfkB_1B_2$, but not in $\Delta zwf pfkB_1B_2$. When trying to delete *gdh* in the $\Delta zwf pfkB_1B_2$ mutant, some undisrupted *gdh* copies were kept in some of its multiple genomic copies, resulting in the merodiploid mutant *gdh*/ $\Delta gdh zwf pfkB_1B_2$. This indicates that *sll1709* is essential in this genetic background. Δzwf , $\Delta pfkB_1B_2$ and $\Delta zwf pfkB_1B_2$ grew similar to the WT under both autotrophic and mixotrophic conditions, whereas the growth of Δgdh was impaired under mixotrophic conditions. That the mutant ($\Delta zwf pfkB_1B_2$) in which both the key enzymes of EMP and OPP pathway were degraded, was able to enhance its growth under mixotrophic conditions, came as a surprise. This observation clearly contradicts the widely held belief that *Synechocystis* relies on the EMP and OPP pathway to degrade glucose under mixotrophic conditions (Yoshikawa, *et al.*, 2013), nevertheless it indicates that *Synechocystis* might bypass these two pathways by GDH for glucose degradation in the light. Under autotrophic conditions, Δgdh , $\Delta gdh zwf$ and $\Delta gdh pfkB_1B_2$ had no phenotype concerning their growth compared to the WT (Fig. 4.30). However under mixotrophic conditions the $\Delta gdh pfkB_1B_2$ mutant did not reach the same optical density at 750 nm as the WT and $\Delta gdh zwf$ could not grow at all (Fig. 4.30). It might be concluded that the OPP pathway is more important than the EMP pathway under mixotrophic conditions when GDH is missing, this is however opposed by the assumption that *Synechocystis* prefers the EMP pathway (Knowles, *et al.*, 2003; Jansén, *et al.*, 2010). For the merodiploid mutant *gdh*/ $\Delta gdh zwf pfkB_1B_2$, the cells could grow neither under autotrophic conditions nor under mixotrophic conditions in liquid cultures, while the mutant could grow on agar plates (Fig. 4.31). This result supports the hypothesis above about the function of GDH encoded by *sll1709* under mixotrophic conditions. However, it could not be confirmed within this study that *sll1709* really encodes for a glucose dehydrogenase. The alternative genes of a GDH *slr1608* is currently deleted and the respective

mutant will be characterized in order to find out whether one or both of these two enzymes catalyze the oxidation of glucose to gluconate.

5.2.2 Characterization of the ED pathway in *Synechocystis*

The fact that the mutant $\Delta zwf pfkB_1 B_2$ in which the key enzymes of both the EMP and the OPP pathway were knocked out could still enhance its growth under mixotrophic conditions came as a surprise (Fig. 4.31). It was thus searched for an additional to date not noticed glucose degradation pathway. Glucose can be degraded into gluconate by GDH as discussed above. Gluconate can be further degraded either in the OPP pathway or alternatively in the Entner-Doudoroff pathway (ED), which was never described in cyanobacteria (Fig. 1.3). The Entner-Doudoroff pathway (ED) is another glucose degradation pathway besides EMP and OPP, which is found in archaea and many bacteria (Flamholz, *et al.*, 2013). The key enzyme of this pathway is the KDPG aldolase. It is still unknown whether the ED pathway operates in cyanobacterium to date (Fabris, *et al.*, 2012; Chavarría, *et al.*, 2013). If one molecule glucose is degraded by the ED pathway, the cells gain one ATP, zero ATP in the OPP pathway, and two ATP by the EMP pathway (Table 1.1). The organisms, which hold the ED pathway mainly belong to facultative anaerobic and aerobic strains and are thus able to gain ATP via aerobic respiration (Flamholz, *et al.*, 2013).

The gene *slI0107(eda)* is annotated as KDPG aldolase in *Synechocystis*. The sequence of the enzyme SII0107 from *Synechocystis* was aligned with the well characterized KDPG aldolase from *E. coli* (Fig. 4.37). Seven out of eight conserved amino acids were conserved in SII0107 from *Synechocystis* (Table 4.5). Only the arginine at position 49 was replaced by an asparagine, which is also found in the KDPG aldolase in *Clostridium pasteurianum* (Fuchs, *et al.*, 2006). It can be concluded by these results that SII0107 might be a KDPG aldolase in *Synechocystis*. An in-depth protein alignment analysis that was carried out in our group revealed that 96% of all totally sequenced cyanobacteria hold a KDPG aldolase, only 4% hold the key enzyme of the EMP pathway alone, 58 % hold the key enzymes of both the EMP and ED pathway (PFK and KDPB-aldolase) and remarkably 38 % of all sequenced cyanobacteria hold the key enzyme of the ED pathway alone but no key enzyme of the EMP pathway (Fährnich and Gutekunst, unpublished). This clearly indicates that most cyanobacteria might hold the ED pathway. Interestingly, *Prochlorococcus* and

Synechococcus, which both live in oligotrophic marine environment, hold only the KDPG aldolase (Fähnrich and Gutekunst, unpublished). This might be due to the necessity to live most economically under these nutrient-limited conditions. It has been shown in some microbes that the expression of unnecessary proteins can limit their growth (Scott, *et al.*, 2010; Schuetz, *et al.*, 2012). The protein costs for the ED pathway were shown to be lower than the protein costs for the EMP pathway per molecule glucose degraded (Flamholz, *et al.*, 2013), which might be the reason why cyanobacteria in oligotrophic environments prefer the ED pathway over the EMP pathway.

In order to run the ED pathway a gluconate kinase and a 6-phosphogluconate dehydratase are needed beside the KDPG aldolase (Fig. 4.38). Protein sequence alignment analysis (Table 4.6) revealed that the hypothetical protein Slr0207 which has a conserved gluconate kinase domain might function as a of gluconate kinase in *Synechocystis*. The gluconate kinase transfers gluconate to 6P-gluconate in the ED pathway (Fig. 4.38). The gene *slr0452* in *Synechocystis* was found to be similar to the gene which encodes 6-phosphogluconate dehydratase in *E. coli*. Even though the function of all these candidate proteins/genes needs to be verified experimentally, these results indicated that *Synechocystis* might degrade glucose via the ED pathway.

5.2.3 Transcription levels of the key genes of the EMP, OPP and ED pathways in *Synechocystis*

The faster growth rate observed in *Synechocystis* cells grown under mixotrophic conditions can be ascribed to the activities of enzymes associated with the glucose degradation pathways (Yang, *et al.*, 2002; Lee, *et al.*, 2007). In this study, the expression ratio of key genes of the EMP (*pfkB1*, *pfkB2*), OPP (*zwf*) and ED (*eda*) pathways in *Synechocystis* under mixotrophic conditions to autotrophic conditions were determined by qRT-PCR in order to check the impact of exogenous glucose on the glucose metabolism.

As shown in figure 4.40 the growth of cells incubated with glucose was enhanced from day 2 on and the glucose was totally consumed on day 5. Therefore in order to evaluate the significance of different pathways under mixotrophic conditions, the period between day 2nd and 5th is especially important. As shown in figure 4.41 the

transcription of the key enzymes of the EMP (PfkB1, PfkB2) and OPP (ZWF) pathway was rather down than upregulated whereas the transcription of the KDPG aldolase (encoded by *eda*) and the putative *gdh* (*sl11709*) that might both participate in the ED pathway were enhanced. These results indicate that the ED pathway might be induced under mixotrophic conditions rather than the EMP or OPP pathway. This is conflict with DNA microarray analysis that revealed that, the expression levels of genes which encode the glyceraldehyde-3-phosphate dehydrogenase from the EMP pathway and 6-phosphogluconate dehydrogenase and ribose-5-phosphate isomerase from the OPP pathway were higher under mixotrophic conditions than under autotrophic conditions. (Yoshikawa, *et al.*, 2013).

As expected, the expression of *pfkB1*, *pfkB2* and *zwf* was elevated after one day under heterotrophic conditions (10 mM glucose and darkness) while the expression of *gdh* and *eda* declined (Fig. 4.45). This indicates that the EMP and OPP pathways might be more important under heterotrophic conditions (Jansén, *et al.*, 2010).

The results show that it is highly likely that *Synechocystis* degrades glucose via the Entner-Doudoroff (ED) pathway under mixotrophic conditions. As the key enzyme of the ED pathway was shown to be highly abundant in the genomes of most sequenced cyanobacteria, it is furthermore likely that this to date unnoticed pathway operates in cyanobacteria. Knowing how glucose is degraded in *Synechocystis* is not only important to understand its glucose metabolism but might also help to get a deeper understanding for its hydrogen metabolism, as both are tightly connected.

6 Summary

In the present work, the effects of exogenous glucose on physiology and metabolism of the single cell model organism *Synechocystis* sp. PCC 6803 grown in the light was investigated. Glucose is degraded to pyruvate, which can be decarboxylated to acetyl-CoA either by the PDH complex (pyruvate dehydrogenase complex) or by PFOR (pyruvate: ferredoxin/ flavodoxin oxidoreductase). A mutant ($\Delta nifJ$), in which PFOR encoded by *nifJ* was deleted, was characterized under mixotrophic conditions. Furthermore, the glucose degradation pathways in *Synechocystis* were studied in detail. The results are summarized as follows:

1. PFOR counts as an enzyme that is only active under anoxic conditions even though it has been shown that the gene is transcribed in the presence of oxygen in some cyanobacteria (Neuer, *et al.*, 1982; Schmitz, *et al.*, 2001). It was shown in this study that *nifJ* is transcribed under fermentative, autotrophic and mixotrophic conditions as *pdhA* (encoding a subunit of the PDH complex). This study revealed that the growth of $\Delta nifJ$ was impaired under mixotrophic conditions (10 mM glucose and light). Its photosynthetic rate declined stronger under mixotrophic conditions than in the WT. The addition of DCMU, which blocks the photosynthetic electron transport chain, resulted in a similar growth of $\Delta nifJ$ and WT in the presence of glucose. It was therefore hypothesized that PFOR might be an important electron sink under mixotrophic conditions. This was supported by the observation that the activity of the cytochrome bd-type oxidase, which is a good indicator for the reduction state of the photosynthetic electron transport chain, was increased in $\Delta nifJ$ compared to the WT. Whereas PFOR reduces ferredoxin, the PDH complex reduces NAD^+ to NADH, when pyruvate is converted to acetyl-CoA. Therefore the NADH/ NAD^+ ratio was enhanced in $\Delta nifJ$ pointing to a high reduction grade of the cells. NMR analyses revealed that only $\Delta nifJ$ but not the WT excreted ethanol into the medium. It was assumed that $\Delta nifJ$ regenerates NAD^+ by ethanol production. It was hypothesized that the PDH complex might be inactivated by the high NADH/ NAD^+ ratio in $\Delta nifJ$ as known in mammals (Patel, *et al.*, 2006). This would inhibit the production of acetyl-CoA and thereby block the TCA cycle, which could be a reason for the impaired growth in $\Delta nifJ$ under mixotrophic conditions. This hypothesis was supported by the fact that the growth phenotype of $\Delta nifJ$ under mixotrophic conditions could be partly rescued by the addition of acetate, which can be converted to acetyl-CoA.

2. Both PFOR and the hydrogenase were shown to be essential for growth under nitrate limited mixotrophic conditions.

3. Two glucose degradation pathways namely the EMP (glycolysis or Embden-Meyerhoff) and the OPP (oxidative pentose phosphate) pathway are known in *Synechocystis*. It was shown in this study that the triple mutant $\Delta zwf pfb_1 B_2$ in which all genes encoding the key enzymes of EMP (*pfb₁*, *pfb₂*) and OPP (*zwf*) pathways were deleted, could enhance its growth under mixotrophic conditions as the WT. This came as a surprise and led to the hypothesis that an additional to date unnoticed glucose degradation pathway might operate in *Synechocystis*. Via protein alignments all genes encoding for enzymes needed for the ED (Entner-Doudoroff) pathway were identified. Sll0107 was found annotated as KDPG aldolase, which is the key enzyme of the ED pathway. A protein alignment between Sll0107 (encoded by *eda*) and the well-characterized KDPG aldolase from *E. coli* showed that 7 out of 8 amino acids critical for the enzyme activity are conserved in Sll0107. This indicated that Sll0107 might function as KDPG aldolase in *Synechocystis*. Additionally two candidate genes (*sll1709* and *slr1608*) were identified that might encode for GDH. *sll1709* could not be completely deleted from the triple mutant $\Delta zwf pfb_1 B_2$, which might indicate that *sll1709* is essential in this genetic background in *Synechocystis*. Under mixotrophic conditions the transcripts of *pfb₁* and *pfb₂* (EMP) and *zwf* (OPP) were rather down regulated whereas the transcription of *gdh* and *eda* (possibly involved in the ED pathway) was up regulated. Under heterotrophic conditions the expression levels of these genes were reversed. This indicates that the ED pathway might be of importance under mixotrophic conditions in *Synechocystis*.

The two main findings of this study are that: (a) In *Synechocystis* sp. PCC 6803 PFOR seems to operate in the presence of oxygen and is an important electron sink under mixotrophic conditions; (b) *Synechocystis* sp. PCC 6803 might hold the Entner-Doudoroff pathway beside the EMP and OP pathways and might degrade exogenous glucose via this pathway especially under mixotrophic conditions in the light.

7 Zusammenfassung

In der vorliegenden Arbeit wurde der Einfluss von exogener Glukose auf die Physiologie und den Metabolismus des einzelligen Modellorganismus *Synechocystis* sp. PCC 6803 untersucht. Glukose wird zu Pyruvat abgebaut, welches entweder durch den PDH Komplex (Pyruvat Dehydrogenase Komplex) oder durch die PFOR (Pyruvate: Ferredoxin/Flavodoxin Oxidoreduktase) weiter zu Acetyl-CoA decarboxyliert werden kann. Eine Mutante ($\Delta nifJ$), in welcher die PFOR, die von *nifJ* kodiert wird, ausgeschaltet war, wurde unter mixotrophen Bedingungen charakterisiert. Darüberhinaus wurden Glukose Abbauwege in *Synechocystis* detailliert untersucht. Die Ergebnisse werden im Folgenden zusammengefasst:

1. Die PFOR gilt als ein Enzym, welches nur unter anoxischen Bedingungen aktiv ist, obwohl gezeigt wurde, dass das Gen in einigen Cyanobakterien in Gegenwart von Sauerstoff exprimiert wird (Neuer, *et al.*, 1982; Schmitz, *et al.*, 2001). In dieser Studie wurde gezeigt, dass *nifJ* unter autotrophen, fermentativen und mixotrophen Bedingungen transkribiert wird, ebenso wie *pdhA*, welches für eine Untereinheit des PDH Komplexes kodiert. Es zeigte sich, dass das Wachstum von $\Delta nifJ$ unter mixotrophen Bedingungen (10 mM Glukose und Licht) beeinträchtigt war. Die photosynthetische Rate nahm in der Mutante unter mixotrophen Bedingungen stärker ab als im WT. Eine Zugabe von DCMU, welches den photosynthetischen Elektronentransport unterbricht, resultierte in einem ähnlichen Wachstum von $\Delta nifJ$ und WT in Gegenwart von Glukose. Es wurde daher die Hypothese aufgestellt, dass die PFOR eine wichtige Elektronensenke unter mixotrophen Bedingungen sein könnte. Diese Hypothese wurde unterstützt durch die Beobachtung, dass die Aktivität der Cytochrome bd-Typ Oxidase, welche ein guter Indikator für den Reduktionsgrad der photosynthetischen Elektronentransportkette ist, in $\Delta nifJ$ im Vergleich zum WT erhöht war. Während die PFOR Ferredoxin reduziert, reduziert der PDH Komplex NAD^+ zu NADH wenn Pyruvat zu Acetyl-CoA umgesetzt wird. Daher war das NADH/NAD^+ Verhältnis in der $\Delta nifJ$ Mutante erhöht, was auf einen hohen Reduktionszustand in den Zellen hinweist. NMR Analysen zeigten, dass $\Delta nifJ$ aber nicht der WT Ethanol ins Medium abgaben. Es wurde angenommen, dass $\Delta nifJ$ Ethanol produziert um NAD^+ zu regenerieren. Es wurde die Hypothese aufgestellt, dass der PDH Komplex durch das hohe NADH/NAD^+ Verhältnis inaktiviert wird, wie dies aus Säugetieren bekannt ist (Patel, *et al.*, 2006). Dies würde die Produktion von AcetylCoA und damit den Zitratzyklus hemmen, was für das beeinträchtigte Wachstum von $\Delta nifJ$ unter mixotrophen Bedingungen verantwortlich sein könnte. Diese Hypothese wird unterstützt durch die Beobachtung, dass die Beeinträchtigung

des Wachstums von $\Delta nifJ$ unter mixotrophen Bedingungen durch die Zugabe von Acetat (welches zu AcetylCoA umgesetzt werden kann) teilweise aufgehoben werden konnte.

2. Es wurde gezeigt, dass sowohl die PFOR als auch die Hydrogenase unter nitratlimitierten, mixotrophen Bedingungen essentiell sind.

3. Zwei Glukose Abbauwege, der EMP (Glykolyse oder Embden-Meyerhoff) und der OPP (Oxidativer Pentose Phosphat) Weg sind in *Synechocystis* bekannt. In der vorliegenden Arbeit wurde gezeigt, dass die Dreifachmutante $\Delta zwf pfkB_1 B_2$, in welcher alle Gene, welche für die Schlüsselenzyme des EMP (*pfkB₁*, *pfkB₂*) und OPP (*zwf*) Weges kodieren, ausgeschaltet wurden, ihr Wachstum unter mixotrophen Bedingungen wie der WT steigern konnte. Dies war überraschend und führte zu der Hypothese, dass ein bis dato unbeachteter Glukose Abbauweg in *Synechocystis* aktiv sein könnte. Über Protein-Vergleiche konnten alle Gene, welche für Enzyme, die für den ED (Entner-Doudoroff) Weg gebraucht werden, identifiziert werden. Sll0107 wurde als KDPG Aldolase annotiert vorgefunden, welche das Schlüsselenzym des ED Wegs ist. Protein-Vergleiche zwischen Sll0107 (kodiert von *eda*) und der gut charakterisierten KDPG Aldolase aus *E. coli* zeigten, dass 7 der 8 Aminosäuren, die kritisch für die Enzymaktivität sind, in Sll0107 konserviert sind. Das weist darauf hin, dass Sll0107 in *Synechocystis* als KDPG Aldolase fungieren könnte. Darüberhinaus wurden zwei Kandidatengene (*sll1709* und *slr1608*) identifiziert, welche für eine GDH kodieren könnten. *sll1709* konnte nicht vollständig aus dem Genom der Dreifachmutante $\Delta zwf pfkB_1 B_2$ deletiert werden, was darauf hinweisen könnte, dass *sll1709* in diesem genetischen Hintergrund essentiell sein könnte. Unter mixotrophen Bedingungen war die Transkription von *pfkB1* und *pfkB2* (EMP) und *zwf* (OPP) eher runter und die Transkription von *gdh* and *eda* (möglicherweise in den ED Weg involviert) eher hoch reguliert. Unter heterotrophen Bedingungen war die Expression dieser Gene umgekehrt. Dies weist darauf hin, dass der ED Weg in *Synechocystis* unter mixotrophen Bedingungen von Bedeutung sein könnte.

Die beiden Hauptaussagen dieser Arbeit sind, dass: (a) Die PFOR in *Synechocystis* sp. PCC 6803 in Gegenwart von Sauerstoff aktiv zu sein scheint und eine wichtige Elektronensenke unter mixotrophen Bedingungen ist; (b) *Synechocystis* sp. PCC 6803 neben dem EMP und OPP Weg den Entner-Doudoroff Weg betreibt und dass dieser Weg insbesondere für den Abbau von Glukose unter mixotrophen Bedingungen im Licht von Bedeutung sein könnte.

8 Future perspectives

Some more experiments need to be carried out in order to understand the mixotrophic metabolism of *Synechocystis* sp. PCC 6803 more deeply. They can be described as follows:

1. It has been shown that the growth of $\Delta nifJ$ is impaired under mixotrophic conditions and that the NADH / NAD⁺ ratio is elevated in the mutant compared to the WT. The reaction that is catalyzed by NifJ is alternatively carried out by the PDH complex. This raises the question why the PDH complex is not able to compensate for the lack of NifJ under mixotrophic conditions. The assumption was put forward that the PDH complex might be phosphorylated and inactivated under high NADH concentrations as was shown for mammals (Patel, *et al.*, 2006). In order to test this hypothesis, western blots should be carried out that allow to discriminate between a phosphorylated and unphosphorylated form of the PDH complex.
2. Two candidate genes that might code for a glucose dehydrogenase (*sll1709* and *slr1608*) were found in *Synechocystis* sp. PCC 6803. The *sll1709* deletion mutant was characterized in this study. The construction of a *slr1608* mutant is under way. The phenotype of this mutant should be characterized under different growth conditions.
3. All the associated proteins of the Entner-Doudoroff pathway have been identified in *Synechocystis* sp. PCC 6803 by protein alignment. The function of these proteins needs to be verified experimentally. The construction of a mutant with a deleted putative KDPG aldolase (the key enzyme of the ED pathway) is underway. This mutant needs to be characterized under autotrophic and mixotrophic conditions. In order to investigate whether this enzyme is truly a KDPG aldolase, enzymatic tests with the WT and the mutant need to be carried out.

9 References

- Affourtit C, Krab K, Moore AL (2001) Control of plant mitochondrial respiration. *Biochimica et Biophysica Acta (BBA)-Bioenergetics* **1504**(1): 58-69.
- Allard J, Grochulski P, Sygusch J (2001) Covalent intermediate trapped in 2-keto-3-deoxy-6-phosphogluconate (KDPG) aldolase structure at 1.95-Å resolution. *Proceedings of the National Academy of Sciences* **98**(7): 3679-3684.
- Allen MM, Smith AJ (1969) Nitrogen chlorosis in blue-green algae. *Archiv für Mikrobiologie* **69**(2):114-120.
- Ananyev G, Carrieri D, Dismukes, GC (2008) Optimization of metabolic capacity and flux through environmental cues to maximize hydrogen production by the cyanobacterium "Arthrospira (Spirulina) maxima". *Applied and Environmental Microbiology* **74**(19): 6102-6113.
- Anderson SL, McIntosh L (1991) Light-activated heterotrophic growth of the cyanobacterium *Synechocystis* sp. strain PCC 6803: a blue-light-requiring process. *Journal of Bacteriology* **173**(9): 2761-2767.
- Antal TK, Lindblad P (2005) Production of H₂ by sulphur-deprived cells of the unicellular cyanobacteria *Gloeocapsa alpicola* and *Synechocystis* sp. PCC 6803 during dark incubation with methane or at various extracellular PH. *Journal of Applied Microbiology* **98**(1): 114-120.
- Aoki M, Katoh S (1983) Size of the plastoquinone pool functioning in photosynthetic and respiratory electron transport of *Synechococcus* sp. *Plant and Cell Physiology* **24**(8): 1379-1386.
- Appel J, Phunpruch S, Steinmüller K, Schulz R (2000) The bidirectional hydrogenase of *Synechocystis* sp. PCC 6803 works as an electron valve during photosynthesis. *Archives of Microbiology* **173**(5-6):333-338.
- Asada K (2000) The water–water cycle as alternative photon and electron sinks. *Philosophical Transactions of the Royal Society of London Series B: Biological Sciences* **355**(1402): 1419-1431.
- Bar-Even A, Flamholz A, Noor E, Milo R (2012) Rethinking glycolysis: on the biochemical logic of metabolic pathways. *Nature Chemical Biology* **8**(6):509-517.
- Barz M, Beimgraben C, Staller T, Germer F, Opitz F, Marquardt C, Appel J (2010) Distribution analysis of hydrogenases in surface waters of marine and freshwater environments. *PloS One* **5**(11): e13846.
- Beck C, Von Meyenburg HK (1968) Enzyme pattern and aerobic growth of *Saccharomyces cerevisiae* under various degrees of glucose limitation. *Journal of Bacteriology* **96**(2): 479-486.
- Benemann JR, Weare NM (1974) Nitrogen fixation by *Anabaena cylindrical*. *Archives of Microbiology* **101**(1): 401-408.

- Berry S, Schneider D, Vermaas WF, Rögner M (2002) Electron transport routes in whole cells of *Synechocystis* sp. strain PCC 6803: the role of the cytochrome bd-type oxidase. *Biochemistry* **41**(10):3422-3429.
- Blankenship RE, Hartman H (1998) The origin and evolution of oxygenic photosynthesis. *Trends in Biochemical Sciences* **23**(3): 94-97.
- Bothe H, Falkenberg B, Nolteernsting U (1974) Properties and function of the pyruvate: Ferredoxin oxidoreductase from the blue-green alga *Anabaena cylindrica*. *Archives of Microbiology* **96**(1): 291-304.
- Buick R (2008) When did oxygenic photosynthesis evolve? *Philosophical Transactions of the Royal Society B: Biological Sciences* **363**(1504): 2731-2743.
- Burgdorf T, Lenz O, Buhrke T, Van der Linden E, Jones AK, Albracht SPJ, Friedrich B (2006) [NiFe]-hydrogenases of *Ralstonia eutropha* H16: modular enzymes for oxygen-tolerant biological hydrogen oxidation. *Journal of Molecular Microbiology and Biotechnology* **10**(2-4): 181-196.
- Büchel C, Zsiros O, Garab G (1998) Alternative cyanide-sensitive oxidase interacting with photosynthesis in *Synechocystis* PCC6803 Ancestor of the terminal oxidase of chlororespiration? *Photosynthetica* **35**(2): 223-231.
- Carrieri D, McNeely K, De Roo AC, Bennette N, Pelczer I, Dismukes GC (2009) Identification and quantification of water-soluble metabolites by cryoprobe-assisted nuclear magnetic resonance spectroscopy applied to microbial fermentation. *Magnetic Resonance in Chemistry* **47**(S1): S138-S146.
- Carrieri D, Momot D, Brasg IA, Ananyev G, Lenz O, Bryant DA, Dismukes GC (2010) Boosting autofermentation rates and product yields with sodium stress cycling: application to production of renewable fuels by cyanobacteria. *Applied and Environmental Microbiology* **76**(19): 6455-6462.
- del Castillo T, Ramos JL, Rodríguez-Herva JJ, Fuhrer T, Sauer U, Duque E (2007) Convergent peripheral pathways catalyze initial glucose catabolism in *Pseudomonas putida*: genomic and flux analysis. *Journal of Bacteriology* **189**(14): 5142-5152.
- Catling DC, Claire MW (2005) How Earth's atmosphere evolved to an oxic state: a status report. *Earth and Planetary Science Letters* **237**(1): 1-20.
- Chavarría M, Nikel PI, Pérez-Pantoja D, Lorenzo V (2013) The Entner–Doudoroff pathway empowers *Pseudomonas putida* KT2440 with a high tolerance to oxidative stress. *Environmental Microbiology*.
- Chenchik A, Diachenko L, Moqadam F, Tarabykin V, Lukyanov S, Siebert PD (1996) Full-length cDNA cloning and determination of mRNA 5' and 3' ends by amplification of adaptor-ligated cDNA. *Biotechniques* **21**(3): 526-535.
- Constant P, Chowdhury SP, Hesse L, Pratscher J, Conrad R (2011) Genome data mining and soil survey for the novel group 5 [NiFe]-hydrogenase to explore the diversity and ecological importance of presumptive high-affinity H₂-oxidizing bacteria. *Applied and Environmental Microbiology* **77**(17): 6027-6035.

- Conway T (1992) The Entner-Doudoroff pathway: history physiology and molecular biology. *FEMS Microbiology Letters* **103**(1):1-27.
- Cooley JW, Howitt CA, Vermaas WF (2000) Succinate: quinol oxidoreductases in the cyanobacterium *Synechocystis* sp. strain PCC 6803: presence and function in metabolism and electron transport. *Journal of Bacteriology* **182**(3): 714-722.
- Cooley JW, Vermaas WF (2001) Succinate dehydrogenase and other respiratory pathways in thylakoid membranes of *Synechocystis* sp. strain PCC 6803: capacity comparisons and physiological function. *Journal of Bacteriology* **183**(14): 4251-4258.
- Cournac L, Mus F, Bernard L, Guedeney G, Vignais P, Peltier G (2002) Limiting steps of hydrogen production in *Chlamydomonas reinhardtii* and *Synechocystis* PCC 6803 as analysed by light-induced gas exchange transients. *International Journal of Hydrogen Energy* **27**(11): 1229-1237.
- Cournac L, Guedeney G, Peltier G, Vignais PM (2004) Sustained photoevolution of molecular hydrogen in a mutant of *Synechocystis* sp. strain PCC 6803 deficient in the type I NADPH-dehydrogenase complex. *Journal of Bacteriology* **186**(6): 1737-1746.
- De Deken RH (1966) The Crabtree effect: a regulatory system in yeast. *Journal of General Microbiology* **44**(2): 149-156.
- De Marsac NT (1977) Occurrence and nature of chromatic adaptation in cyanobacteria. *Journal of Bacteriology* **130**(1): 82-91.
- Deibel RH, Niven CF (1964) Pyruvate fermentation by *Streptococcus faecalis*. *Journal of Bacteriology* **88**(1): 4-10.
- Deng MD, Coleman JR (1999) Ethanol synthesis by genetic engineering in cyanobacteria. *Applied and Environmental Microbiology* **65**(2): 523-528.
- DeRuyter YS, Fromme P (2008) Molecular structure of the photosynthetic apparatus. *The Cyanobacteria Molecular Biology Genomics and Evolution* 217-269.
- Dixon RA (1984) The genetic complexity of nitrogen fixation *Journal of General Microbiology* **130**(11):2745-2755.
- Douglas SE (2004) Chloroplast origins and evolution. *The Molecular Biology of Cyanobacteria* Springer Netherlands 91-118.
- Eiler A (2006) Evidence for the ubiquity of mixotrophic bacteria in the upper ocean: implications and consequences. *Applied and Environmental Microbiology* **72**(12): 7431-7437
- Entner N, Doudoroff M (1952) Glucose and gluconic acid oxidation of *Pseudomonas saccharophila*. *Journal of Biological Chemistry* **196**(2): 853-862.
- Fabris M, Matthijs M, Rombauts S, Vyverman W, Goossens A, Baart GJ (2012) The metabolic blueprint of *Phaeodactylum tricornutum* reveals a eukaryotic Entner–Doudoroff glycolytic pathway. *The Plant Journal* **70**(6): 1004-1014.

- Feng X, Bandyopadhyay A, Berla B, Page L, Wu B, Pakrasi HB, Tang YJ (2010) Mixotrophic and photoheterotrophic metabolism in *Cyanothece* sp ATCC 51142 under continuous light. *Microbiology* **156**(8): 2566-2574.
- Fiechter A, Fuhrmann GF, Käppeli O (1981) Regulation of glucose metabolism in growing yeast cells. *Advances in Microbial Physiology* **22**: 123-183.
- Flamholz A, Noor E, Bar-Even A, Liebermeister W, Milo R (2013) Glycolytic strategy as a tradeoff between energy yield and protein cost. *Proceedings of the National Academy of Sciences* **110**(24): 10039-10044
- Fontecilla-Camps JC, Volbeda A, Cavazza C, Nicolet Y (2007) Structure/function relationships of [NiFe]- and [FeFe]-hydrogenases. *Chemical Reviews* **107**(10): 4273-4303.
- Fraenkel AS (1996) Combinatorial games: Selected bibliography with a succinct gourmet introduction. *The Electronic Journal of Combinatorics [electronic only]* Research-paper.
- Fuchs G, Schlegel HG (2006) *Allgemeine Mikrobiologie: Begründet von Hans-Günter Schlegel* Georg Thieme Verlag.
- Fuhrer T, Fischer E, Sauer U (2005) Experimental identification and quantification of glucose metabolism in seven bacterial species. *Journal of Bacteriology* **187**(5): 1581-1590.
- Fujita Y, Murakami A, Ohki K (1987) Regulation of photosystem composition in the cyanobacterial photosynthetic system: the regulation occurs in response to the redox state of the electron pool located between the two photosystems. *Plant and Cell Physiology* **28**(2): 283-292.
- Fukui S, Tanaka A (1982) Immobilized microbial cells. *Annual Reviews in Microbiology* **36**(1): 145-172.
- Gancedo JM (1998) Yeast carbon catabolite repression. *Microbiology and Molecular Biology Reviews* **62**(2): 334-361.
- Gantt E (1994) Supramolecular membrane organization In *The molecular biology of cyanobacteria* Springer Netherlands 119-138.
- Gill R T, Katsoulakis E, Schmitt W, Taroncher-Oldenburg G, Misra J, Stephanopoulos G (2002) Genome-wide dynamic transcriptional profiling of the light-to-dark transition in *Synechocystis* sp. strain PCC 6803. *Journal of Bacteriology* **184**(13): 3671-3681.
- Gilmore AM (2004) Excess light stress: probing excitation dissipation mechanisms through global analysis of time- and wavelength-resolved chlorophyll a fluorescence. *Chlorophyll a Fluorescence* Springer Netherlands 555-581.
- Grigorieva G, Shestakov S (1982) Transformation in the cyanobacterium *Synechocystis* sp. 6803. *FEMS Microbiology Letters* **13**(4): 367-370.

- Gründel M, Scheunemann R, Lockau W, Zilliges Y (2012) Impaired glycogen synthesis causes metabolic overflow reactions and affects stress responses in the cyanobacterium *Synechocystis* sp PCC 6803. *Microbiology* **158**(Pt 12): 3032-3043.
- Gutekunst K, Chen X, Schreiber K, Kaspar U, Makam S, Appel J (2014) The bidirectional NiFe-hydrogenase in *Synechocystis* sp. PCC 6803 is reduced by flavodoxin and ferredoxin and is essential under mixotrophic nitrate-limiting conditions. *Journal of Biological Chemistry* **289**(4): 1930-1937.
- Gutthann F, Egert M, Marques A, Appel J (2007) Inhibition of respiration and nitrate assimilation enhances photohydrogen evolution under low oxygen concentrations in *Synechocystis* sp. PCC 6803. *Biochimica et Biophysica Acta (BBA)-Bioenergetics* **1767**(2): 161-169.
- Hauf W, Schlebusch M, Hüge J, Kopka J, Hagemann M, Forchhammer K (2013) Metabolic Changes in *Synechocystis* PCC6803 upon Nitrogen-Starvation: Excess NADPH Sustains Polyhydroxybutyrate Accumulation. *Metabolites* **3**(1): 101-118.
- Herranen M, Battchikova N, Zhang P, Graf A, Sirpiö S, Paakkarinen V, Aro EM (2004) Towards functional proteomics of membrane protein complexes in *Synechocystis* sp. PCC 6803. *Plant Physiology* **134**(1): 470-481.
- Heyer H, Stal L, Krumbein WE (1989) Simultaneous heterolactic and acetate fermentation in the marine cyanobacterium *Oscillatoria limosa* incubated anaerobically in the dark. *Archives of microbiology* **151**(6): 558-564.
- Heyer H, Krumbein WE (1991) Excretion of fermentation products in dark and anaerobically incubated cyanobacteria. *Archives of Microbiology* **155**(3): 284-287.
- Hihara Y, Kamei A, Kanehisa M, Kaplan A, Ikeuchi M (2001) DNA microarray analysis of cyanobacterial gene expression during acclimation to high light. *The Plant Cell Online* **13**(4): 793-806.
- Hormann H, Neubauer C, Asada K, Schreiber U (1993) Intact chloroplasts display pH 5 optimum of O₂-reduction in the absence of methyl viologen: indirect evidence for a regulatory role of superoxide protonation. *Photosynthesis Research* **37**(1): 69-80.
- Horner DS, Heil B, Happe T, Embley TM (2002) Iron hydrogenases-ancient enzymes in modern eukaryotes. *Trends in Biochemical Sciences* **27**(3): 148-153.
- Horner DS, Hirt RP, Kilvington S, Lloyd D, Embley TM (1996) Molecular data suggest an early acquisition of the mitochondrion endosymbiont. *Proceedings of the Royal Society of London Series B: Biological Sciences* **263**(1373): 1053-1059.
- Howitt CA, Vermaas WF (1998) Quinol and cytochrome oxidases in the cyanobacterium *Synechocystis* sp. PCC 6803. *Biochemistry* **37**(51): 17944-17951.
- Huang F, Parmryd I, Nilsson F, Persson AL, Pakrasi HB, Andersson B, Norling B (2002) Proteomics of *Synechocystis* sp. strain PCC 6803 identification of plasma membrane proteins. *Molecular & Cellular Proteomics* **1**(12): 956-966.
- Jansén T, Kurian D, Raksajit W, York S, Summers ML, Mäenpää P (2010) Characterization of trophic changes and a functional oxidative pentose phosphate

- pathway in *Synechocystis* sp. PCC 6803. *Acta Physiologiae Plantarum* **32**(3): 511-518.
- Jarmuszkiewicz W, Sluse-Goffart CM, Hryniewiecka L, Michejda J, Sluse FE (1998) Electron partitioning between the two branching quinol-oxidizing pathways in *Acanthamoeba castellanii* mitochondria during steady-state state 3 respiration. *Journal of Biological Chemistry* **273**(17): 10174-10180.
- Jones LW, Myers J (1964) Enhancement in the blue-green alga *Anacystis nidulans*. *Plant Physiology* **39**(6): 938.
- Kahlon S, Beeri K, Ohkawa H, Hihara Y, Murik O, Suzuki I, Kaplan A (2006) A putative sensor kinase Hik31 is involved in the response of *Synechocystis* sp. strain PCC 6803 to the presence of glucose. *Microbiology* **152**(3): 647-655.
- Kaneko T, Sato S, Kotani H, Tanaka A, Asamizu E, Nakamura Y, Tabata S (1996) Sequence analysis of the genome of the unicellular cyanobacterium *Synechocystis* sp. strain PCC6803 II Sequence determination of the entire genome and assignment of potential protein-coding regions. *DNA research* **3**(3): 109-136.
- Kaspar U (2010) Investigations on the Electron Transfer to the Bidirectional [NiFe]-Hydrogenase of *Synechocystis* sp. PCC 6803 Master thesis. Christian-Albrechts-Universitaet zu Kiel.
- Kim BH, Gadd GM (2008) Bacterial physiology and metabolism. *Cambridge: Cambridge University Press*.
- Kirsch R (2012) Physiologie und biotechnologie der pflanzlichen zelle. Bachelor thesis Christian-Albrechts-Universitaet zu Kiel.
- Kletzin A, Adams MW (1996) Molecular and phylogenetic characterization of pyruvate and 2-ketoisovalerate ferredoxin oxidoreductases from *Pyrococcus furiosus* and pyruvate ferredoxin oxidoreductase from *Thermotoga maritime*. *Journal of Bacteriology* **178**(1): 248-257.
- Knight E, Hardy RWF (1966) Isolation and characteristics of flavodoxin from nitrogen-fixing *Clostridium pasteurianum*. *Journal of Biological Chemistry* **241**(12): 2752-2756.
- Knowles VL, Plaxton WC (2003) From genome to enzyme: analysis of key glycolytic and oxidative pentose-phosphate pathway enzymes in the cyanobacterium *Synechocystis* sp. PCC 6803. *Plant and Cell Physiology* **44**(7): 758-763.
- de Kok A, Hengeveld AF, Martin A, Westphal AH (1998) The pyruvate dehydrogenase multi-enzyme complex from Gram-negative bacteria. *Biochimica et Biophysica Acta (BBA)-Protein Structure and Molecular Enzymology* **1385**(2): 353-366.
- Koksharova O, Wolk C (2002) Genetic tools for cyanobacteria. *Applied Microbiology and Biotechnology* **58**(2): 123-137.
- Krasikov V, Aguirre von Wobeser E, Dekker HL, Huisman J, Matthijs HC (2012) Time-series resolution of gradual nitrogen starvation and its impact on

- photosynthesis in the cyanobacterium *Synechocystis* PCC 6803. *Physiologia Plantarum* **145**(3): 426-439.
- Krebs HA (1970) The history of the tricarboxylic acid cycle. *Perspectives in Biology and Medicine* **14**(1): 154.
- Kruger NJ, von Schaewen A (2003) The oxidative pentose phosphate pathway: structure and organization. *Current Opinion in Plant Biology* **6**(3): 236-246.
- Kujat SL, Owttrim GW (2000) Redox-regulated RNA helicase expression. *Plant Physiology* **124**(2): 703-714.
- Kurian D, Jansèn T, Mäenpää P (2006) Proteomic analysis of heterotrophy in *Synechocystis* sp. PCC 6803. *Proteomics* **6**(5): 1483-1494.
- Käppeli O, Sonnleitner B, Blanch HW (1986) Regulation of sugar metabolism in *Saccharomyces*-type yeast: experimental and conceptual considerations. *Critical Reviews in Biotechnology* **4**(3): 299-325.
- Leach CK, Carr NG (1971) Pyruvate: Ferredoxin oxidoreductase and its activation by ATP in the blue-green alga *Anabaena variabilis*. *Biochimica et Biophysica Acta (BBA)-Bioenergetics* **245**(1): 165-174.
- Lee S, Ryu JY, Kim SY, Jeon JH, Song JY, Cho HT, Park YI (2007) Transcriptional regulation of the respiratory genes in the cyanobacterium *Synechocystis* sp PCC 6803 during the early response to glucose feeding. *Plant Physiology* **145**(3): 1018-1030.
- Lichtenthaler HK (1987) Chlorophylls and carotenoids: Pigments of photosynthetic biomembranes. *Methods in Enzymology* **148**: 350-382.
- Lindberg P, Schütz K, Happe T, Lindblad P (2002) A hydrogen-producing hydrogenase-free mutant strain of *Nostoc punctiforme* ATCC 29133. *International Journal of Hydrogen Energy* **27**(11): 1291-1296.
- Lindblad P, Christensson K, Lindberg P, Fedorov A, Pinto F, Tsygankov A (2002) Photoproduction of H₂ by wildtype *Anabaena* PCC 7120 and a hydrogen uptake deficient mutant: from laboratory experiments to outdoor culture. *International journal of hydrogen energy* **27**(11): 1271-1281.
- Lindel F (2012) Charakterisierung der nifJ--Mutante von *Synechocystis* sp. PCC 6803 unter mixotrophen Bedingungen Bachelor thesis Christian-Albrechts-Universitaet zu Kiel.
- Ludwig M, Bryant DA (2011) Transcription profiling of the model cyanobacterium *Synechococcus* sp. strain PCC 7002 by Next-Gen (SOLiD™) sequencing of cDNA *Frontiers in microbiology* **2**.
- Marc J, Feria-Gervasio D, Mouret JR, Guillouet SE (2013) Impact of oleic acid as co-substrate of glucose on “short” and “long-term” Crabtree effect in *Saccharomyces cerevisiae*. *Microbial Cell Factories* **12**(1): 83.

- Mattevi A, Obmolova G, Schulze E, Kalk KH, Westphal AH, de Kok A, Hol WG (1992) Atomic structure of the cubic core of the pyruvate dehydrogenase multienzyme complex. *Science* **255**(5051):1544-1550.
- Maxwell K, Johnson GN (2000) Chlorophyll fluorescence-a practical guide. *Journal of Experimental Botany* **51**(345): 659-668.
- McConnell MD, Koop R, Vasil'ev S, Bruce D (2002) Regulation of the distribution of chlorophyll and phycobilin-absorbed excitation energy in cyanobacteria. A structure-based model for the light state transition. *Plant physiology* **130**(3):1201-1212.
- McNeely K, Xu Y, Ananyev G, Bennette N, Bryant DA, Dismukes GC (2011) *Synechococcus* sp strain PCC 7002 nifJ mutant lacking pyruvate: ferredoxin oxidoreductase. *Applied and Environmental Microbiology* **77**(7): 2435-2444.
- McNeely K, Xu Y, Bennette N, Bryant DA, Dismukes GC (2010) Redirecting reductant flux into hydrogen production via metabolic engineering of fermentative carbon metabolism in a cyanobacterium. *Applied and Environmental Microbiology* **76**(15): 5032-5038.
- Mehler AH (1951) Studies on reactions of illuminated chloroplasts: I Mechanism of the reduction of oxygen and other hill reagents. *Archives of Biochemistry and Biophysics* **33**(1): 65-77.
- Melis A (1999) Photosystem-II damage and repair cycle in chloroplasts: what modulates the rate of photodamage *in vivo*? *Trends in plant science* **4**(4): 130-135.
- Metz JG, Pakrasi HB, Seibert M, Arntzer CJ (1986) Evidence for a dual function of the herbicide-binding D1 protein in photosystem II. *FEBS Letters* **205**(2): 269-274.
- Meyer J (2007) [FeFe] hydrogenases and their evolution: a genomic perspective. *Cellular and Molecular Life Sciences* **64**(9): 1063-1084.
- Moezelaar R, Stal LJ (1994) Fermentation in the unicellular cyanobacterium *Microcystis* PCC7806. *Archives of Microbiology* **162**(1-2): 63-69.
- Moore AL, Leach G, Whitehouse DG, van den Bergen CW, Wagner AM, Krab K (1994) Control of oxidative phosphorylation in plant mitochondria: the role of non-phosphorylating pathways. *Biochimica et Biophysica Acta (BBA)-Bioenergetics* **1187**(2) 145-151.
- Müller M (1988) Energy metabolism of protozoa without mitochondria. *Annual Reviews in Microbiology* **42**(1): 465-488
- Nakao M, Okamoto S, Kohara M, Fujishiro T, Fujisawa T, Sato S, Nakamura Y (2010) CyanoBase: the cyanobacteria genome database update 2010. *Nucleic Acids Research* **38**(suppl 1): D379-D381.
- Neuer G, Bothe H (1982) The pyruvate: Ferredoxin oxidoreductase in heterocysts of the cyanobacterium *Anabaena cylindrical*. *Biochimica et Biophysica Acta (BBA)-General Subjects* **716**(3): 358-365.

- Nicholls P, Obinger C, Niederhauser H, Peschek GA (1992) Cytochrome oxidase in *Anacystis nidulans*: stoichiometries and possible functions in the cytoplasmic and thylakoid membranes. *Biochimica et Biophysica Acta (BBA)-Bioenergetics* **1098**(2): 184-190.
- Oesterhelt C, Schmäzlin E, Schmitt JM, Lokstein H (2007) Regulation of photosynthesis in the unicellular acidophilic red alga *Galdieria sulphuraria*. *The Plant Journal* **51**(3): 500-511.
- Oren A, Shilo M (1979) Anaerobic heterotrophic dark metabolism in the cyanobacterium *Oscillatoria limnetica*: sulfur respiration and lactate fermentation. *Archives of Microbiology* **122**(1): 77-84.
- Osanai T, Kanesaki Y, Nakano T, Takahashi H, Asayama M, Shirai M, Tanaka K (2005) Positive regulation of sugar catabolic pathways in the cyanobacterium *Synechocystis* sp. PCC 6803 by the group 2 σ factor SigE. *Journal of Biological Chemistry* **280**(35): 30653-30659.
- Paczia N, Nilgen A, Lehmann T, Gätgens J, Wiechert W, Noack S (2012) Extensive exometabolome analysis reveals extended overflow metabolism in various microorganisms. *Microbial Cell Factories* **11**(1): 1-14.
- Patel MS, Korotchkina LG (2006) Regulation of the pyruvate dehydrogenase complex. *Biochemical Society Transactions* **34**(2): 217-222.
- Peekhaus N, Conway T (1998) What's for Dinner? Entner-Doudoroff Metabolism in *Escherichia coli*. *Journal of Bacteriology* **180**(14): 3495-3502.
- Pelroy RA, Rippka R, Stanier RY (1972) Metabolism of glucose by unicellular blue-green algae. *Archiv für Mikrobiologie* **87**(4): 303-322.
- Peschek GA (1987) Respiratory electron transport. *The cyanobacteria* 119-161.
- Pfannschmidt T (2003) Chloroplast redox signals: how photosynthesis controls its own genes. *Trends in Plant Science* **8**(1): 33-41.
- Pils D, Gregor W, Schmetterer G (1997) Evidence for in vivo activity of three distinct respiratory terminal oxidases in the cyanobacterium *Synechocystis* sp. strain PCC6803. *FEMS Microbiology Letters* **152**(1): 83-88.
- Pils D, Schmetterer G (2001) Characterization of three bioenergetically active respiratory terminal oxidases in the cyanobacterium *Synechocystis* sp. strain PCC 6803. *FEMS Microbiology Letters* **203**(2): 217-222.
- Plaga W, Lottspeich F, Oesterhelt D (1992) Improved purification crystallization and primary structure of pyruvate: ferredoxin oxidoreductase from *Halobacterium halobium*. *European Journal of Biochemistry* **205**(1): 391-397.
- Postma E, Verduyn C O R N E L I S, Scheffers W A & Van Dijken J P (1989) Enzymic analysis of the Crabtree effect in glucose-limited chemostat cultures of *Saccharomyces cerevisiae*. *Applied and environmental microbiology* **55**(2) 468-477.

- Ragsdale SW (2003) Pyruvate ferredoxin oxidoreductase and its radical intermediate. *Chemical Reviews* **103**(6): 2333-2346.
- Reed RH, Stewart WDP (1985) Osmotic adjustment and organic solute accumulation in unicellular cyanobacteria from freshwater and marine habitats. *Marine Biology* **88**(1): 1-9.
- Reher M, Fuhrer T, Bott M, Schönheit P (2010) The nonphosphorylative Entner-Doudoroff pathway in the thermoacidophilic euryarchaeon *Picrophilus torridus* involves a novel 2-keto-3-deoxygluconate-specific aldolase. *Journal of Bacteriology* **192**(4): 964-974.
- Rieger M, KÄPpeli O, Fiechter A (1983) The role of limited respiration in the incomplete oxidation of glucose by *Saccharomyces cerevisiae*. *Journal of General Microbiology* **129**(3): 653-661.
- Rippka R (1972) Photoheterotrophy and chemoheterotrophy among unicellular blue-green algae. *Archiv für Mikrobiologie* **87**(1): 93-98.
- Rippka R, Deruelles J, Waterbury JB, Herdman M, Stanier RY (1979) Generic assignments strain histories and properties of pure cultures of cyanobacteria. *Journal of General Microbiology* **111**(1): 1-61.
- Roberts AG, Kramer DM (2001) Inhibitor "Double Occupancy" in the Qo Pocket of the Chloroplast Cytochrome b6f Complex. *Biochemistry* **40**(45): 13407-13412.
- Rodríguez-Ezpeleta N, Brinkmann H, Burey SC, Roure B, Burger G, Löffelhardt W, Lang BF (2005) Monophyly of primary photosynthetic eukaryotes: green plants red algae and glaucophytes. *Current Biology* **15**(14): 1325-1330.
- Romano AH, Conway T (1996) Evolution of carbohydrate metabolic pathways. *Research in Microbiology* **147**(6): 448-455.
- Saiki RK, Gelfand DH, Stoffel S, Scharf SJ, Higuchi R, Horn GT, Erlich HA (1988) Primer-directed enzymatic amplification of DNA with a thermostable DNA polymerase. *Science* **239**(4839): 487-491.
- Sambrook J, Fritsch EF, Maniatis T (1989) *Molecular cloning* New York: Cold spring harbor laboratory press **2**:14-9.
- Sanger F, Nicklen S, Coulson AR (1977) DNA sequencing with chain-terminating inhibitors. *Proceedings of the National Academy of Sciences* **74**(12): 5463-5467.
- Stanier RY, Bazine GC (1977) Phototrophic prokaryotes: the cyanobacteria. *Annual Reviews in Microbiology* **31**(1): 225-274.
- Sagan L (1967) On the origin of mitosing cells. *Journal of Theoretical Biology* **14**(3): 225-IN6.
- Sauer J, Schreiber U, Schmid R, Völker U, Forchhammer K (2001) Nitrogen starvation-induced chlorosis in *synechococcus* pcc 7942 low-level photosynthesis as a mechanism of long-term survival. *Plant Physiology* **126**(1):233-243.

- Schmetterer G (1994) Cyanobacterial respiration. *The molecular biology of cyanobacteria* Springer Netherlands 409-435.
- Schmitz O, Gurke J, Bothe H (2001) Molecular evidence for the aerobic expression of *nifJ* encoding pyruvate: ferredoxin oxidoreductase in cyanobacteria. *FEMS Microbiology Letters* **195**(1): 97-102.
- Schopf JW (1993) Microfossils of the Early Archean Apex chert: new evidence of the antiquity of life. *Science* **260**(5108): 640-646
- Schopf JW (2002) The fossil record: tracing the roots of the cyanobacterial lineage. *The ecology of cyanobacteria* Springer Netherlands 13-35
- Schopf JW (2006) Fossil evidence of Archaean life. *Philosophical Transactions of the Royal Society B: Biological Sciences* **361**(1470): 869-885.
- Schreiber U, Klughammer C, Kolbowski J (2012) Assessment of wavelength-dependent parameters of photosynthetic electron transport with a new type of multi-color PAM chlorophyll fluorometer. *Photosynthesis Research* **113**(1-3): 127-144.
- Schreiber U, Schliwa U, Bilger W (1986) Continuous recording of photochemical and non-photochemical chlorophyll fluorescence quenching with a new type of modulation fluorometer. *Photosynthesis Research* **10**(1-2): 51-62.
- Schuetz R, Zamboni N, Zampieri M, Heinemann M, Sauer U (2012) Multidimensional optimality of microbial metabolism. *Science* **336**(6081): 601-604.
- Schwarz D, Nodop A, Hüge J, Purfürst S, Forchhammer K, Michel KP, Hagemann M (2011) Metabolic and transcriptomic phenotyping of inorganic carbon acclimation in the cyanobacterium *Synechococcus elongatus* PCC 7942. *Plant Physiology* **155**(4): 1640-1655.
- Schütz K, Happe T, Troshina O, Lindblad P, Leitão E, Oliveira P, Tamagnini P (2004) Cyanobacterial H₂ production-a comparative analysis. *Planta* **218**(3): 350-359.
- Scott M, Gunderson CW, Mateescu EM, Zhang Z, Hwa T (2010) Interdependence of cell growth and gene expression: origins and consequences. *Science* **330**(6007): 1099-1102.
- Serebryakova LT, Sheremetieva M, Tsygankov AA (1998) Reversible hydrogenase activity of *Gloeocapsa alpicola* in continuous culture. *FEMS Microbiology Letters* **166**(1): 89-94
- Serebryakova LT, Tsygankov AA (2007) Two-stage system for hydrogen production by immobilized cyanobacterium *Gloeocapsa alpicola* CALU 743. *Biotechnology progress* **23**(5): 1106-1110.
- Shah VK, Stacey G, Brill WJ (1983) Electron transport to nitrogenase purification and characterization of pyruvate: flavodoxin oxidoreductase the *nifj* gene product. *Journal of Biological Chemistry* **258**(19): 12064-12068.
- Shestakov SV, Khyen NT (1970) Evidence for genetic transformation in blue-green alga *Anacystis nidulans*. *Molecular and General Genetics MGG* **107**(4): 372-375.

- Shima S, Thauer RK (2007) A third type of hydrogenase catalyzing H₂ activation. *The Chemical Record* **7**(1): 37-46.
- Siebers B, Schönheit P (2005) Unusual pathways and enzymes of central carbohydrate metabolism in Archaea. *Current Opinion in Microbiology* **8**(6): 695-705.
- Singh AK, Sherman LA (2005) Pleiotropic effect of a histidine kinase on carbohydrate metabolism in *Synechocystis* sp. strain PCC 6803 and its requirement for heterotrophic growth. *Journal of Bacteriology* **187**(7): 2368-2376.
- Smith AJ, London J, Stanier RY (1967) Biochemical basis of obligate autotrophy in blue-green algae and thiobacilli. *Journal of Bacteriology* **94**(4): 972-983
- Stanier RY, Bazine GC (1977) Phototrophic prokaryotes: the cyanobacteria. *Annual Reviews in Microbiology* **31**(1): 225-274.
- Stal LJ, Moezelaar R (1997) Fermentation in cyanobacteria1. *FEMS microbiology Reviews* **21**(2): 179-211.
- Summers ML, Wallis JG, Campbell EL, Meeks JC (1995) Genetic evidence of a major role for glucose-6-phosphate dehydrogenase in nitrogen fixation and dark growth of the cyanobacterium *Nostoc* sp. strain ATCC 29133. *Journal of Bacteriology* **177**(21): 6184-6194
- Sveshnikov DA, Sveshnikova NV, Rao KK, Hall DO (1997) Hydrogen metabolism of mutant forms of *Anabaena variabilis* in continuous cultures and under nutritional stress. *FEMS Microbiology Letters* **147**(2): 297-301.
- Sweeney NJ, Laux DC, Cohen PS (1996) Escherichia coli F-18 and E coli K-12 eda mutants do not colonize the streptomycin-treated mouse large intestine. *Infection and Immunity* **64**(9): 3504-3511.
- Takahashi H, Uchimiya H, Hihara Y (2008) Difference in metabolite levels between photoautotrophic and photomixotrophic cultures of *Synechocystis* sp. PCC 6803 examined by capillary electrophoresis electrospray ionization mass spectrometry. *Journal of Experimental Botany* **59**(11): 3009-3018.
- Tamagnini P, Axelsson R, Lindberg P, Oxelfelt F, Wünschiers R, Lindblad P (2002) Hydrogenases and hydrogen metabolism of cyanobacteria. *Microbiology and Molecular Biology Reviews* **66**(1): 1-20.
- Tamoi M, Miyazaki T, Fukamizo T, Shigeoka S (2005) The Calvin cycle in cyanobacteria is regulated by CP12 via the NAD (H)/NADP (H) ratio under light/dark conditions. *The Plant Journal* **42**(4):504-513.
- Teeling H, Fuchs BM, Becher D, Klockow C, Gardebrecht A, Bennke CM, Amann R (2012) Substrate-controlled succession of marine bacterioplankton populations induced by a phytoplankton bloom. *Science* **336**(6081): 608-611.
- Thauer RK (1998) Biochemistry of methanogenesis: a tribute to Marjory Stephenson: 1998 Marjory Stephenson Prize Lecture. *Microbiology* **144**(9): 2377-2406.

- Thauer RK, Jungermann K, Decker K (1977) Energy conservation in chemotrophic anaerobic bacteria. *Bacteriological Reviews* **41**(1): 100.
- Thauer RK, Klein AR, Hartmann GC (1996) Reactions with molecular hydrogen in microorganisms: evidence for a purely organic hydrogenation catalyst. *Chemical Reviews* **96**(7): 3031-3042.
- Tittmann K (2009) Reaction mechanisms of thiamin diphosphate enzymes: redox reactions. *FEBS Journal* **276**(9): 2454-2468.
- Toepel J, Welsh E, Summerfield TC, Pakrasi HB, Sherman LA (2008) Differential transcriptional analysis of the cyanobacterium *Cyanothece* sp. strain ATCC 51142 during light-dark and continuous-light growth. *Journal of Bacteriology* **190**(11): 3904-3913.
- Thomas JC, Ughy B, Lagoutte B, Ajlani G (2006) A second isoform of the ferredoxin: NADP oxidoreductase generated by an in-frame initiation of translation. *Proceedings of the National Academy of Sciences* **103**(48): 18368-18373.
- Tsygankov A (2004) Hydrogen production by suspension and immobilized cultures of phototrophic microorganisms Technological aspects. *Biohydrogen III Renewable Energy System by Biological Solar Energy Conversion Elsevier Oxford* 57-74.
- Tu CJ, Shrager J, Burnap RL, Postier BL, Grossman AR (2004) Consequences of a deletion in *dspA* on transcript accumulation in *Synechocystis* sp. strain PCC6803. *Journal of Bacteriology* **186**(12): 3889-3902.
- Van der Oost J, Bulthuis BA, Feitz S, Krab K, Kraayenhof R (1989) Fermentation metabolism of the unicellular cyanobacterium *Cyanothece* PCC 7822. *Archives of Microbiology* **152**(5): 415-419.
- Whitton BA, Potts M (Eds) (2000) *The Ecology of Cyanobacteria: their diversity in time and space* Springer.
- Verhees C, Kengen S, Tuininga J, Schut G, Adams M, de VOS W, Van Der Oost J (2003) The unique features of glycolytic pathways in Archaea. *Biochemical Journal* **375**: 231-246.
- Vermaas WF (2001) Photosynthesis and respiration in cyanobacteria. *eLS*.
- Vernotte C, Astier C, Olive J (1990) State 1-state 2 adaptation in the cyanobacteria *Synechocystis* PCC 6714 wild type and *Synechocystis* PCC 6803 wild type and phycocyanin-less mutant. *Photosynthesis Research* **26**(3): 203-212.
- Vemuri GN, Altman E, Sangurdekar DP, Khodursky AB, Eiteman MA (2006) Overflow metabolism in *Escherichia coli* during steady-state growth: transcriptional regulation and effect of the redox ratio. *Applied and Environmental Microbiology* **72**(5): 3653-3661.
- Vemuri GN, Eiteman MA, McEwen JE, Olsson L, Nielsen J (2007) Increasing NADH oxidation reduces overflow metabolism in *Saccharomyces cerevisiae*. *Proceedings of the National Academy of Sciences* **104**(7): 2402-2407.

- Vignais PM, Billoud B, Meyer J (2001) Classification and phylogeny of hydrogenases1. *FEMS Microbiology Reviews* **25**(4): 455-501.
- Vignais PM, Billoud B (2007) Occurrence classification and biological function of hydrogenases: an overview. *Chemical Reviews* **107**(10): 4206-4272.
- Volkmer T, Schneider D, Bernát G, Kirchhoff H, Wenk SO, Rögner M (2007) Ssr2998 of *Synechocystis* sp PCC 6803 is involved in regulation of cyanobacterial electron transport and associated with the cytochrome b6f complex. *Journal of Biological Chemistry* **282**(6): 3730-3737.
- Wetz MS, Wheeler PA (2004) Response of bacteria to simulated upwelling phytoplankton blooms.
- Williams JG (1988) [85] Construction of specific mutations in photosystem II photosynthetic reaction center by genetic engineering methods in *Synechocystis* 6803. *Methods in Enzymology* **167**: 766-778.
- Xu Y (2010) *Synechococcus* sp PCC 7002: A Robust and Versatile Cyanobacterial Platform for Biofuels Development. Doctoral dissertation Pennsylvania State University.
- Yang C, Hua Q, Shimizu K (2002) Metabolic Flux Analysis in *Synechocystis* Using Isotope Distribution from ^{13}C -Labeled Glucose. *Metabolic Engineering* **4**(3): 202-216.
- Yoshikawa K, Hirasawa T, Ogawa K, Hidaka Y, Nakajima T, Furusawa C, Shimizu H (2013) Integrated transcriptomic and metabolomic analysis of the central metabolism of *Synechocystis* sp. PCC 6803 under different trophic conditions. *Biotechnology Journal*.
- Zhang S, Bryant DA (2011) The tricarboxylic acid cycle in cyanobacteria. *Science* **334**(6062): 1551-1553.

Acknowledgement

This PhD study was carried out from October 2010 to February 2014 under the supervision of Prof. Dr. Rüdiger Schulz and Dr. Kirstin Gutekunst.

My deepest and sincere gratitude goes first and foremost to Prof. Dr. Rüdiger Schulz, for providing me the opportunity to work as PhD student and explore my minds in Germany, for his constant encouragement and guidance, for his support which inspired me greatly to work in the projects.

I would like to express my heartfelt gratitude to Dr. Kirstin Gutekunst who introduced me to the cyanobacteria world. Her valuable and constructive suggestions, interesting ideas, patient explanation and constant scientific training ensured the well planning and development of the projects. She encouraged me to not only grow as a qualified student, but also as an independent thinker. I also appreciate her useful comments and language editing, which have greatly improved the thesis. Without her help this work will be not succeeded.

I would like to give my sincere thanks to Dr. Jens Appel for his excellent discussion. He provided me much valuable information as guidance of my projects.

I would like to thank Prof. Sönnichsen for discussing the project and for performing so many NMR measurements with me.

I would like to thank Prof. Schönheit for his excellent knowledge and deep discussion about the glucose degradation pathways and further cooperation with our group.

I would like to thank Prof. Bilger for being my second referee.

I would like to thank Dr. Rena Isemer and gave me many helpful advices for qRT-PCR experiments.

I would like to thank Fabian Lindel for conducting PAM measurement, oxygen evolution and consumption measurement with me. And also thank Nora Burhenne, Rebekka Kirsch and Kristina Rauff. They are very good cooperators. I am enjoyed quite a lot to work together with them.

I would like to thank Dr. Opayi Mudium, Ursula Kaspar, Karoline Schreiber, Heiner Burgstaller, Claudia Marquardt and Sandra Pusch. They are very nice friends and very good colleagues. Their passion for science and willingness to study motivated me. They also give me lots of help for experiments and my daily life. I would like to thank the whole team in our laboratory for the generous exchange of ideas, their kindness and nice atmosphere they have created. They provided an enjoyable environment to study and made my life in Kiel a truly memorable experience and their friendship is invaluable to me. Especially I want to show grateful appreciation for Heiner Burgstaller once more for setting up qRT-PCR system for our group.

The financial support from “Fazit Stiftung” for learning and reasearching is gratefully acknowledged.

Finally, I would like to send my deepest gratitude to my family. I thank my parents for caring about me in my life, for thirty years support of my studies and their faith in me. I thank my caring and supportive wife, Dan Shen, for giving advice in my studies and sharing my life for eight years.

Affidavit

Herewith, I declare that the work is my genuine work apart from the supervisor's guidance and nothing but the references and tools mentioned in my thesis have been used to conduct this work.

The thesis has not been submitted either partially or wholly as part of a doctoral degree to another examining body.

Besides this, I declare that the thesis has been prepared subject to the Rules of Good Scientific Practice of the German Research Foundation.

Parts of this dissertation have been published in:

Kirstin Gutekunst, Xi Chen, Karoline Schreiber, Ursula Kaspar, Srinivas Makamand, and Jens Appel. . The bidirectional NiFe-hydrogenase in *Synechocystis* sp. PCC 6803 is reduced by flavodoxin and ferredoxin and is essential under mixotrophic, nitrate-limiting conditions[J]. Journal of Biological Chemistry, 2014, 289 (4): 1930-1937. Doi: 10.1074/jbc. M113. 526376.

Kiel, den

(Xi Chen)

Curriculum Vitae

Name	Xi Chen
Date of birth	27.11.1983
Place of birth	Fujian, China
Nationality	P. R. China
1990-1996	Elementary School, Fuqing, Fujian, China
1996-1999	Middle School, Fuqing, Fujian, China
1999-2003	High School, Fuqing, Fujian, China
2003-2007	B.Sc. Department of Plant Genetic and Breeding, China Agricultural University, Beijing, China Thesis: Investigation of cotton quality regionalism in China Supervisor: Dr. Wenxin Liu
2007-2010	MSc. Department of Crop Science, Zhejiang University, Hangzhou, China Thesis: Investigation and utilization of intron length polymorphism in conifers Supervisor: Prof. Dr. Weiren Wu
2010-present	PhD student, Department of Biology, Christian-Albrechts- University of Kiel, Germany Thesis: Characterization of <i>Synechocystis</i> sp. PCC 6803 under mixotrophic conditions Supervisor: Prof. Dr. Rüdiger Schulz

Dr. Kirstin Gutekunst